

Title	Development of a lab on a chip electrochemical immunosensor array for the detection of polycyclic aromatic hydrocarbons (PAHs) in environmental of water
Authors	Felemban, Shifa Jameel
Publication date	2020-01
Original Citation	Felemban, S. J. 2020. Development of a lab on a chip electrochemical immunosensor array for the detection of polycyclic aromatic hydrocarbons (PAHs) in environmental of water. PhD Thesis, University College Cork.
Type of publication	Doctoral thesis
Rights	© 2020, Shifa Jameel Felemban. - <a href="https://creativecommons.org/licenses/by-nc-nd/4.0/">https://creativecommons.org/licenses/by-nc-nd/4.0/</a>
Download date	2023-05-05 03:37:18
Item downloaded from	<a href="http://hdl.handle.net/10468/10462">http://hdl.handle.net/10468/10462</a>

# **Development of a lab on a Chip Electrochemical Immunosensor Array For the Detection of Polycyclic Aromatic Hydrocarbons (PAHs) in Environmental of Water**

A thesis submitted for the degree of Ph.D.

by

Shifa Jameel Felemban, B.Sc. M.Sc.  
**112220253**

Under the supervision of

Dr. Eric Moore  
Dr. Patricia Vazquez



Based on research work carried out at

School of Chemistry  
University College Cork  
Cork  
Ireland

**January 2020**

Research supported by Ministry of Higher Education of Saudi Arabia and Umm Al-Qura University

## **CERTIFICATE OF APPROVAL**

---

**PH.D. THESIS**

---

This is to certify that the Ph.D. thesis of

**Shifa Jameel Felemban**

Has been approved by the Examining Committee for the thesis requirement for the

Doctor of Philosophy degree in Chemistry at the January 2020 graduation.

Thesis Committee: \_\_\_\_\_

\_\_\_\_\_

\_\_\_\_\_

\_\_\_\_\_

\_\_\_\_\_

**To my father's soul, mother, siblings and all people who love me.**

## ACKNOWLEDGEMENTS

First of all: all the praises and thanks be to Allah for all the blessings He has bestowed on me. Without his blessings, this achievement would not have been possible. Secondly: I would like to thank and acknowledge the financial support of Ministry of Higher Education of Saudi Arabia and Umm Al-Qura University.

The last four years at Tyndall and UCC have been very rewarding and I have met many wonderful people. Today I want to take the opportunity to thank all the people I met who made my life and work interesting and fun by sharing their knowledge and views and the many friends I have made here. In particular to all the people who in one-way or another were with me, supported me and shared with me all my 4 years in which has been done this thesis.

To Dr. **Eric Moore** for being my supervisor, for his support throughout all this time and for being directly responsible for this work. To Dr. **Patricia Vazquez** for being my co-supervisor for her time, suggestions and excellent contributions. **Patricia** has dedicated countless hours to making me a better researcher, and I will always be grateful for her . Both provided me with valuable support and advice that led to exciting and successful projects. To Dr. **Anna Hogen** for her support in the validation work and optimism and for making of every moment at chemistry lab a great memory. I am also grateful to my monitor Dr. **James Rohan** for his advice to improve the quality of my research.

I would like to express my sincere gratitude to the LSI team. Especially to the lab manger of LSI lab at Tyndall National Institute **Eileen** and to all the **colleagues** of the Dr. Eric Moore team, with whom I've had the pleasure to work during all these years, for all the good times we've had together in the lab. To my **Family** for their listening, helping me and providing me a lot of joy. To my **fiancée** for waiting me a long time.

**“Anyone who has never made a mistake has never tried anything new. “**  
**-Albert Einstein-**



## DECLARATION

I hereby declare that this thesis is my original work and it has been written by me in its entirety. I have duly acknowledged all the sources of information that has been used in this thesis.

This thesis has also not been submitted for any degree in any university previously.

Signed \_\_\_\_\_ **Shifa Jameel Felemban** \_\_\_\_\_

Student Number \_\_\_\_\_ **112220253** \_\_\_\_\_

Date \_\_\_\_\_ / \_\_\_\_ / **2020** \_\_\_\_\_

## **SUMMARY THESIS (ABSTRACT)**

Polycyclic aromatic hydrocarbons (PAHs) are a very large group of organic compounds made of carbon and hydrogen atoms. These compounds present an important impact as environmental pollutants. They are a primary concern for human health, as PAHs have been reported to increase the risk of cancer in humans. It is therefore of high importance to avail of a method to detect them in any matter that humans may get in contact with, such as food, soil and water. The European Drinking Water Directive (98/83/EC) recommends a value of 0.01ng/ml as a limit for Benzo[a]pyrene (BaP) levels in drinking water. Traditionally, detection of PAHs in the environment was done using commercial equipment such as HPLC-fluorescence detection and Gas Chromatography-Mass Spectrometry (GC-MS). However, these techniques are often expensive, use large amounts of toxic solvents, are time-consuming, and non-portable [8,9]. In this research, immunosensors were used for BaP determination in water sample. Immunosensors are affinity biosensors based on the specific interaction between antigens and antibodies; this interaction could be monitored by several techniques including electrochemistry. Voltammetric detection with the immunosensor provides an approach, which could be performed in small portable instrument for in-field measurements. Electrochemistry technique has several advantages compared to other techniques; it is easy to apply and also have the advantages of miniaturisation, portability, real measurement time, low-cost production and fabrication without reducing their levels of detection or sensitivity. This thesis is to address the shortcomings of the current techniques. The study presented in this thesis described the development of the immunosensors with electrochemical detection for detection of polycyclic aromatic hydrocarbon in environmental monitoring of water.

This work shows how the integration of electrochemical techniques with an immunoassay method can reach limits of detection as low as required for the analysis of water samples in situ and in real time. In particular, we targeted to detect the presence of (BaP) in water. Results obtained by optical and electrochemical detections were validated with Gas Chromatography-Mass Spectrometry (GC-MS). The usage of this method as a complement to the electrochemical studies, not only increased the quality of the research, but also helped in the construction and improvement of immunosensors. They were not reliable, but also represent accurate characteristics to be employed in miniaturised sensor and fluidic system. This thesis is organized in six chapters and a brief explanation for each of them is shown below:

Chapter 1 is a general introduction about the essential concepts and conditions used in this thesis. Chapter 2 offers an understanding of the key principles of optical immunoassay involved in this thesis. An optical immunoassay using a 96-well microtiter plate as a solid surface was developed. Chapter 3 the application of the developed electrochemical immunosensors was discussed. Chapter 4, focuses on the design, fabrication and characterization of a Q-sens (Lab On a Chip) that was developed for use in electrochemical application. Chapter 5 demonstrates the validation study in order to confirm that the applied developed method for a PAH was suitable for its intended use. The validation could compare the reliability and sensitivity of the developed results. Chapter 6 represents the conclusion and future perspectives.



**Basis:**

The objective of the work presented is to develop an electrochemical sensing array to detect PAHs in the environment, as they represent a toxic threat for health in water and the current detection methods are time consuming and non-portable.

**Hypothesis:**

The research will focus on the integration of a sensor arrays with immunoassay and electrochemical detection methods. Water samples will be spiked with PAHs and tested using the immunosensor arrays. ELISA will be used to help validate the electrochemical analysis This project show the work done towards the optimisation of the immunoassay protocol for PAHs detection in water samples, and its transfer into a lab-on-a chip application that has a particular focus on environmental screening.

**Research strategy:**

The first year aim of the research was to optimize ELISA reagents and detection methods. The second year and first half of the third year of the research were for integrating the immunoassay method with lab on a chip platform. The second half of the third year was for the interfaces between lab on a chip platform and the bio recognition element modified with the addition of metal nanoparticle, magnetic beads. During the last year the research terminated with final testing and comparison system.

## CONTENTS INDEX

CHAPTER I General Introduction	1
1.1 Biosensors	2
1.1.1 Biosensing Components	3
1.1.1.1 Antibodies	3
1.1.1.2 Enzymes	4
1.1.2 Bio-transducer Components	4
1.1.2.1 Electrochemical Biosensors	4
1.1.2.1.1 Electrochemical Techniques	6
A. Amperometric Transducers	6
B. Voltammetric Transducers	6
• Linear Sweep Voltammetry (LSV)	6
• Cyclic Voltammetry (CV)	7
C. Conductometric Transducers	8
D. Impedimetric Transducers	8
E. Potentiometric Transducers	9
1.1.2.1.2 Microfluidic Electrochemical Cell	9
1.1.2.2 Optical Biosensors	11
1.1.2.3 Other Biosensors	12
1.2 Molecular Recognition	13
1.2.1 Binding forces and Interaction involved in molecular recognition	13
1.2.1.1 Electrostatic and Hydrophobic Interaction	13
1.2.1.2 Covalent Bonding	13
1.2.1.3 Hydrogen Bonding	13

1.2.1.4	Specific Interaction	14
1.2.2	Types of Molecular Recognition	14
1.2.2.1	Static molecular recognition	14
1.2.2.2	Dynamic molecular recognition	14
1.3	Antibody-Antigen Interactions	15
1.4	Immunoassay	17
1.4.1	Types of Immunoassays	19
1.4.2	Enzyme-Linked Immunosorbent Assay (ELISA)	20
1.4.3	Signal Generation in Immunoassays	22
1.4.4	Electrochemical immunoassay applications	24
1.4.5	Immunoassay Optimisation	27
1.4.6	Immunoassay Buffers	28
1.4.7	Immunoassay Validation	29
•	Define Calibration Model	30
•	The limit of detection [LOD]	31
1.5	Immobilisation strategies for biomolecules onto solid surfaces	32
1.5.1	Enhancement of the recognition antibody	33
1.5.2	Improvement platform and recognition performance	34
•	Magnetic beads	35
1.6	Lab-on-a-Chip Immunoassay Systems	37
1.6.1	Substrates Used for Microfluidic Chip Design	39
1.6.2	Microfluidic Channel Design and Fabrication	39
1.6.3	Analyte Delivery, Mixing and Washing	40

1.6.4	Antibody Integration	40
1.7	Trends in instrumentation and technology	41
1.8	Water pollution	46
1.9	Polycyclic aromatic hydrocarbons (PAHs)	47
1.9.1	Health issues pertaining to PAHs	48
1.9.2	Analysis of PAHs	51
1.9.3	Surface Functionalisation Techniques	53
1.9.4	Haptens and their conjugates	57
1.9.4.1	Pyrene as hapten	58
1.9.4.2	Benzo[a]pyrene to haptene	58
1.9.5	Proteins	59
1.9.6	The conjugates of carrier proteins	62
1.10	Perspective	63
1.11	References	65
 <u>CHAPTER II Immunoassay protocols (ELISA)</u>		
2.1	Introduction	91
2.2	Objective	91
2.3	Experimental	92
2.3.1	Materials	92
2.3.2	Instrumentations	93
2.3.3	Procedures	93
2.3.3.1	Preparation of phenanthrene-protein coating conjugate	93
2.3.3.2	Matrix Assisted Laser Desorption ionization / mass spectrometer (MALDI-TOF /MS) test for determination of the average PHE to BSA ratio	95

• Principle	96
• Sample preparation required: For the measurements of the coating conjugate ratio	96
• The protocol of MALDI-TOF / mass spectrometry (MS) test	97
2.3.3.3 Immunoassay buffer solutions	97
2.3.3.4 Checkerboard ELISA protocol of immunoassays reagents	98
• Reagents required	99
• The protocol of checkerboard ELISA	100
2.3.3.5 Optimisation of AP Labelling	101
2.3.3.6 Antibody immobilisation time	101
2.3.3.7 Capture assay: monoclonal mouse antibody 4D5 specific to BaP concentration	102
2.3.3.8 Displacement assay on microplate	103
2.3.3.9 Use of a spiked sample	104
2.4 Results and Discussion	104
2.4.1 Development of immunoassay protocol	104
2.4.2 Optimisation of buffer solutions	104
2.4.3 Optimisation of coating conjugate	105
2.4.4 (MALDI-TOF /MS) test for determination of the average binding PHEN to BSA ratio	107
2.4.5 Optimisation checkerboard ELISA titration assay	111
2.4.6 Optimisation of antibody immobilisation time	112
2.4.7 Optimisation of AP labeling	113

2.4.8	Optimisation of monoclonal mouse antibody	
	4D5 specific to BaP concentration	114
2.4.9	Displacement assay	116
2.4.10	Measurements of tap water	117
2.5	Conclusion	118
2.6	References	119

### CHAPTER III Electrochemical Immunosensors

#### Part 1: Screen-printed electrodes (SPEs)

#### Part 2: Nanoparticles (NPs)

3.1	Immunosensors	122
3.2	Objective of electrochemical immunosensors	125
3.2.1	Part 1: Screen-printed electrodes (SPEs)	125
3.2.1.1	Introduction	125
3.2.1.2	Experimental	127
3.2.1.2.1	Materials	127
3.2.1.2.2	Instrumentations	128
3.2.1.2.3	Procedures	128
•	Preparation of phenanthrene–protein coating conjugate	128
•	Screen-printed electrodes (SPE) cleaning	128
•	Capture assay: optimization of monoclonal mouse	
	4D5 antibody specific to Benzo[a]pyrene (BaP)	129
•	Michaelis – Menten Kinetics.	130
•	Displacement assay on SPE.	130
3.2.1.3	Results and Discussion	131
•	Development of immunoassay protocol for SPEs	131
•	Optimisation of coating conjugate	131

• Optimisation of monoclonal primary antibody	132
• Optimisation of <i>p</i> APP ( Michaelis – Menten Kinetics)	133
• Displacement assay on SPE.	134
3.2.1.4 Conclusion	136
3.3 Objective of electrochemical immunosensors	136
3.3.1 Part 2: Nanoparticles (NPs)	136
3.3.1.1 Introduction	137
3.3.1.2 Experimental	139
3.3.1.2.1 Materials	139
3.3.1.2.2 Instrumentations	140
3.3.1.2.3 Procedures	140
• Preparation of PEG-ferromagnetic particles	140
• Capture assay: Optimisation of monoclonal mouse antibody 4D5 specific to BaP	141
• Displacement assay on ferromagnetic particles surface	142
3.3.1.3 Results and Discussion	142
• Development of immunoassay protocol for ferromagnetic particles	142
• Optimisation of monoclonal mouse 4D5 antibody specific to Benzo[a]pyrene (BaP)	143
• Displacement assay on ferromagnetic particles	145
3.3.4 Conclusion	147
3.3.5 References	148

## CHAPTER IV Development and Characterisation

### of a lab on a chip electrochemical immunosensor array

4.1	Aim and Novelty	153
4.2	Introduction	154
4.3	Materials and Methods	155
4.3.1	Reagents	155
4.3.2	Instrumentations	155
4.3.3	The fabrication of the biochip	156
4.3.4	Characterisation and preparation of the gold chip	157
4.3.4.1	Studies on the influence of scan rate	157
4.3.4.2	Gold chip cleaning protocols	158
4.3.4.3.	Gold chip modification procedure	
	(Self Assembled Monolayers (SAM))	158
4.3.4.4	Contact angle measurements	159
4.3.4.5	Amperometric detection	159
4.3	Lab on a chip design	159
4.5	Smarter-SI Q-Sense (Measurement GUI)	163
4.5.1	Raspian Desktop	163
4.5.2	GUI – Tabs	163
4.5.3.	GUI – Pump and Valve Control Tab	164
<b>4.5.4</b>	<b>GUI – Measurement Control Tab</b>	164
<b>4.5.5</b>	<b>GUI – App Control Tab</b>	165
4.6	Results and Discussions	166
4.6.1	Characterisation of the gold chip	166
4.6.1.1	Influence of scan rate	168



4.6.1.2	Influence of gold chip cleaning protocols	159
4.6.1.3	Gold chip arrays modification procedure (Self-Assembled Monolayers (SAM))	170
4.6.1.4	Contact angle measurements	171
4.6.1.5	Amperometric detection	172
4.7	Development of an integrated sensing system (Lab On a Chip)	173
4.7.1	Proof of concept	173
4.7.2	Troubleshooting and future work	176
4.6	Conclusion	178
4.7	References	179
<u>CHAPTER V Comparison Gas Chromatography</u>		
<u>-Mass Spectrometry (GC-MS)</u>		
5.1	Comparitive Study	181
5.2	Introduction	182
5.2.1	Conventional PAHs Analysis Methods	182
5.2.2	Environmental monitoring study (Drinking Water)	183
5.2.3	Study with coal tar	184
5.3	Objective	185
5.3.1	Experimental	186
5.3.1.1	Standards and reagents	185
5.3.1.2	GC-MS conditions and instrumentation	186
5.3.1.3	Water extraction	187
5.3.1.4	Disks preparation	187
5.3.1.5	Extraction of sample	188

5.3.1.6 Elution of the sample	189
5.3.2 Sample analysis with GC-MS	190
5.3.2.1 Response Factor (RF) and Relative Response Factors (RRFs)	
experiment	195
5.3.2.2 Relative standard deviation (RSD)	197
5.3.2.3 Spiked and recovery experiments	198
5.3.3 Conclusions	201
5.3.4 References	201
<u>CHAPTER VI Conclusions and Future work</u>	
6.1 Conclusion	204
6.2 Suggestions for Future perspective	207
6.3 References	209

## **LIST OF FIGURES**

### CHAPTER I

Figure 1.1: Schematic of different types of biosensor. The biocomponent are immobilised on biocompatible layer, resulting in a change of physical or chemical properties of the elements that can be detected by a measuring tool	2
Figure 1.2: A general structure of an individual immunoprotein molecule	3
Figure 1.3 A typical Linear Sweep Voltammetry. The slop shows the scan rate of the experiment (volts per unite time).	7
Figure 1.4: Laminar Flow: the flow of a fluid when each particle of the fluid follows a smooth path, top, versus turbulent flow, irregular flow that is characterised by tiny whirlpool regions, bottom.	10

Figure 1.5: A typical response plot for each assay is illustrated and ELISA assays: capture and displacement assays	21
Figure 1.6. (a) Hydrolysis Enzymatic reaction of pNPP to chromogenic p-nitrophenol catalyzed with alkaline phosphatase AP (b) Upon the reaction of the pAPP with AP, 2 electron were generated with p- aminophenol (pAP) as a final product	24
Figure 1.7: Limit of blank (LOB), limit of detection (LOD), and limit of quantitation (LOQ) based on the blank	30
Figure. 1.8: Schematic representation of homogeneous (bead-based) and heterogeneous immunoassay formats available for ‘lab-on-a-chip’ applications	41
Figure 1.9: Diagram showing characteristic diffusion profiles of (a) a macroelectrode and (b) a microelectrode. The arrows indicate the direction of analyte diffusion to the surface of the electrode. In the case of the microelectrode the diffusion is a faster mass transport and therefore to a higher response.	45
Figure 1.10: Environmental water monitoring parameters	47
Figure 1.11: Structure of selected PAHs. Highlighted compounds comprise the Environmental Protection Agency (EPA) list of 16 priorities PAH	50
Figure 1.12: Electrochemical detection using an immunological reaction by measuring the alkaline phosphatase (AP) enzymatic reaction towards the substrate para-aminophenyl phosphate (pAPP). Two electrons were generated with a new product (para-aminophenyl (pAP)	54

Figure 1.13: Schematic representation of Fe <sub>3</sub> O <sub>4</sub> /PANI/Nafion-based immunosensor using multi-HRP-HCS-Ab2 bioconjugates as labels	55
Figure 1.14: Synthesis of ruthenium tris(bipyridine)-pyrene butyric acid (PAH-Ru) conjugate	56
Figure 1.15: Various haptens required for producing different antibodies	57
Figure 1.16: Coupling approaches for linking antibodies to surfaces.	
In its natural state an antibody has primary amines, carboxyls and hydroxyls as target groups for antibody immobilisation. Amine group is the most abundant of all native pendent groups on an antibody. Carboxyl group is another viable group for antibody functionalisation.	61

## CHAPTER II

Figure 2.1: Schematic of preparation of coating conjugate. The crosslinker EDAC helps the coupling of AAD with the BSA hydroxyl group. This combination provides the coating conjugate with amine groups, where finally hapten phenanthrene-9-carboxaldehyde binds.	95
Figure 2.2: Mass analyser- Mechanism of TOF separates ions according to their mass (m)-to charge (z) (m/z) ratios	96
Figure 2.3: checkerboard capture assay was performed with different concentration of the capture antibody and the detection antibody. Each column 1-12 contains a capture antibody dilution factor. Each row A-H contains a detection antibody dilution factor	98
Figure 2.4: Capture assay	103
Figure 2.5: Displacement assay	103
Figure 2.6: The serial dilution of the protein sample was performed on a 96 well ELISA microplate.. The typical behaviour of a protein curve	

measured at 590 nm (n=2).	106
Figure 2.7: Typical behaviour of a PHEN curve measured at 532 nm	106
Figure 2.8: Determination of hapten density on BSA-PHEN conjugates using MALDI-TOF method	110
Figure 2.9: Absorbance signals detected for different incubation times between the antibody and the solid surface. The points correspond to the average signal of absorbance $\pm$ S.D. calculated for n=3 repetitions	113
Figure 2.10: Optimisation detection antibody dilution. The antibody immobilisation time was 60 min. The dilution points correspond to the average signal of absorbance $\pm$ S.D. calculated for n=3 repetitions	114
Figure 2.11: Calibration curve obtained with the absorbance found for each concentration of the monoclonal mouse 4D5 antibody (7.8 ng/ml to 10 $\mu$ g/ml) (n=3)	115
Figure 2.12: Variation of absorbance with log of concentration of the BaP	117
<b><u>CHAPTER III</u></b>	
Figure 3.1: Antibody orientations on immunosensors A) random immobilization B) oriented immobilisation	124
Figure 3.2: Kanichi Research Services Ltd screen-printed electrode	129
Figure 3.3: (a) Example of a cyclic voltammetry plot obtained from the application of the capture assay. (b) Calibration curve obtained with the current peaks found for each concentration of the monoclonal mouse 4D5 antibody. The control was without a primary antibody.	133
Figure 3.4: Calibration curve of pAPP from amperometry readings in a stirred batch	134

Figure 3.5.: (a) Example of a typical linear sweep voltammetry plot obtained from the application of the displacement assay (b) Calibration curve obtained with the current peaks found for each concentration Benzo[a]pyrene (BaP) (range of concentrations from 0.01 ng/ml to 10 µg/ml) 135

Figure 3.6: Schematic reaction of carboxyl-amine. Carboxyl-amine crosslinker presents hetero-bifunctional chemistry (EDC). The carboxyl group of the antibody reacts with the amine on the surface 141

Figure 3.7: Schematic of typical EI steps using magnetic beads [Fe<sub>3</sub>O<sub>4</sub>] as solid surface material for immobilisation of immunoreagents. The immunocomplex is composed of a capture antibody (Ab1) and a secondary antibody (Ab2) labelled with redox enzyme (E). The magnetic bead-capture ELISA conjugate is attached to the screen-printed-electrode by magnetic attraction for electrochemical measurements. 143

Figure 3.8: (a) Example of a typical linear sweep voltammetry plot obtained from the application of the capture assay. (b) Calibration plot for the monoclonal mouse 4D5 antibody using magneto-electrochemical immunoassay. 144

Figure 3.9: A schematic illustrates a typical ELISA format involved in the displacement assay. 145

Figure. 3.10: (a) Example of a typical linear sweep voltammetry plot obtained from the application of the displacement assay (b) Calibration curve obtained with the current peaks found for each concentration Benzo[a]pyrene (BaP) (range of concentrations from 0.01 ng/ml to 10 µg/ml). 146

#### CHAPTER IV

Figure 4.1: Amperometric detection using an AP used as enzyme label. The substrate used was *p*APP. With the potential applied at 300 mV. Upon

the reaction of the <i>p</i> APP with AP, 2 electrons were generated with	
<i>p</i> - aminophenol ( <i>p</i> AP) as a final product	154
Figure 4.2: Fabricated chip in a three-electrode system	156
Figure 4.3: Electrochemical sensing array, with interface for connection	
to PalmSens detector and reservoir device for sample addition	157
Figure 4.4: (left) Microfluidic cartridge with immunosensor and	
(right) fluidic manifold with valves to control fluid	160
Figure 4.5: The fluid channels across the chip , fluidic cell with electrode	
chip electronics, portable pump and valve control Tab.	161
Figure 4.6: Images of a euro coin to help clarify dimensions of the chip	161
and the microfluidic cell with the chip.	
Figure 4.7: Control module, containing interfaces for microfluidics,	
immunosensor and user display	162
Figure 4.8: Q-sense system desktop	163
Figure 4.9: Q-sense system Tabs	163
Figure 4.10: Q-sense system pump and valve control Tab	164
Figure 4.11: Q-sense system measurement control Tab	164
Figure 4.12: Q-sense system App control Tab	165
Figure 4.13: Simulations of liquid flow from inlet to outlet at microfluidic	
capsule	166
Figure 4.14: Influence of the scan reates of 5 mM ferri/ferrocyanide	
at bare chip. Supporting electrolyte was 0.1M KCL	167
Figure 4.15: Studies on different chip cleaning protocols. CV was scanned in	
5 mM ferri/ferrocyanide redox couple with a 50 mV /s scan rate	169
Figure 4.16: CVs of (i) bare Au: (ii) 20 hours 11-MUA SAM (iii) activation	

with EDC/NHS and (iv) immobilisation of primary monoclonal antibody.	
Electrolyte used was 5 mM ferri/ferrocyanide redox couple in 0.1M KCL with	
a 0.05 V /s scan rate.	171
Figure 4.17: Contact angle tests before and after modification	
of the gold chip with 11-MUA SAM	172
Figure 4.18: Typical signal for amperometric detection. The chip modified	
AP consisting bilayer (immunoassay format) was measured in DEA	
solution pH 9.5 at a potential of 300 mV. The substrate pAPP was injected	
10 seconds	173
Figure 4.19 Electrochemical detection of bare chip. Electrolyte used was	
5 mM ferri/ferrocyanide in 0.1M KCL	174
Figure 4.20: The amperometric tests with typical signal of Q-sense.	
The gold chip array modified AP consisting bilayer (immunoassay format)	
was measured in DEA solution	175
Fuiger 4.21: The Pyrex glass substrate, Example of Q-Sens immunosensor in	
H2020 project SMARTER-Si. This immunosensor is being used for water quality	
monitoring.	177
 <u>CHAPTER V</u>	
Figure 5.1: Agilent 6890/5973 gas chromatography-mass Spectrometry	
(GC-MS) instrument	187
Figure 5.2: The setup for disk conditioning.	188
Figure 5.3: Elution apparatus	189
Figure 5.4: Standard curves obtained GC-MS for BaP .A 30.0 m, 0.25 mm i.d.	
HP-5MS capillary column, Injection volume 5.0 ul, Injection temperature	
250 0C	192



Figure 5.5: Chromatogram of the individual compounds in the 15 PAHs mix. Peak ID : (a) Nap, (b) Ace, (c) Flo, (d) Phe, (e) Anth, (f ) Flan, (g) Pyr, (h) B[a]a, (i)

Figure 5.6: The total ion chromatogram of the 6 internal standards Chry,( j) B[b]f, (k)B[e]a, (l) B[k]f, (m) B[a]p, (n) Pery and (o) Ind. Peak ID: Naphthalene D8,1,4-Dichlorobenzene D4, Acenaphthylene

D10, Phenanthrene-D10, Chrysene D12, Perylene D12 194

Figure 5.7: GC calibration curve of PAH (BaP) with internal standard

Peak ID: Naphthalene D8,1,4-Dichlorobenzene D4, Acenaphthylene

D10, Phenanthrene-D10, Chrysene D12, Perylene D12 196

Figure 5.8: the total ion chromatogram of real sample (tap water).

All the spiked ISs were found in the sample 199

## LIST OF TABLES

### CHAPTER I

Table 1.1: The three types of electrochemical cell	5
Table 1.2: Electroanalytical characteristics of the biosensors	11
Table1.3: Types of Immunoassays: Immunoassays can be divided into two kinds: homogenous and heterogeneous	19
Table 1.4: Buffers used for immunoassay formats	28
Table 1.5: The effects of PAHs in short and long contacts	49

### CHAPTER II

Table 2.1: Different coating conjugates concentrations. Control (PSB buffer)=0, MW (PHEN)=206.24. MW of BSA =66430.3 kDa	111
Table 2.2: Recovery study for Tap water sample with three different concentrations of BaP. ELISA format used was displacement assay	117

### CHAPTER III

Table 3.1: immunosensor types depending on the techniques of detection	123
--	-----

### CHAPTER IV

Table 4.1: Influence of scan rate on the peak potential for 5 Mm ferrocyanide. The scan rate were 5 mV/s, 10 mV/s, 20 mV/s, 50 mV/s, 100 mV/s, 150 mV/s and 200 mV/s.	168
---	-----

### CHAPTER V

Table 5.1: Physicochemical properties of BaP	183
Table 5.2: Agilent 6890/5973 gas chromatography-mass Spectrometry conditions	186
Table 5.3: GC-MS conditions under time scheduled selected ion monitoring	191
Table 5.4: Internal Standard with number of rings, molecular mass, and \	
retention time	194
Table 5.5: Calibration Curve with Internal Standard	196
Table 5.6: The average and standard deviation of the PAH solutions and real sample (tap water) and the relative standard deviation of the retention times and the peak areas	198
Table 5.7: The recovery percentages of spiked (IS) found in tap water sample.	199
Table 5.8 : Comparison of optical and electrochemical immunosensors performance with GC-MS	200

### CHAPTER VI

Table 6.1: The challenges environmental monitoring and the possible solutions	208
---	-----

## LIST OF ABBREVIATIONS

<b>IDES</b>	<b>interdigitated electrode structure</b>
<b>Ig</b>	<b>immunoglobulins</b>
<b>IPA</b>	<b>isopropanol</b>
<b>ISE</b>	<b>ion selective electrode</b>
<b>K<sub>3</sub>Fe(CN)<sup>6</sup></b>	<b>potassium ferricyanide</b>
<b>K<sub>4</sub>Fe(CN)<sup>6</sup></b>	<b>potassium ferrocyanide</b>
<b>KCl</b>	<b>potassium chloride</b>
<b>LOD</b>	<b>limit of detection</b>
<b>LSV</b>	<b>linear sweep voltammetry</b>
<b>mAb</b>	<b>monoclonal antibodies</b>
<b>MeOH</b>	<b>methanol</b>
<b>NaCl</b>	<b>sodium chloride</b>
<b>NaCNBH<sub>4</sub></b>	<b>sodium cyanoborohydride</b>
<b>NaOH</b>	<b>sodium hydroxide</b>
<b>NHS</b>	<b>N-hydroxysuccinimide</b>
<b>PAH</b>	<b>polycyclic aromatic hydrocarbon</b>
<b>pAPP</b>	<b>para aminophenyl phosphate</b>
<b>PBS</b>	<b>phosphate buffered saline</b>

<b>HPLC</b>	<b>high performance liquid chromatography</b>
<b>Ag/AgCl</b>	<b>silver/silver chloride</b>
<b><i>p</i>NPP</b>	<b>para nitrophenyl phosphate</b>
<b>Pt</b>	<b>platinum</b>
<b>R<sub>ct</sub></b>	<b>charge transfer resistance</b>
<b>SAM</b>	<b>self-assembled monolayers</b>
<b>SPCE</b>	<b>screen-printed carbon electrodes</b>
<b>SPE</b>	<b>solid phase extraction</b>
<b>TRIS</b>	<b>tris[hydroxymethyl]aminomethane</b>
<b>ΔE<sub>p</sub></b>	<b>peak-to-peak separation</b>
<b>11-MUA</b>	<b>11-mercaptoundecanoic acid</b>
<b>AAD</b>	<b>adipic acid dihydrazide</b>
<b>ACN</b>	<b>acetonitrile</b>
<b>AP</b>	<b>alkaline phosphatase</b>
<b>Au</b>	<b>gold</b>
<b>BaP</b>	<b>benzo[a]pyrene</b>
<b>BSA</b>	<b>bovine serum albumin</b>
<b>BSA-PHEN</b>	<b>bovine serum albumin-phenanthrene</b>
<b>CV</b>	<b>cyclic voltammetry</b>

<b>DEA</b>	<b>Diethanolamine</b>
<b>HCL</b>	<b>hydrochloric acid</b>
<b>DMSO</b>	<b>dimethyl sulfoxide</b>
<b>DNA</b>	<b>deoxyribonucleic acid</b>
<b>ECIA</b>	<b>electrochemical immunoassay</b>
<b>EDC</b>	<b>1-ethyl-3-(3-dimethylaminopropyl) carbodiimide</b>
<b>EDTA</b>	<b>ethylenediaminetetraacetic acid</b>
<b>EIS</b>	<b>electrochemical impedance spectroscopy</b>
<b>ELISA</b>	<b>enzyme-linked immunosorbent assay</b>
<b>EPA</b>	<b>environmental protection agency</b>
<b>FeCl<sub>3</sub></b>	<b>ferric chloride</b>
<b>GC/MS</b>	<b>gas chromatography/mass spectrometry</b>
<b>H<sub>2</sub>O</b>	<b>water</b>



# **Chapter 1**

## **General Introduction**





# 1. General Introduction

## **Motivation**

Since their first appearance in 1962, biosensors have undergone gradual development, improvement and innovation. This advancement is attributed to their outstanding features and growth potential. Biosensors are a low cost option compared to other methods currently in use, such as the early immunoassays (ELISA). Integration of biosensors with lab-on-a chip platforms and their ability to perform environmental monitoring and testing demonstrates the significant opportunities that they offer when successfully integrated and properly implemented. There are many requirements for biosensors, in order to be cost- effective tools, they need to produce fast results and have a low-cost production. There are many challenges pertaining to environmental monitoring of pollutants, food analysis, and pharmaceutical development. However, despite these challenges, biosensors are already in use. The impact of biosensors on the quality of life can be important if the key limitations related to cost and some existing technical barriers are overcome. In addition, their commercial potential can be increased by reducing the cost of production [1].

## 1.1 Biosensors

According to the International Union of Pure and Applied Chemistry (IUPAC), a biosensor is defined as a self-contained and integrated receptor-transducer device, which provides selective quantitative or semi-quantitative analytical data using a bio-receptor and transducer to effect spatial contact. [2]. The Biosensor & Bioelectronics defines biosensors as analytical devices that incorporate biological material, such as tissue, antibodies, microorganisms, organelles, nucleic acids, cell receptors, and enzymes, and biologically derived materials or biomimic, which are linked with a physicochemical transducer. The transducer may be thermometric, magnetic, electrochemical, piezoelectric, optical or micromechanical [3]. Figure 1.1 below depicts the principal parts of a biosensor.

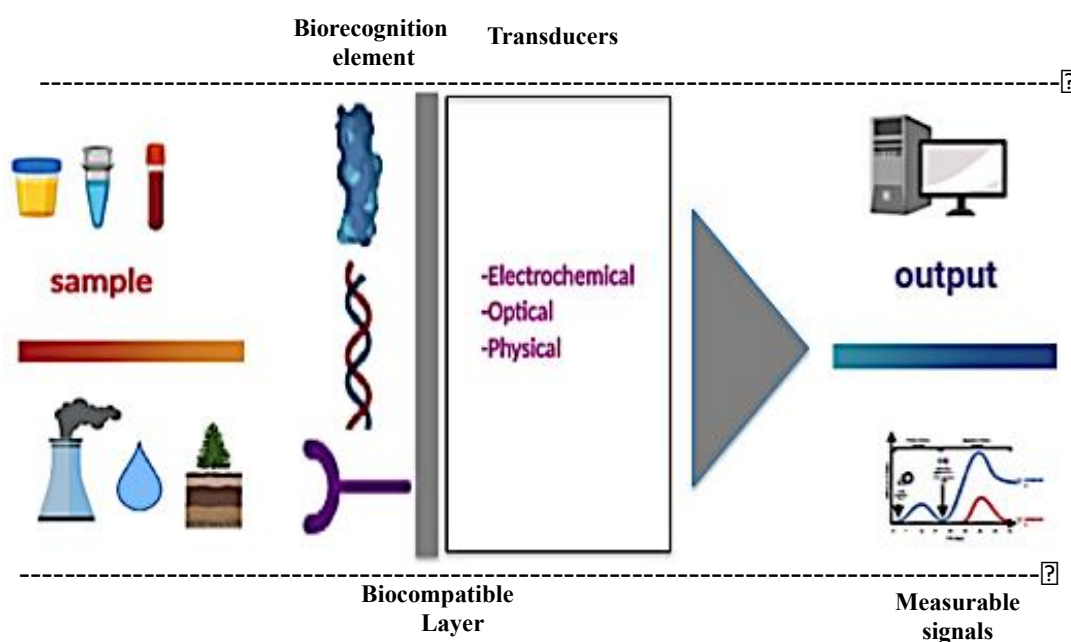


Figure 1.1: Schematic of different types of biosensor. The biocomponent is immobilised on a biocompatible layer, resulting in a change of physical or chemical properties of the elements that can be detected by a measuring tool.

### 1.1.1 Biosensing Components

The two main types of recognition element within biosensing devices are affinity and catalytic. The affinity type constitutes antibodies and nucleic acids. The catalytic part consists of cells, enzymes, and tissues [4].

#### 1.1.1.1 Antibodies

Antibodies can be used to develop immunosensors. They use the immobilisation of antibodies (Abs) as a biological recognition component to detect the specific antigen. Figure 1.2 below shows schematic representation of an antibody's Y-shape structure [5].

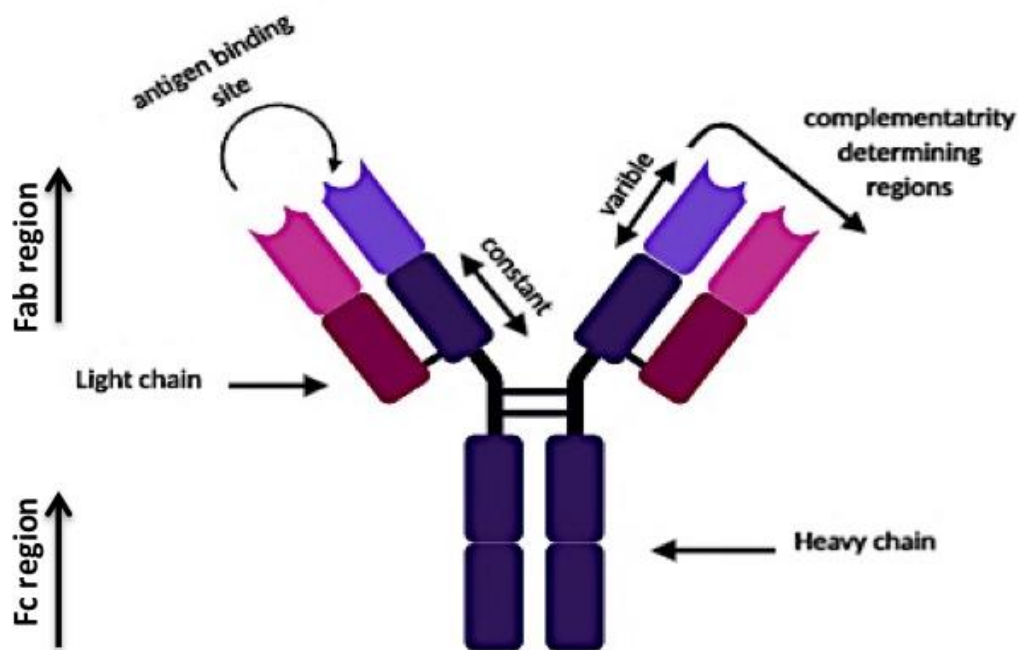


Figure 1.2: A general structure of an individual immune protein molecule

In addition, immunosensors are mainly used in rapid detection methods, with the exception of glucose biosensors [6]. They use labelled antibodies or antigens, coupled with other compounds, to complete the recognition step. Transducers, such

as an electrochemical impedance spectroscopy (EIS) and a surface plasmon resonance (SPR), can work in different modes. Therefore, they may be used under a label-free detection mode. This detection mode may be modified to competitive, non-competitive and displacement assay formats, thereby eliminating the need to use label or chemical compounds, which may affect the sensitivity of the sensors [7].

#### **1.1.1.2 Enzymes**

An enzyme is a protein that catalyses the chemical reaction in living system at significant rates. The ideal enzyme label has to be very high catalytic activity toward a specific substrate. Glucose oxidase [8] and urease [9] are some of the major enzymes utilised. In some instances, enzymes inside cells, such as bacterial cells can be used to detect atrazine [10].

#### **1.1.2 Bio-transducer Components**

A transducer is a tool that converts the biorecognition event into a detectable electronic signal [11]. Biosensors use different types of transducers, such as the electrochemical, optical acoustic and calorimetric transducers. Electrical transducers are commonly used, because they can be operated with little difficulty and contain rapid response immunosensors [12].

##### **1.1.2.1 Electrochemical Biosensors**

Electrochemical biosensors contain an electrochemical transducer and a transduction component. IUPAC defines an electrochemical biosensor a self-contained integrated element, which gives analytical data using a biochemical receptor, which spatially contacts with an electrochemical transduction component. These types of biosensors are commonly used to measure the current yielded during oxidation and reduction reactions. At present, they are numbers of transducers that have been used in electrochemical detection including voltammetric, amperometric,

potentiometric and impedimetric. These are all used in the measurement of pollution in water. Biosensor electrodes play a significant role in the performance of electrochemical cells. An electrochemical analyser measures targets since it can measure current in each electrochemical cell. An electrochemical cell has three types of electrodes; the reference electrode (RE); the counter electrode (CE); and the working electrode (WE); the Table 1.1 below explains the three types.

Table 1.1: The three types of electrochemical cell.

<p><b>Working Electrode (WE)</b></p>	<p>WE (cathodic or anodic) is where the electrically driven chemical reaction and electron transport take place. They represent the location where the electrochemical reactions take place (oxidative &amp; reductive). WE selection also has two main aspects; the target analyte redox behaviour and the current in the background over the potential region, which is essential for measurement. Other WE selection features include; [electrochemical potential window, mechanical characteristics, accessibility, electrical response, cost and toxicity] [13.14].</p>
<p><b>Reference Electrode (RE)</b></p>	<p>RE produces a constant potential [15] such as Ag/AgCl. Low impedance and non-polarizable electrodes are suitable, because they prevent changing of the RE potential. In addition, high impedance not only heightens the susceptibility of the method to noise from power lines and it also decreases rise time.</p>

<p><b>Counter Electrode (CE)</b></p>	<p>In an electrochemical cell, CE ensures that current does not run through the reference electrode, since such a flow would change the reference electrodes potential. It is made of inert materials; hence it does not participate in electrochemical reactions [16]. It can be used together with WE to measure other variables. In this case, the WE acts as a cathode while the CE can be used as an anode.</p>
--	--

#### **1.1.2.1.1 Electrochemical Techniques**

##### **A. Amperometric Transducers**

This type of transducers measures currents resulting from an electrochemical reaction. They work upon the premise that current can only be produced in the process of bio-recognition of an electro-active species after the application of a steady potential on the working electrode. This potential can force the species to donate or accept electrons. The rate at which electron are transferred is represented by the current in order to complete the recognition process.

##### **B. Voltammetric Transducers**

Voltammetric transducers can be used to detect the current that is recorded as a function of the applied potential. Here the peak current is equivalent to a specific chemical and is directly related to the species concentration. Low noise, higher sensitivity, and detection of a variety of compounds with different peak potentials in one experiment are some of its benefits. Data concerning particular chemical reactions are acquired by plotting the current produced by the analyte at the potential applied to the working electrode [17].

- **Linear Sweep Voltammetry (LSV)**

Linear sweep voltammetry is a widely used electrochemical technique that utilises the change in potential as a linear function of time. In tandem with the Nernst equation, linear sweep voltammetry can determine unknown species and concentration of electrolytic solutions. Figure 1.3 shows a sample linear sweep voltammogram when the potential is applied versus time. The slope can be applied to calculate the scan rate of the voltage. The scan begins on the left at zero current. As the voltage increases, current also starts to flow reaching a peak before dropping as shown in Figure 1.3. Oxidation and reduction of species is reported as a peak and trough, respectively in the voltammogram

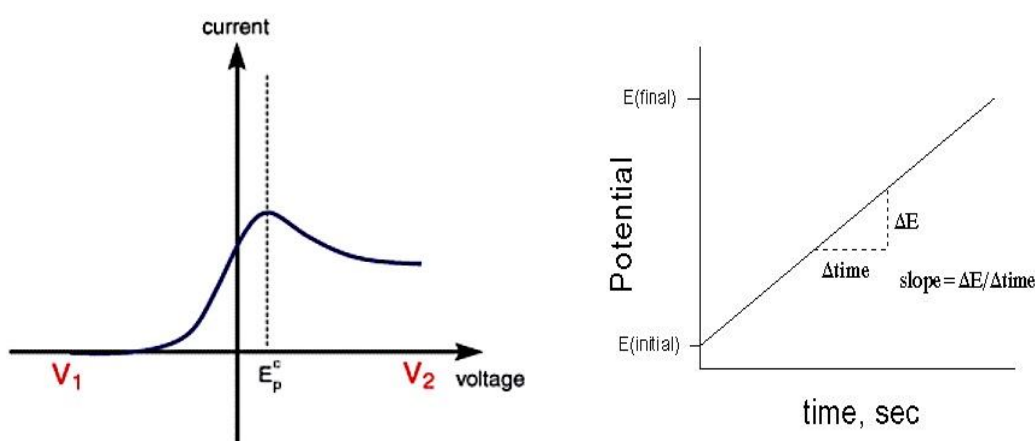


Figure 1.3: A typical Linear Sweep Voltammetry. The slope shows the scan rate of the experiment (volts per unit time).

- **Cyclic Voltammetry (CV)**

It is an effective electrochemical technique widely used to examine the reduction and oxidation processes and study the performance of electrodes. It is also used in the characterization of electron transfers involving biofilms or microbial cells. The redox reaction caused by the working electrode can be either of the individual steps depending on the system: the rate of mass transfer of the electroactive species, the

rate of absorption or desorption on the electrode surface, the rate of electron transfer between the electroactive species and the electrode, or the rate of individual chemical reactions. The electric potential and concentration of the species involved in the redox reaction can be described by the Nernst Equation in equation 1 (at 298 K):

$$E = E^0 + \frac{0.059}{n} \log_{10} \frac{[Ox]}{[Red]} \quad \text{Equation 1}$$

Where E is the applied potential,  $E^0$  the formal potential, n is the number of electrons gained in the reduction, [Ox] as the concentration of oxidized species and [Red] as the concentration of reduced species.

### **C. Conductometric Transducers**

Conductometric transducer monitors the ionic concentration of a species, which leads to a change in electrical conductivity. It contains two electrodes and an AC voltage, which is employed through the electrodes. An alteration in conductance between the electrodes occurs when the ionic composition changes. The technique does not require RE. They are, therefore, inexpensive and simple to miniaturise. The main disadvantage of conductometric transducer compared to amperometric and potentiometric transducers is their relatively lower sensitivity. [18].

### **D. Impedimetric Transducers**

This transducer recognises changes in impedance generated as a result of immobilising biomaterials on the electrodes causing a change in capacitance and the transfer of electrons between the electrodes. Electrochemical impedance spectroscopy (EIS), which is associated with this type of transducer, characterises the function and properties of biomaterial-functionalised electrodes [19].



## **E. Potentiometric Transducers**

In potentiometric transducer, a transmembrane potential is yielded by a biological detection reaction. Potentiometric biosensors are used to detect potential with regard to an identified electrode. A high impedance voltmeter is used to measure the potential. Based on the Nernst equation, this biosensor connects the electrode potential (E) of identified electrode depending on the concentration of oxidized or reduced species [20].

### **1.1.2.1.2 Microfluidic Electrochemical Cell**

This cell operates as an alternative to the conventional cell and contains metal microelectrodes. It greatly improves the handling of the sample and the cleaning of the electrodes. It also allows on site real-time monitoring, hence provide much better pollution control [21]. Three major materials are used as electrodes in this type of cell; gold film or graphite-epoxy as (WE); silver-epoxy composite as pseudo-(RE); and graphite-epoxy composite as (CE). The potential of the reference electrode is stable and well defined in aqueous systems. The potential of a pseudo reference electrode varies depending on the electrolyte. Pseudo-reference electrode is simple, and because this is immersed directly into the electrolyte used in the microelectrodes, the impedance effect is small. In pseudo-reference electrode there is no contamination of the test solution by electrolyte molecules or ions that a reference electrode might transfer. In contrast to conventional cell, the electrochemical response of microelectrodes may differ from that observed at conventional sized electrode in that nonlinear diffusion is the predominant mode of mass transport. The difference in mass transfer from the solution toward the electrode has many important implications that make microelectrodes very appealing in electroanalytical chemistry.

Moreover they possess a smaller time constant, and heightened signal-to-noise ratio. Cyclic voltammetry characterizes the performance of the microfluidic cell. The benefits of microfluidic cells include reduced solution consumption, less waste generation, online/in-line recognition; and minimal interference.

LOC is a platform that combines many laboratory functions on one chip. Advantages of LOC: low fluid volume consumption, faster analysis and response times. LOC is also compact and small leading resulting in low fabrication costs. Fluid flow within microfluidic channels is laminar since it is normally characterised by low Reynolds numbers. Reynolds number is a ratio between inertial force ( $\rho v_s$ ) and viscous force ( $\mu/L$ ). Laminar flow is particles of liquid that flow in a uniform way (straight lines). These liquid layers do not mix with neighboring layers due to its small size of the channel and opposite of turbulent flow (Figure 1.4).

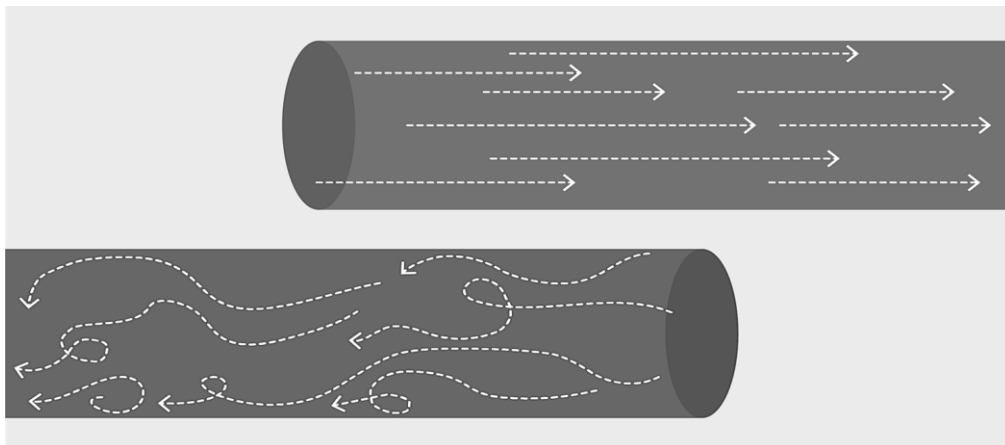


Figure 1.4: Laminar Flow: the flow of a fluid when each particle of the fluid follows a smooth path, top, versus turbulent flow, irregular flow that is characterised by tiny whirlpool regions, bottom.

Table 1.2: Electroanalytical characteristics of biosensors

<b>Electroanalytical Features</b>	<b>Description</b>
<b>Linear Range</b>	They have a range of analyte concentration in which the reaction of the sensor occurs linearly.
<b>Detection limit</b>	This is the lowest amount of a substance that the sensor signal can distinguish in the absence of a control sample.
<b>Sensitivity</b>	Their sensitivity enables them to respond to the required magnitude of the input signal that is required to produce an output with a specific signal-to-noise ratio.
<b>Selectivity</b>	The ratio of the signal output combined with the analyte alone compared with that of the interfering substance alone while keeping the analyte concentration constant.
<b>Reproducibility</b>	Their reproducibility determines the extent to which a sequence of observations shifts over time.
<b>Stability</b>	The biosensors' stability depends on sensor geometry and process of preparation.
<b>Response time</b>	Their response time is divided into two: steady state response time, which indicates the time required to reach 95% of the biosensors' response; and transient, which is the period required for the first output signal to reach its optimum after the addition of an analyte.

### 1.1.2.2 Optical Biosensors

Optical biosensor is based on the change of the optical properties of biological elements. Absorbance measurement is the simplest optical detection in biosensors, in which changes in analytes concentration that adsorb a certain wavelength of light can be determined.

### **1.1.2.3 Other Biosensors**

Other biosensors, such as the acoustic, thermometric, piezoelectric calorimetric, and magnetic biosensors work using distinct characteristics. Acoustic-based biosensors work based on surface or bulk-acoustic waves. Calorimetric transducers operate using changes in temperatures that result from the biochemical response at the sensing area. Biomimetic design has shown a promising future in the arena of nanomaterial technology. The biomimetic design combines three different technologies like genetic engineering, bioinformatics and biotechnology. These pose a large number of challenges to the field of biosensors. Different molecules have been designed specifically with special structural features by biomimetic processes that mimic similar behavior of enzymes and proteins. Biosensor technology has advanced at a fast pace, with the synthesis of artificial molecules like biomimetic molecules, molecular imprinting polymers, aptamers and peptide nucleic acids. These artificial molecules are helping to address a number of issues, including the use of animals in the production of element and arduous labeling of elements with smart tags. The merging of biosensors with different technologies, such as information and communication technologies, three dimensional printing, solar cells and organic light emitting diodes [OLED] will represent significant progress in the role of biosensors in specific and selective environmental analysis. Biosensor technology still has to address a range of challenges in regard to the spatial and temporal distribution of the hazardous chemicals. Environmental issues can be handled proficiently with the aid of these interdisciplinary technologies, as nano sized micro detectors, which have rapid and multi detection sensors, are likely to be designed in the near future.

## **1.2 Molecular Recognition**

The success of biosensing is dependent upon molecular recognition. Molecular recognition refers to the ability of a molecule to detect another through bonding interactions and molecular geometry. Several forces and bonding processes are involved in molecular recognition and include hydrogen bonding, hydrophobic forces, and metal coordination. These and other forces are described below. In molecular recognition, the interaction between the host and the guest results in a detectable change. Molecular recognition is the basis of many processes in biology such as enzyme catalysis, receptor substrate binding, and the assembly of multiprotein complexes.

### **1.2.1 Binding forces and Interaction involved in molecular recognition**

#### **1.2.1.1 Electrostatic and Hydrophobic Interaction**

Electrostatic interaction occurs between charged molecules and surfaces with opposite charges and is exploited in molecular recognition. Hydrophobic interactions have a lipophilic property, which makes them a good substitute for the bio recognition of molecules.

#### **1.2.1.2 Covalent Bonding**

Covalent bonds giving high reversibility are usually incorporated into host molecules. The formation of a reversible covalent bond between two molecules follows a molecular recognition event. The strongest chemical bonds are formed by those covalent bonds having the highest energy forms.

#### **1.2.1.3 Hydrogen Bonding**

Hydrogen bonds provide directionality and specificity of interaction, which are important for molecular recognition. Hydrogen bonds occur between a protein and its ligands (protein, nucleic acid or substrate). Although H-bonds have less energy

(1 kcal/mol) than covalent bonds (100 kcal/mol), their multiplicity confers rigidity to protein/DNA structure, geometry, and specificity to intermolecular interactions.

#### **1.2.1.4 Specific Interaction**

Deterioration in functionality as a result of improved orientation and stability can be prevented by specific interaction-mediated immobilisation of molecules using DNA hybridisation or antibody-protein A/G interaction. As protein A/G combines the domains of protein A and G, it has the additive property of forming both proteins, which are useful for biosensing applications. Protein A/G can be used as an immunological tool given that pathogenic bacteria such as *Streptococcus* and *Staphylococcus* have protein A and G on their surfaces, which bind IgG. Protein A binds to the Fc portion of IgG with affinity, which depends on the subclass of IgG and the species. The specificity of protein G for IgGs is broader than that of A, depending on the source and can bind to both the Fab and the Fc portions of the antibody molecule with affinities varying based on the species [22].

### **1.2.2 Types of Molecular Recognition**

#### **1.2.2.1 Static molecular recognition**

This type of recognition resembles the interaction between lock and key. It exhibits a complex reaction in which the host and the guest molecule react in a ratio of 1:1 to form a host-guest molecule. To obtain advanced static molecular recognition, it is important to make recognition sites that are specific for guest molecules [23].

#### **1.2.2.2 Dynamic molecular recognition**

In dynamic molecular detection, the binding of the first guest to the first host-binding site affects the subsequent binding of the second guest to the second binding site. In addition, in a positive allosteric system, the attachment of the first

guest increases the association constant of the second guest, while in a negative system the association constant is reduced. The dynamic nature of binding provides the method for controlling binding in biological systems [23].

### **1.3 Antibody-Antigen Interactions**

Affinity refers to the strength of binding between an antigenic site and an antibody-binding site. Affinity is the equilibrium constant that describes the antigen-antibody interactions. It is the sum of the attractive and repulsive forces operating between an antigenic site and an antibody-binding site. The reactions are noncovalent and irreversible since antibodies do not irreversibly alter the antigen that binds them. The interaction process involves hydrophobic, electrostatic, and van der Waals forces and hydrogen bonds. Van der Waals forces are the weak electric forces that contribute to intermolecular bonding between neutral molecules. The contribution of each interaction varies with the type of antigen or antibody involved. Immunoglobulin-antigen interactions typically occur between the paratope on the antibody at which the antigen binds and the epitope. When the epitope and the paratope bind, they become attracted as a result of long-range electrostatic forces, which overwhelm the hydration energies. After the expulsion of the water molecules, the molecules attract each other creating a distance that makes it possible for short-range forces, such as the van der Waals, to draw two complementary surfaces together. The strength of the binding depends on how the two interacting surfaces fit. If there are high salt concentrations, resulting extreme pH can disrupt the interaction between an antibody and its antigen.

The process of measuring the binding strength between an antibody and an epitope is known as affinity. This interaction can be described by introducing the affinity constant  $K_a$  for the reaction



Therefore, the amount of antigen-antibody complex formed at equilibrium can be expressed by the following formula.

$$K_a = [Ab - Ag] / [Ab][Ag] \quad \text{Equation [2]}$$

Where-:

- I.  $K_a$  is the affinity constant
- II.  $[Ab-Ag]$  is the molar concentration of the antibody-antigen complex
- III.  $[Ab]$  is the molar concentration of unoccupied antibodies and
- IV.  $[Ag]$  is the molar concentration of the free antigen.

Association and dissociation rate constants are defined as follows:

$$V_{ass} = k_{ass} [Antibody][Antigen] \quad V_{diss} = k_{diss} [Complex] \quad \text{Equation [3]}$$

where  $V_{ass}$  and  $V_{diss}$  represent the rates of association and dissociation, respectively, and  $k_{ass}$  and  $k_{diss}$  represent the rate constants of association and dissociation, respectively.

At equilibrium  $V_{ass}$  is equal to  $V_{diss}$  and from eqns [1] and [3], the following equation is obtained:

$$K_a = k_{ass}/k_{diss} \quad \text{Equation [4]}$$

Antibodies with high-affinity bind larger quantities of antigen with higher stability in a shorter compared to those with low affinity. The existence of additional binding sites on antibodies and antigens affects the stability of antigen-antibody complexes. The binding intensity between multivalent antibodies or multivalent antigens is termed as avidity. Avidity is influenced by factors that include the affinity of the antibody for the epitope, the number of antibody or antigen binding sites, and the resulting structure of the antibody-antigen complexes. [24-33].



The section below provides to offer a comprehensive and fundamental introduction to immunoassays and sets a context for subsequent chapters specific key elements of immunoassays. Immunoassay formats that range from non-competitive to competitive are available. These formats and their signaling systems, such as the colorimetric approach are examined. Lastly, the electrical signal transduction technique, which is used in the subsequent generation of immunoassays, is described.

#### **1.4 Immunoassays:**

Immunoassays are biochemical tests that use highly sensitive immunoglobulin (Ig) (antibodies) as binders to detect the existence of molecules present at low concentrations. Therefore, antibodies play an integral role in the immune system and are nature's major detection tool. They are located on the surface of B-cells (B-lymphocytes) and have the ability to detect the presence of any foreign antigens. The B-cells can recognise and signal the existence of a wide range of antigens that consists of molecules, such as prions, toxins, viruses, drugs, and aberrant biomolecules that attack our bodies. Immunoglobulin proteins exist in various formats. The five isotypes of antibodies are IgG, IgA, IgD, IgE, and IgM. Due to their high natural affinities and excellent half-lives, antibodies are the priority of targeted therapeutics and diagnostics. The half-life is the amount of time needed for an antibody to reduce to one-half its initial level value. The term is commonly used to describe how long stable antibody survives. Antibodies can be easily manipulated using standard molecular biological methods into customised antibodies that are structured to perform effectively in their chosen application. Investment in antibody-based diagnostics and therapeutics in the biopharmaceutical

industry has been heavy. Therapeutics is the largest and fastest growing class of biopharmaceuticals [34, 35].

**Antibodies occur in three forms:**

- (i) Polyclonal antibodies- which are produced by mixing different B-cell clones.
- (ii) Monoclonal antibodies - which is secreted from a single clone of B-cells.
- (iii) Recombinant antibodies - which results from genetic manipulation of antibody genes [36, 37].

This piece of research focused on the environmental application of immunoassays, and, in particular, on the quantification of polycyclic aromatic hydrocarbons (PAHs) in polluted water. Years of studies have greatly advanced the development of immunoassays that are now used to detect PAHs in soil and water samples. Some available immunoassays can be used to determine PAH concentration. Examples of this include chemiluminescence immunoassays (CLIA); fluoroimmunoassays (FIA); radioimmunoassays (RIA); and enzyme-linked immunosorbent assays (ELISA). These examples differ from each other in relation to their form of detection, be it UV, fluorimetric, amperometric or potentiometric [38].

- **Commercial immunoassays**

There is a relatively large number of commercially available immunoassay PAH detection Kits used in PAH. For example, BTEX RaPID Assay® is a rapid-field or laboratory enzyme immunoassay (from JJS technical services) that is able to analyse small aliphatic PAHs and carcinogenic PAHs (> 4 aromatic rings) [39]. Commercial immunoassays can sample-specific (e.g., designed for use with soil or water). Ensys PAH is a soil test kit that can be purchased from Strategic Diagnostic

Inc. The kit is used both as a qualitative and semi-quantitative assay, as it gives only an approximate value of the PAH concentrations present in soil [40]. Rapid Assay® PAH test kit (from Tigret Inc.) is used for qualitative, semi-quantitative, and quantitative analysis of PAHs in water (well water, surface water, and groundwater) [41]. Envirogard® (by JSS Modern Water) also detects PAH in water, and it includes the 16 PAH compounds listed under the Environmental Protection Agency (EPA) regulations. These kits are both rapid and reliable [42].

#### 1.4.1 Types of Immunoassays:

Table 1.3: Types of Immunoassays: Immunoassays can be divided into two kinds: homogenous and heterogeneous.

Types of Immunoassays	Schematic for Immunoassay Types	Description
<b>Homogeneous</b>	<p>The diagram illustrates two scenarios for a homogeneous immunoassay. In the first, a test antigen (X) competes with an enzyme-labeled antigen (X-E) for a limited amount of antibody. The enzyme-labeled antigen reacts with a substrate to produce a product. In the second scenario, the enzyme is inactivated when it forms a complex with the antigen, resulting in no reaction (N.R.).</p>	<b>Homogeneous</b> assays do not require the separation of the bound reagents from unbound material. Fluorescence polarisation immunoassays (FPIA) are examples of homogenous immunoassays.
<b>Heterogeneous</b>	<p>The diagram shows a 7-step process for a heterogeneous immunoassay: 1. Incubate to attach antibody to plastic surface (microplate well). 2. Wash and block unoccupied sites on surface. 3. Incubate with test solution to attach antigen. 4. Wash. 5. Incubate with enzyme-linked antibody. 6. Wash. 7. Incubate with substrate to form chromophoric product.</p>	<b>Heterogeneous</b> assays, on the other hand, segregate the free analyte from the reagent-bound analyte. An enzyme-linked immunosorbent assay (ELISA) is a heterogeneous immunoassay.

### **1.4.2 Enzyme-Linked Immunosorbent Assay (ELISA)**

Enzyme-linked immunosorbent assay (ELISA) is a strategy used to distinguish the presence of an analyte in a sample. It is regularly the 'gold standard' upon which different immunoassays are based. It is a quick, delicate, specific and reproducible strategy dependent on the ability of immunoglobulin to distinguish a particular antigen. ELISA can be utilized in numerous formats, with various read-outs. The chosen assay relies upon the recognition requirements, concentration of the analyte, the structure and size of the analyte and on whether the analyte is soluble or membrane-bound. ELISA is commonly used because of its high-throughput capacities, (it can measure numerous samples in a moderately brief timeframe). Immunoassay can be divided into 'immunometric' and 'competitive' assays (Fig. 1.4). Immunometric are also referred to as sandwich assays. They require the use of two specific antibodies. The first immobilised antibody captures the target by attaching to one of its antigenic sites.

The second detection antibody then attaches and produces a signal that is directly proportional to the concentration of the target in the sample. In the competitive assay, a free antigen and a labelled antigen compete in order to attach to the immobilised antibody. The higher the target level in the assay, the lower the amount of labelled antigen present for binding. Thus, the signal produced is inversely proportional to the concentration of the free target, as illustrated by the curve in Figure 1.5. A number of formats are commonly used such as capture and displacement assays described in Figure 1.5.

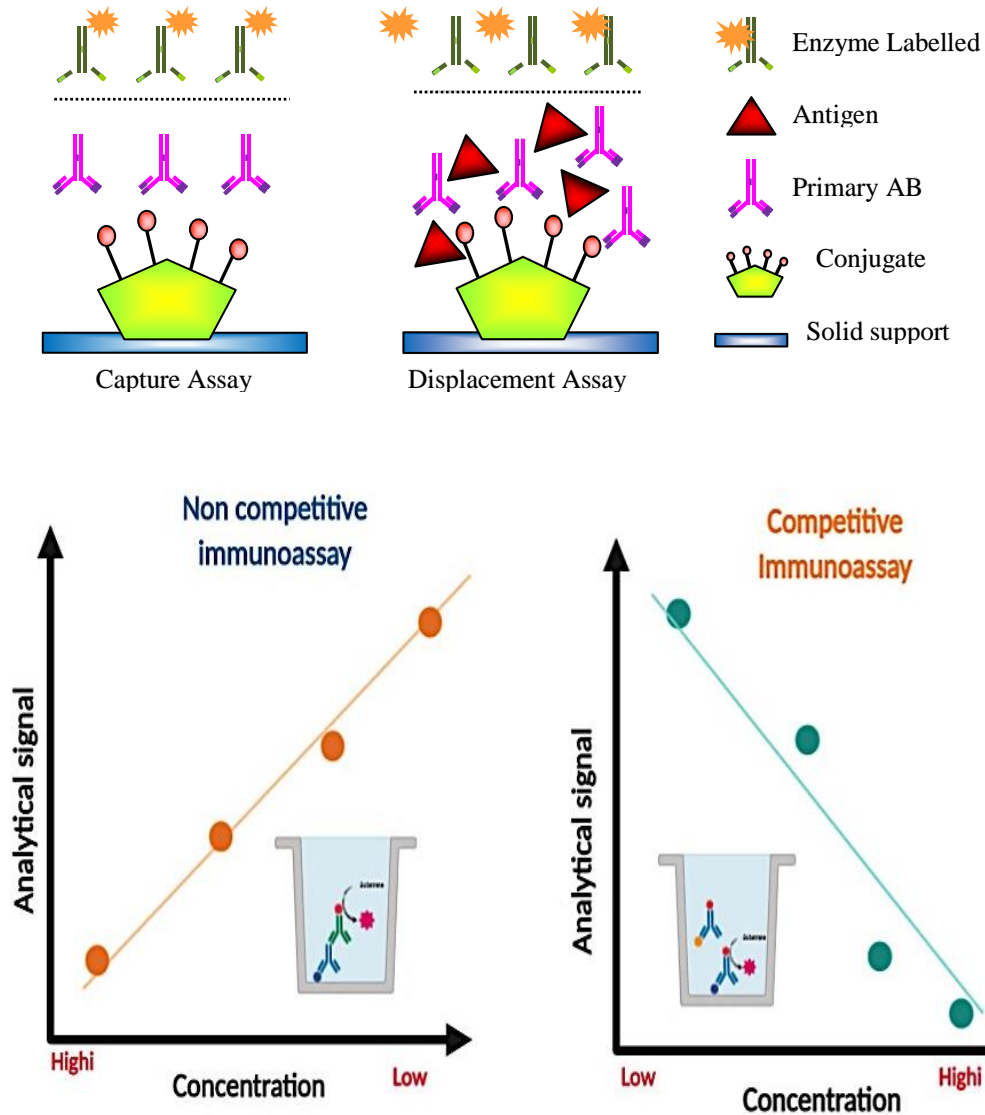


Figure 1.5: A typical response plot for each assay is illustrated and ELISA assays: capture and displacement assays.

Immunometric assays are commonly used to detect molecules, such as viruses and proteins since they can facilitate the binding of more than one antibody. Competitive immunoassays must recognize small molecules (toxins). They use an analyte-specific recognition antibody and a ‘tracer’ molecule, a labelled version of the target analyte. The tracer is frequently labelled with a fluorophore or an enzyme that can produce a measurable signal [43-46].

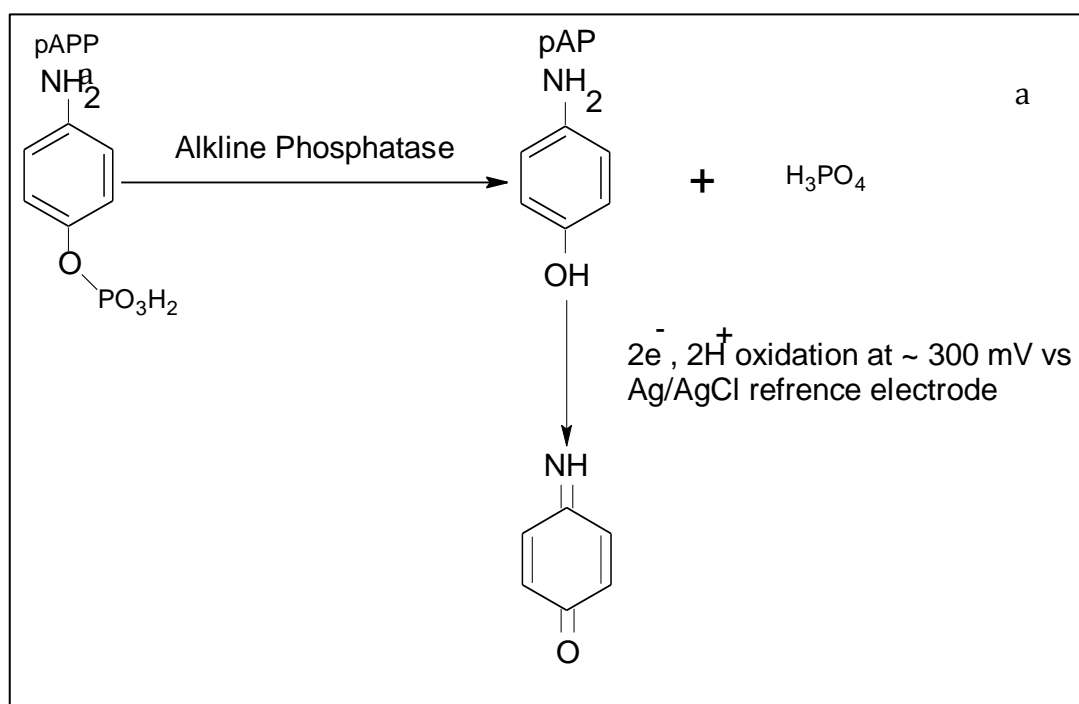
### **1.4.3 Signal Generation in Immunoassays:**

Identification methodologies can be characterized as ‘labelled’ and ‘label-free’ signaling methods. Labeled immunoassays utilize an antibody connected to a compound, fluorescent label, radiolabel, colorimetric or nanoparticle. In the case of labelled immunoassays, one of the reagents of immunoassay test is coupled with a label or something similar. It can be a fluorescent particle, a quantum dot, a dynamic redox atom or enzyme. Labelled immunoassays, allow for identification of an analyte with a high sensitivity and low limits of detection [47]. Electrochemical strategies can be used in various configurations. Over the last number of years work has been carried out which has resulted in flow cell innovation being combined with electrochemical detection to make a range of labelled immunoassays. Some of the previous works are outlined here [47]. The combination of electrochemical recognition with advanced ELISA innovation has permitted the improvement of high throughput techniques, which allow the completion of numerous assays in short periods. The first historically speaking immune response detection methods applied the utilisation of radiolabels [48]. Rosalyn Yalow and Solomon Aaron Berson announced the primary use of radiolabels in an immunoassay to identify insulin during the 1950s [48, 49].

Hazardous working situations, problems with waste elimination and potential medical problems related to dealing with radioactivity resulted in a rapid advancement in alternative detection methods. Current methods are more secure since they do not present health risks to the operator and waste produced can be discarded relatively easily.

Nowadays, radiolabels have been generously replaced with recognition techniques that provide high sensitivities, while utilising much safer methodologies. Colourimetry is a system that is utilized to measure coloured substances in a sample.

Upon enzymatic activity, chromogenic substrates produce coloured compounds. The catalyst, soluble phosphatase (AP), is an alternative indicator, which generates the enzymatic label (Figure 1.6). It has an estimated molecular weight of 86 kDa. Because of its large size, antibodies with AP must be produced carefully, to guarantee that the conjugation level does not hamper access for target binding. AP is more costly than peroxidase. A drawback associated with having AP is that it is active in alkaline conditions and inactive in inorganic buffers or in chelating agents. However, acidic conditions ( $\text{pH} < 4.5$ ) attributes may be beneficially utilized as reaction stopping agents. The AP substrates are non-toxic and moderately steady. For instance, p-nitrophenyl phosphate (pNPP) remains constant for a considerable period at  $4^\circ\text{C}$  [50-51].



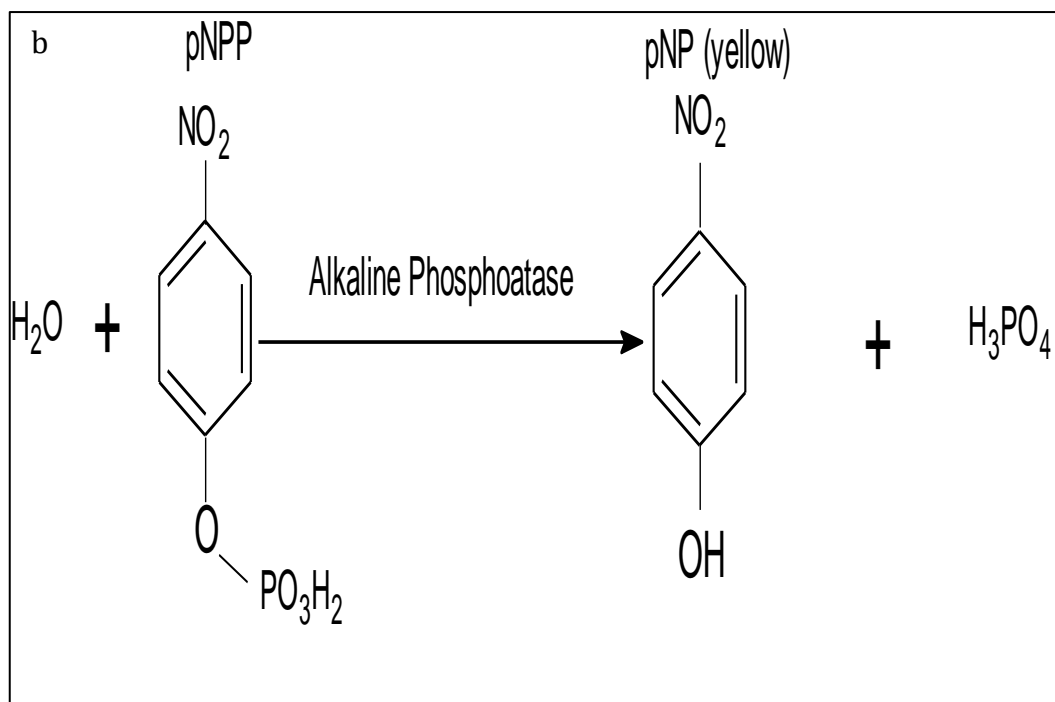


Figure 1.6: (a) Upon the reaction of the *p*APP with AP, 2 electrons were generated with *p*-aminophenol. (b) Hydrolysis Enzymatic reaction of *p*NPP to chromogenic *p*-nitrophenol catalyzed with alkaline phosphatase AP

#### 1.4.4 Electrochemical immunoassay applications

Transduction techniques simplify detection mechanisms, reduce assay times, and decrease the number of assay steps and assist in facilitating the multiplexing of immunoassays. Electrochemical transducers are a fundamental part of immunoassay motioning, so, electrochemistry identifies with the production of an electric current amid a chemical response. The most widely recognized kind of electrochemical reaction utilised in biotechnology is the oxidation response or redox reaction, during which electrons are exchanged between two connecting species. Electrochemical systems are frequently utilised for use in coloured and thick media [53, 54]. Electrochemical immunoassay transducers can accomplish high sensitivities. Electrochemical immunosensors, for the most part, have low power prerequisites and are equipped for being combined into mechanised



recognition platforms [54]. The application of electrochemical biosensors was first recorded in the 1960s. These early biosensors used enzymes, such as in the initial paper by Leyland Clark, where glucose oxidase was utilized as a catalyst to facilitate the reaction between glucose and oxygen. Its consumption could be measured by oxygen electrodes [55]. The management of diabetes is usually done by electrochemical biosensors, which can measure the level of blood glucose [56]. Electrochemical biosensors are generally quick to detect analytes and are uncomplicated. They can also be easily carried and are less sensitive to interferences than optical ELISA. These advantages make them more favourable than other immunoassays. In addition, the commercialisation of economical screen-printed methods and the production of desirable ink formulations necessitate the mass production of electrochemical sensors, which potentially reduces production costs.

Early enzymatic biosensors was based on the production or consumption of electroactive substrates, such as hydrogen peroxide or oxygen, while the second-generation biosensors was based on electroactive substances, such as ferrocene compounds [56, 57]. Third generation biosensors involved directing an enzyme to a substrate [56,58]. However, all of these stages need electrochemical oxidation or reduction reaction to occur. One major issue arises as a result of the interactions of antibody-antigen interactions, which are based on hydrogen bonding and other non-covalent interactions meaning that the detection of reactions using electrochemical biosensors is challenging since there is no generation of electrochemically active species.

However, labelling of different elements of the immunoassay or using ‘label-free’ electrochemical techniques such as AC impedance can effectively address this challenge. An antibody component is bound onto a surface. When put in a solution with its antigen, a recognition reaction takes place where the antigen is attached. Detection of this binding, however, requires a transduction reaction where this binding is transformed into a signal. An early illustration of an electrochemical immunosensor was published in 1991 [59]. The reader is referred to [60] for an account of research in this field up until 1997, while more recent information can be found in other reviews [61–63]. Electrochemical immunoassays and immunosensors are not costly compared to techniques such as surface plasmon resonance (SPR), rapid, and quantitative (unlike lateral-flow assays). Additionally, coloured or turbid solutions do not interfere with them. The base electrodes essential for these tests can be mass-produced using standard screen-printing technology.

Additionally, only small quantities of highly costly biological reagents are required, which minimises the cost of production. These benefits make electrochemical methods highly effective for high output mass- screening programmes. Screen-printing micro fabrication technology is an emerging field, where sensor devices have been fabricated on the screen-printed electrodes (SPE) [64]. The main advantages of these electrodes are that they are cheap, planar, miniature, disposable and thick film electrodes. These electrodes are mainly of pocket size and are easy for on site monitoring. [65] There are different configurations of SPE in the market that have wide applicability as per the requirement of the customer.

The configuration of the working and reference electrodes is called the first generation SPE while the configuration of the working electrode, reference electrode and auxiliary electrode is called the second generation SPE [66]. Recently there are also multiplex working electrodes like eight SPE and 96 SPE that have been used for detection of multiple biomarkers simultaneously. [67] Recent SPEs have been designed, which replace solid substrates with paper substrates for development of novel electroanalytical tools for the detection of a broad spectrum of biomolecules. [68]. In the medical field, there are SPE biosensors that take the form of technologies that can be worn or tattoos imprinted on skin for sensing medical conditions like heart rate, skin temperature, activity of brain, hemoglobin in blood and blood pressure. [69].

**1.4.5 Immunoassay Optimisation:** In order to measure biological compound with remarkable accuracy, sensitivity and specificity, the optimisation of various aspects of the assay must be ensured. It is essential at this phase to prepare enough immunoassay reagents that are destined to be adequate for the entire test. All analyte reagents and antibody agent (ideally very refined to decrease any form of test interference) should be fully characterised from the outset. Creating and purifying more analyte or antibody during a test will require re-optimisation of the concentration of reagents and conditions that could influence the reproducibility of the experiment. These reagents ought to be stored with the goal that recurrent use does not affect the respectability of the sample (for example store in vials at  $-20^{\circ}\text{C}$  ideally at  $-80^{\circ}\text{C}$ ). Ligand binding assays (LBA) are techniques that rely upon a specific method of attaching an analyte to an antibody. Commonly these are reversible binding occasions governed by the laws of mass action [70].

Law of mass action states that unbound reactants is in equilibrium with bound reactants. It shows that the rate of forward reaction equals the rate of backward reaction. In LBA format the specific binding of an antigen to an antibody involves reversible non-covalent interactions governed by the laws of mass action. The laws of mass action relates to the assay's sensitivity in that the sensitivity of the assay is proportional to value of  $K_a$  (the amount of the antigen-antibody complexes). Reasonable test optimisation ought to be embraced to guarantee that the assay is carrying out to its maximum capabilities. For instance, minimum dilution, coating, detection, washing concentration solutions and incubation period ought to be assessed experimentally.

**1.4.6 Immunoassay Buffers:** The antibody/antigen reaction is made to work effectively under physiological situations. Therefore, physiological pH and ionic strength should be utilized. Widely used buffers in immunoassays are described in (Table 1.4).

Table 1.4 Buffers used for immunoassay formats.

Application	Buffer	pH
<b>Coating</b>	50 mM carbonate/bicarbonate: 0.05g NaCl, and 2.1g sodium hydrogen carbonate, bring to 500 ml with deionised H <sub>2</sub> O.	9.5
<b>Washing</b>	3.0285 g Tris in 500 mL diH <sub>2</sub> O Discard 250 µl of the mixed solution and add a 250 µl Tween 20.	7.4
<b>Blocking</b>	3.0285 g Tris in 500 mL diH <sub>2</sub> O.	7.4
<b>Substrate</b>	4.793 ml of diethanolamine reagent (DEA) into 500 mL	9.5

#### **1.4.7 Immunoassay Validation:**

In its most conventional structure, an immunoassay is a bioanalytical technique involving the specific binding of an immune protein agent (antibody) with its analyte. Detection is accomplished by the addition of a reporter label that generates a reaction to the analyte [71]. The goal of assay validation is to have the capacity to characterize an assay as far as statistically measurable parameters are concerned with estimated certainty.

The designation of validated analysis is possibly merited when it has been described as far as its ability to classify tests regarding the presence or absence of a specific target [72]. Analytical strategy validation combines all the procedures that show that a particular technique used for the quantitative test of analytes in an obtained sample, e.g., blood, plasma, serum, urine, sweat or milk, is dependable and reproducible for the expected use [73]. The basic parameters for validation are include yet are not constrained by (1) accuracy, (2) precision, (3) selectivity, (4) reproducibility, and (5) stability. Validation procedures include documenting using specific research investigations; and ensuring that the experimental characteristics of the technique are appropriate and reliable for the intended, analytical purposes. The acceptability of analytical information corresponds straightforwardly to the criteria used to validate the method.

Limit of blank (LOB), limit of detection (LOD), and limit of quantitation (LOQ) terms are used to determine the smallest concentration of an analyte that can be reliably detected by an analytical method. International Conference on Harmonization [ICH] Q2 suggests these methods for measuring limits.

These methods of limit determination uses the mean and standard deviation of blank samples to set the limits (see Equation 1 and Figure 1.7):

$$\text{LOB} = \text{Mean blank} + 1.645 * \text{Stdev blank (one sided 95\%)}$$

$$\text{LOD} = \text{Mean blank} + 3.3 * \text{Stdev blank (one sided 95\% * 2)}$$

$$\text{LOQ} = \text{Mean blank} + 10 * \text{Stdev blank (one sided 95\% * 6)}$$

[Eq. 1].

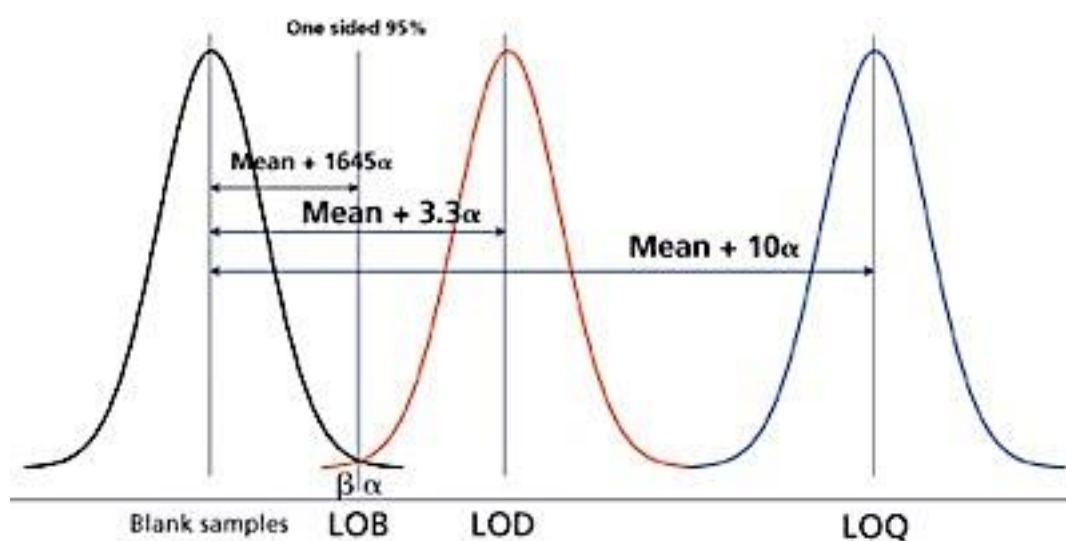


Figure 1.7: Limit of blank (LOB), limit of detection (LOD), and limit of quantitation (LOQ) based on the blank.

- **Define Calibration Model:**

The choice and arrangements of standard plots are central in the design, validation and utilisation of all quantitative assay strategies. Calibrations curves arranged from heterogeneous, contaminant, and/or poorly characterised analytes are more likely to generate uncertainty and greater variability [74]. The calibration plot model picked should be the model that yields the best fit to our data. A substandard curve fitting will produce test percentage error and enlarge the amount of substance at which the limit of quantification (LOQ) can be characterized. LBA detects the signal of a

progression of interactions that follow the law of mass action, bringing about a nonlinear and frequently sigmoidal calibration curve. Four-parameter logistic regression is regularly utilised to fit the LBA calibration curve [75]. It is advised the calibration model be set up at least three times with no less than eight different concentrations in duplicate. The utilisation of the correlation coefficient is not suggested for affirmation of the regression model [76]. For a model to be useful, it is recommended that the mean %RE of calibrators within the intended validity range be commonly close to 10% [77]. Sometimes, if contrasts in bias and precision are insignificant, it might be desirable to choose a straightforward model rather than a precise but complex one. The least complicated model that sufficiently illustrates the concentration reaction should be utilized [78].

- **The limit of detection [LOD]:**

This is the most minimal concentration of target in an assay that can be recognized yet not quantified [79]. The limit of detection is frequently mistaken for the sensitivity of the test strategy. The sensitivity of an analytical approach is dependent upon the capacity of the technique to separate small contrasts in concentration or mass of the assay target. In experimental terms, sensitivity is represented by the incline of the calibration plot that is given by plotting the analytical response against the target concentration [79]. LOD is a fixed parameter used to describe an analytical confirmatory strategy. It may be characterised as the most minimal analyte concentration likely to be dependably recognised from the limit of the blank (LOB) and at which recognition is feasible. In this way, it is larger than LOB.

## **1.5 Immobilisation strategies for biomolecules onto solid surfaces**

Picking the most reasonable immobilisation technique is fundamental in the advancement of any test, as it must enable the ligand to hold its action and furthermore guarantee that the fitting binding sites are presented to the coupling antibody [80]. Immobilisation of an antibody to any surface can be accomplished through physical, covalent or affinity techniques. Physical adsorption interferes with ionic, hydrophobic and polar between inter-molecular reactions (reacting groups in different molecules) that can happen between an antibody and chosen surfaces [81]. Physical adsorption is a less costly and simple antibody binding strategy. It can, however, result in the random orientation of the antibody onto the solid phase, and may lead to the diminished presentation of critical sites. It should be noted that physically absorbed proteins can be removed effectively by washing with a detergent. Covalent immobilization can be done by connecting directly with reactive groups (for example  $\text{NH}_2$  – $\text{COOH}$  or – $\text{SH}$ ) or by chemically functionalising the proteins to empower linkage [80] Pierce Thermo Scientific offers a range of immobilization technique kits [82]. Before beginning the immobilization procedure for an antibody, the following factors ought to be studied or optimized:

- Choose either a direct or capture attachment methodology;
- Indicate the purity and concentration of the antibody;
- Search for the ideal solution pH for the immobilization response;
- Identify residues in the antibody agreeable for attachment, for example, cysteine;
- Control the perfect incubation time;
- Select the ideal ionic quality response solution;
- Find the most suitable coupling procedure based on the groups accessible and the requirement for a linker (or not)



- Amine
- Carboxyl
- Thiol
- Aldehyde
- Pegylation
- Maleimid

The immunoassay has developed extremely since its introduction in 1959 [83]. These have been driven by an increase quest for sensitive, specific and quick detection methods while reducing expenses and eliminating the need for highly experienced personnel. Developments in immunoassay efficiency have taken place in two areas the enhancement of the recognition antibody and improvement of the recognition platform.

### **1.5.1 Enhancement of the recognition antibody**

The main properties of antibodies, particularly their greater affinity and specificity for an analyte, make them favourable in numerous applications in biotechnology, diagnostic, and biomedical areas. The introduction of hybridoma technology in 1975 and the subsequent ability to create monoclonal antibodies (mAbs) have resulted in an increase in antibody study and advancement. Consequently, the area of monoclonal antibodies has grown into a thriving industry and has a substantial impact on rich sources of diagnostic, therapeutic, and research reagents. The universal increase in demand for immunoassay testing was around \$15.6 billion and \$16.3 billion in 2011 and 2012 respectively. This market was expected to surge to an estimated \$20.5 billion by 2017 [84] with the research in antibodies reaching nearly \$2 billion and \$2.2 billion in 2013 and 2014 respectively. The market is expected to reach approximately \$3 billion in 2019 [85].

The initial challenges resulting from immunogenicity of murine mAbs have been minimised or eliminated, by the advancement of mechanisms to generate chimeric, humanised and fully human antibodies [86]. The global demand for antibody drugs was estimated to be worth \$63.4 billion in 2013. This market is anticipated to expand to nearly \$122.6 billion globally in 2019, based on the BCC Research [87].

### **1.5.2 Improvement in platform and recognition performance**

New antibody molecules with higher affinity and specificity properties could profoundly affect the next generation of immunoassay research. However, recognition antibodies comprise of only one of the numerous elements that require further research to reduce the level of analytical detection. Advancements in antibodies, platforms, signal production and acquisition have all played a significant role in the recent generation immunoassay growth. The combination of nanosised materials into different assays is the primary focus of the whole field of biosensors research. Nanosized materials involve a broad range of organic or inorganic components where one dimension is at least  $< 100$  nm. Nano, a Greek prefix, refers to the smallest natural parts while the term nanotechnology describes the manipulation of the materials that show powerful electrical, mechanical, chemical or optical features [88]. These components have been evaluated and optimised to provide essential tunability, intensities and longevities that are larger than common labels or dyes [89]. Nanoparticles possess various chemical and physical characteristics that enable them to produce the outcomes that allow them to be used as probes in analysis [90]. A broad range of nanomaterials, such as enzyme- loaded carbon nanotubes, nanoparticles, and semiconductor nanoparticles, have been utilised to improve the signal produced by the antigen-antibody interaction [91].

Nanomaterials have been used extensively as immunosensors. A potentiometric immunosensor with nanoparticles has been magnetically functionalised with an antibody to human (IgG). The immunosensor was a carbon paste electrode that used for the detection of the analyte of interest. For the antibody coupling to the nanoparticles a covalent immobilisation method was used and the linear response range was from 0.1 to 1.2 ng mL<sup>-1</sup> [92]. Another study revealed the application of magnetite nanorods for carcino embryonic antigen within a range of 1.5-80 ng mL<sup>-1</sup> with a detection limit of 0.9 ng mL<sup>-1</sup> [93]. The nanoparticles of the complex CoFe<sub>2</sub>O<sub>4</sub> were used for the fabrication of immunosensors that were used for the detection of a-Ferroprotein. Analysis yielded similar result with the ELISA results from human serum samples. [94]

- **Magnetic beads:**

The synthesis of magnetic beads can be carried out by three general methods. In the first method the magnetic particles are synthesised inside polymer matrix. In the second method polymer is synthesized in the presence of magnetic particles. In the third method the beads are prepared from pre-formed polymer and magnetic particles. Electrochemical immunosensors use magnetic (MBs) beads for the separation and transport of antibodies [95]. Their high surface area, low toxicity, chemical and physical stabilities, and biocompatibility make them effective [96]. The process allows antibodies to react with the magnetic beads before adding onto the electrode surface using an external attraction. DropSens currently offers a custom made external attraction to be used alongside with their SPEs. This method does not involve the electrode in the immunological process since it can lead to passivation [97].

Magnetic particles (MPs) have been determined to be a stable solid phase in immunoassays and electrochemical Immunosensors [98,99]. In the case of Electrochemical Immunosensors (EI), the immunoassay reagents are generally added on the working area of the electrochemical cell (transducer). In magneto-electrochemical immunoassay (EMIs), MBs are utilised as a solid surface and the immunoreaction takes place in the outer electrochemical cell. The entire test, typically, takes place in a test vial. In every incubation and wash step, immunoassay reagents are blended in a shaker and collected on the wall of the glassy vial by utilising a commercially accessible attractive separator. After the immunoreactions, the MBs coupled with the immunoassay reagents are moved to an electrochemical setup and identification follows. MBs can be attractively collected onto the working area of the electrochemical cell [100], and the measurement is conducted. A correlation between the two strategies, EI and EMI, has been accounted for by Centi et al. [101].

Electrochemical identification was carried out on (SPEs). Although the two techniques were improved for electrochemical immunosensing, EMI made it possible to achieve quicker and progressively more sensitive immunochemical detection. Other announced methods for magneto-electrochemical immunosensing (EMI) have focused for instance on MBs as reasonable carriers of covalently attached enzymes for planar biosensors [102]. MBs are chemically and physically steady materials. They are biocompatible, and they can be effectively and immediately collected from vast volumes of tests by applying attractive powers.

The outside of MBs can be synthetically modified, which permits the connection of biomolecules, such as DNA, chemicals or antibodies. These favourable circumstances permit a large number of immunoassay designs [103-104]. Additionally, the use of modified MBs in immunoassays as a solid phase for immunoassay reagents can develop the efficiency of the immunological response because of the expanded surface (high stacking of immunoassay reagents permitted). Immunoreactions can benefit from quicker assay motion since MBs can be scattered effectively into the solution with just a delicate shake. The analyte does not have to migrate far in the MBs colloidal suspension. EMI can be scaled down, and the entire immunoassay can be automated. Possible sampling and magnetic separation methods for scaled down and automated EMI methods have been identified [105]. An integrated microfluidic approach based on magnetic beads as both attachment phase and molecule carriers have been created for quick and low-volume immunoassays utilising MB [106]. The absolute time required for the already developed approach based on magnetic beads was less than 20 min with the incubation times included, and the test volume used was under 50  $\mu$ l for 5 repetitive assays. The key components in the presented approach were a detector and a magnetic separator.

## **1.6 Lab-on-a-Chip Immunoassay Systems**

Lab-on-a-Chip shows a main technology to enhance sensor performances in terms of being able to decrease the use of reagents and the waste volumes, automation. Miniature and portable sensors help to overcome the difficulties associated with multi residue analysis and real time in field measurements. In addition, eco-designed portable devices have been constructed which have advantages, such as

relatively low cost and high automation during environmental analysis. This research focuses on lab on chip platform that is effective for analysis of PAH environmental pollutants. Immunoassays are the best quality level system for recognising a panel of biologically critical antigens. Besides, latest trends are characterised by the combination of biomedical designing and immunoassay improvements, leading to the generation of miniaturised microfluidic systems with the capacity to recognise relevant analytes in a quick, sensitive and dependable way. The current 'lab-on-a-chip' immunoassay is characterised by four key components (I) accessible surfaces, (ii) microfluidic platform design and manufacture, (iii) systems for the transporting and mixing of immunoassay compounds and (iv) the combination of antibodies as recognition components. A detailed explanation of 'lab-on-a-chip' immunoassay platforms to illustrate the huge potential for sensitive recognition and the nature of assessment for multiple elements exceeds the scope of this discussion.

With the evolution and enhancement of other immunoanalysis platforms particular emphasis has been placed on the advancement of miniaturised configurations where the test is completed using networks of enclosed channels whose configurations match in the micron scale. In such tests, immunoassay samples (e.g. buffer containing the target of interest) show laminar flow characteristics where fluidic streams flow parallel to each other, with mixing taking place by diffusion [107]. These fluidic platforms have numerous benefits over standard immunoassays. Firstly, the reduced dimensions of integrated techniques lead to a significant decrease in the number of reagents that are required for immunoanalysis.

This integration can be a significant consideration where costly chemical reagents are needed. Secondly, the increased surface-to-volume ratio exhibited by these miniaturized components facilitates quicker antibody/antigen interactions and consequently leads to quicker assessment. Thirdly, most lab-on-a-chip platforms can be transformed to incorporate automation systems, which can influence the development of the assay reproducibility.

**1.6.1 Substrates Used for Microfluidic Chip Design:** the fabricating and production of the fluidic system is determined by the selected substrates. These combine silicon, glass and polymers [108– 110]. When choosing a substance for utilization in a 'lab-on-a-chip' immunoassay, it is important to choose a substrate that enables the planned assay to be produced logically and cost-effectively, without any detrimental impact on any of the assay compounds by not exhibiting any toxicity-related properties should be chosen. In addition, the component chosen must be much perfectly with the identification methodology to be connected. For instance, in the case of an immunoassay where fluorescently labelled detection antibodies are to be integrated, it is fundamental that the material does not have any natural fluorescent properties that might interfere with the investigation. Also, the material ought to effortlessly permit fluidic channels to be integrated for the benefit of sample delivery and mixing (if pertinent), and should also be preferably fit towards the mass-transfer of analytical parts [111, 112].

**1.6.2 Microfluidic Channel Design and Fabrication:** A computer-aided design (CAD) approach is commonly chosen to structure the microstructures of a microfluidic platform. Several economically accessible platforms (for example AutoCAD, DraftSight, SolidWorks and Creo), which give a schematic description of the last microfluidic channel can be selected. When designing the structure, it is

necessary to consider the following: (I) the relative size of the analytical system, (ii) the number of paths required for use and (iii) the channel measurements, with attention being paid to length, width and stature. In most instances, no less than one valve (for test addition) and channel should be provided for each reagent. Channels should be short and conceivable to limit the transfer distance. However they must be of adequate length to prevent cross-contamination between various reagents caused by minor fluctuations in flow driving force [113]. Finally, when planning such models, it is necessary to integrate a waste-accumulation channel for encouraging the simple expulsion of waste reagents, e.g., unwanted antibody and wash buffers.

**1.6.3 Analyte Delivery, Mixing and Washing:** When conventional heterogeneous immunoassays are produced in microtitre plates with at least 96 test wells, they usually require approximately six successive steps to be specific to an analyte (I) preparation of the test samples (ii) introduction of bioreagents (for example antigens, antibodies) by means of pipetting, (iii) incubation time, (iv) wash solution (v) substrate production and (vi) recognition (for instance colourimetric). These procedures are comparative for microfluidic uses, and the implementation of innovative methodologies for analyte transfer and subsequent washing is to develop immunoassay sensitivity and performance [114, 115]. The pressure-driven flow can obtain the delivery of immunoreactants solutions through the microfluidic channels [116].

**1.6.4 Antibody Integration:** Microfluidic immunoassay configurations can be both heterogeneous and homogeneous. Homogeneous immunoassays include interactions among antibodies and antigens in a buffer, and for microfluidics-based immunoassays bound and unbound antibodies are normally discriminated by their



electrophoretic mobility properties in microchannels [114]. Interestingly, heterogeneous measurements routinely use antibodies, which are directly attached on the solid phase of the microdevice or on the other hand, are cross-linked to micrometre sized particles that are combined inside a system (Fig. 1.8). The viability of the antibody immobilisation method profoundly affects test performance, with a specific focus on sensitivity.

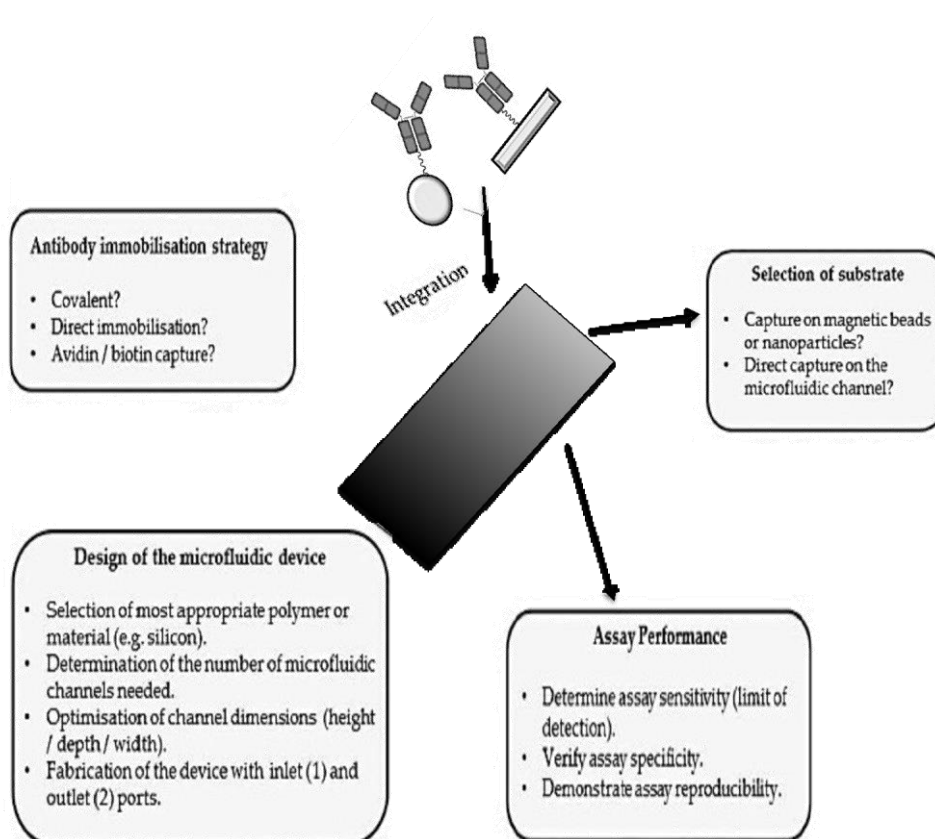


Figure. 1.8: Schematic representation of homogeneous (bead-based) and heterogeneous immunoassay formats available for 'lab-on-a-chip' applications.

## 1.7 Trends in instrumentation and technology

Analysis of water in the required environment by electroanalytical instrumentation has developed to a great extent. Factors including sensitivity, specificity, and minimum time for sample preparation, cost and portability have been greatly

improved in modern equipment. These modern devices, such as remote sensors, mini lab on a chip instruments and electrode technologies are utilized for the *in situ* analysis of pollutants in large water bodies, such as rivers. Hanrahan et al., [117] have outlined the major issues that have to be addressed for the development of *in situ* electrochemical devices. They reported that modification of certain factors, such as stability for long term use, changes in natural conditions, (such as oxygen or convection) specificity and reversible electrochemical processes have to be taken into account in order to improve the response of the sensors. These factors affect the calibration for *in situ* analysis, thereby reducing inaccuracies when taking measurements [118]. Different factors including pH, ionic strength and temperature changes are related to depth in sediments and water. The surface layers of fresh water and sea water, the interface of water and sediment, and estuaries may exhibit very strong gradients of ionic strength and pH. They may affect not only the metal speciation but also the rate of electron transport at the electrode which in turn will influence the signals obtained during analysis. Electroanalytical techniques are appropriate for integration in lab on a chip system, thanks to miniaturisation of detectors and electronics.

Polymer micro machining systems and micro electromechanical systems (MEMS) are used for construction of electro chemical sensing based portable analysing systems and lab chips for different environmental analysis [119]. These miniature devices are placed on the contaminated sites, which aid in the analysis of sample in a relatively quick timeframe. Namour et al [120] discussed various microsensors equipped with amperometric, conductometric and voltammetric technologies for the analysis of major pollutants targeted in the EU water framework directive. The

major drawback limiting sensors applications in ambient water is that the lack of ruggedness (the ability of an analytical system to remain unaffected by variations in method parameters) of receptor in different conditions of the environment. Screen printing technology is the most outstanding progress with respect to electrodes design and fabrication for environmental water monitoring. The base for multiple developments in environmental analysis for the screen printed electrodes is mainly bismuth, carbon and gold working areas. Application to water sample, mainly focused on trace element detection have obtained promising methods for in field sensing of toxic pollutants in water. Li et al [120] have reported on a wide variety of uses of screen printed electrodes have been used in different environmental analysis. Another promising method in this arena is the introduction of imprinted polymer molecules in working electrode designs which exhibited superior performance in the detection of pollutants in water [121].

There has been a constant demand of chemical information about water bodies, as consequence of intensive water research, stricter guidelines for environment protection and growing public concern. Monitoring points for the pollutants depend on the density and location. In situ and on-site monitoring, the concept of geosensor networks has been used for the miniaturisation and simplification of the devices. There is now demand for the development of wireless analytical devices which would reduce the analysis time for detection of water pollutants. The most significant factors are the management of data from a range of sources and the control of errors in analysis. Thus, the concept of screening and monitoring emerging tools (SMET) has emerged in order to address these issues.

Electrochemical sensors are the most common method used to overcome the limitations resulting from the aforementioned challenges, so they will play a significant role in the detection of ambient water bodies. The organic light emitting diode (OLED) has been become an emerging technology in different spheres of research, during the last decade, whereby diodes are the source of excitation. It has an organic semiconductor layer that is placed between two electrodes that emits light in the presence of an electric field. Digital displays and portable systems are also made using OLED. OLED devices are also designed as sensing equipment [122], which have been widely used for environmental analysis [123].

Tsopela et al. [124] reported the construction of a lab on chip designed integrated OLED which was acted as an electrochemical micro sensor for the analysis of the toxicity of water. Significant improvements in sensitivity can be achieved using microarrays and nanoarrays techniques. A comparative study between the microelectrodes and planar electrodes indicated that the diffusion profile of microelectrodes is hemispherical while that of planar electrodes are linear (Figure 1.9). The hemispherical diffusion pattern of the microelectrodes increases the sensitivity as well as responses that do not depend on the flow of the analyte. However the signals produced by the microelectrodes are smaller than that of the larger electrodes. Thus, an array of microelectrodes is required to generate a strong response.

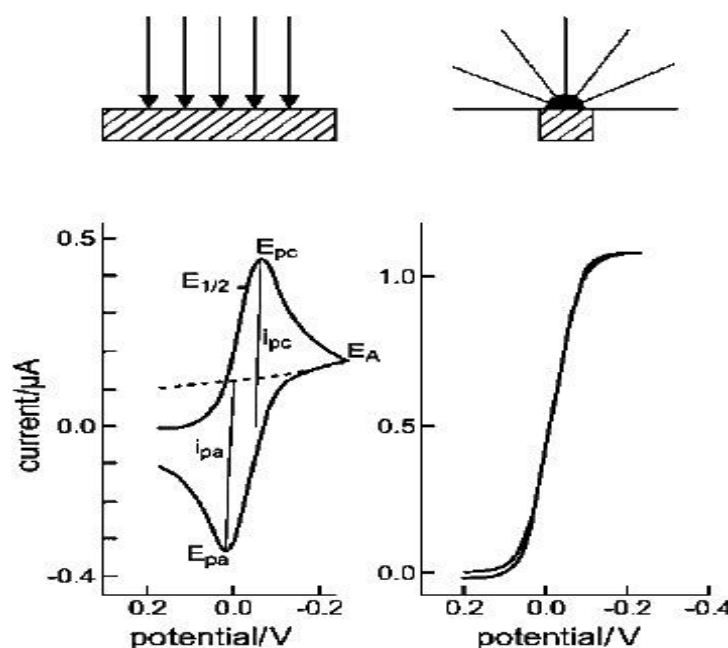


Figure 1.9: Diagram showing characteristic diffusion profiles of (a) a macroelectrode and (b) a microelectrode. The arrows indicate the direction of analyte diffusion to the surface of the electrode. In the case of the microelectrode the diffusion is a faster mass transport and therefore to a higher response.

Precaution should be taken when constructing an array of electrodes to ensure that they are properly spaced, to avoid the overlap of the diffusion profiles and to be sure that the qualities of the individual microelectrodes are displayed. Reports reveal various design of microarrays based on different techniques. Nanoarrays have also been reported using carbon nanotubes. A recent report discussed the design of immunosensors using a label free electrochemical immunosensors technique. The report described fabricated gold microelectrode arrays with a finger thickness of 5  $\mu m$  being designed by photolithographic methods. Thiols were absorbed on the microelectrode arrays to which cortisol specific monoclonal antibodies were attached covalently which could sense 1 pM – 100 nM cortisol [125].

Five by five arrays of gold microelectrodes were designed by photolithographic methods having a dimension of  $25 \times 25 \mu\text{m}$  which were deposited with diisocyanate cross-linked antibodies. The recognition of aflatoxin M1 in milk was reported by a HRP labeled immunoassay having a detection limit of  $8 \text{ pg mL}^{-1}$  and a dynamic range of detection within  $10\text{--}100 \text{ pg mL}^{-1}$  [126].

## **1.8 Water pollution**

Diseases arising from water borne toxic chemicals pose a constant threat for both developing as well as developed countries. Rainwater is a medium for transporting the pollutants from the atmosphere to the earth's surface. Anthropogenic and natural substances transfer to water bodies and ground water. According to the European Environmental Agency [127], approximately 25% of the groundwater in Europe is polluted. Human activities in various arenas have led to an increase in pollutants e.g., nitrates in groundwater. Another source of pollution of the groundwater is the disposal of untreated wastewater and solid wastes to the water bodies. The sources of the chemicals present in water are either natural or from different human activities. Natural sources of chemical pollutants include climate, soil erosion and leaching and weathering of rocks. Human sources of chemicals are related to complex industrial activities, such as oil drilling and mining. Other human sources are sewage wastes, fuel leakages and solid wastes. Certain agricultural activities produce different chemicals, such as fertilizers and pesticides, which find their way into the ground water from the fields. Additionally the construction sites also generate large chemicals that are released into the ground. The main categories of water pollutants are shown in Figure 1.10.

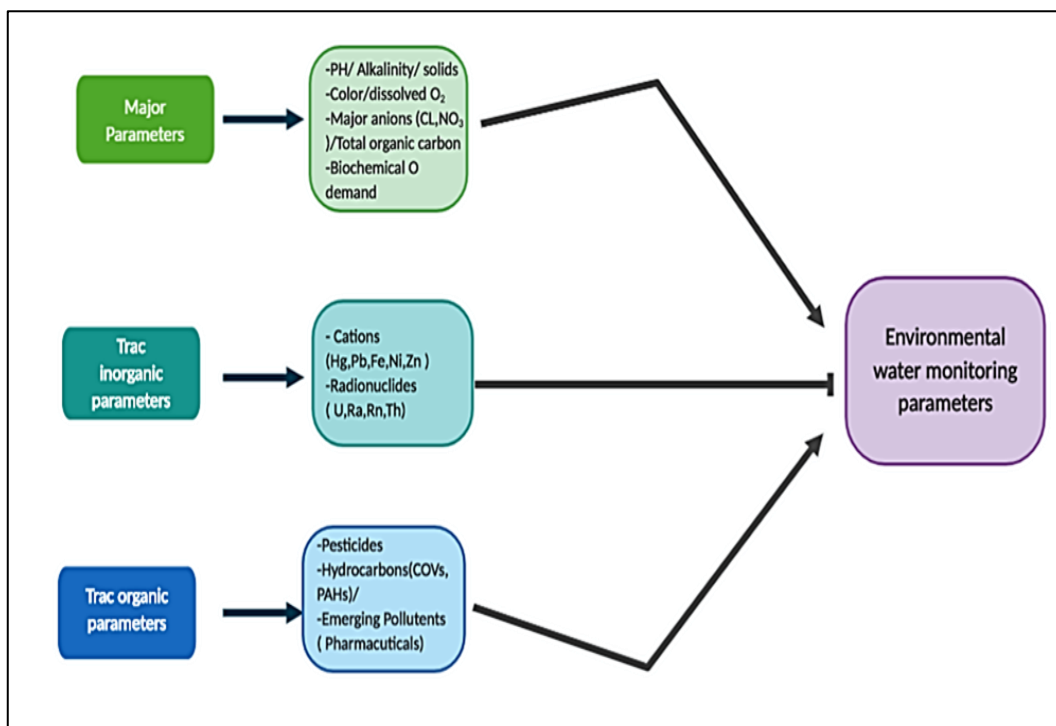


Figure 1.10: Environmental water monitoring parameters.

### 1.9 Polycyclic aromatic hydrocarbons (PAHs)

PAHs are a type of contaminant present in environmental pollutants. The structure of PAHs comprises of two or more fused aromatic rings. The molecules in the vapour phase (a molecule that is a mixture of two phases at room temperature) contain PAHs having between two and four fused aromatic rings. PAHs have been identified as one of the major risks associated with food consumption and environmental safety. Historically, much public attention has been given to PAHs due to their toxic and carcinogenic effects. Molecules of PAHs having more than four fused rings are present as particles in the atmosphere. PAHs can be found in aqueous phases, such as ground water, surface water and drinking water. However the concentration of these compounds is very low in ground water. The concentration of the contaminant in surface water is very high due to contaminations from oil products carried by wastewater during disposal. Drinking

water becomes contaminated as result of the water pipes used to supply water. Contaminant molecules diffuse from the coal tar that is used as a coating for the water pipes to the water flowing through the pipes. PAHs are both generated by natural processes as well as anthropogenic processes. Natural sources of the contaminant are volcanic eruptions and forest fire. Other sources relate to the incomplete combustion of wood, gasoline and coal. Additionally this contaminant enters the environment from the emissions of cooking gas and fuel used in vehicles. Emissions from tobacco smoking also contribute a minor amount of PAHs to the environment. Only small quantities of PAHs are made for commercial purpose. The contaminants present in air, water and soil matrixes usually have PAHs as their major constituent [128-137]. However the concentration of the pollutant differs based on its locality, sources and the matrix. Its concentration is lower in water than in air and soil as it is a hydrophobic molecule and has poor affinity towards water. Industrial pollutants and oil leakages are two factors attributed to the contamination of soil by PAHs [138,139].

#### **1.9.1 Health issues pertaining to PAHs**

PAH molecules can enter the human body [140] via number of routes: contact, ingestion and inhalation [134-136]. The health impacts of PAHs depend upon the type of contact route, PAHs concentration and contact time [137]. The consequences of exposure to these pollutants are shown in Table 1.5.



Table 1.5: The effects of PAHs in short and long contacts.

Short contact	Long-standing contact
<ul style="list-style-type: none"> <li>-Impaired lung function and coronary heart conditions as consequence of inhalation</li> <li>-Intake of water contaminated with PAHs has resulted in diarrhea, vomiting and nausea conditions.</li> <li>- When the human skin is exposed to PAHs, it results in irritation, swelling and allergic reactions of the skin [141-143]</li> </ul>	<ul style="list-style-type: none"> <li>-Detrimental effects on the reproductive and development systems.</li> <li>- Kidney and liver infection,</li> <li>-Cataract inducement</li> <li>-Jaundice.</li> <li>-Malfunction of red blood cells (RBCs) [144-146]</li> </ul>

The lipophilic character of these molecules aids in their accumulation in the human body. Some PAHs form carcinogenic species that bind to the DNA in humans and animals through metabolism. Metabolic processes involving PAHs lead to the production of toxic metabolites that can attach to DNA, resulting in gene mutation. Some occupational exposure may cause lung and skin cancers [147]. The Environmental Protection Agency has identified 16 PAHs as major pollutants (Figure 1.11). The Scientific Committee on Food of the European Commission analysed 33 potent PAHs of which 15 were found to be both genotoxic and carcinogenic [148]. In the European Union (European Union under the Drinking Water Directive [149] the limit of concentration values of PAHs permitted in water is set at 0.1 µg/L. Among all the toxic PAHs, benzo[a] pyrene (BaP) is the most widely studied compound based on its carcinogenic character whose limit value has been defined for various matrices. The maximum limit of BaP for drinking water is 0.01 µg/L. Additionally, the annual mean limit and 24-hour limit in air are 0.01µg/m<sup>3</sup> and 0.0025 µg/m<sup>3</sup>.

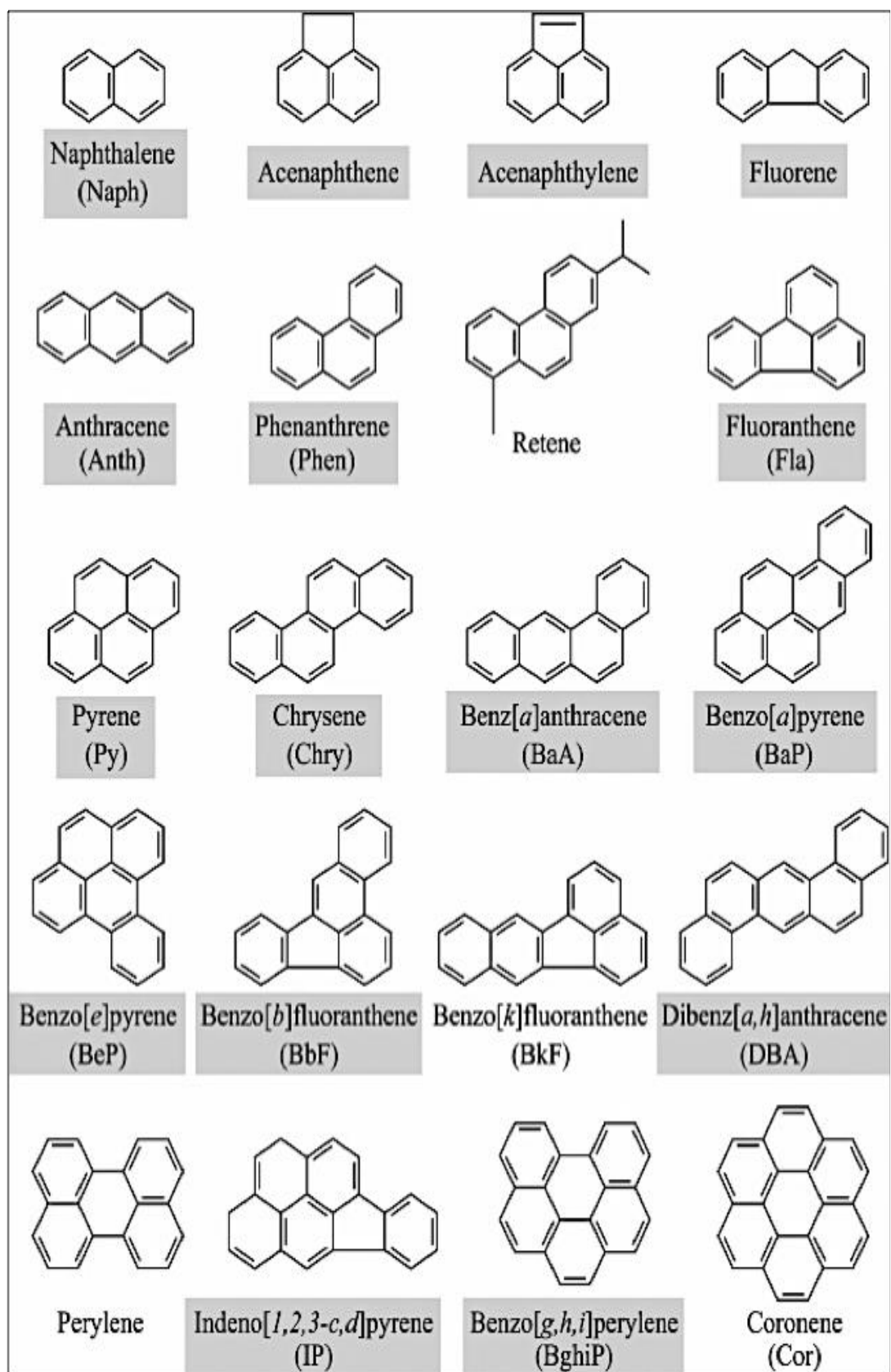


Figure 1.11: Structure of selected PAHs. Highlighted compounds comprise the Environmental Protection Agency (EPA) list of 16 priorities PAH [149].

### **1.9.2 Analysis of PAHs**

Presently, the common traditional analytical methods used to detect PAHs include, gas chromatography/mass spectrometry (GC/MS), including chemical ionization MS, ion trap MS, TOF/MS, and isotope-ratio MS (IRMS), and high-performance liquid chromatography (HPLC) with fluorescence detection or ultraviolet detection (HPLC/UV). There are several advantages that are associated with the use of these standard analysis techniques, such as accuracy, reliability, and sensitivity. They present, however, some limitations. Some of these disadvantages include the fact that their processes involve high-risk loss of analytes during sample separation, in addition to using an extensive amount of hazardous organic solvents. With the various limitations of the traditional chromatographic techniques, there is demand for low-cost, sensitive, rapid, on-site, environmentally as well as human friendly techniques that can be carried out by public healthcare providers and institutions who are keen to improve the quality of water. Thus, this is where new emerging techniques like immunoassay come in [150,151].

Lux et al. [152] pointed out that these methods require sophisticated equipment and present a lack of real-time detection. When studying several groups of PAHs simultaneously, the extraction process can be complicated when PAHs of similar properties are included in the sample, as similar characteristics make the identification process difficult [153]. Molaei et al. [154] note that alternative approaches, such as single-drop microextraction, solid-phase microextraction, and stir bar sportive extraction methods have been introduced to reduce costs, pollution, and shorten processing time.

Manoli et al. [155] discussed a new model of magnetic solid-phase extraction (MSPE). The MSPE process uses magnetic material as adsorbents and comes with several advantages, including the ability to detect PAHs in crude samples. For decades, using a highly reliable GC-MS method solved the difficulty of detecting PAHs in crude samples. However, GC-MS has its limitations. Generally, even though GC-MS is extremely precise and sensitive, it involves very expensive equipment and is therefore not available to all laboratories or consumers [156]. Additionally, there has been an increasing demand for low-cost, sensitive, rapid, and on-site detection techniques by public health care providers and institutions who are keen to improve the quality of water [153] and want to understand the mechanisms of creation of PAHs in the environment. In addition to conventional PAH detection methods, the impact of pollutants on environmental water have been monitored using biological systems, including biomarkers and biomonitors [157].

These biological techniques can measure the impact of anthropogenic activities in order to ensure compliance with environmental guidelines and regulations [158]. Biomonitoring involves the use of indicator organisms, for instance, filter-feeding mollusk bivalves [159,160]. As such, this technique is important because it can identify the early presence of water pollutants entering water sources [161-164]. On the other hand, biomonitoring can only be used to detect the presence of pollutants, not to identify or quantify a specific pollutant in water [165]. As a result, biomonitoring is limited in its application, and compared to other state-of-the-art methods such as immunoassay techniques, does not provide a persuasive performance [166].

A range of immunological assays including immunosensors, fluorescent and chemiluminescent immunoassays and Enzyme Linked Immuno Sorbent Assays (ELISA) have been developed for the analysis of PAHs. Immunosensors are created through the integration of immunoassay methods in micro-devices. As a compact analytical device, an immunosensor presents a surface where antigen-antibody complex can be detected and also converted into electrical and biomechanical signals using transducers. The final detected signals can then be processed, recorded and displayed [167].

### **1.9.3 Surface Functionalisation Techniques**

In relation to state of the art techniques, Ahmad and Moore [168] reported on the performance of an electrochemical immunosensor for the detection of benzo[a]pyrene (BaP) in water samples. Detection was done electrochemically by a common reaction used to create an electrochemical signal in immunological reactions, produced by the substrate para-aminophenyl phosphate (*p*APP) (an example of an immunoassay with a *p*APP reaction is shown in Figure 1.12). In this reaction, an alkaline phosphatase enzyme [AP], which was linked to a secondary antibody, was reduced (by hydrolysis of the substrate *p*APP) to para-aminophenyl [pAP], freeing hydrogen ions in the process. The difference in potential created by the two hydrogens was then measured, as it an electrical signal proportional to the presence of the target analyte. The same authors also used surface functionalization techniques like optimization of surface substrates and active redox probes to increase the sensitivity of the sensor.

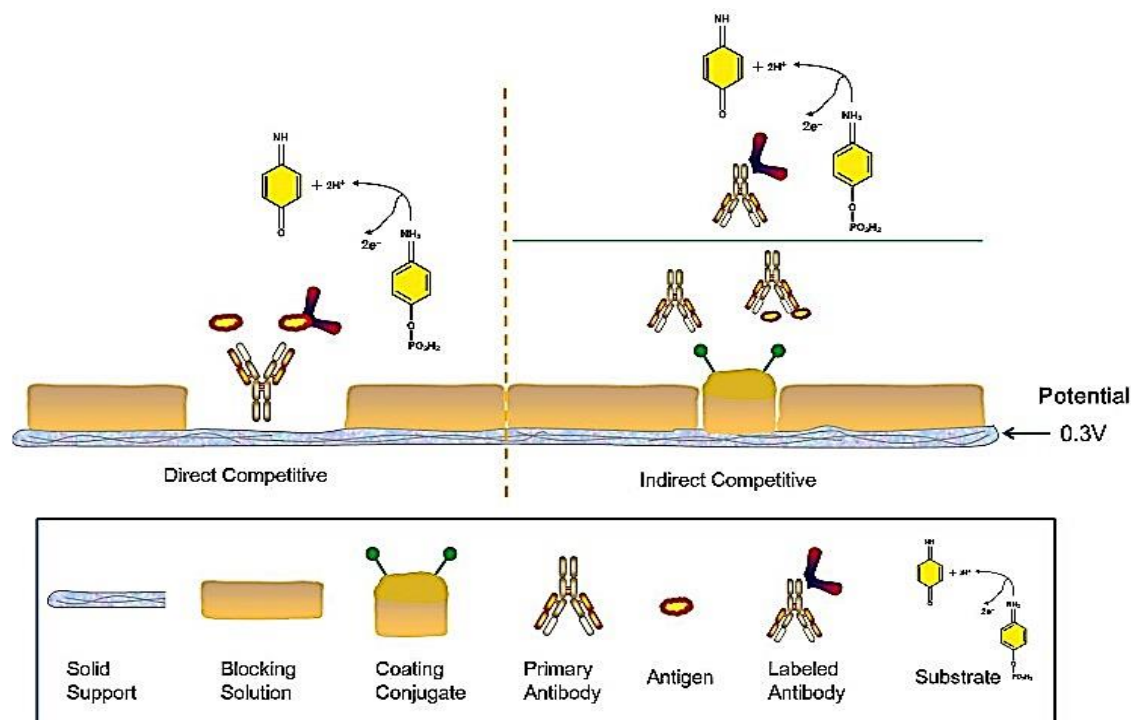


Figure1.12: Electrochemical detection using an immunological reaction by measuring the alkaline phosphatase (AP) enzymatic reaction towards the substrate para-aminophenyl phosphate (pAPP). Two electrons were generated with a new product (para-aminophenyl (pAP)) [168].

There are several possible surface functionalisation techniques for improving PAH detection. However, the current section will focus on three key approaches that are widely discussed in the literature in terms of improving immunosensor performance. These surface functionalisation techniques include optimisation of substrate surface reaction, redox-active probes and layer-by-layer technique. In optimisation of surface substrates focuses on improving the sensitivity and selectivity of immunosensors by enhancing antigen-antibody binding and enzymatic reactions [169]. For example, the authors of [170] used a biocompatible polyaniline (PANI) layer and iron oxide to develop an electrochemical immunosensor platform for sensitive detection of benzo[a]pyrene (BaP).

The role of  $\text{Fe}_3\text{O}_4/\text{PANI}$  on a Nafion/ITO surface is to capture the BaP antigen with the aid of glutaraldehyde. Fabricated Multi-HRP-HCS-Ab2 labels were added at the end of the assay (see Figure 1.13). The technique works through immunoreaction between the BaP antigen and the primary antibody (Ab1) in the sample solution. The authors reported a linear response in the range of 8 pM to 2 nM and a detection limit of 4 pM, which is highly sensitive, compared to conventional PAH detection techniques.

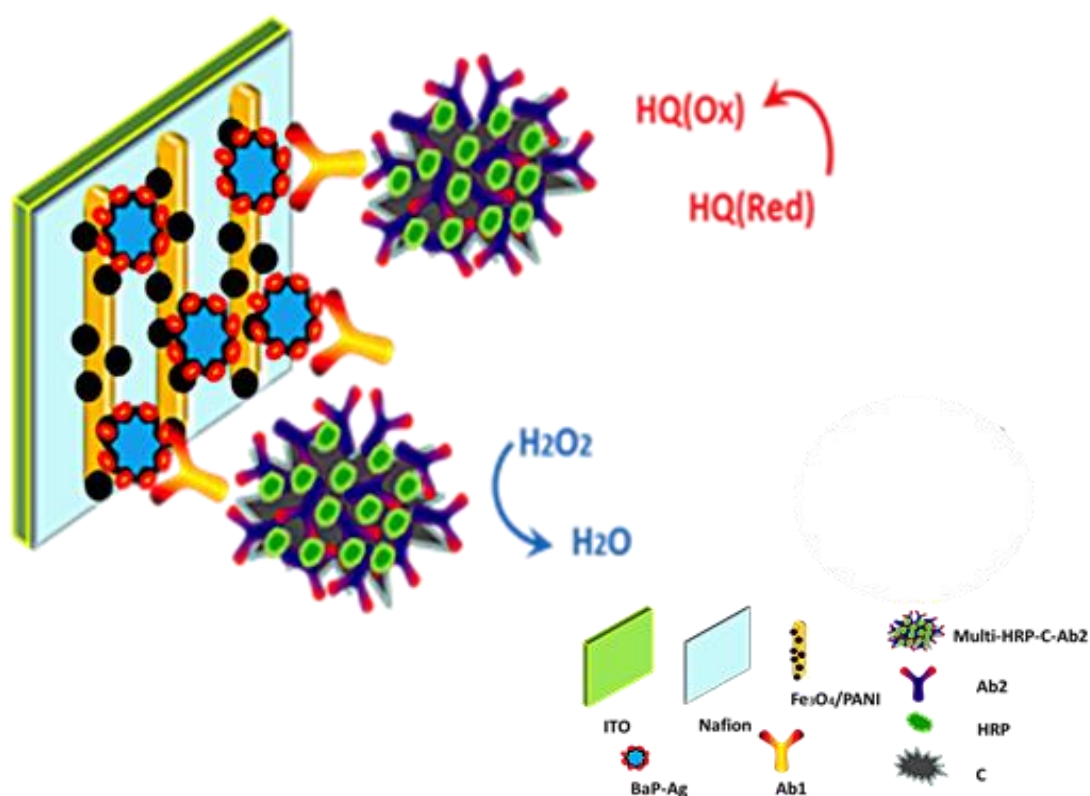


Figure1.13: Schematic representation of  $\text{Fe}_3\text{O}_4/\text{PANI}/\text{Nafion}$ -based immunosensor using multi-HRP-HCS-Ab2 bioconjugates as labels [170].

Redox-probes offer efficient PAH detection in polluted water as indicated in Figure 1.14. In PAH detection, the objective of this technique was to amplify the redox cycling provided by the probes in order to obtain high electrochemical signals. The use of redox probes is useful as it can simultaneously detect multiple PAHs [171]. Figure 1.14 shows how a ruthenium tris(bipyridine)-pyrene butyric acid conjugate (PAH-Ru) was synthesized as a redox-labelled tracer [171]. For the PAH-Ru conjugate to be used as a tracer in PAH immunoassays, it needs to be detected by anti-PAH antibodies.

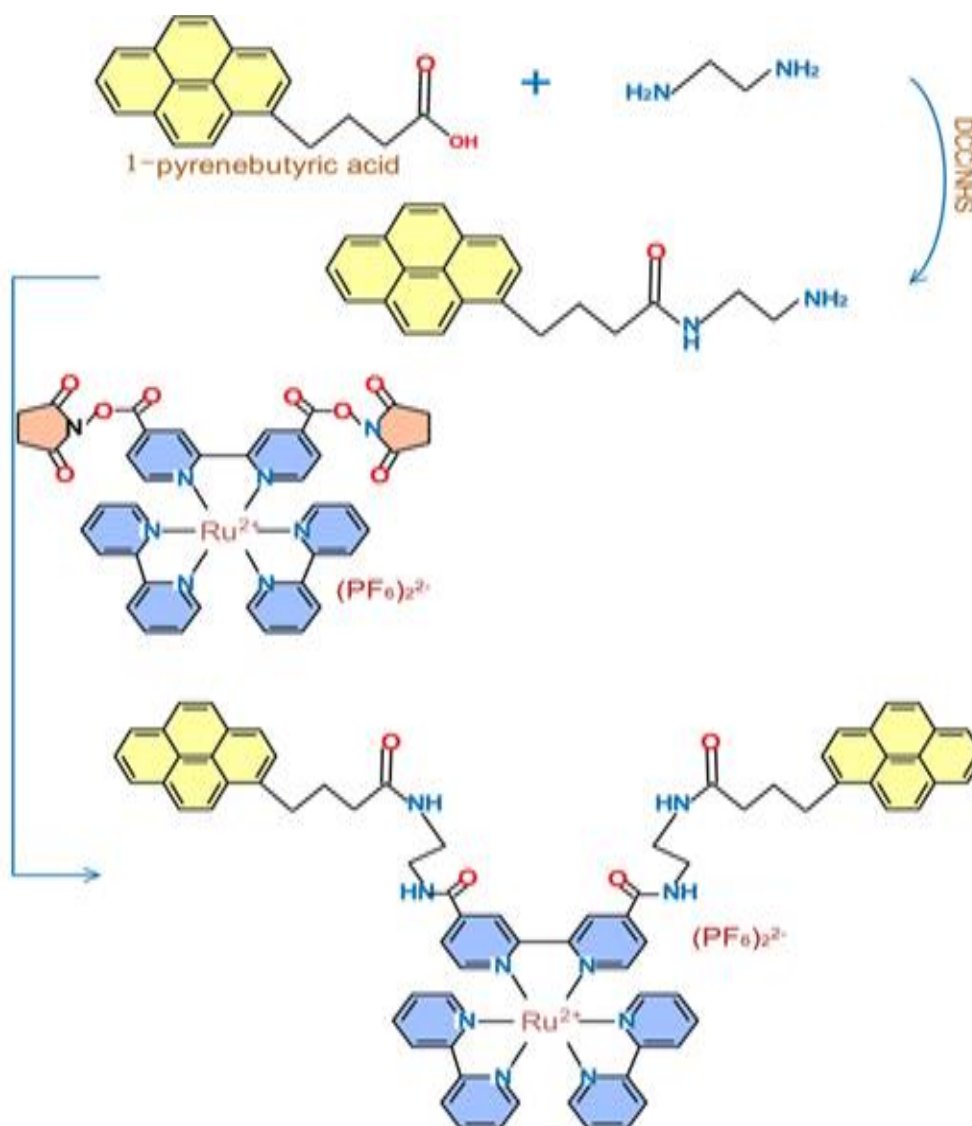


Figure 1.14: Synthesis of ruthenium tris(bipyridine)-pyrene butyric acid (PAH-Ru) conjugate



### 1.9.4 Haptens and their conjugates

The molecular weight of the PAHs is low and hence fails to induce an immune response. Thus, these molecules have to be conjugated to large carrier proteins with the aim of generating an immune response. However, the main drawback with the PAHs molecules is that they do not form covalent bond easily with the carrier molecules. Thus the PAHs are converted to haptens that easily form the required covalent bond with the carrier protein. The various haptens required for producing different antibodies are shown in figure 1.15 [172-173].

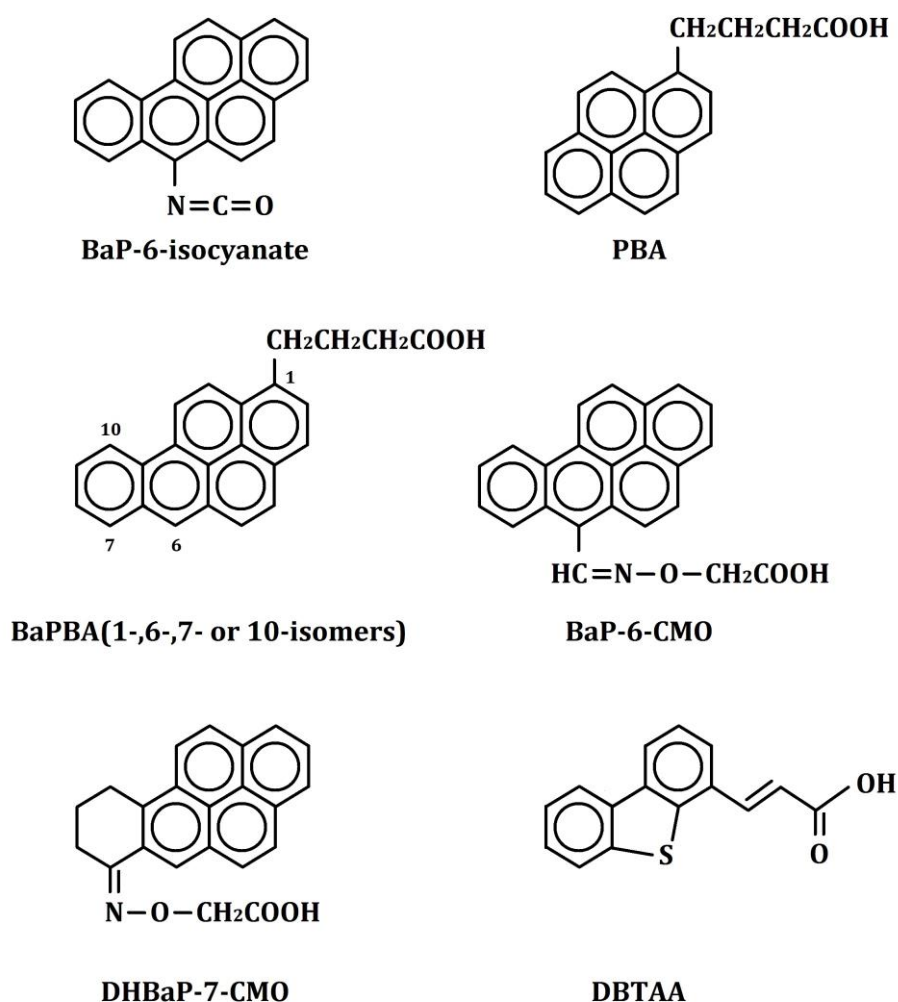


Figure 1.15: Various haptens required for producing different antibodies

#### **1.9.4.1 Pyrene as Hapten**

Pyrene that has been found abundantly in the environment consists mainly of 3 to 5 fused aromatic rings. Based on this, the pyrene molecule that contains 4 fused rings called 4-ring pyrene, has been considered as the standard hapten for immunoassays. Additionally 1-pyrene butyric acid, which is also a 4-ring pyrene, is available commercially, and can be conveniently conjugated to carrier proteins. Thus, the additional work of derivatisation can be avoided. The main aim of the study was to produce polyclonal antibodies by conjugating 1-pyrene butyric acid to carrier proteins and produce pAbs to be used in ELISA [173]. It was found that the Ab for PBA was more sensitive than PYR. Thus a monoclonal antibody was prepared using PBA and applied for detection of some other poly aromatic hydrocarbons in water [174].

#### **1.9.4.2 Benzo[a]pyrene as Hapten**

Benzo[a]pyrene has been used widely as target analyte as it is very toxic in nature. The derivatives of benzo[a]pyrene have to be synthesised in the laboratory as they are not commercially available. Recently, the metabolites of benzo[a]pyrene have been identified in urine with the help of immunological assays for which two monoclonal antibodies (4D5 and 10C10) were produced with the hapten of benzo[a]pyrene-6-isocyanate (Figure 1.12) [175]. Another immunogen used for producing broad specific monoclonal antibodies BaP-13 and rigorous specific monoclonal antibodies 22F12 is benzo[a]pyrene butyric acid [176, 177]. BaP-13 was obtained from 1-benzo[a]pyrene butyric acid which was specific towards to 21 parent poly aromatic hydrocarbons along with its 10 derivatives [176]. 22F12 antibody was the most selective and sensitive Ab to 6-benzo[a]pyrene butyric acid, 7-benzo[a]pyrene butyric acid or 10-benzo[a]pyrene butyric acid.

The LOD for benzo[a]pyrene was 24 ng/L [177]. Another recent report provided a detailed study about where mice were immunised with 10-benzo [a] pyrene butyric acid –protein conjugate and 110 obtained by hybridoma cell lines were detected by a new biochip noncompetitive direct chemiluminescence immunoassay [178]. The hapten of benzo[a]pyrene butyric acid was used for development of single chain variable antibodies against the poly aromatic hydrocarbons [179]. Also another hapten synthesized for benzo[a]pyrene was 6- benzo[a]pyrene carboxaldehyde-O-carboxymethyloxime. The limit of detection was 0.5µg/L for the time resolved fluoroimmunoassay of this hapten in water [180]. Another two synthesized haptens were 9,10-dihydrobenzo [a] pyrene-7 (8H)-one—7-(O-carboxymethyl) oxim and 1-hydroxy pyrene used for immunoassays of urine [181, 182].

### **1.9.5 Proteins**

Proteins can quickly lose their shape and hence their activity upon functionalisation and attachments. Physicochemical properties of the protein and the surface play a key role when the procedure to modify the surfaces has to be taken. The recognition of proteins using antibodies primarily relies on the retention of binding affinity. Consequently, advanced strategies are needed to protect the bio-detection component [183]. After extensive examination, the immobilization of antibodies (or their fragments) on stable structures is broadly used in the life science zone. The successful application of antibodies to immunoassay-based uses is aided by the existence of necessary parameters. These parameters have various characteristics, such as antibody size, labeling, immobilization ability, sensitivity, selectivity, orientation, and stability. However, the capture and the detection of antibodies is a critical aspect for assay advancement, and the technique adopted may have considerable impacts on the assay. The capacity to design more sensitive and

reliable methods is dependent upon improvement of assay-specific antibodies to boost these general performance properties. The ability to improve antibodies with regard to modification and suitability for the applications is vital to robust biosensor advancement. Similarly, knowledge-driven methods to enhance surface chemistry, conjugation, and immobilization are critical to the development of the next generation of immunoassay methods. Research on antibody immobilization has led to the evolution of numerous mechanisms, which facilitate the introduction of sophisticated study tools and systems for better analysis [184, 185]. Therefore, the current antibody-based immunoassay platforms are better than traditional analytical approaches. In a typical situation, antibodies are deposited evenly on a solid surface in high amount and with the required orientations, such that they retain their effectiveness and avert non-specific bindings.

The deposition of the active antibody onto the assay surface is essential in matching the reporter molecule to the secondary antibody. The orientation and the activity of the antibody on the immunoassay surface depend on the mode of antibody immobilisation. Therefore, the quantity and activity of the immobilized antibody affect the immunoassay's sensitivity [186]. There are two essential modes of antibody immobilisation, passive and covalent attachment. These modes rely on the antibody and the chemical properties of the solid phase upon which covalent immobilization is required [187]. The absorption of proteins on the substrate is one of the simplest processes used to capture antibodies Figure 1.16.

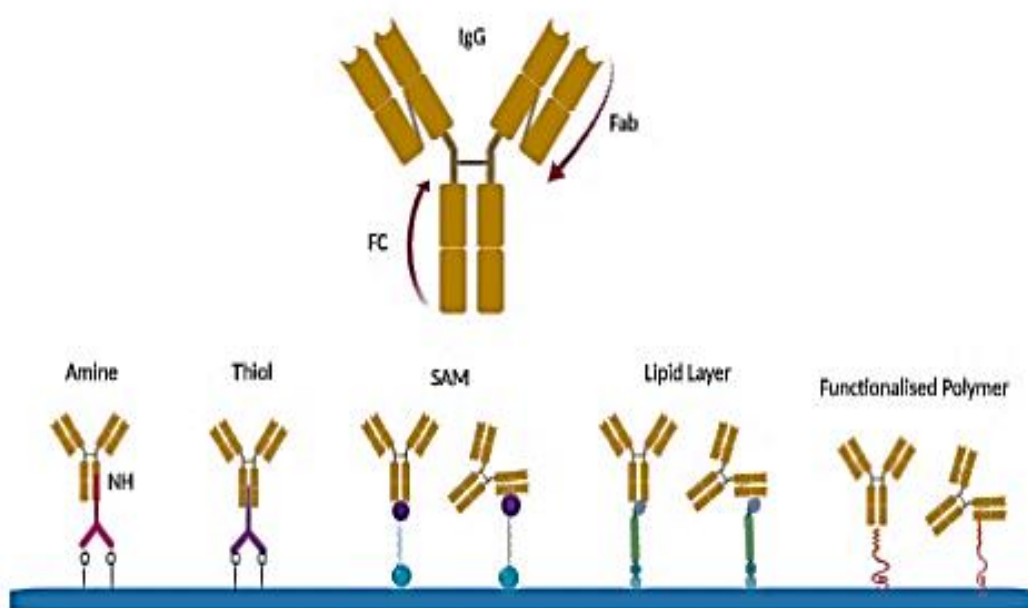


Figure1.16: Coupling approaches for linking antibodies to surfaces. In its natural state an antibody has primary amines, carboxyls and hydroxyls as target groups for antibody immobilisation. Amine group is the most abundant of all native pendent groups on an antibody. Carboxyl group is another viable group for antibody functionalisation.

However, the success of this approach depends on random orientation and denaturation. For crosslinking antibodies to the surface the availability of the functional reactive groups on both the partners is needed. The strategy of antibody immobilization influences the orientation on the surface, which eventually affects the activity of the antibodies. Thus, effective immobilisation of antibodies for all immunoassay methods needs novel and well-designed modes to maximize the sensitivity of the test.

### **1.9.6 The conjugates of carrier proteins**

The most common carrier proteins in the conjugation with haptens are ovalbumin (OVA), keyhole limpet hemocyanin (KLH) and bovine serum albumin (BSA). The hapten derivative containing functional groups like thiol, amine, hydroxyl and carboxylic acid are bonded covalently to the carrier proteins by using different techniques [188]. This binding step is very significant as the efficiency and quality of the antibodies depend on the binding ratio of the hapten-protein conjugates in the immunoassays. The strength and specificity of the immune response is dictated by the ratio of the hapten to the carrier protein. The average ratio of binding of haptens to carrier protein is analysed by various techniques, such as gel electrophoresis and matrix assisted laser desorption ionization time of flight mass spectrometry (MALDI-TOF-MS) [189, 190]. These techniques can estimate the binding ratio accurately. No technique currently exists for estimation of all the hapten-protein conjugates. It was reported that the synthesis, characterization and the calculation of the binding average of PBA-OVA and PBA-BSA were by MALDI-TOF-MS, IR and UV –visible spectroscopy [191]. These two methods were very useful to determine the binding ratio of the haptens to the carrier protein. Immunological assays are highly selective and sensitive and relatively inexpensive. These immunoassays are used for the analysis of both broad specific and class selective PAHs [192]. The PAHs present in biological samples, soil and water can be detected with the aid of commercially available ELISA kits [193,194]. Sufficient antibodies are required for the analysis of PAH by immunoassays. However the search for novel antibodies for immunoassays, equipped with quantitative structure activity relationship (QSAR) methods is still a significant area of research.

### 1.10 Perspective

Toxic compounds present in the environment consist of different poly aromatic hydrocarbons, so it is essential to establish a technique that can identify different poly aromatic hydrocarbons simultaneously. Recent reports indicate that the generic antibodies or specific antibodies can be analyzed using multi tracer co-marking or multi antibody coating with the help of ELISA [195]. Structural activity relationship is a relationship between a biological activity of a molecular system and its geometric and chemical characteristics (electronic and crystal structures of a molecule). The multi analyte ELISA is based on the technique of cross reactivity of the broad specific antibodies to different poly aromatic hydrocarbons since there is a structural similarity between the different poly aromatic hydrocarbons. Data pertaining to the cross reactivity of different poly aromatic hydrocarbons has still not been completely investigated. Molecular modelling as well as Quantitative Structure-Activity Relationship (QSAR) has been used extensively in the immunoassays relating to the environment for understanding the physical and chemical interactions of haptens and antibodies [196-201]. These interactions have been studied by both two-dimensional and three-dimensional QSAR studies including comparative molecular field analysis [200,201], regression analysis [197], principal component analysis and Hantzsch method [199]. The different analogues of poly aromatic hydrocarbons and their cross binding to different antibodies have made them suitable candidates for QSAR studies. An ELISA kit has been developed for the QSAR studies relating to poly aromatic hydrocarbons [202]. An ELISA study of quantitative structure and cross reactivity relationship of polycyclic aromatic hydrocarbons was conducted. The study was done with the aid of published data on multiple regression analysis and comparative molecular field

analysis [203,204]. The main aim of the study was to investigate the effect of molecular property on the cross reactivity of ELISA and the probable cross reactivity of QSAR studies. The results indicated that the major factors that affected the immunoassays of polycyclic aromatic hydrocarbons were their hydrophobic property and solubility. Additionally it was found that the cross reactivity can be effectively predicted by QSAR studies. However there are certain fundamental problems associated with QSAR that still need further attention to be solved [205]. Another study reported a modified method for analysing the binding of haptens to monoclonal antibodies through the use of homogeneous modeling and ligand docking [206]. A three dimensional model of the variable fragments of the antibodies was constructed on the high resolution crystallographic structures in order to study the factors responsible for binding affinities of monoclonal antibodies and the haptens. This is a promising method for studying the interactions between antibodies and haptens. Antibodies play a significant role in immunoassays for haptens of low molecular weight in immunoassays. There is still a dearth of information about haptens and antibodies for polycyclic aromatic hydrocarbons. Interdisciplinary work between synthetic chemists and immunological chemists will provide greater insights in this arena and synthesise high quality antibodies. There is a wide scope for developing broad spectrum, monoclonal, polyclonal, conventional and novel antibodies for use in the immunoassay of poly aromatic hydrocarbons [207-208].



### 1.11 References:

1. Luong JH, Male KB, Glennon JD. Biosensor technology: Technology push versus market pull. *Biotech Adv.* 2008 Sep 1;26(5):492-500.
2. Thévenot DR, Toth K, Durst RA, Wilson GS. Electrochemical biosensors: Recommended definitions and classification. *Anal Letters.* 2001 Mar 31;34(5):635-59.
3. Turner A, Karube I, Wilson GS. *Biosensors: Fundamentals and applications.* Oxford University Press; 1987.
4. Patel PD. (Bio) sensors for measurement of analytes implicated in food safety: A review. *TrAC Trends in Analyt Chem.* 2002 Feb 1;21(2):96-115.
5. Conroy PJ, Hearty S, Leonard P, O’Kennedy RJ. Antibody production, design and use for biosensor-based applications. In *Seminars in cell & developmental biology* 2009 Feb 1 (Vol. 20, No. 1, pp. 10-26). Academic Press.
6. Chambers JP, Arulanandam BP, Matta LL, Weis A, Valdes JJ. Biosensor recognition elements. Texas Univ at San Antonio Dept of Biology; 2008 Jan.
7. Zhang QD, March G, Noel V, Piro B, Reisberg S, Tran LD, Hai LV, Abadia E, Nielsen PE, Sola C, Pham MC. Label-free and reagentless electrochemical detection of PCR fragments using self-assembled quinone derivative monolayer: Application to *Mycobacterium tuberculosis*. *Bios and Bioelect.* 2012 Feb 15;32(1):163-8.
8. Retama JR, Cabarcos EL, Mecerreyes D, Lopez-Ruiz B. Design of an amperometric biosensor using polypyrrole-microgel composites containing glucose oxidase. *Bios and Bioelect.* 2004 Dec 15;20(6):1111-7.
9. Palomera N, Balaguera M, Arya SK, Hernández S, Tomar MS, Ramírez-Vick JE, Singh SP. Zinc oxide nanorods modified indium tin oxide surface for

- amperometric urea biosensor. *Journal of Nanosc and Nanotech.* 2011 Aug 1;11(8):6683-9.
10. Das N, Reardon KF. Fiber-optic biosensor for the detection of atrazine: Characterization and continuous measurements. *Anal Letters.* 2012 Jan 1;45(2-3):251-61.
  11. McGrath TF, Elliott CT, Fodey TL. Biosensors for the analysis of microbiological and chemical contaminants in food. *Anal and Bioanal Chem.* 2012 Apr 1;403(1):75-92.
  12. Chaubey A, Malhotra B. Mediated biosensors. *Bios and Bioelect.* 2002 Jun 26;17(6-7):441-56.
  13. Radhakrishnan J, Wang S, Ayoub IM, Kolarova JD, Levine RF, Gazmuri RJ. Circulating levels of cytochrome c after resuscitation from cardiac arrest: a marker of mitochondrial injury and predictor of survival. *American Jour of Physi-Heart and Circ Phys.* 2007 Feb;292(2):H767-75.
  14. Zhou F, Xing D, Wu B, Wu S, Ou Z, Chen WR. New insights of transmembranal mechanism and subcellular localization of noncovalently modified single-walled carbon nanotubes. *Nano Letters.* 2010 Apr 6;10(5):1677-81.
  15. Inzelt G, Lewenstam A, Scholz F. *Handbook of reference electrodes.* Heidelberg:: Springer; 2013 Jan 1.
  16. Thomas FG, Henze G. *Introduction to voltammetric analysis: Theory and practice.* Csiro Publishing; 2001 Apr 15.
  17. Bard AJ, Faulkner LR. *Fundamentals and applications. Electrochem Methods.* 2001;2:482.

18. Mikkelsen SR, Rechnitz GA. Conductometric transducers for enzyme-based biosensors. *Anal Chem.* 1989 Aug 1;61(15):1737-42.
19. Yu CJ, Wan Y, Yowanto H, Li J, Tao C, James MD, Tan CL, Blackburn GF, Meade TJ. Electronic detection of single-base mismatches in DNA with ferrocene-modified probes. *Journal of the American Chem Society.* 2001 Nov 14;123(45):11155-61.
20. Bard AJ, Faulkner LR, Leddy J, Zoski CG. *Electrochemical methods: Fundamentals and applications.* New York: Wiley; 1980.
21. Chand R, Han D, Kim YS. Voltammetric analysis on a disposable microfluidic electrochemical cell. *Bulletin of the Korean Chem Society.* 2013 Apr 20;34(4):1175-80.
22. Kato K, Lian LY, Barsukov IL, Derrick JP, Kim H, Tanaka R, Yoshino A, Shiraishi M, Shimada I, Arata Y, Roberts GC. Model for the complex between protein G and an antibody Fc fragment in solution. *Struct.* 1995 Jan 1;3(1):79-85.
23. Shinkai S, Ikeda M, Sugasaki A, Takeuchi M. Positive allosteric systems designed on dynamic supramolecular scaffolds: toward switching and amplification of guest affinity and selectivity. *Acc of Chem Resrch.* 2001 Jun 19;34(6):494-503.
24. Goldberg RJ. A Theory of Antibody—Antigen Reactions. I. Theory for Reactions of Multivalent Antigen with Bivalent and Univalent Antibody2. *Journal of the American Chem Society.* 1952 Nov;74(22):5715-25.  
[doi:10.1021/ja01142a045](https://doi.org/10.1021/ja01142a045).
25. Sahini M, Sahimi M. *Applications of percolation theory.* CRC Press; 1994 Jan 27.

26. Spiers JA. Goldberg's theory of antigen-antibody reactions in vitro. *Immun.* 1958 Apr;1(2):89.
27. Janeway CA, Travers P, Walport M, Shlomchik M. *Immunobiology: The immune system in health and disease*. London: Current Biology; 1996 Mar.
28. Sela-Culang I, Kunik V, Ofran Y. The structural basis of antibody-antigen recognition. *Front in Immun.* 2013 Oct 8;4:302.
29. Mian IS, Bradwell AR, Olson AJ. Structure, function and properties of antibody binding sites. *Jour of Molec Bio.* 1991 Jan 5;217(1):133-51.
30. Van Oss CJ, Good RJ, Chaudhury MK. Nature of the antigen-antibody interaction: Primary and secondary bonds: optimal conditions for association and dissociation. *Journal of Chromatography B: Biomed Sc and Applic.* 1986 Apr 11;376:111-9.
31. Absolom DR. The nature of the antigen-antibody bond and the factors affecting its association and dissociation. *CRC Critic Reviews in Immuno.* 1986;6(1):1-46.
32. Lisova O, Belkadi L, Bedouelle H. Direct and indirect interactions in the recognition between a cross-neutralizing antibody and the four serotypes of dengue virus. *Jour of Molec Recog.* 2014 Apr;27(4):205-14.
33. Braden BC, Dall'Acqua W, Eisenstein E, Fields BA, Goldbaum FA, Malchiodi EL, Mariuzza RA, Schwarz FP, Ysern X, Poljak RJ. Protein motion and lock and key complementarity in antigen-antibody reactions. *Pharma Acta Helvetiae.* 1995 Mar 1;69(4):225-30.
34. Almagro JC. Natural and man-made V-gene repertoires for antibody discovery. *Fro in Immuno.* 2012 Nov 15;3:342.

35. Conroy PJ, Law RH, Gilgunn S, Hearty S, Caradoc-Davies TT, Lloyd G, O'Kennedy RJ, Whisstock JC. Reconciling the structural attributes of avian antibodies. *Jour of Bio Chem*. 2014 May 30;289(22):15384-92.
36. Leenaars M, Hendriksen CF. Critical steps in the production of polyclonal and monoclonal antibodies: evaluation and recommendations. *Ilar Journal*. 2005 Jan 1;46(3):269-79.
37. Zhu K, Dietrich R, Didier A, Doyscher D, Märtlbauer E. Recent developments in antibody-based assays for the detection of bacterial toxins. *Toxins*. 2014 Apr;6(4):1325-48.
38. Bansal V, Kumar P, Kwon EE, Kim KH. Review of the quantification techniques for polycyclic aromatic hydrocarbons (PAHs) in food products. *Crit Rev in Food Sc and Nutri*. 2017 Oct 13;57(15):3297-312.
39. Fillmann G, Bicego MC, Zamboni A, Fileman TW, Depledge MH, Readman JW. Validation of immunoassay methods to determine hydrocarbon contamination in estuarine sediments. *Journal of the Braz Chem Soc*. 2007;18(4):774-81.
40. National Environmental Methods Index (NEMI), Strategic diagnostics Inc., EPA Method 4035 7061301. 2018. Available online: [file:///C:/Users/hp/AppData/Local/Packages/Microsoft.MicrosoftEdge\\_8wekyb3d8bbwe/TempState/Downloads/7061301%20\(1\).pdf](file:///C:/Users/hp/AppData/Local/Packages/Microsoft.MicrosoftEdge_8wekyb3d8bbwe/TempState/Downloads/7061301%20(1).pdf) (Accessed 27<sup>th</sup> November, 2019).
41. National Environmental Methods Index (NEMI), Strategic diagnostics Inc., Rapid Assay PAH Test Kit A00156/A00157. 2018. Available online: [file:///C:/Users/hp/AppData/Local/Packages/Microsoft.MicrosoftEdge\\_8wekyb3d8bbwe/TempState/Downloads/7061301%20\(1\).pdf](file:///C:/Users/hp/AppData/Local/Packages/Microsoft.MicrosoftEdge_8wekyb3d8bbwe/TempState/Downloads/7061301%20(1).pdf)

- [b3d8bbwe/TempState/Downloads/A00157%20\(1\).pdf](b3d8bbwe/TempState/Downloads/A00157%20(1).pdf) (Accessed 27<sup>th</sup> November, 2019).
42. National Environmental Methods Index (NEMI), Strategic diagnostics Inc., EPA method summary - 70620. 2018. Available online: [https://www.nemi.gov/methods/method\\_summary/5630/](https://www.nemi.gov/methods/method_summary/5630/) (A Accessed 27<sup>th</sup> November, 2019).
43. Jeong MS, Ahn DR. A microwell plate-based multiplex immunoassay for simultaneous quantitation of antibodies to infectious viruses. *Analyst*. 2015;140(6):1995-2000.
44. Abcam. Available online: <http://www.abcom.com> (accessed on 27<sup>th</sup> November, 2019).
45. Byrne B, Stack E, Gilmartin N, O’Kennedy R. Antibody-based sensors: Principles, problems and potential for detection of pathogens and associated toxins. *Sensors*. 2009 Jun;9(6):4407-45.
46. Uraipong C, Wong V, Lee NA. A testosterone specific competitive enzyme immunoassay for monitoring water quality. *Bulletin of Envir Contam and Toxi*. 2013 May 1;90(5):585-90.
47. Díaz-González M, González-García MB, Costa-García A. Recent advances in electrochemical enzyme immunoassays. *Electroanalysis: An International Journal Devoted to Fundamental and Practic Aspects of Electroanaly*. 2005 Nov;17(21):1901-18.
48. Yalow RS, Berson SA. Assay of plasma insulin in human subjects by immunological methods. *Nature*. 1959 Nov 21;184(4699):1648-9.
49. Yalow RS, Berson SA. Immunoassay of endogenous plasma insulin in man. *The Journal of Cli Invest*. 1960 Jul 1;39(7):1157-75.

50. Kuznetsov BA, Shumakovich GP, Koroleva OV, Yaropolov AI. On applicability of laccase as label in the mediated and mediatorless electroimmunoassay: Effect of distance on the direct electron transfer between laccase and electrode. *Bio and Bioelectr.* 2001 Jan 1;16(1-2):73-84.
51. Du D, Yan F, Liu S, Ju H. Immunological assay for carbohydrate antigen 19-9 using an electrochemical immunosensor and antigen immobilization in titania sol-gel matrix. *Journal of Imm Met.* 2003 Dec 1;283(1-2):67-75.
52. Liu Y, Li Y. An antibody-immobilized capillary column as a bioseparator/bioreactor for detection of *Escherichia coli* O157: H7 with absorbance measurement. *Anal Chem.* 2001 Nov 1;73(21):5180-3.
53. Ghindilis AL, Atanasov P, Wilkins M, Wilkins E. Immunosensors: Electrochemical sensing and other engineering approaches. *Bio and Bioelectr.* 1998 Jan 1;13(1):113-31.
54. Sharma MK, Rao VK, Agarwal GS, Rai GP, Gopalan N, Prakash S, Sharma SK, Vijayaraghavan R. Highly sensitive amperometric immunosensor for detection of *Plasmodium falciparum* histidine-rich protein 2 in serum of humans with malaria: Comparison with a commercial kit. *Journal of Clin Microb.* 2008 Nov 1;46(11):3759-65.
55. Clark Jr LC, Lyons C. Electrode systems for continuous monitoring in cardiovascular surgery. *Annals of the New York Ac of Sci.* 1962 Oct;102(1):29-45.
56. Wang J. Glucose biosensors: 40 years of advances and challenges. *Electroanalysis: An Internl Journal Dev to Fundam and Prac Asp of Electroanal.* 2001 Aug;13(12):983-8.

57. Cass AE, Davis G, Francis GD, Hill HA, Aston WJ, Higgins IJ, Plotkin EV, Scott LD, Turner AP. Ferrocene-mediated enzyme electrode for amperometric determination of glucose. *Anal Chem.* 1984 Apr 1;56(4):667-71.
58. Degani Y, Heller A. Direct electrical communication between chemically modified enzymes and metal electrodes. I. Electron transfer from glucose oxidase to metal electrodes via electron relays, bound covalently to the enzyme. *Journal of Phy Chem.* 1987 Mar;91(6):1285-9.
59. John R, Spencer M, Wallace GG, Smyth MR. Development of a polypyrrole-based human serum albumin sensor. *Analytica Chimica Acta.* 1991 Jan 1;249(2):381-5.
60. Hock B. Antibodies for immunosensors a review. *Analytica Chimica Acta.* 1997 Jul 30;347(1-2):177-86.
61. Cosnier S. Affinity biosensors based on electropolymerized films. *Electroanalysis: An Internl Journal Dev to Fund and Prac Asp of Electroanal.* 2005 Oct;17(19):1701-15.
62. Rodriguez-Mozaz S, de Alda MJ, Barceló D. Biosensors as useful tools for environmental analysis and monitoring. *Anal and Bioanal Chem.* 2006 Oct 1;386(4):1025-41.
63. Centi S, Laschi S, Mascini M. Strategies for electrochemical detection in immunochemistry. *Bioanal.* 2009 Oct;1(7):1271-91.
64. García-Miranda Ferrari A, Foster C, Kelly P, Brownson D, Banks C. Determination of the electrochemical area of screen-printed electrochemical sensing platforms. *Biosen.* 2018 Jun;8(2):53.



65. Li M, Li YT, Li DW, Long YT. Recent developments and applications of screen-printed electrodes in environmental assays—A review. *Analytica Chimica Acta*. 2012 Jul 13;734:31-44.
66. Tudorache M, Bala C. Biosensors based on screen-printing technology, and their applications in environmental and food analysis. *Anal and Bioanal Chem*. 2007 Jun 1;388(3):565-78.
67. Yáñez-Sedeño P, Campuzano S, Pingarrón JM. Multiplexed electrochemical immunosensors for clinical biomarkers. *Sensors*. 2017 May;17(5):965.
68. Devarakonda S, Singh R, Bhardwaj J, Jang J. Cost-effective and handmade paper-based immunosensing device for electrochemical detection of influenza virus. *Sensors*. 2017;17(11):2597.
69. Windmiller JR, Wang J. Wearable electrochemical sensors and biosensors: A review. *Electroanal*. 2013 Jan;25(1):29-46.
70. Miller KJ, Bowsher RR, Celniker A, Gibbons J, Gupta S, Lee JW, Swanson SJ, Smith WC, Weiner RS, Crommelin DJ, Das I. Workshop on bioanalytical methods validation for macromolecules: summary report. *Pharmaceutical Research*. 2001 Sep 1;18(9):1373-83.
71. Lipton CR, Dautlick JX, Grothaus GD, Hunst PL, Magin KM, Mihaliak CA, Rubio FM, Stave JW. Guidelines for the validation and use of immunoassays for determination of introduced proteins in biotechnology enhanced crops and derived food ingredients. *Food and Agric Imm*. 2000 Jun 1;12(2):153-64.
72. Crowther JR. Validation of Diagnostic Tests. In *The ELISA guidebook*. Springer Science & Business Media; 2001.
73. Food and Drug Administration. Guidance for industry: bioanalytical method validation. US Department of Health and Human Services. Food and Drug

- Administration, Center for Drug Evaluation and Research, Center for Biologics Eval and Rsrch. 2001 May.
74. Lee JW, Devanarayan V, Barrett YC, Weiner R, Allinson J, Fountain S, Keller S, Weinryb I, Green M, Duan L, Rogers JA. Fit-for-purpose method development and validation for successful biomarker measurement. *Pharm Resrch*. 2006 Feb 1;23(2):312-28.
  75. Nix B, Wild D. Calibration curve-fitting. *The immunoassay handbook*. Nature Pub Group, New York. 2003:233-45.
  76. Kelley M, DeSilva B. Key elements of bioanalytical method validation for macromolecules. *The AAPS Jour*. 2007 Jun 1;9(2):E156-63.
  77. Findlay JW, Smith WC, Lee JW, Nordblom GD, Das I, DeSilva BS, Khan MN, Bowsher RR. Validation of immunoassays for bioanalysis: a pharmaceutical industry perspective. *Jour of Pharm and Biom Anal*. 2000 Jan 1;21(6):1249-73.
  78. Huber L. *Validation and Qualification in Analytical laboratories* 2nd edition, New York: Informa Healthcare USA.
  79. Huber L. *Validation of analytical methods*. Agilent technologies. 2010 Mar 1;12.
  80. Jason-Moller L, Murphy M, Bruno J. Overview of Biacore systems and their applications. *Current protocols in protein science*. 2006 Aug;45(1):19-3.
  81. Rusmini F, Zhong Z, Feijen J. Protein immobilization strategies for protein biochips. *Biomacro*. 2007 Jun 11;8(6):1775-89.
  82. Thermo scientific pierce protein biology. Available online: <http://www.piercenet.com>. (Accessed on 27th November, 2019)

83. Yalow RS, Berson SA. Assay of plasma insulin in human subjects by immunological methods. *Nature*. 1959 Nov 21;184(4699):1648-9.
84. Immunoassays: Technologies and global markets. Available online: <http://www.bccresearch.com/pressroom/bio/immunoassays-technologies-global-markets> (Accessed 27th November, 2019).
85. Global markets for research antibodies. Available online: <http://www.bccresearch.com/market-research/biotechnology/research-antibodies-global-markets-report-bio141a.html> (Accessed 27th November, 2019).
86. Nissim A, Chernajovsky Y. Historical development of monoclonal antibody therapeutics. In *Therapeutic Antibodies 2008* (pp. 3-18). Springer, Berlin, Heidelberg.
87. Antibody Drugs: Technologies and global markets. Available online: <http://www.bccresearch.com/market-research/> (Accessed 27th November, 2019).
88. Zeenia KA, Yaguchi T, Sunil CK, Hirano T, Wadhwa R, Taira K. Mortalin imaging in normal and cancer cells with quantum dot immuno-conjugates. *Cell Resrch*. 2003 Dec;13(6):503.
89. Myers FB, Lee LP. Innovations in optical microfluidic technologies for point-of-care diagnostics. *Lab on a Chip*. 2008;8(12):2015-31.
90. Sun C, Yang J, Li L, Wu X, Liu Y, Liu S. Advances in the study of luminescence probes for proteins. *Jour of Chroma B*. 2004 Apr 25;803(2):173-90.
91. Tang D, Tang J, Su B, Chen G. Ultrasensitive electrochemical immunoassay of staphylococcal enterotoxin B in food using enzyme-nanosilica-doped carbon

- nanotubes for signal amplification. *Jour of Agric and Food Chem.* 2010 Sep 28;58(20):10824-30.
92. Li J, Gao H. A renewable potentiometric immunosensor based on Fe<sub>3</sub>O<sub>4</sub> nanoparticles immobilized anti-IgG. *Electroanalysis: An Internl Jour Dev to Fundam and Prac Asp of Electroanal.* 2008 Apr;20(8):881-7.
  93. Fu X, Wang J, Li N, Wang L, Pu L. Label-free electrochemical immunoassay of carcinoembryonic antigen in human serum using magnetic nanorods as sensing probes. *Microchimica Acta.* 2009 Jun 1;165(3-4):437-42.
  94. Wang L, Gan X. Antibody-functionalized magnetic nanoparticles for electrochemical immunoassay of  $\alpha$ -1-fetoprotein in human serum. *Microch Acta.* 2009 Jan 1;164(1-2):231.
  95. Rusling JF. Nanomaterials-based electrochemical immunosensors for proteins. *The Chem Rec.* 2012 Feb 10;12(1):164-76.
  96. Kuramitz H. Magnetic microbead-based electrochemical immunoassays. *Anal and Bioanal Chem.* 2009 May 1;394(1):61-9.
  97. Ricci F, Adornetto G, Palleschi G. A review of experimental aspects of electrochemical immunosensors. *Electrochimica Acta.* 2012 Dec 1;84:74-83.
  98. Guesdon JL, Avrameas S. Magnetic solid phase enzyme-immunoassay. *Immunochem.* 1977 Jun 1;14(6):443-7.
  99. Robinson GA, Hill HA, Philo RD, Gear JM, Rattle SJ, Forrest GC. Bioelectrochemical enzyme immunoassay of human choriogonadotropin with magnetic electrodes. *Clin Chem.* 1985 Sep 1;31(9):1449-52.
  100. Oreno-Guzmán M, González-Cortés A, Yáñez-Sedeño P, Pingarrón JM. A disposable electrochemical immunosensor for prolactin involving affinity

- reaction on streptavidin-functionalized magnetic particles. *Anal Chimica Acta*. 2011 Apr 29;692(1-2):125-30.
101. Centi S, Laschi S, Mascini M. Improvement of analytical performances of a disposable electrochemical immunosensor by using magnetic beads. *Talanta*. 2007 Sep 15;73(2):394-9.
  102. Suls J, Jacobs P, Sansen W. A new technique of enzyme entrapment for planar biosensors. *Bios and Bioel*. 1995 Jan 1;10(8):xv-ix.
  103. Zacco E, Pividori MI, Alegret S, Galvé R, Marco MP. Electrochemical magnetoimmunosensing strategy for the detection of pesticides residues. *Anal Chem*. 2006 Mar 15;78(6):1780-8.
  104. Kuramitz H. Magnetic microbead-based electrochemical immunoassays. *Anal and Bioanal Chem*. 2009 May 1;394(1):61-9.
  105. Choi JW, Ahn CH, Bhansali S, Henderson HT. A new magnetic bead-based, filterless bio-separator with planar electromagnet surfaces for integrated bio-detection systems. *Sensors and Actuators B: Chemical*. 2000 Aug 25;68(1-3):34-9.
  106. Choi JW, Oh KW, Thomas JH, Heineman WR, Halsall HB, Nevin JH, Helmicki AJ, Henderson HT, Ahn CH. An integrated microfluidic biochemical detection system for protein analysis with magnetic bead-based sampling capabilities. *Lab on a Chip*. 2002 Feb 7;2(1):27-30.
  107. Sia SK, Whitesides GM. Microfluidic devices fabricated in poly (dimethylsiloxane) for biological studies. *Electroph*. 2003 Nov;24(21):3563-76.
  108. Guber AE, Hecke M, Herrmann D, Muslija A, Saile V, Eichhorn L, Gietzelt T, Hoffmann W, Hauser PC, Tanyanyiwa J, Gerlach A. Microfluidic lab-on-a-

- chip systems based on polymers—fabrication and application. *Chem Eng Jour.* 2004 Aug 1;101(1-3):447-53.
109. Alrifaiy A, Lindahl OA, Ramser K. Polymer-based microfluidic devices for pharmacy, biology and tissue engineering. *Polymers.* 2012 Sep;4(3):1349-98.
  110. Nge PN, Rogers CI, Woolley AT. Advances in microfluidic materials, functions, integration, and applications. *Chem Reviews.* 2013 Feb 14;113(4):2550-83.
  111. Ng JM, Gitlin I, Stroock AD, Whitesides GM. Components for integrated poly (dimethylsiloxane) microfluidic systems. *Electroph.* 2002 Oct;23(20):3461-73.
  112. Eribol P, Uguz AK, Ulgen KO. Screening applications in drug discovery based on microfluidic technology. *Biomicrofl.* 2016 Jan 28;10(1):011502.
  113. Gao Y, Hu G, Lin FY, Sherman PM, Li D. An electrokinetically-controlled immunoassay for simultaneous detection of multiple microbial antigens. *Biomed Microd.* 2005 Dec 1;7(4):301.
  114. Ng AH, Uddayasankar U, Wheeler AR. Immunoassays in microfluidic systems. *Anal and Bioanal Chem.* 2010 Jun 1;397(3):991-1007.
  115. Nhan V. Lab on a chip for multiplexed immunoassays to detect bladder cancer using multifunctional dielectrophoretic manipulations. *Lab on a Chip.* 2015;15(14):3056-64.
  116. Lin FY, Sabri M, Erickson D, Alirezaie J, Li D, Sherman PM. Development of a novel microfluidic immunoassay for the detection of *Helicobacter pylori* infection. *Anal.* 2004;129(9):823-8.
  117. Hanrahan G, Patil DG, Wang J. Electrochemical sensors for environmental monitoring: design, development and applications. *Jour of Environ Monit.* 2004;6(8):657-64.

118. Buffle J, Tercier-Waeber ML. Voltammetric environmental trace-metal analysis and speciation: from laboratory to in situ measurements. *TrAC Tr in Anal Chem.* 2005 Mar 1;24(3):172-91.
119. Namour P, Lepot M, Jaffrezic-Renault N. Recent trends in monitoring of European water framework directive priority substances using micro-sensors: a 2007–2009 review. *Sensors.* 2010 Sep;10(9):7947-78.
120. Li M, Li YT, Li DW, Long YT. Recent developments and applications of screen-printed electrodes in environmental assays—A review. *Anal Chimica Acta.* 2012 Jul 13;734:31-44.
121. Jang A, Zou Z, Lee KK, Ahn CH, Bishop PL. State-of-the-art lab chip sensors for environmental water monitoring. *Meas Sc and Tech.* 2011 Jan 24;22(3):032001.
122. Liu R, Cai Y, Park JM, Ho KM, Shinar J, Shinar R. Organic light-emitting diode sensing platform: Challenges and solutions. *Adv Funct Mat.* 2011 Dec 20;21(24):4744-53.
123. Tsopela A, Laborde A, Salvagnac L, Séguy I, Izquierdo R, Juneau P, Temple-Boyer P, Launay J. Light emitting devices and integrated electrochemical sensors on lab-on-chip for toxicity bioassays based on algal physiology. In 2015 Transducers-2015 18th International Conference on Solid-State Sensors, Actuators and Microsystems (TRANSDUCERS) 2015 Jun 21 (pp. 1621-1624). IEEE.
124. Tsopela A, Laborde A, Salvagnac L, Ventalon V, Bedel-Pereira E, Séguy I, Temple-Boyer P, Juneau P, Izquierdo R, Launay J. Development of a lab-on-chip electrochemical biosensor for water quality analysis based on microalgal photosynthesis. *Bios and Bioelect.* 2016 May 15;79:568-73.

125. Arya SK, Chornokur G, Venugopal M, Bhansali S. Dithiobis (succinimidyl propionate) modified gold microarray electrode based electrochemical immunosensor for ultrasensitive detection of cortisol. *Bios and Bioelect.* 2010 Jun 15;25(10):2296-301.
126. Parker CO, Lanyon YH, Manning M, Arrigan DW, Tothill IE. Electrochemical immunochip sensor for aflatoxin M1 detection. *Anal Chem.* 2009 Jun 2;81(13):5291-8.
127. European Environment Agency. European waters-current status and future challenges: synthesis. Office for Official Publ. of the Europ. Union; 2012.
128. Baklanov A, Hänninen O, Slørdal LH, Kukkonen J, Bjergene N, Fay B, Finardi S, Hoe SC, Jantunen M, Karppinen A, Rasmussen A. Integrated systems for forecasting urban meteorology, air pollution and population exposure. *Atm Chem and Phy.* 2007 Feb 15;7(3):855-74.
129. Latimer JS, Zheng J. and Fate of PAHs in the Marine Environment. *PAHs: An Ecotoxicol Persp.* 2003 Jul 25:9.
130. Menzie CA, Potocki BB, Santodonato J. Exposure to carcinogenic PAHs in the environment. *Environ Sci & Tech.* 1992 Jul;26(7):1278-84.
131. Arey J, Atkinson R. Photochemical reactions of PAHs in the atmosphere. *PAHs: An ecotoxicol persp.* 2003 Mar 14:47-63.
132. Di Toro DM, McGrath JA, Hansen DJ. Technical basis for narcotic chemicals and polycyclic aromatic hydrocarbon criteria. I. Water and tissue. *Environ Toxic and Chem: An International Journal.* 2000 Aug;19(8):1951-70.
133. Kim KH, Jahan SA, Kabir E, Brown RJ. A review of airborne polycyclic aromatic hydrocarbons (PAHs) and their human health effects. *Enviro intl.* 2013 Oct 1;60:71-80.



134. Armstrong B, Hutchinson E, Unwin J, Fletcher T. Lung cancer risk after exposure to polycyclic aromatic hydrocarbons: a review and meta-analysis. *Environ hea persp.* 2004 Apr 7;112(9):970-8.
135. CCME (Canadian Council of Ministers of the Environment).. Canadian soil quality guidelines for potentially carcinogenic and other PAHs: scientific criteria document.
136. Suess MJ. The environmental load and cycle of polycyclic aromatic hydrocarbons. *Sc of the Tot Environ.* 1976 Nov 1;6(3):239-50.
137. Directive C. On the quality of water intended for human consumption. *Off Jour of the Euro Comm.* 1998 Dec 5;330:32-54.
138. Moorthy B, Chu C, Carlin DJ. Polycyclic aromatic hydrocarbons: from metabolism to lung cancer. *Toxic Sc.* 2015 Apr 23;145(1):5-15.
139. Vo-Dinh T, Fetzer J, Campiglia AD. Monitoring and characterization of polyaromatic compounds in the environment. *Talanta.* 1998 Sep 28;47(4):943-69.
140. Ma Y, Harrad S. Spatiotemporal analysis and human exposure assessment on polycyclic aromatic hydrocarbons in indoor air, settled house dust, and diet: A review. *Environ intl.* 2015 Nov 1;84:7-16.
141. Dahlstrom DL, Bloomhuff AB. ACGIH®(American Conference of Governmental Industrial Hygienists).
142. Unwin J, Cocker J, Scobbie E, Chambers H. An assessment of occupational exposure to polycyclic aromatic hydrocarbons in the UK. *Annals of Occupational Hygiene.* 2006 Mar 21;50(4):395-403.

143. Polycyclic aromatic hydrocarbons, selected non-heterocyclic. Available online: <http://www.inchem.org/documents/ehc/ehc/ehc202> (Accessed on 27th November, 2019).
144. Abdel-Shafy HI, Mansour MS. A review on polycyclic aromatic hydrocarbons: source, environmental impact, effect on human health and remediation. Egypt Jour of Petrol. 2016 Mar 1;25(1):107-23.
145. Diggs DL, Huderson AC, Harris KL, Myers JN, Banks LD, Rekhadevi PV, Niaz MS, Ramesh A. Polycyclic aromatic hydrocarbons and digestive tract cancers: a perspective. Jour of environ sc and heal, part c. 2011 Oct 1;29(4):324-57.
146. Olsson AC, Fevotte J, Fletcher T, Cassidy A, Mannetje AT, Zaridze D, Szeszenia-Dabrowska N, Rudnai P, Lissowska J, Fabianova E, Mates D. Occupational exposure to polycyclic aromatic hydrocarbons and lung cancer risk: a multicenter study in Europe. Occl and environ med. 2010 Feb 1;67(2):98-103.
147. Pratt MM, John K, MacLean AB, Afework S, Phillips DH, Poirier MC. Polycyclic aromatic hydrocarbon (PAH) exposure and DNA adduct semi-quantitation in archived human tissues. Interl jour of environ resrch and public health. 2011 Jul;8(7):2675-91.
148. Purcaro G, Moret S, Conte LS. Overview on polycyclic aromatic hydrocarbons: occurrence, legislation and innovative determination in foods. Talanta. 2013 Feb 15;105:292-305.
149. Nowacka A, Włodarczyk-Makula M. Monitoring of polycyclic aromatic hydrocarbons in water during preparation processes. Polycyclic Aromatic Compounds. 2013 Oct 20;33(5):430-50.

150. Plaza-Bolaños P, Frenich AG, Vidal JL. Polycyclic aromatic hydrocarbons in food and beverages. Analytical methods and trends. Jour of Chrom A. 2010 Oct 8;1217(41):6303-26.
151. de Boer J, Law RJ. Developments in the use of chromatographic techniques in marine laboratories for the determination of halogenated contaminants and polycyclic aromatic hydrocarbons. Jour of Chrom A. 2003 Jun 6;1000(1-2):223-51.
152. Lux G, Langer A, Pschenitza M, Karsunke X, Strasser R, Niessner R, Knopp D, Rant U. Detection of the carcinogenic water pollutant benzo [a] pyrene with an electro-switchable biosurface. Anal Chem. 2015 Apr 10;87(8):4538-45.
153. Zhang L, Duan D, Liu Y, Ge C, Cui X, Sun J, Fang J. Highly selective off-on fluorescent probe for imaging thioredoxin reductase in living cells. Jour of the Amer Chem Society. 2013 Dec 18;136(1):226-33.
154. Molaei S, Saleh A, Ghoulipour V, Seidi S. Centrifuge-less Emulsification Microextraction Using Effervescent CO<sub>2</sub> Tablet for On-site Extraction of PAHs in Water Samples Prior to GC-MS Detection. Chrom. 2016 May 1;79(9-10):629-40.
155. Manoli E, Kouras A, Samara C. Profile analysis of ambient and source emitted particle-bound polycyclic aromatic hydrocarbons from three sites in northern Greece. Chemos. 2004 Sep 1;56(9):867-78.
156. Mostert MM, Ayoko GA, Kokot S. Application of chemometrics to analysis of soil pollutants. TrAC Trends in Anal Chem. 2010 May 1;29(5):430-45.
157. Vo-Dinh T, Fetzer J, Campiglia AD. Monitoring and characterization of polyaromatic compounds in the environment. Talanta. 1998 Sep 28;47(4):943-69.

158. Hund K, Traunspurger W. Ecotox-evaluation strategy for soil bioremediation exemplified for a PAH-contaminated site. *Chemos*. 1994 Jul 1;29(2):371-90.
159. Hwang HM, Wade TL, Sericano JL. Concentrations and source characterization of polycyclic aromatic hydrocarbons in pine needles from Korea, Mexico, and United States. *Atmos Env*. 2003 May 1;37(16):2259-67.
160. Kielhorn J, Boehncke A. Polynuclear aromatic hydrocarbons. Guidelines for drinking-water quality, Addendum to Vol. 2. Health criteria and other supporting information. 1998:123-52.
161. Hamza-Chaffai A. Usefulness of bioindicators and biomarkers in pollution biomonitoring. *Internl Jour of Biotech for Wellness Industr*. 2014 Apr 15;3(1):19-26.
162. Del Carlo M, Di Marcello M, Perugini M, Ponzielli V, Sergi M, Mascini M, Compagnone D. Electrochemical DNA biosensor for polycyclic aromatic hydrocarbon detection. *Microchimica Acta*. 2008 Oct 1;163(3-4):163-9.
163. Gu MB, Chang ST. Soil biosensor for the detection of PAH toxicity using an immobilized recombinant bacterium and a biosurfactant. *Bios and Bioelect*. 2001 Dec 1;16(9-12):667-74.
164. Song Y, Jiang B, Tian S, Tang H, Liu Z, Li C, Jia J, Huang WE, Zhang X, Li G. A whole-cell bioreporter approach for the genotoxicity assessment of bioavailability of toxic compounds in contaminated soil in China. *Environ Pollut*. 2014 Dec 1;195:178-84.
165. Jones JM, Anderson JW, Tukey RH. Using the metabolism of PAHs in a human cell line to characterize environmental samples. *Environ Tox and Pharma*. 2000 Jan 1;8(2):119-26.

166. Fent K. Fish cell lines as versatile tools in ecotoxicology: assessment of cytotoxicity, cytochrome P4501A induction potential and estrogenic activity of chemicals and environmental samples. *Toxi in Vitro*. 2001 Aug 1;15(4-5):477-88.
167. Butler GJ, Neale R, Green AC, Pandeya N, Whiteman DC. Nonsteroidal anti-inflammatory drugs and the risk of actinic keratoses and squamous cell cancers of the skin. *Jour of the Amer Acad of Dermat*. 2005 Dec 1;53(6):966-72.
168. Ahmad A, Moore EJ. Comparison of cell-based biosensors with traditional analytical techniques for cytotoxicity monitoring and screening of polycyclic aromatic hydrocarbons in the environment. *Anal Letters*. 2009 Jan 20;42(1):1-28.
169. Zheng X, Tian D, Duan S, Wei M, Liu S, Zhou C, Li Q, Wu G. Polypyrrole composite film for highly sensitive and selective electrochemical determination sensors. *Electroch Acta*. 2014 Jun 1;130:187-93.
170. Lin M, Liu Y, Sun Z, Zhang S, Yang Z, Ni C. Electrochemical immunoassay of benzo [a] pyrene based on dual amplification strategy of electron-accelerated Fe<sub>3</sub>O<sub>4</sub>/polyaniline platform and multi-enzyme-functionalized carbon sphere label. *Anal Chimica Acta*. 2012 Apr 13;722:100-6.
171. Wei MY, Wen SD, Yang XQ, Guo LH. Development of redox-labeled electrochemical immunoassay for polycyclic aromatic hydrocarbons with controlled surface modification and catalytic voltammetric detection. *Bios and Bioelect*. 2009 May 15;24(9):2909-14.
172. Li K, Chen R, Zhao B, Liu M, Karu AE, Roberts VA, Li QX. Monoclonal antibody-based ELISAs for part-per-billion determination of polycyclic

- aromatic hydrocarbons: effects of haptens and formats on sensitivity and specificity. *Anal Chem.* 1999 Jan 15;71(2):302-9.
173. Székács A, Le HM, Knopp D, Niessner R. A modified enzyme-linked immunosorbent assay (ELISA) for polycyclic aromatic hydrocarbons. *Anal Chimica Acta.* 1999 Nov 8;399(1-2):127-34.
  174. Meng XY, Li YS, Zhou Y, Zhang YY, Yang L, Qiao B, Wang NN, Hu P, Lu SY, Ren HL, Liu ZS. An enzyme-linked immunosorbent assay for detection of pyrene and related polycyclic aromatic hydrocarbons. *Anal Biochem.* 2015 Mar 15;473:1-6.
  175. Gomes M, Santella RM. Immunologic methods for the detection of benzo [a] pyrene metabolites in urine. *Chem Resrch in Tox.* 1990 Jul;3(4):307-10.
  176. Scharnweber T, Fisher M, Suchanek M, Knopp D, Niessner R. Monoclonal antibody to polycyclic aromatic hydrocarbons based on a new benzo [a] pyrene immunogen. *Fresenius' Jour of Anal Chem.* 2001 Nov 1;371(5):578-85.
  177. Scharnweber T, Fisher M, Suchanek M, Knopp D, Niessner R. Monoclonal antibody to polycyclic aromatic hydrocarbons based on a new benzo [a] pyrene immunogen. *Fresenius' Jour of Anal Chem.* 2001 Nov 1;371(5):578-85.
  178. Karsunke XY, Pschenitza M, Rieger M, Weber E, Niessner R, Knopp D. Screening and characterization of new monoclonal anti-benzo [a] pyrene antibodies using automated flow-through microarray technology. *Jour of Immuno met.* 2011 Aug 31;371(1-2):81-90.
  179. Karsunke XY, Wang H, Weber E, McLean MD, Niessner R, Hall JC, Knopp D. Development of single-chain variable fragment (scFv) antibodies against hapten benzo [a] pyrene: a binding study. *Anal and Bioanal Chem.* 2012 Jan 1;402(1):499-507.

180. Ius A, Bacigalupo MA, Roda A, Vaccari C. 006 Development of a time-resolved fluoroimmunoassay of benzo (a) pyrene in water. *Fresenius' Jour of Anal Chem.* 1992 Jan 1;343(1):55-6.
181. Roda A, Bacigalupo MA, Ius A, Minutello A. Development and applications of an ultrasensitive quantitative enzyme immuno-assay for benzo (a) pyrene in environmental samples. *Environ Tech.* 1991 Nov 1;12(11):1027-35.
182. Roda A, Simoni P, Mirasoli M, Baraldini M, Violante SF. Development of a chemiluminescent enzyme immunoassay for urinary 1-hydroxypyrene. *Anal and Bioanal Chem.* 2002 Apr 1;372(7-8):751-8.
183. Kusnezow W, Hoheisel JD. Solid supports for microarray immunoassays. *Jour of Molec Recog.* 2003 Jul;16(4):165-76.
184. Angenendt P. Progress in protein and antibody microarray technology. *Drug Disc Today.* 2005 Apr 1;10(7):503-11.
185. Liu Y, Li CM. Advanced immobilization and amplification for high performance protein chips. *Anal Letters.* 2012 Jan 1;45(2-3):130-55.
186. Bonroy K, Frederix F, Reekmans G, Dewolf E, De Palma R, Borghs G, Declerck P, Goddeeris B. Comparison of random and oriented immobilisation of antibody fragments on mixed self-assembled monolayers. *Jour of Immuno Met.* 2006 May 30;312(1-2):167-81.
187. Wong LS, Khan F, Micklefield J. Selective covalent protein immobilization: strategies and applications. *Chem Reviews.* 2009 Jul 2;109(9):4025-53.
188. Marco MP, Gee S, Hammock BD. Immunochemical techniques for environmental analysis II. Antibody production and immunoassay development. *Trends in Anal Chem.* 1995 Sep 1;14(8):415-25.

189. Singh KV, Kaur J, Varshney GC, Raje M, Suri CR. Synthesis and characterization of hapten– protein conjugates for antibody production against small molecules. *Biocon Chem.* 2004 Jan 21;15(1):168-73.
190. Chan EC, Ho PC. Preparation and characterization of immunogens for antibody production against metanephrine and normetanephrine. *Jour of Immuno Met.* 2002 Aug 1;266(1-2):143-54.
191. ZHANG YF, GAO ZX, SUN HW, DAI SG. Characterization of hapten-protein conjugates for immunoassay of polycyclic aromatic hydrocarbons (PAHs). *Chem Resrch in Chinese Uni.* 2008 Nov 1;24(6):697-700.
192. Fähnrich KA, Pravda M, Guilbault GG. Immunochemical detection of polycyclic aromatic hydrocarbons (PAHs). *Anal Letters.* 2002 May 8;35(8):1269-300.
193. EMON JM, Gerlach CL. A status report on field-portable immunoassay. *Environ Sc & Tech.* 1995 Jul 1;29(7):312A-7A.
194. Krämer PM. A strategy to validate immunoassay test kits for TNT and PAHs as a field screening method for contaminated sites in Germany. *Anal Chimica Acta.* 1998 Dec 4;376(1):3-11.
195. Zhang H, Wang S, Fang G. Applications and recent developments of multi-analyte simultaneous analysis by enzyme-linked immunosorbent assays. *Jour of Immuno Met.* 2011 May 31;368(1-2):1-23.
196. Zhang H, Wang S, Fang G. Applications and recent developments of multi-analyte simultaneous analysis by enzyme-linked immunosorbent assays. *Jour of Immuno Met.* 2011 May 31;368(1-2):1-23.
197. Xu ZL, Xie GM, Li YX, Wang BF, Beier RC, Lei HT, Wang H, Shen YD, Sun YM. Production and characterization of a broad-specificity polyclonal



- antibody for O, O-diethyl organophosphorus pesticides and a quantitative structure–activity relationship study of antibody recognition. *Anal Chimica Acta*. 2009 Aug 4;647(1):90-6.
198. Xu ZL, Shen YD, Beier RC, Yang JY, Lei HT, Wang H, Sun YM. Application of computer-assisted molecular modeling for immunoassay of low molecular weight food contaminants: A review. *Anal Chimica Acta*. 2009 Aug 11;647(2):125-36.
199. Yuan M, Liu B, Liu E, Sheng W, Zhang Y, Crossan A, Kennedy I, Wang S. Immunoassay for phenylurea herbicides: application of molecular modeling and quantitative structure–activity relationship analysis on an antigen–antibody interaction study. *Anal Chem*. 2011 May 16;83(12):4767-74.
200. Liu YH, Jin MJ, Gui WJ, Cheng JL, Guo YR, Zhu GN. Hapten design and indirect competitive immunoassay for parathion determination: Correlation with molecular modeling and principal component analysis. *Anal Chimica Acta*. 2007 May 22;591(2):173-82.
201. Delaunay-Bertoncini N, Pichon V, Hennion MC. Experimental comparison of three monoclonal antibodies for the class-selective immunoextraction of triazines: Correlation with molecular modeling and principal component analysis studies. *Jour of Chromat A*. 2003 May 30;999(1-2):3-15.
202. Nording M, Haglund P. Evaluation of the structure/cross-reactivity relationship of polycyclic aromatic compounds using an enzyme-linked immunosorbent assay kit. *Anal Chimica Acta*. 2003 Jul 1;487(1):43-50.
203. Zhang YF, Ma Y, Gao ZX, Dai SG. Predicting the cross-reactivities of polycyclic aromatic hydrocarbons in ELISA by regression analysis and CoMFA methods. *Anal and Bioanal Chem*. 2010 Jul 1;397(6):2551-7.

204. Zhang YF, Zhang L, Gao ZX, Dai SG. Investigating the quantitative structure-activity relationships for antibody recognition of two immunoassays for polycyclic aromatic hydrocarbons by multiple regression methods. *Sensors*. 2012 Jul;12(7):9363-74.
205. Cronin MT, Schultz TW. Pitfalls in QSAR. *Journal of Molecular Structure: Theochem*. 2003 Mar 7;622(1-2):39-51.
206. Pellequer JL, Chen SW, Keum YS, Karu AE, Li QX, Roberts VA. Structural basis for preferential binding of non-ortho-substituted polychlorinated biphenyls by the monoclonal antibody S2B1. *Jour of Molec Recog: An Interdiscp Jour*. 2005 Jun;18(4):282-94.

**Chapter 2:**

**Immunoassay protocols**

**(ELISA)**



## **2.1 Introduction**

Immunoassays measure the presence of target that is present at low concentration. The focus of this chapter is on the immunoassay of PAHs. Immunoassays use bioanalytical processes in the detection of analytes, such as lipids, carbohydrates, and proteins in solutions by means of the interaction of an antibody (immunoglobulins (Ig)).

## **2.2 Objective**

The main aim of the presented work was to study an immunoassay method based on (ELISA) for the detecting of PAHs in environmental monitoring of drinking water. In particular, the research focused on measuring the presence and concentration of (BaP) in drinking water. Heterogeneous immunoassays were used for all ELISA formats. Incubation and washing steps were conducted in heterogeneous immunoassay multiple mixing. The properties of the analyte to be detected and the sensitivity of the assays must be considered in order to carry out the competitive or non-competitive assays. In this study the heterogeneous immunoassay was subdivided into competitive or non-competitive assays. With regard to competitive assays, the labelled antigen and the antigen to be analysed compete to attach to the immobilized antibody. In non-competitive assays, the antigens bind to the excess of the immobilized antibodies, which are on the solid surface and are detected after binding to the secondary antibodies. The typical response curves for these assays can be directly or indirectly proportional to the concentration of the antigen in the sample. The optimisation of different reagents and conditions was carried out to ensure the accuracy, sensitivity and specificity of the immunoassay assays. To immobilise the immunoreactants, the assays took place in a 96-well ELISA microplate.

The ELISA microplates were used as solid surfaces for immunoreactions. The microplate was made from hydrophobic polystyrene (PS) with flat bottom. This type

of plate was used in order to minimize edge effects and to ensure optimal optical conditions for data collection. The antigens were screened via ELISA technique using the 96-well ELISA plat reader. The detection approach used was an enzymatic labeled signaling system. Colourimetry technique was used to measure the yellow coloured product in a solution. Upon enzymatic reaction, chromogenic substrates produced coloured compounds. Spectrophotometer (absorbance plate reader) at 405 nm read the absorbance signal. The wavelength depends on the type of the substrate and the enzyme label used in the ELISA technique. In this study a *p*-nitrophenyl phosphate (*p*NPP) substrate and an alkaline phosphatase (AP) label enzyme were applied for all optical assays. A *p*-nitrophenyl phosphate (*p*NPP) substrate is non-toxic and remains stable for many months at 4<sup>0</sup>C .It is used for detecting alkaline phosphatase (AP) label enzyme in ELISA experiments. Alkaline phosphatase (AP) label enzyme has a high specific activity, stability for long periods in appropriate storage condition and inexpensive reagent. Alkaline phosphatase (AP) label enzyme also has also a low background and reaction rates, which increases sensitivity over the incubation periods. The substrate chosen for detection of AP enzyme activity was *p*NPP that dephosphorylates into (*p*NP), a soluble chromophore with a maximum molar extinction coefficient at 405 nm under alkaline conditions.

## **2.3 Experimental**

### **2.3.1 Materials:**

For the synthesis of BSA-PHEN coating conjugate: bovine serum albumin (BSA), adipic acid dihydrazide (AAD), phosphate buffered saline (PBS), 1-ethyl-3-(3-dimethylaminopropyl) carbodiimide (EDAC), diethanolamine dimethyl sulfoxide (DMSO), phenanthrene-9-carboxaldehyde, sodium cyanoborohydride (NaCNBH<sub>4</sub>) , sodium hydroxide were bought from Sigma (Dublin, Ireland). In order to adjust pH, hydrochloric acid (HCL) 37% was bought from KMG ULTRA CHEMICALS LTD

(England) and sodium hydroxide (NaOH) was bought from Sigma (Dublin, Ireland). Monoclonal mouse antibody 4D5 specific to BaP was bought from Santa Cruz (Heidelberg, Germany). Sodium hydrogen carbonate, sodium chloride, detergent Tween-20, Tris salt, BaP, alkaline phosphatase (AP) labelled goat anti-mouse antibodies (whole molecule), a *p*-nitrophenyl phosphate (*p*NPP) substrate agent and diethanolamine reagent (DEA) were all purchased from Sigma (Dublin, Ireland). All reagents were of analytical grade or better and any water used in the solutions was nanopure water. A Micro BCA™ Protein Assay Reagent kit was provided by Pierce (Rockford, IL). In order to ensure optical detection a standard 96 well ELISA microplate was bought from Greiner bio-one (Germany).

### **2.3.2 Instrumentations:**

Slide-A-Lyzer™ Dialysis cassettes 10K (0.5-3 ml) from Thermo Scientific were used for the purification of proteins. For ELISA applications, EL Read 2000 microplate reader was provided by biochrom.co.UK. For incubation, a Biometra OV3 Incubator (Gottingen, Germany) was set at 37 °C.

### **2.3.3 Procedures.**

#### **2.3.3.1 Preparation of phenanthrene-protein coating conjugate**

Bioconjugation is a method to link and combine two biomolecules to form a complex that can be used as a detecting probe in ELISA. The use of a coating conjugate was necessary because the small molecule Benzo[a]pyrene (BaP) is non-immunogenic, and therefore does not induce an immune response unless coupled with macromolecules such as bovine serum albumin (BSA) protein. Coating conjugate was a method to combine more biomolecules to form a complex that could be used as a detecting probe in the immunoassay.

The preparation procedure of the coating conjugate (carbodiimide method) has been published [1]. It consists of the following steps:

- 1) The BSA (carrier) was covalently coupled with the hapten phenanthrene-9-carboxaldehyde and adipic acid dihydrazide (AAD) was used to activate the BSA agent.
- 2) Adipic acid dihydrazide (79.8 mg) was dissolved in (2400  $\mu$ l) phosphate buffered saline (PBS, pH 7.4) under a fume hood.
- 3) 24 mg of BSA was mixed with 1386.4 mg of EDAC and added to the AAD solution.
- 4) The resultant mixture was placed in ice and stirred for 4 h using a magnetic stirrer in the fume hood.
- 5) The coating conjugate solution was inserted into Slide-A-Lyzer<sup>TM</sup> using a disposable syringe. Dialysis cassettes of 10kDa MWCO (0.5-3 ml) were used and the cassette were immersed in PBS buffer for 2 hours with 3 changes of fresh buffer of 750 ml each.
- 6) A volume of 1800  $\mu$ l of the obtained conjugate solution was mixed with a freshly made dilution of phenanthrene-9- carboxaldehyde (0.6 mg) in 1200  $\mu$ l dimethyl sulfoxide (DMSO), and was left to react for 2 hours at room temperature under the fume hood.
- 7) A preparation of 24  $\mu$ l of NaCNBH<sub>4</sub> (5 M) in NaOH (1 M) was then added to the solution previously obtained and left to mix for 1 hour. This solution was purified in a dialysis cassette as explained in the previous step. The resultant solution was the final coating conjugate (Figure 2.1).



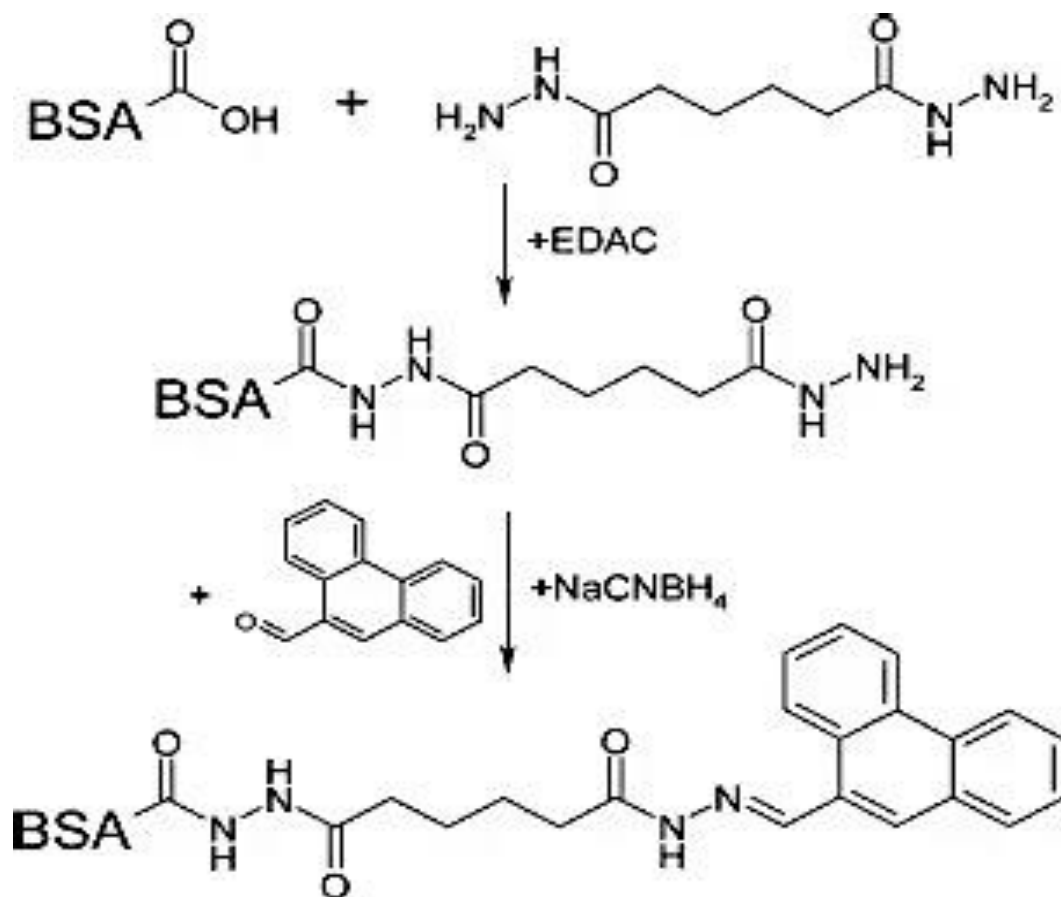


Figure 2.1: Schematic of preparation of coating conjugate. The crosslinker EDAC helps the coupling of AAD with the BSA hydroxyl group. This combination provides the coating conjugate with amine groups, where finally hapten phenanthrene-9- carboxaldehyde binds.

### 2.3.3.2 Matrix Assisted Laser Desorption ionization / mass spectrometer (MALDI-TOF /MS) test for determination of the average PHE to BSA ratio:

- **Required items:**

- 1) A sample to be analyzed (a coating conjugate BSA-PHEN).

A matrix substance  $\alpha$ -Cyano-4-hydroxycinnamic acid (Bruker Matrix HCCA).

$\alpha$ -Cyano-4-hydroxycinnamic acid was used as matrix in developing the detection of low concentration protein digests on MALDI-TOF.

- **Principle:**

Matrix Assisted Laser Desorption ionization / mass spectrometer (MALDI-TOF /MS) is a soft ionization method where the sample (a coating conjugate BSA-PHEN) is mixed in a matrix (Bruker Matrix HCCA) and then the matrix absorbs the laser light energy at a certain wavelength (Figure 2.2). The wavelength is dependent upon the type of the sample. The matrix transforms the laser energy into excitation energy, which then heats the surface of matrix. The result from the heating surface is photons and then collect, analyze and detect the resulting ions.

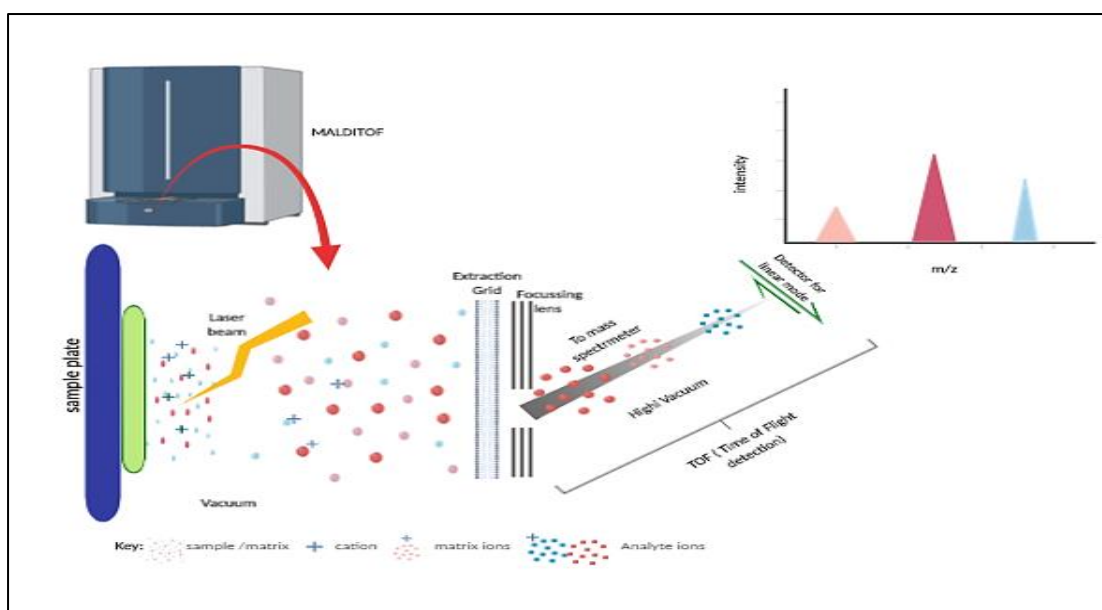


Figure 2.2: Mass analyser- Mechanism of TOF where separates ions according to their mass (m)-to charge (z) ( $m/z$ ) ratios

- **Sample preparation required: For the measurements of the coating conjugate ratio.**

The first step was synthesis of coating conjugate (BSA-PHEN) as it described in the previous section (from step 1 to step 5). From the step 6 a five different concentrations were prepared. A volume of 1800  $\mu\text{l}$  all of the obtained conjugate solution was mixed with a freshly made dilution of phenanthrene-9- carboxaldehyde ( $C_1=0.5$ ,  $C_2=0.125$ ,  $C_3=0.062$ ) mg/ml in 1200  $\mu\text{l}$  dimethyl sulfoxide (DMSO).

It was left to react for 2 hours at room temperature under the fume hood. As in step 7 the same process was done for all dilutions.

- **The protocol of MALDI-TOF / mass spectrometry (MS) test.**

The first step of the MALDI preparation was to mix the sample and matrix solutions in a suitable ratio. The matrix was able to embed and isolate the sample. The selection of the matrix was suitable for the molecular weight of the protein to be analyzed. The aliquoted samples were defrosted and mixed on the target plate as a thin film. 1µl was taken from each sample and allowed to dry at room temperature. (If the matrix was not added to the sample within 30 min it could not be used). The sample was overlaid on sample spot with 1ul of HCCA and allowed to dry. A homogeneous preparation had to be observed. MALDI-TOF-MS samples were examined using the Broker Biotyper Microflex LT. The samples were analyzed using flexcontrol software. The mass range used was 19 kDa to 121 kDa. The samples were analyzed in a linear mode (4.4 x 2776v). The mode of ionization was singly charged ions. Positive ion detection was used because of the sample had a protein with a functional group (amines). Positive ion detection is where the sample accepts a proton ( $H^+$ ). Various frequencies of the laser to detect any peaks were applied; the frequency of 240Hz was where it found the information. There were 240 shots added for each successful run.

### **2.3.3.3 Immunoassay buffer solutions:**

Suitable buffer solutions for immunoassay development in this research were produced in house to minimize non-specific binding. Buffers were used to protect the proteins activity against degradation or denaturation of the material. Antibodies may bind to other proteins with lower affinities. These non-specific interactions can be removed by a number of different approaches. The addition of surfactants approach such as Tween-20 decreases hydrophobic interactions. Non-specific binding and matrix effects can have a background noise and using washing and blocking solutions

can help to remove this background noise. 1 M HCL and 1 M NaOH were used for adjusting the pH of all buffers.

#### 2.3.3.4 Checkerboard ELISA protocol of immunoassays reagents:

A checkerboard ELISA involves different dilutions of each reagent used against each other on the microplate wells in order to obtain the optimal dilution values of reagent concentrations (Figure 2.3). The capture was a mouse monoclonal and the detection antibody was an anti-mouse secondary antibody. The species of capture antibody is raised and should be different from the species of our sample. The species of these antibodies were different in order to prevent cross-reactivity from the detection antibody with sample. A capture antibody always binds to the target antigen; therefore, detection antibody should be directed against the species of the capture antibody.

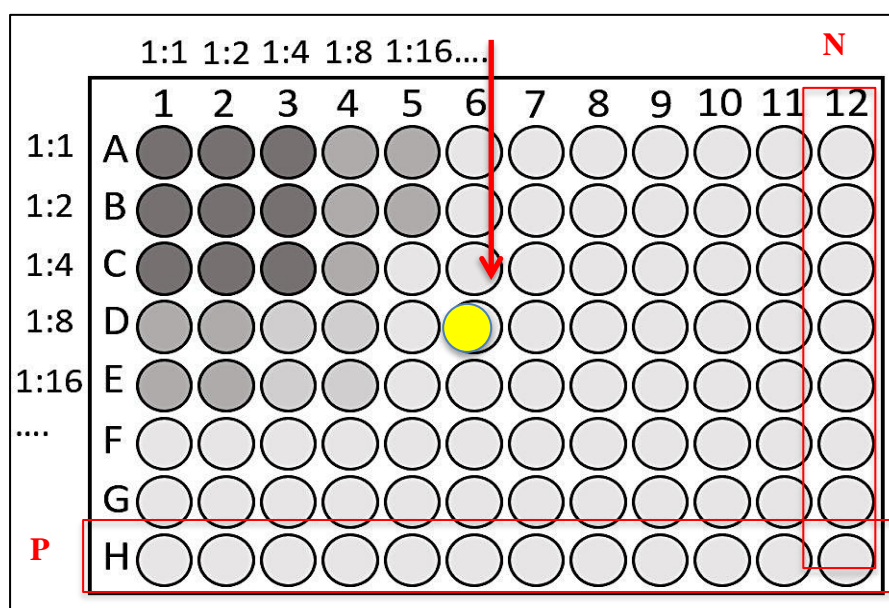


Figure 2.3: checkerboard capture assay was performed with different concentration of the capture antibody and the detection antibody. Each column 1-12 contains a capture antibody dilution factor. Each row A-H contains a detection antibody dilution factor.

#### • Reagents required:

1) The detection limit of the assay depends on the affinity of the chosen antibody. The antibody at the plate should be the one with the highest affinity and provide the most

sensitive detection. Monoclonal mouse antibody (4D5 specific to BaP) was used at the desired concentration in bicarbonate/carbonate buffer (10 µg/ml). The recommended coating concentration should be between 1 to 10 µg/ml because of the protein-binding capacity of 100-400 ng/cm<sup>2</sup>. ELISA plate captures around 100–400 ng of IgG/cm<sup>2</sup>. This is commercially available as high-binding plate. Typical coating conditions involve adding 50-100 µl of buffer, containing antigen or antibody at a concentration of 1-10 µg/ml, and incubating overnight at 4°C or for 1 hour at 37°C.

2) Detection antibody (alkaline phosphatase (AP) labelled goat anti-mouse antibodies) was at desired concentration 1/1000 dilution.

3) Washing buffer (Tris 50 mM+0.05 % Tween 20). Tween-20 reduces nonspecific binding by blocking unreacted sites and retaining protein structure.

4) Blocking reagent (1% BSA in Tris 0.05M buffer solution) was used to reduce the non-specific binding of detection antibodies to the plate surface itself. The blocking buffer had an unrelated protein that did not react with any of the antibodies that were used in the detection step.

5) Colour producing substrate (a *p*-nitrophenyl phosphate (*p*NPP) substrate agent in DEA buffer 0.1 M). Diethanolamine (DEA) buffer has favourable reaction kinetics and good sensitivity compared to most buffer immunoassays.

6) Incubation times of 1 hour at 37°C, or overnight at 4°C or of 2 hours at room temperature to ensure optimal performance and reproducibility of the assay.

- **The protocol of checkerboard ELISA**

1) Bicarbonate/carbonate buffer (100 µL) was added to each well of the microplate. Then, using a multichannel pipette. 100 µL of the capture antibody solution into each well in column 1. The solution was pipetted up and down in order to mix it correctly. Using new tips, 100 µL from each well in column 1 was added to column 2. This process was repeated until column 11 was reached.

Column 12 was a positive control (no capture antibody).

2) The plate was incubated at 37°C for 1 hour in order to allow the capture antibody to bind to the microplate. Adsorption took place passively due to hydrophobic interactions between the amino acids side chains on the capture antibody used for coating and the microplate surface. It was key to put the plate in a moist condition in order to minimise evaporation.

3) The volume of blocking solution used was 250 µl. This was incubated at 37°C for 1 hour in order to fully block the plate.

4) The plate was washed with 3XTris (300 µl) per well. The microplate was blotted dry using clean tissue.

5) 100-µl blocking buffer solution was added to all the wells in the 96-well plate. In this stage the previous blocking buffer, which was used for the blocking step, was also used to dilute the detection antibody.

6) The detection antibody was diluted in a separate vial before being added to the plate. 100 µL of the detection antibody solution was added into each well in row A. The solution was pipetted up and down in order to mix it correctly. Using new tips, 100 µL from each well in row A was added to row B. This process was repeated until row G was reached. Row H was a negative control (no detection antibody).

7) The microplate was incubated and washed. A *p*-nitrophenyl phosphate (*p*NPP) substrate agent was added, a signal was generated and the absorbance of the solution in microplate was read on EL Read 2000 microplate reader at the wavelength 405 nm.

#### **2.3.3.5 Optimisation of AP Labelling**

The aim of this experiment was to develop an optical immunoassay using the microplate for optimising of AP labelling. The monoclonal mouse antibody 4D5 specific to BaP at desired concentration was incubated at 37°C for 1 hour in bicarbonate/carbonate buffer. This test was performed using capture assay. Then the

microplate was blocked by blocking solution and incubated at 37°C for 1 hour and washed. Six different dilutions (1: 1000, 1:3000, 1:5000, 1:7000, 1:9000 and 1:11000) were prepared in triplicate (n=3) in order to maximise the optimal dilution for the immunoassay. The plate then was incubated at 37°C for 1 hour and washed. The final step of the immunoassay was the addition of (*p*NPP) substrate agent; microplate reader at the wavelength 405 nm generated the signal. The optimal dilution was chosen for carrying out the further immunoassays.

#### **2.3.3.6 Antibody immobilisation time**

This experiment was carried out in order to achieve the optimal immobilization time of monoclonal mouse antibody 4D5 specific to BaP (capture antibody) at the desired concentration onto the microplate. Five different immobilization times (20 min, 30 min, 40 min, 50 min and 60 min) between the monoclonal mouse antibody and the plate were tested in triplicates (n=3) in order to optimize the immobilization time of the immunoassay. The plate was incubated for 1 hour at 37°C. Then the detection antibody solution (1/3000) was added. As was the case with the all the pervious experiments, the final immunoassay steps were repeated.

#### **2.3.3.7 Capture assay: monoclonal mouse antibody 4D5 specific to BaP concentration:**

50 µl of the previously obtained coating conjugate (BSA-PHEN, concentration 6.0 µg/ml) was added to each well of the microplate and allowed to bind for 60 minutes at 37 °C. The microplate was washed with Tris 0.05 M + 0.05 % Tween 20 (pH 7.4) three times to remove any unbound coating, and dried on a clean tissue. 200 µl of blocking solution Tris 0.05 M (pH 7.4) was added to all wells of the microplate to reduce background interferences. The treated wells were left to incubate for 60 minutes at 37 °C. The wells were washed with Tris 0.05 M +0.05 % Tween 20 (pH 7.4) 3 times to remove unbound materials from the previous step. For the primary antibody step, a

serial dilution of monoclonal mouse 4D5 antibody in 10 different concentrations was prepared. 50  $\mu$ l of each concentration was applied to the wells and allowed to bind for 60 minutes at 37 °C. The wells were washed with Tris 0.05M +0.05 % Tween 20 (pH 7.4) 3 times to remove unbound materials of previous step and dried on a clean tissue. Finally, 50ul of AP labeled antibody dilution (anti-mouse IgG, 1/3000 dilution) were added to each well of the microplate, and the wells were incubated for 60 minutes at 37 °C.

Before the incubation, the wells were washed with Tris 0.05 M +0.05 % Tween 20 (pH 7.4) three times and dried on a clean tissue. After the last step of the capture assay was completed, the microplate was introduced to the spectrophotometric reader. Absorbance was measured for the AP label reaction and a solution of the substrate *p*NPP in Diethanolamine buffer (DEA, 0.1 M, pH 9.5) at 405 nm. The optimal concentration was chosen to carry out the immunoassays. The diagram for capture assay is shown in Figure 2.4.

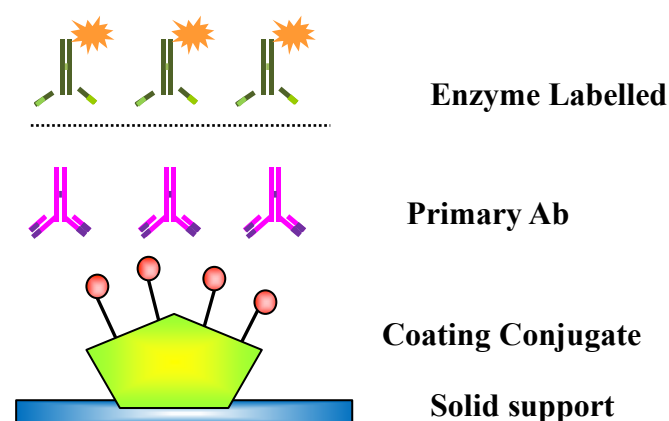


Figure 2.4 Capture assay

#### 2.3.3.8 Displacement assay on microplate:

In this assay the target analyte binds to the primary antibody (in our case 4D5 mAb) and displaces it from the surface of the microplate. The amount of the antibodies left



in the wells will attach to the secondary antibody, in our case the AP labelled anti-IgG. Optimized values of each reagent concentration (see previous sections) were carried out for each well. A serial dilution of the analyte under test (BaP in DMSO) was prepared by using blocking buffer (Tris 0.05 M). Three replicates were carried out for each concentration of BaP (n=3). The prepared microplate was introduced to the spectrophotometric reader in order to measure individual responses at 405 nm. The diagram for indirect displacement assay is shown in Figure 2.5.

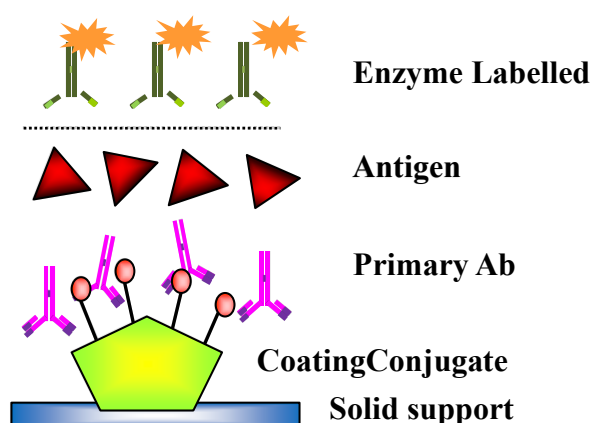


Figure 2.5: Displacement assay

### 2.3.3.9 Use of a spiked sample

Drinkable water was collected from LSI lab in Tyndall national institute. Sensitivity of the assay was measured by analysing a triplicate of water sample using a displacement assay. For recovery experiment, the known amount of BaP was spiked in the tap water sample. Spiked sample was prepared in blocking solution at three different dilutions; 10,50,100 ng/ml of BaP.

## 2.4 Results and Discussion:

### 2.4.1 Development of immunoassay protocol

The main aim of this work was to develop an optical immunoassay using microplate for the detection of Benzo[a]pyrene (BaP) in drinking water. In this study, optimizations of different reagents were performed on the wells in order to obtain the

optimal concentration for a maximum antibody-antigen affinity. We chose a displacement assay form as it allowed us to reach low limits of detection and to obtain good assay sensitivity. This format is commonly used when the antigen is small and non immunogenic. Optimisation of immunoassay working reagents was individually done and then studied the response of the system before reaching the saturation. Optimisation of the assay was achieved through using the following criteria: concentrations of coating conjugate, checkerboard ELISA, antibody immobilisation time, optimisation of AP labelling and optimisation of monoclonal mouse antibody concentration: The following subsections will describe the results obtained in detail and link it to the final displacement assay used.

#### **2.4.2 Optimisation of buffer solutions**

In the previous immunoassay research conducted by our group, the influence of several immunoassay parameters was prepared and studied in order to obtain the optimal conditions for the immunoassay measurements. These include the pH of immunoassay buffers, incubation time and the PAH solvents. In addition, the optimum concentration of each immunoreactant has been studied resulting in maximum antigen-antibody affinity reactions. In this research the same immunoassay buffers and conditions were utilized and results were as predicted. The most suitable blocking solution buffer was 1% BSA. It showed a good ability to block the free sites on the solid surface. The presence of the blocking agents can reduce the steric hindrance and denaturation of the proteins bound to the surface. PAH is insoluble in water and lipophilic compound and for dilution PAHs the most suitable organic solvent found was DMSO. It showed a better response with a high sensitivity and limit of detection when studied in comparison with different organic solvents such as acetone and methanol. In order to achieve the maximum enzyme activity, the enzyme used in this research worked best in alkaline environment and a pH range of pH 7-9 was used for the substrate.

### 2.4.3 Optimisation of coating conjugate

The concentration of the carrier protein BSA was determined using A Micro BCA™ kit. The concentration of the protein sample was determined on a 96 well ELISA microplate. The typical behaviour of a standard protein curve measured at the wavelength 590 nm means that, if the carrier protein concentration increases, the absorbance (optical density) would increase linearly (Figure 2.6). The concentration of BSA sample in the ready coating conjugate was calculated based on the standard curve of the protein. The total concentration of coating conjugate sample was 0.163 mg/ml.

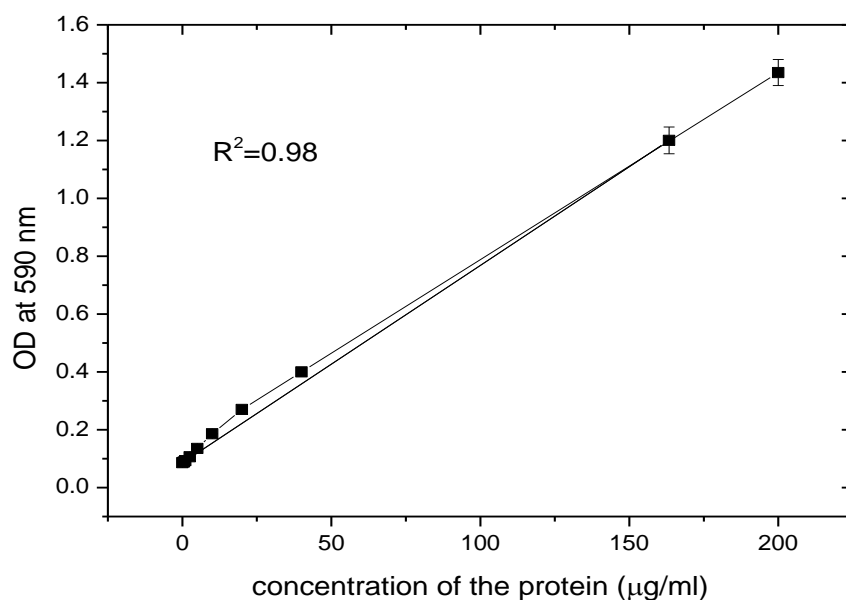


Figure 2.6: The serial dilution of the protein sample was performed on a 96 well ELISA microplate. The typical behaviour of a protein curve measured at 590 nm (n=2).

The concentration of the hapten was measured by using the UV spectroscopy at 532nm (parameters: start wavelength = 200 nm and the end wavelength = 450 nm, the scan step = 1.0 nm, the scan speed = 500 nm/min, temperature was off, run mode = standard, repeat time =30 and (n =3).

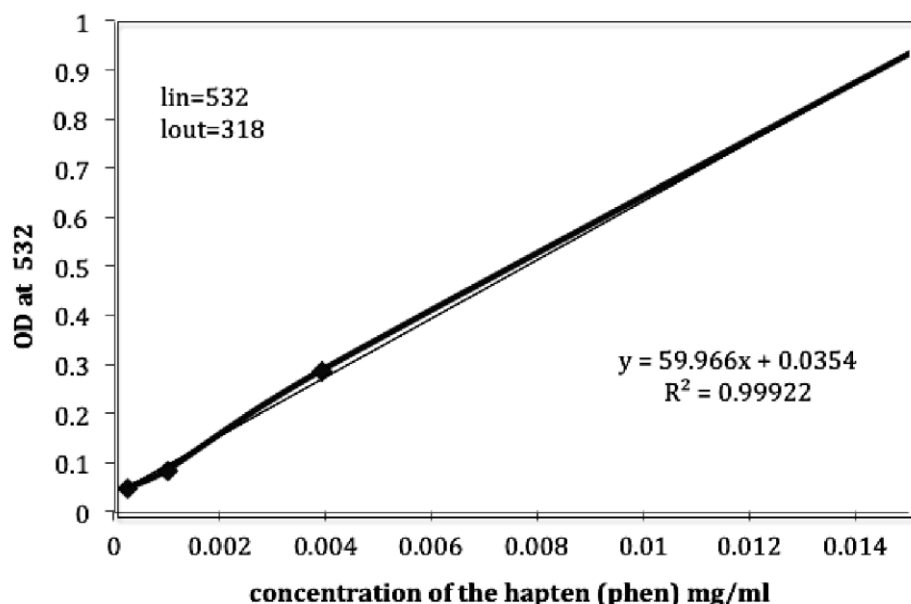


Figure 2.7: The typical behaviour of a PHEN curve measured at 532 nm

The average hapten to carrier protein ratio was manually calculated as 16.45 molecules of hapten per molecule carrier protein for the prepared coating conjugate. It is critical for a successful immunoassay to use an optimized concentration for the coating conjugate. As mentioned earlier, hapten needs to couple with macromolecules such as bovine serum albumin (BSA) protein, in order to take part in an immunogenic reaction. In our experimental work, we optimized this value by working with a serial dilution of the coating conjugate. This was done in order to ascertain which value produced the maximum output signal without reaching saturation. We used a standard ELISA plate and measure the absorbance as a response. The final value that was used for the bioconjugate was 6 µg/ml.

#### **2.4.4 (MALDI-TOF /MS) test for determination of the average binding PHEN to BSA ratio:**

MALDI-TOF experiment was done before being used for the immunisation and assay purposes. The selection of the conjugation method was governed by the functional group of the hapten. The method was useful for monitoring the conjugation for specific antibody against analyte of interest [2-4]. The most used carrier protein for conjugation is (BSA). BSA has a large number of functional group available for hapten conjugation; BSA solubility in buffers is high above pH 5.5 due to its low molecular size. There has been huge progress in recent years in protein-hapten conjugates for the antibody's response with applications in immunoassays for environmental pollutants [5-8]. The phenanthrene-9-carboxaldehyde hapten was cross-linked (coupled) with the BSA carrier protein to obtain the immunogenic reaction. The complex of such conjugates had to always be stable and reproducible. This led to consistent hapten-protein stoichiometries, resulting in small variations and desired immune response. Synthesis of the phenanthrene-9-carboxaldehyde hapten coupled with the BSA carrier protein was the most important factor for specific antibody against PAHs in optical immunoassay applications. The functional group of the phenanthrene-9-carboxaldehyde selected the type of the conjugation technique to be carried out. Current methods apply amine, carboxyl, hydroxyl groups on the hapten and the protein [9,10]. It was important to study the prepared conjugates in order to measure the phenanthrene-9-carboxaldehyde density on BSA protein surface. The higher ratio of coating conjugate increases the intensity and quality of the immune response. However, there is a chance that a high density of substitution could negatively influence the performance of immune response produced [11]. In addition, the complex of coating conjugate is not always reproducible, even in preferable experimental situations. Accurate selection of hapten concentration for coating

conjugate is an important factor in immune response generation. In this study, the hapten (phenanthrene-9-carboxaldehyde) was coupled to carrier protein (BSA). The binding efficiency of hapten-carrier conjugate was optimised by taking different hapten-carrier concentrations.

Five different concentrations were prepared for immunization purpose. A volume of 1800  $\mu$ l of the obtained conjugate solution was mixed with a freshly made dilution of phenanthrene-9-carboxaldehyde (C1=1, C2=0.5, C3=0.25, C4=0.125, C5=0.062) mg/ml in dimethyl sulfoxide (DMSO) solvent. The Phenanthrene-9-carboxaldehyde [PHEN] was synthesized in the LSI laboratory at Tyndall National Institute for coupling with BSA protein. The BSA-PHEN conjugates prepared were characterized using the MALDI-TOF method at Cork Institute of Technology. The masses were analyzed twice. Unfortunately, in the first run, there were no peaks found in any of the concentrations.

The procedure started adding a 1  $\mu$ l from each different concentration on the sample spot area, which was then overlaid that with 1  $\mu$ l of the matrix. The MALDI was set to analyze the sample between 3kDa and 20 kDa, i.e., the conventional range. The protein in our solution was greater than this range. The protein molecular weight used in the range of 66 kDa. The second run was done after receiving advice from the manufacture of MALDI on how to change the mass range in order to run the sample. The samples were run this time with a little more success. As was expected, there was no peak in the control PBS sample. Two samples (C<sub>1</sub>, C<sub>3</sub>) returned no peaks. These two samples were run a few times but still no peaks were obtained. The screenshot of the screen of the MALDI for the analysis of these two showed fuzzy lines. These were noises, and no definitive peaks; hence the lack of mass spectra. All samples were freshly prepared at the same time and under the same conditions. However, these samples may have deteriorated.

Data for the other three concentrations ( $C_2$ ,  $C_4$ ,  $C_5$ ) was obtained and figure 2.7 showed their three peaks. In the Figure 2.6 the peaks found unusual in their mass spectra, it was expected to have only one peak for the hapten-carrier conjugate in each mass spectra. C20-A42 paint program shows the mass spectra for these three peaks. The clarity was poor and there was a lot of noise even after background noise subtraction.

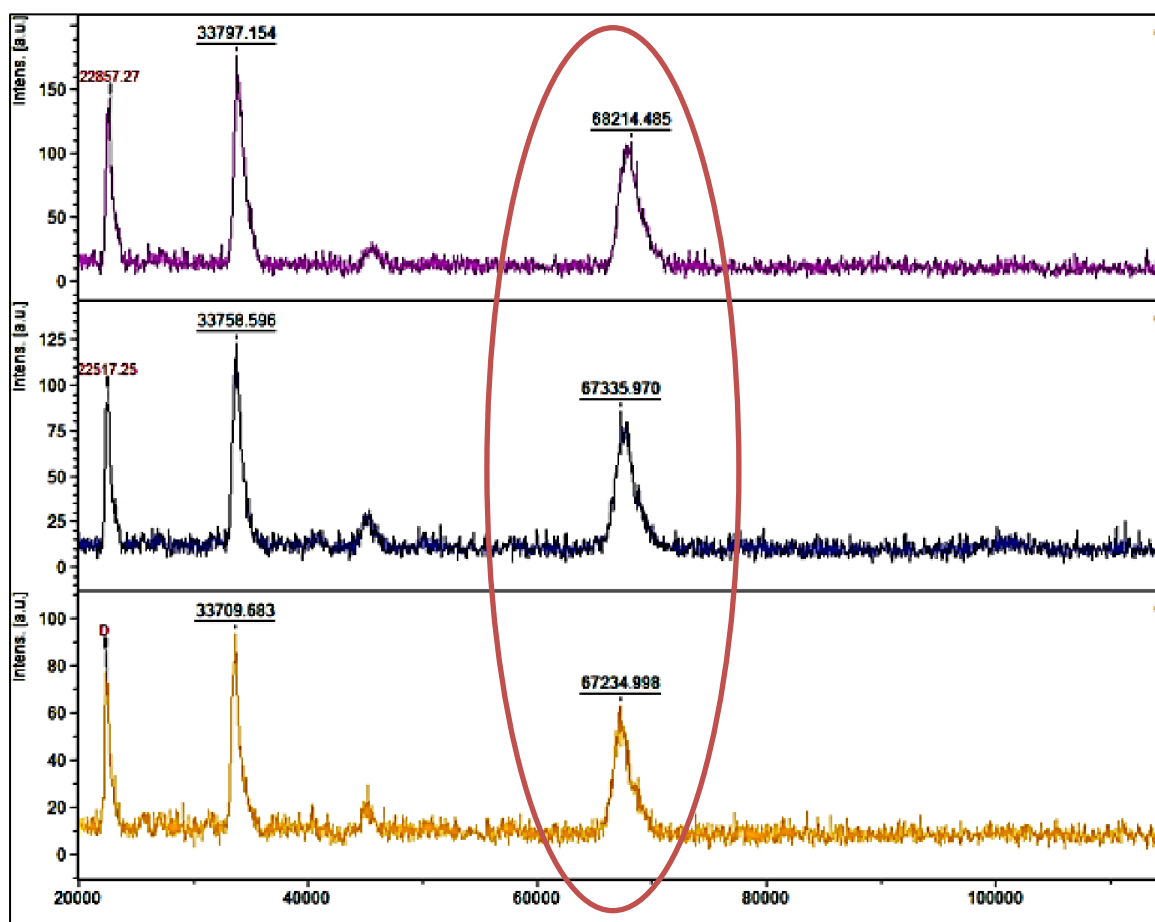


Figure 2.8: Determination of hapten density on BSA-PHEN conjugates using MALDI-TOF method

The preliminary data below the conjugation density for each hapten in increasing concentrations ( $C_2$ ,  $C_4$ ,  $C_5$ ) resulted in a noticeable improvement in the molecular weight of the sample as determined by watching the peak change of mass spectra (Figure 2.8). The shift in molecular weight due to the combination of hapten molecules to BSA matched the number of hapten molecules per BSA molecule. Obvious coupling for the PHEN to BSA, at different concentrations, was roughly same (Table 2.1).

Table 2.1: Different coating conjugates concentrations. Control (PSB buffer) =0, MW (PHEN)=206.24.  
MW of BSA =66430.3 kDa.

Mass spectrometry MALDI-TOF				
Concentration	Carrier-hapten concentration (mg/ml)	Observed mass (kDa)	Change in mass ( $\Delta M$ )	$\Delta M/Mh$ (hapten density)
C2	0.5	68214.485	1784	8.65 (9)
C4	0.125	67335.970	905.674	4.48(5)
C5	0.062	67234.99	804.69	3.90 (4)

#### 2.4.5 Optimisation checkerboard ELISA titration assay

In order to achieve the best results, the dilution factors of the two antibodies must be optimized. If the antibodies are too concentrated, these will saturate the assay. If the antibodies are not concentrated enough, the response will be difficult to measure. In order to attain a strong signal, we used a checkerboard titration for optimal concentration of two variables at once. The resulting combination was the working concentration. Each well was a different ratio of the two variables. Checkerboard titration was used only to acquire the optimal concentration of the two variables, but the optimal ratio of concentrations as well. From the checkerboard assay we could get information for the application used, and we got better results. A different pH was tested in columns and rows and antibody controls served as the background controls. In addition, optimal signal-to-noise ratio was determined for the ELISA assay.

Variations in blocking conditions were optimised in the same plate. In this study, the checkerboard titration determined the optimal concentrations of monoclonal mouse antibody (4D5 specific to BaP) and the optimal concentrations of the detection antibody (alkaline phosphatase (AP) labeled goat anti-mouse) on the 96-well microplate.



Capture ELISA assay was carried out to optimise the two antibodies concentrations. Serial dilutions of both components were titrated against each other on the plate. The higher the component concentrations were, the higher the optical density that was obtained. Two appropriate positive (P) and negative (N) controls were used in the immunoassay plate in order to validate the results. Positive control was a sample that was known not to contain capture antibody I wish to detect. Positive control was applied to the wells resulting in the absence of signal from wells. A negative control is a sample that was known not to contain any detecting antibody I wish to detect. Negative control in the assay tested for the presence of non-specific binding. The optimum dilution factors were observed and used for the final assay. The dilution factor of the capture antibody was (1:64), where the concentration (0.0411 µg/ml) and the dilution factor of detection antibody was (1:4). The concentration of detection antibody was (1:3000 dilution).

#### **2.4.6 Optimisation of antibody immobilisation time**

The results obtained were reported in Figure 2.9. Low response values were measured when the incubation times of less than 60 min were used. The absorbance started to increase when the antibody was incubated for more than 20 min. In ELISA, the optimum incubation time for the adsorption of the antibodies to solid surface is important, with respect to the development of a rapid and fast assay. For this reason, the incubation period of the capture antibody was studied. Capture assay was performed for optimisation of the antibody incubation time. The results showed that the incubation time of 60 min at 37 °C is sufficient enough for the antibody binding, thus achieving a good response. After 60 min the absorbance was higher than the recommended value of optical density (OD) range (less than 1.2 to 0.2), become constant and the reaction was concluded. 60 min was used as the minimum time necessary for binding the antibody to the solid surface.

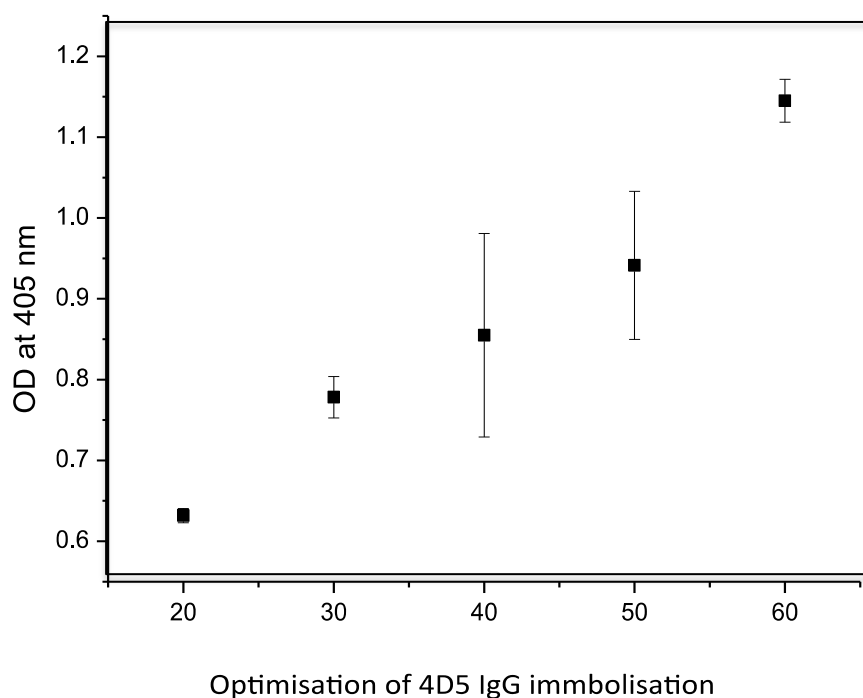


Figure 2.9: Absorbance signals detected for different incubation times between the antibody and the solid surface. The points correspond to the average signal of absorbance  $\pm$  S.D. calculated for  $n=3$  repetitions.

#### 2.4.7 Optimisation of AP Labelling

The results were reported in Figure 2.10. The typical response curve for this assay was directly proportional to the concentration of the antigen in the sample. The optical density (OD) values increased when the detection antibody dilutions increased. In dilution 1:1000 (0.001), the OD value reached to the steady state and showing that the antibodies were saturated. The enzyme-labelled conjugate dilution 1:5000 was used as optimal dilution to carry out the displacement assays. The chosen enzyme-labelled conjugate dilution was the dilution before the saturation state.

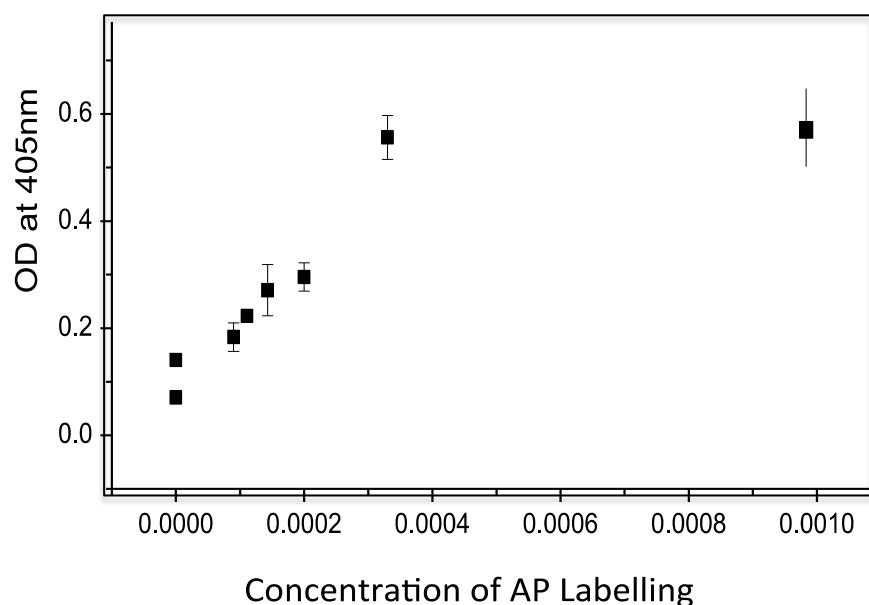


Figure 2.10: Optimisation detection antibody dilution. The antibody immobilisation time of the antibody was 60 min. The dilution points correspond to the average signal of absorbance  $\pm$  S.D. calculated for  $n=3$  repetitions.

#### 2.4.8 Optimisation of monoclonal mouse antibody 4D5 specific to BaP concentration

The aim of this experiment was to optimize the concentration of monoclonal mouse 4D5 antibodies on the wells using capture format. This assay was developed by applying the coating conjugate (6.0  $\mu\text{g/ml}$ ) to the wells. The wells were blocked with 1% BSA in Tris 0.05M, pH 7.4 solution. A serial dilution of monoclonal mouse 4D5 antibody in 10 different concentrations was prepared and placed to the wells. An AP labelled antibody solution (1/3000) dilution was added to each well of the plate. Capture assay for antibody concentration measured after the exposure to the *pAPP*. Detection was absorbance ( $n=3$ ). This assay was developed to measure amounts of antibodies that were present in very low concentrations.

Figure 2.11 illustrates the optimized concentration of monoclonal mouse 4D5 antibody before saturation level of the system. It was found that the optimal concentration was 0.0411 µg/ml; this concentration was used in the final indirect displacement assay.

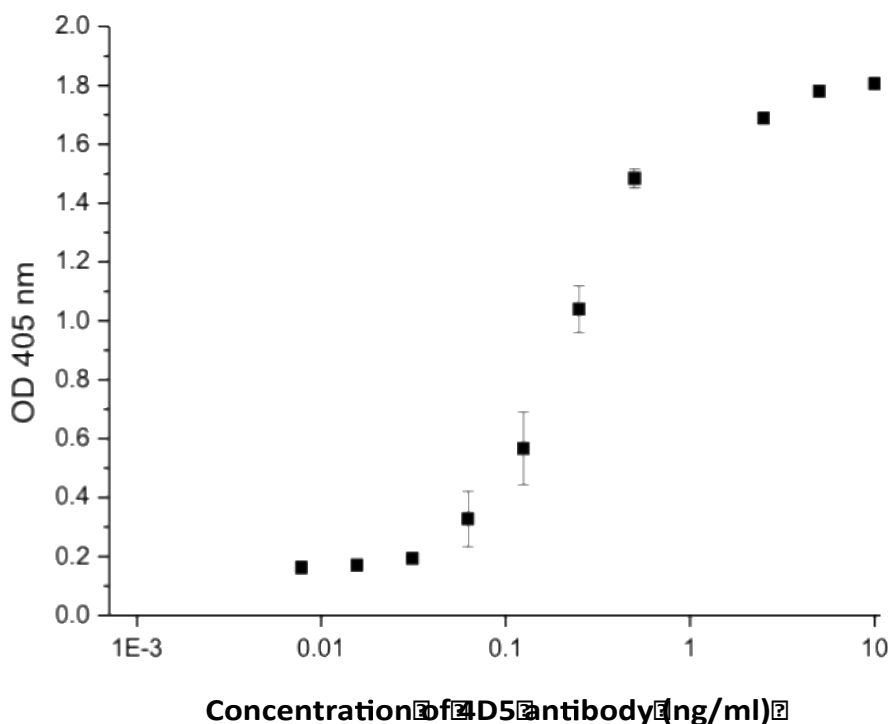


Figure 2.11: Calibration curve obtained with the absorbance found for each concentration of the monoclonal mouse 4D5 antibody (7.8 ng/ml to 10 µg/ml) (n=3).

In the graph the concentration of capture antibody (commercial 4D5 mAb) is on the log scale (X) and the absorbance signal at 405nm is on the linear scale (Y). The performance of the system shows the limit of detection (LOD), the linear range and the saturation area. The International Union of Pure and Applied Chemistry states that (LOD) expressed as a concentration  $C_L$  (or amount,  $q_L$ ), is derived from the smallest measure,  $x_L$ , that can be detected with reasonable certainty for a given analytical procedure. This is represented by equation (1).

$$LOD = \frac{ksb}{m} \quad \text{Equation (1)}$$

The value of  $k$  a numerical factor chosen in accordance with the confidence level desired. The use of  $k = 3$  allows confidence level of 99.86% that a measured sample is greater than or equal to three times the average of the blank signal plus three times the blank signal plus three times the standard deviation of the blank signal.  $S$  is the standard deviation of the response and  $b$  is the slope of the calibration curve. It can be calculated for a linear calibration curve by the slope of the line ( $m$ ), where the equation of the line is given by:

$$y = mx + c \quad \text{Equation (2)}$$

and  $c$  is intercept of the line with the line.

#### **2.4. Displacement assay**

This was the final experiment to detect BaP. In this experiment the wells were coated with 6.0 µg/ml BSA-PHE (optimized concentration of coating conjugate) and blocked with Tris buffer (0.05M). The monoclonal mouse 4D5 antibody (0.0411µg/ml, optimized concentration) was exposed to the coating conjugate (without analyte). In parallel, a serial dilution of the BaP target was prepared (0.51ng/ml to 110 µg/ml). The addition of a specific concentration of BaP should bind to 4D5 antibody immobilized on the surface and carry it away (displace) from the well's surface. The assay was conducted as described in section 2.3.3.8. The results from measurements with absorbance are shown in Figure 2.12. As it can be seen, the performance of the system showed a limit of detection of 0.0137ug/ml. In addition, the response showed a linear range between 0.37 to 0.0137ug/ml. It was possible to prepare the assay on the surface of the wells in about 5 hours, and a single measurement with absorbance was done in minutes.

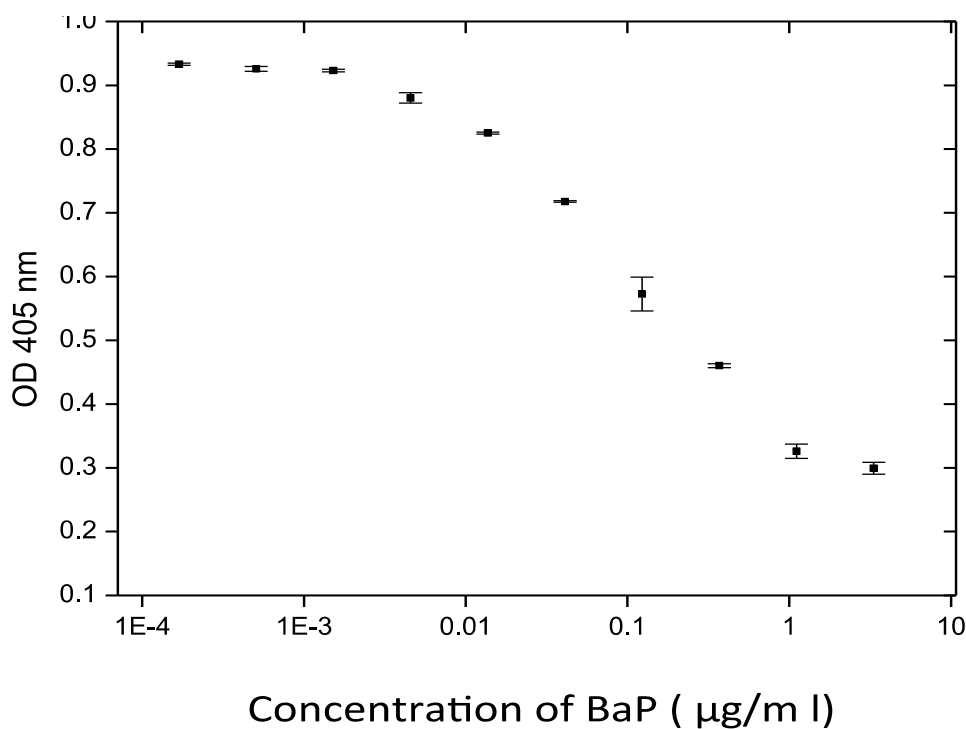


Figure 2.12: Variation of absorbance with log of concentration of BaP

#### 2.4.10 Measurements of tap water

A pre-treatment method was not required for the real sample measurements. A pre-treatment method is a common practice in traditional techniques before measuring the samples. The analysis was carried out in a tap water sample. The tap water was taken from the LSI in Tyndall National Institute, Cork City. The Tris buffer 0.05M concentrations were prepared. The recovery of the spiked BaP in the tap water sample using AP label is illustrated in the Table 2.2 below.

Table 2.2: Recovery study for Tap water sample with three different concentrations of BaP. ELISA format used was displacement assay

BaP	Added: 5 ng/ml		Added: 50 ng/ml		Added: 100 ng/ml	
Sample	Found ng/ml	Recovery (%)	Found ng/ml	Recovery (%)	Found ng/ml	Recovery (%)
Tap water	3.98	78.8	55.43	110.8	26.48	26.5

The displacement assay was carried out. BaP was firstly diluted in DMSO. The blocking buffer used to prepare the serial dilutions was changed to tap water. The assays followed the steps as described in section 2.3.3.8. Absorbance was measured, after one-hour exposure to *p*APP substrate, at 405 nm. The recovery study was carried out to assess the applicability of the developed ELISA format in quantitative analysis of BaP in water. Different concentrations of BaP diluted in blocking buffer (5 ng/ml, 50 ng/ml, 100 ng/ml) were spiked in water sample. Analysis with the spiked water sample achieved unexpected results. It is observed that the higher the amount of BaP spiked in the samples; the less recovery was measured. The acceptable recovery percentage depends on the analyte concentration, if spike recovery fails to fall within the acceptance range, additional optimisation testing (such as changing the reagent diluent or assaying samples at a different dilution) may be necessary.

## **2.5 Conclusion:**

In this chapter the development of an ELISA method for the detection of BaP compound was discussed. Capture and Displacement assays were developed for screening the BaP in a real water sample. Optimisation of different immunoassay reagents and conditions were carried out for obtaining active assay performance. hapten-carrier coating conjugate was synthesised by coupling the interest hapten (phenanthrene-9-carboxaldehyde) with the carrier protein (bovine serum albumin). A Micro BCA Kit was used for quantification of total protein (BSA) and the concentration of the hapten (phenanthrene-9-carboxaldehyde) was determined using UV/VIS spectroscopy. Checkerboard titration assay was carried out to obtain the optimal concentration of the immunoreactants. The optimal concentration of the prepared coating conjugate was 6 µg/ml. In order to gain a good understanding of an

effective coating conjugate for the antibody response, a (MALDI-TOF MS) was used to characterize the coating conjugate resultant. MALDI-TOF MS was used to determine the PHEN-hapten density on BAS-carrier protein surface. Optimisation of immunoassay incubation times was ensured. The optimization of immunoreactant binding time is one of the most important steps when developing ELISA assay. The result showed that the 60 min incubation time at 37°C was the optimal absorbance response under 1.0 at 405 nm. Depending on the instrument specifications and the UV/VIS manufacturer the dynamic range can vary. In our plate reader the best absorbance range values were from 0.2 to 1.5 units at the wavelength 405 nm and the values above 1.5 were excluded. Indirect displacement assay could detect the BaP analyte and the LOD was at 0.0137ug/ml in Tris buffer solution and the liner range was from 0.37 to 0.0137 ug/ml. For the real sample measurements where no pre-treatment methods were used, the analysis was carried out in a tap water sample. For the recovery study the tap water was spiked with known amounts of BaP. The result observed was that the higher concentration of BaP spiked in the water sample, the lower the value of recovery. Further study was performed using the same formats and buffers but using electrochemical cell consisting of three electrodes and electrochemical detection methods for screening and quantifying the concentration of BaP. This is discussed in Chapter 3.

## **2.6 References:**

1. Ahmad A, Moore E. Electrochemical immunosensor modified with self-assembled monolayer of 11-mercaptoundecanoic acid on gold electrodes for detection of benzo [a] pyrene in water. *Analyst*. 2012;137(24):5839-44.
2. Van Emon JM, Seiber JN, Hammock BD. Applications of Immunoassay to Paraquat and other Pesticides. *Bioreg for Pest Ctrl*. 1985 Jan 1;276:307-16.



3. Goodrow MH, Harrison RO, Hammock BD. Hapten synthesis, antibody development, and competitive inhibition enzyme immunoassay for s-triazine herbicides. *Jour of Agric and Food Chem.* 1990 Apr;38(4):990-6.
4. Szurdoki F, Székács A, Le HM, Hammock BD. Synthesis of haptens and protein conjugates for the development of immunoassays for the insect growth regulator fenoxycarb. *Jour of Agric and Food Chem.* 2002 Jan 2;50(1):29-40.
5. Hill AS, McAdam DP, Edward SL, Skerritt JH. Quantitation of bioresmethrin, a synthetic pyrethroid grain protectant, by enzyme immunoassay. *Jour of Agric and Food Chem.* 1993 Nov;41(11):2011-8.
6. Harrison RO, Goodrow MH, Hammock BD. Competitive inhibition ELISA for the s-triazine herbicides: assay optimization and antibody characterization. *Jour of Agric and Food Chem.* 1991 Jan;39(1):122-8.
7. Kramer PM. Biosensors for measuring pesticide residues in the environment: past, present, and future. *Jour of AOAC International (USA).* 1996.
8. Lee JK, Ahn KC, Park OS, Kang SY, Hammock BD. Development of an ELISA for the detection of the residues of the insecticide imidacloprid in agricultural and environmental samples. *Jour of Agric and Food Chem.* 2001 May 21;49(5):2159-67.
9. Szurdoki F, Székács A, Le HM, Hammock BD. Synthesis of haptens and protein conjugates for the development of immunoassays for the insect growth regulator fenoxycarb. *Jour of Agric and Food Chem.* 2002 Jan 2;50(1):29-40.
10. Naar J, Branaa P, Chinain M, Pauillac S. An improved method for the microscale preparation and characterization of hapten– protein conjugates: the use of cholesterol as a model for nonchromophore hydroxylated haptens. *Bioconjugate chemistry.* 1999 Nov 15;10(6):1143-9.

11. Marco MP, Gee S, Hammock BD. Immunochemical techniques for environmental analysis II. Antibody production and immunoassay development. TrAC Trends in Anal Chem. 1995 Sep 1;14(8):415-25.

# **Chapter 3**

## **Electrochemical Immunosensors**

### **Part 1: Screen-printed electrodes (SPEs)**

### **Part 2: Nanoparticles (NPs)**



### 3.1 Immunosensors

Immunosensors are created through the integration of immunoassay methods in a transducer. As a compact analytical device, an immunosensor presents a surface where antigen-antibody complexes can be detected and also converted into electrical and biomechanical signals using transducers. The final detected signals can then be processed, recorded and displayed [1]. The advantages immunosensors in comparison to traditional PAH detection methods, such as Gas Chromatography–Mass Spectrometry (GC-MS) are several, including miniaturization of instrumental devices. They also need minimal reagents, small amount of buffer solutions, little use of organic solvents, and they do not require an extensive cleanup of samples due to potential contamination [2].

Also, immunosensors make it possible to analyse many samples at the same time, and permits in-situ analysis of environmental pollutants' concentrations in a sample [3] [4]. This type allows for the fast screening of multiple samples. The detection of a positive presence of PAHs in samples would indicate the need for further analysis in the laboratory with more standard analytical techniques.

As previously noted, immunosensors are a viable approach to the real-time and fast screening of PAHs [5]. Generally, they are grouped into three groups depending on the techniques of detection as shown in Table 3.1 [6].

Table 3.1: immunosensor types depending on the techniques of detection.

<b>Immunosensors</b>	<b>Definitions</b>
Electrochemical	An antibody can be used as a receptor and can be grouped according to the detection method [7,5], such as electrochemical impedance spectroscopy, potentiometric, conductometric, or amperometric [8-11].
Optical	The antibody-antigen complex triggers changes in the optical characteristics of the substrate, which can be detected by the use of different techniques, such as Total Internal Reflection Fluorescence (TIRF) and Polarisation-Modulation Infrared Reflection-Absorption Spectroscopy (PM-IRRAS) [3]. Additional methods of detection include chemiluminescence, fluorescence [4], and Ramman spectroscopy [12].
Mechanical	The basis in of this type of transduction is the response of a surface to variations in the stress and loading applied to it. Velocity and position can be used in detecting measurement performance [1,13]. In addition, piezoelectric materials (where mechanical stress generates an accumulation of electric charge) such as quartz crystals have been used to immobilize antibodies and antigens [3, 9]. The linking of antibodies to these quartz crystal surfaces allows the immunosensors construction, which can directly determine the connection with their corresponding target.

The standardization of microfabrication techniques in the last 20 years has made the fabrication procedure for immunosensors simple. They allow for the possibility of using surface modification techniques to improve the orientation of the antibodies (Ab) immobilized on them (Figure 3.1), which makes the detection of PAHs in polluted water samples more effective.

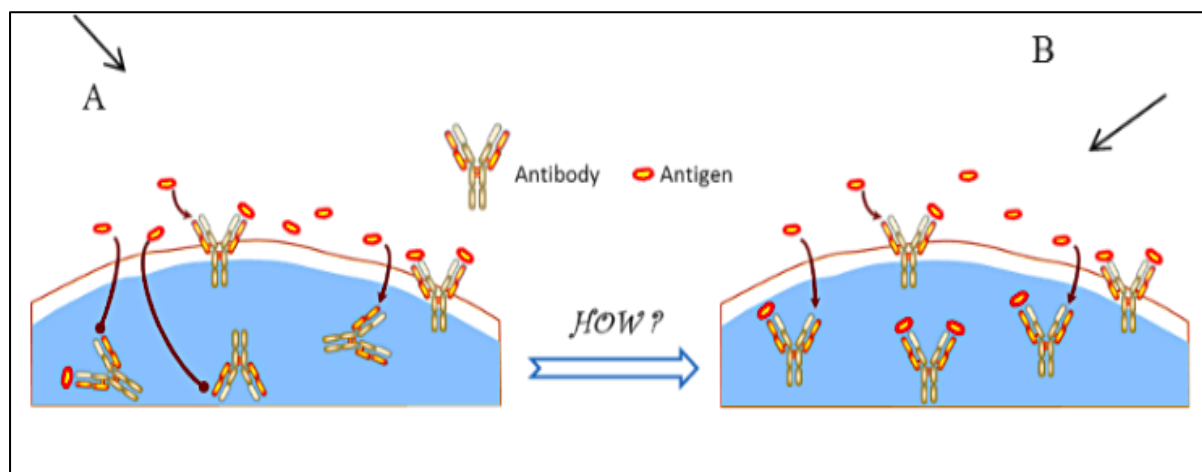


Figure 3.1: Antibody orientations on immunosensors A) random immobilization B) oriented immobilization

[14]

Immunosensors are specific for a particular antigen that is capable of detecting a single target. However, for detection of different disease markers, such as cancers, the process of analysis is very complicated. This challenge has been addressed by the introduction of multiple arrays of sensors where each sensor can analyse a specific antigen. One instance of such an immunosensor has been reported where the electrodes were modified with anti-goat IgG, anti-human IgG and anti-rat IgG. These electrodes were incubated with a mixture of three antigens and selective binding demonstrated [15]. Multiple analyses were also reported applying a flow injection instrument connected with four different electrodes in order to allow simultaneous measurements of four different samples for the detection of one analyte or by applying four separate electrodes, allowing detection of four targets in one sample [16]. Another report stated that specific antibodies immobilized on screen-printed carbon arrays (transducer) to  $\alpha$ -

fetoprotein, carcinoembryonic, and carcinoma antigens. The screen-printed carbon arrays used to identify the antigens and the limit of detections were  $1.1 \mu\text{g L}^{-1}$ ,  $1.7 \mu\text{g L}^{-1}$ ,  $1.2 \text{ IU L}^{-1}$  and  $1.7 \text{ kIU L}^{-1}$ , respectively [17]. IU stands for International Unit and is specific effect when tested according to an internationally accepted biological process. Another group reported the design of gold electrode arrays which were embedded with antigens of five hepatitis variants namely hepatitis A to hepatitis E. Thus, the concentration of viral antigens could be detected [18].

## **3.2 Objective of electrochemical immunosensors**

### **3.2.1 Part 1: Screen-printed electrodes (SPEs)**

This section focuses on how the integration of immunoassay techniques in combination with electrochemical detection can provide a portable and very accurate solution for the detection of water pollutants that are detrimental for human health. In particular, we focused our work on the quantification of polycyclic aromatic hydrocarbons in polluted water. Our integrative approach facilitates a faster detection of this family of organic compounds, by reducing the time of analysis. Additionally, the use of a lab-on-a-chip platform delivers a portable solution that could be used for in situ monitoring. Optimisation of a displacement assay, which investigates the presence and concentration of Benzo[a]pyrene (BaP) in water, allows the miniaturization of the standard ELISA format into a highly accurate system that provides fast results. The limits of detection obtained are comparable to those of state-of-the art tools, and achieve the values set by European Drinking Water Directive ( $0.01 \text{ ng/ml}$ , is the limit for Benzo[a]pyrene (BaP) levels in drinking water).



### 3.2.1.1 Introduction

Polycyclic aromatic hydrocarbons (PAHs) are a very large group of organic compounds made of carbon and hydrogen atoms. These compounds have an important impact on environmental pollutants. They are a primary concern for human health, as PAHs have been reported to increase the risk of cancer in humans [19-24]. It is therefore, very important to identify a method for detecting them in any matter that humans may get in contact with, such as food, soil and water. The European Drinking Water Directive (98/83/EC) recommends a value of 0.01ng/ml as a limit for Benzo [a] pyrene (BaP) levels in drinking water [25]. Currently, detection of PAHs in the environment was done using commercial equipment, such as HPLC-fluorescence detection and Gas Chromatography-Mass Spectrometry (GC-MS). However, these techniques are often expensive, use large amounts of toxic solvents, are time-consuming, and are not portable [26,27]. To address the shortcomings of these commercial techniques, this study presented an alternative electrochemical technique that can be used to detect PAHs within a short time; it is also portable, inexpensive, and environmentally friendly. Electrochemical immunosensors present great advantages in comparison to traditional PAH detection methods, in that they are easy to fabricate and use, without reducing their levels of detection or sensitivity. This work shows how the integration of electrochemical techniques with an immunoassay method can reach limits of detection as low as required for the analysis of water samples in situ and in real time. In particular, we were able to detect the presence of Benzo [a] pyrene (BaP) in water. The development of this system is based on the use of Screen-Printed Electrodes (SPEs), which are integrated with the aforementioned methods (electrochemical techniques with an immunoassay). The SPE system contains a three-electrode set that allows the combination of electrochemical measurements with immune-sensing techniques. The best results obtained were achieved by adapting the protocol of an indirect displacement assay in the SPE platform.

Our findings indicate that the adaptation of the immunoassay protocol reduces detection time to less than 3 hours. The ability of this system to reduce dramatically the performance time of a standard immunoassay (optical immunoassay) and the integration into a portable lab-on-a-chip solution, could represent a future platform for the home-testing for water quality monitoring and avoid costly and inefficient analysis of water samples in dedicated laboratories.

### **3.2.1.2 Experimental**

#### **3.2.1.2.1 Materials**

For the synthesis of BSA-phenanthrene coating conjugate: the following were purchased from Sigma (Dublin, Ireland): bovine serum albumin (BSA), adipic acid dihydrazide (AAD), phosphate buffered saline (PBS), 1-ethyl-3-(3-dimethylaminopropyl) carbodiimide (EDAC), diethanolamine dimethyl sulfoxide (DMSO), phenanthrene-9-carboxaldehyde, sodium cyanoborohydride ( $\text{NaCNBH}_4$ ), and sodium hydroxide. Hydrochloric acid 37% was bought from KMG ULTRA CHEMICALS LTD (England). Slide-A-Lyzer™ Dialysis Cassettes 10K (0.5–3 mL) were purchased from Thermo Scientific and were used for purification of proteins. Monoclonal mouse antibody 4D5 specific to BaP was bought from Santa Cruz (Heidelberg, Germany). Sodium hydrogen carbonate, sodium chloride, detergent Tween-20, Tris salt, BaP, alkaline phosphatase (AP) labelled goat anti-mouse antibodies (whole molecule) were all purchased from Sigma (Dublin, Ireland). In order to ensure optical detection, a standard 96 well ELISA microplate was bought from Greiner bio-one (Germany). For the electrochemical sensor the substrate was para-aminophenyl phosphate (pAPP) salt, which was bought from Gold Biotechnology Inc., USA. Potassium chloride (KCl) and Diethanolamine (DEA) were bought from Sigma (Dublin, Ireland). All reagents were of analytical grade, and any water used in the solutions was nanopure water (having 18.2 megohm ionic purity with little, if any bacteria ( $18.2 \text{ m}\Omega\text{-cm}$ )). Disposable electrochemical

screen-printed electrodes (Kanichi 3 mm Graphite, KRS-1001) were provided by Kanichi Research Services Ltd (UK).

#### **3.2.1.2.2 Instrumentation**

A PalmSens potentiostat (Palm Instrument BV, the Netherlands) was used for the electrochemical measurements. For incubation, a Biometra OV3 Incubator (Gottingen, Germany) was set at 37 °C. A Plasma Cleaner (45watts) (Harrick Plasma, Ithaca, New York) was used for removing organic molecules from the surface of SPEs. A Nitrogen spray gun was used to dry the SPEs between measurements. A UV absorbance reader for ELISA applications was provided by Thermo Fisher. A nanopure water system was bought from ELGA.

#### **3.2.1.2.3 Procedures**

- **Preparation of phenanthrene–protein coating conjugate**

The preparation was completed as described in section 2.3.3.1.

- **Screen-printed electrodes (SPE) cleaning**

The SPEs needed to be cleaned with isopropanol before use, and then dried with a nitrogen gun. The SPEs were additionally treated in a plasma asher (45 watts) for 30 minutes, in order to remove any organic compounds. The SPEs were stored in dry and dark conditions for further application of immunoassay methods and electrochemical detection. The SPE used contained graphite working electrode (0.071cm<sup>2</sup>), graphite counter electrode and Ag/AgCl paste reference electrode (Figure 3.2).

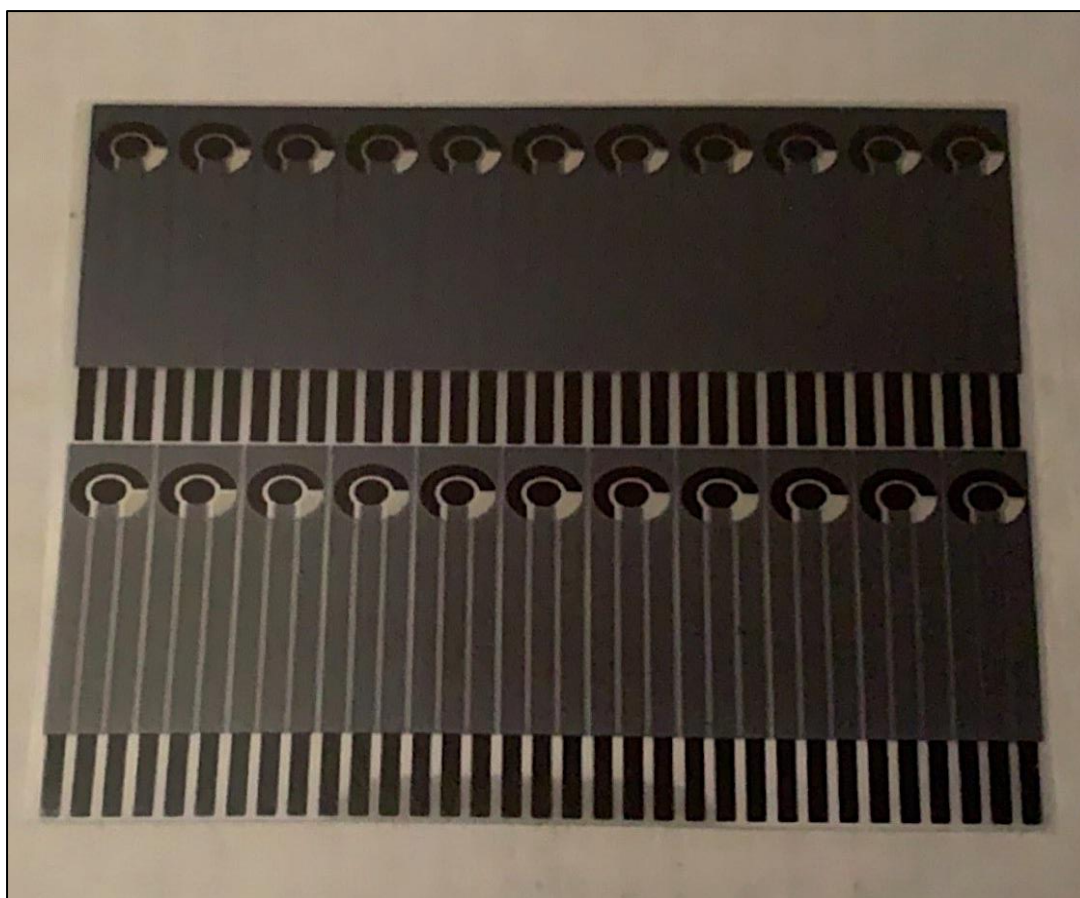


Figure 3.2: Kanichi Research Services Ltd screen-printed electrode

- **Capture assay: optimisation of monoclonal mouse 4D5 antibody specific to Benzo[a]pyrene (BaP)**

1  $\mu$ l of coating conjugate (6.0  $\mu$ g/ml) was added to the working electrode and allowed to bind for 30 minutes at 37 °C. The SPEs were washed with washing buffer three times and dried with the nitrogen spray gun. 4  $\mu$ l of blocking solution was added to electrode, making sure that the working was completely covered and were left to incubate for 30 minutes at 37 °C. Then, the SPEs were washed again using washing buffer three times and were dried with a nitrogen spray. For the primary antibody step, a serial dilution of monoclonal mouse 4D5 antibody in eight different concentrations was prepared. 2  $\mu$ l of each concentration was placed to the SPE working area and allowed to bind for 30 minutes at 37 °C. Then, the SPEs were washed again using washing buffer three times and were dried with a nitrogen spray.

Finally, 2ul of AP labelled antibody was added and the SPEs were incubated for 30 minutes at 37 °C. The electrodes were ready to be measured using Lanier sweep voltammetry detection.

- **Michaelis – Menten Kinetics.**

In AP kinetics, the concentration of the enzyme needs to be taken into consideration. The electrochemical detectable species (pAP) that is observed is the result of the hydrolysis of pAPP substrate (catalysed) by the AP enzyme, which is linked to the secondary antibody. The enzymatic reaction of the substrate (equation 1) involves the combination of a substrate (S) and the enzyme (E) to form a complex (ES). This complex then breaks down into a product (P) and releases the enzyme (E). According to the Michaelis – Menten mechanism the enzyme-substrate complex takes place in first step of mechanism. Equation 1 shows the reaction of the single substrate [28].



The rate  $v$  of this reaction for a fixed enzyme can be explained as shown in (equation 2).

$$v = \frac{V_{max} * [S]}{K_m + [S]} \quad (2)$$

$V_{max}$  is the maximum rate of the reaction (at saturated substrate concentration) and  $K_m$  the Michaelis – Menten constant (corresponds to the substrate concentration determined as half of  $V_m$  ).

- **Displacement assay on SPE.**

In this assay, the target (analyte) displaces the primary antibodies (in our case 4D5 mAB) from the surface of SPEs. The amount of the antibodies left will attach to the secondary antibody, in our case the AP labelled anti-IgG. Optimised concentration values of the reagents were used for each SPE. A serial dilution of BaP was prepared and was used to displace the

primary antibodies that were bound to the surface through the coating conjugate. All washing steps were done with washing buffer 7.4 pH and were dried with a nitrogen spray. The prepared electrodes were connected to potentiostat in order to measure their individual response in a linear sweep voltammetry setting (parameters: Initial voltage = 0.2 V, final voltage = -1.6 V, scan rate 0.05 V/s, sample interval = 0.005V).

### **3.2.1.3 Results and Discussion**

- **Development of immunoassay protocol for SPEs**

The main aim of this work was to develop an electrochemical immunoassay using SPEs for the detection of Benzo[a]pyrene (BaP) in water. In this study, optimisation of different reagents was carried out on the electrodes in order to obtain the optimal concentration for a maximum antibody-antigen affinity. We chose a displacement assay form as it allowed us to reach low limits of detection and to obtain good assay sensitivity. This format is commonly used when the target is small and has only one epitope (the part of an antigen that is recognized by antibody). The optimisations of the main steps of the assay were carried out as follows: optimizations of concentrations of coating conjugate, optimisations of primary antibody concentrations, and optimizations of substrate concentrations. The following subsections will describe the results obtained in detail and link it to the final displacement assay used.

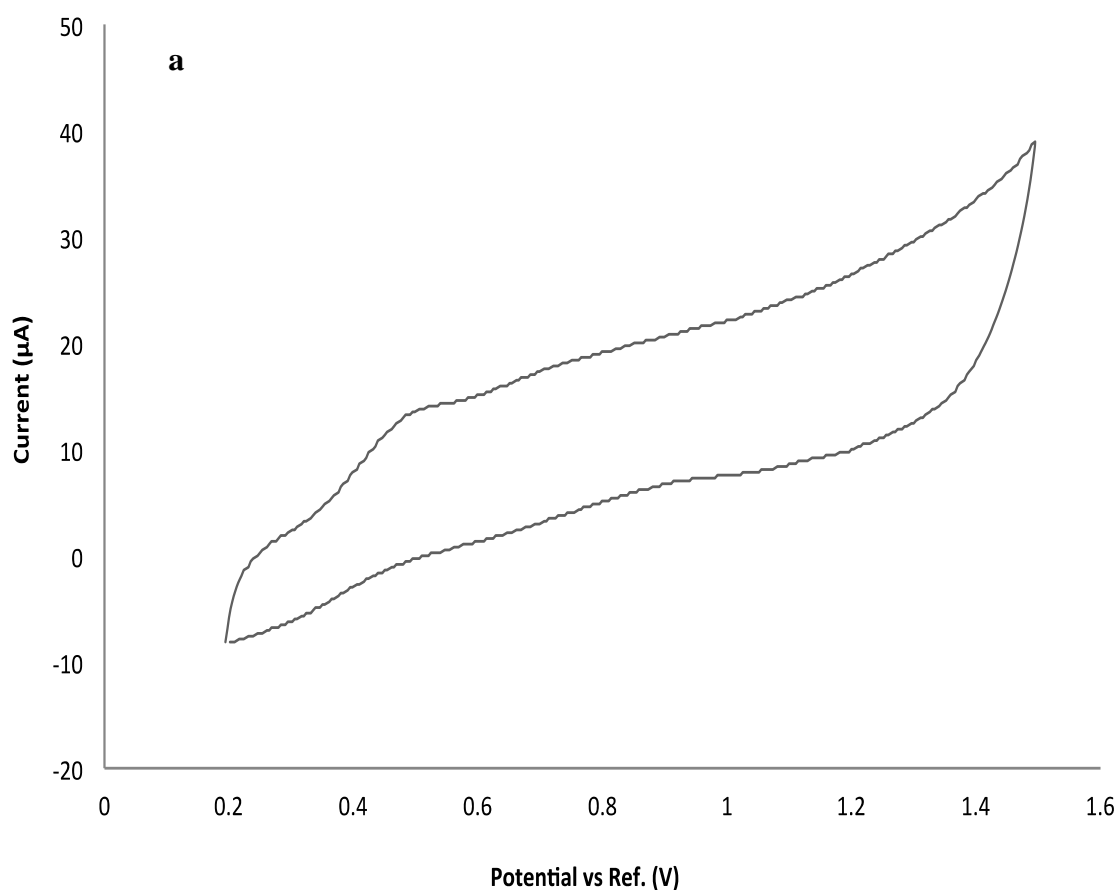
- **Optimisation of coating conjugate.**

The protocol was carried out as described in section 2.3.3.6.

- **Optimisation of monoclonal primary antibody**

The aim of this experiment was to optimize the concentration of monoclonal mouse 4D5 antibody on the SPEs using capture format.

This assay was developed by applying the coating conjugate ( $6.0\text{ }\mu\text{g/ml}$ ) to the SPE working electrodes. The SPEs were blocked with 1% BSA in Tris 0.05M, pH 7.4 solution. A serial dilution of monoclonal mouse 4D5 antibody in eight different concentrations was prepared and applied to the working electrode of the SPEs. Cyclic voltammetry detection was used to study the reaction (Figure 3.3). Figure 3.3 illustrates the optimised concentration of monoclonal mouse 4D5 antibody before saturation level of the system. It was found that the optimal concentration was  $0.37\text{ }\mu\text{g/ml}$ ; this concentration was used in the final indirect displacement assay.



## optimisation of 4D5 ABs

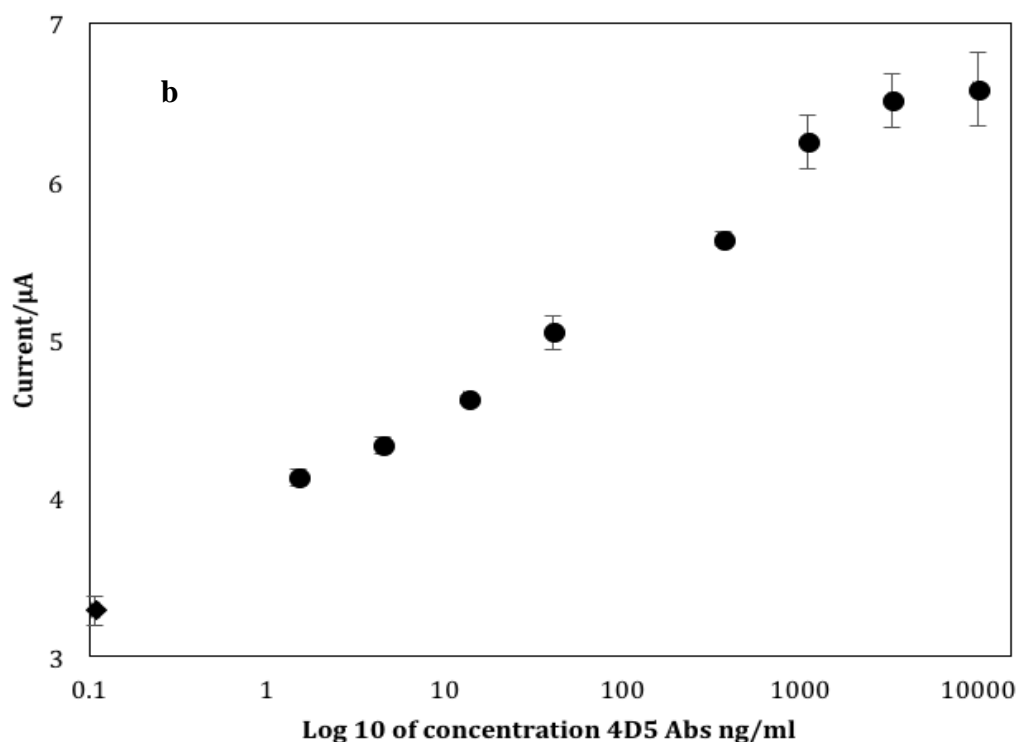


Figure 3.3: (a) Example of a cyclic voltammetry plot obtained from the application of the capture assay. (b) Calibration curve obtained with the current peaks found for each concentration of the monoclonal mouse 4D5 antibody. The control was without a primary antibody.

### • Optimisation of *p*APP (Michaelis – Menten Kinetics)

The enzyme kinetics for the *p*APP substrate was studied at SPEs using amperometry method and the potential was applied 300mV in a stirred solution to determine the concentration of *p*APP that would have a 95% of  $I_{\max}$ . The measurement was set to 50 seconds. The biocomponents were applied onto the electrodes in a capture assay. Different concentration of *p*APP were prepared [1mM-15mM]. The data were fitted by a non-linear regression based on the Michaelis – Menten model. The  $K_m$  of *p*APP 0.15915 mg/ml and the corresponding concentration of *p*APP at 95 % of  $I_{\max}$  was 22.8842 mg/ml.



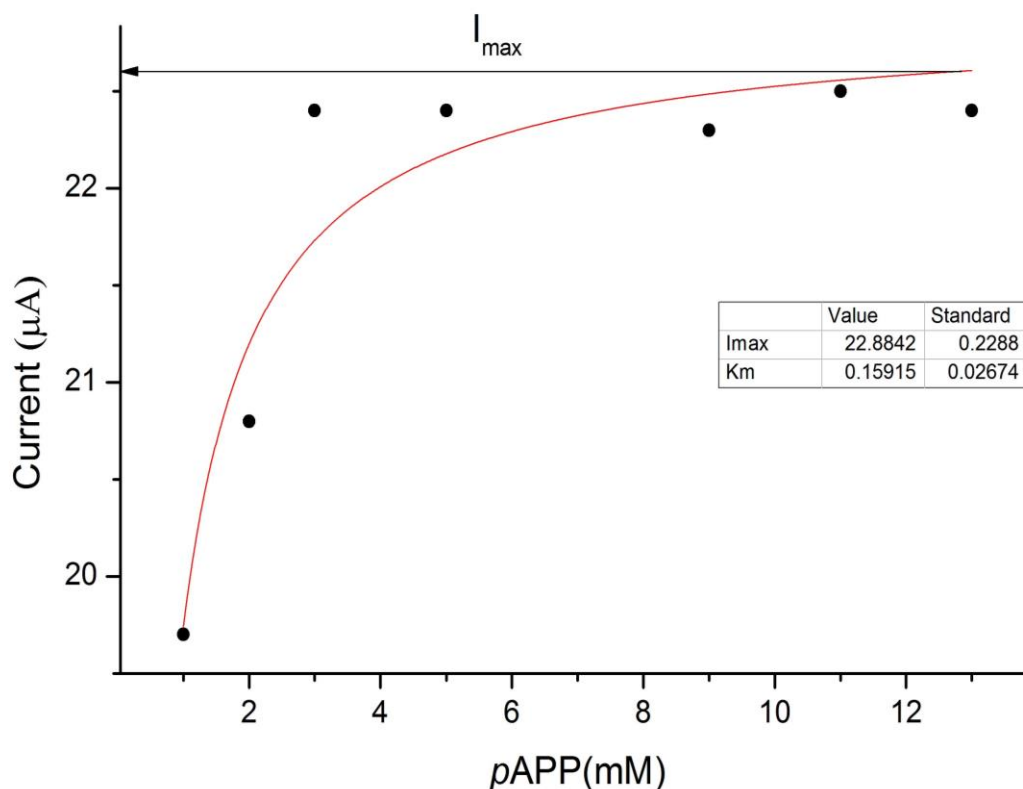


Figure 3.4. Calibration curve of pAPP from amperometry readings in a stirred batch

- **Displacement assay on SPE.**

This was the final experiment to detect BaP. In this experiment the SPEs were coated with 6.0  $\mu\text{g/ml}$  BSA-PHE (optimised concentration of coating conjugate) and blocked with Tris buffer (0.05M). As a next step, the monoclonal mouse 4D5 antibody (0.37  $\mu\text{g/ml}$ , optimised concentration) was exposed to the coating conjugate (with yet no analyte). In parallel, a serial dilution of the BaP target was prepared (10  $\mu\text{g/ml}$  to 0.01ng/ml). The addition of a specific concentration of BaP should bind to the 4D5 antibody immobilized on the surface and carry it way (displace) from the SPE surface. The assay was conducted as described in section 3.2.1.2.3. The results from measurements with linear sweep voltammetry are shown in Figure 3.5. In Figure 3.5 (a) the peak noted at 0.60 V in the linear sweep voltammogram and in (b)

the calibration plot was constructed by plotting the current associated with peak at 0.60 V against the log of BaP concentration.

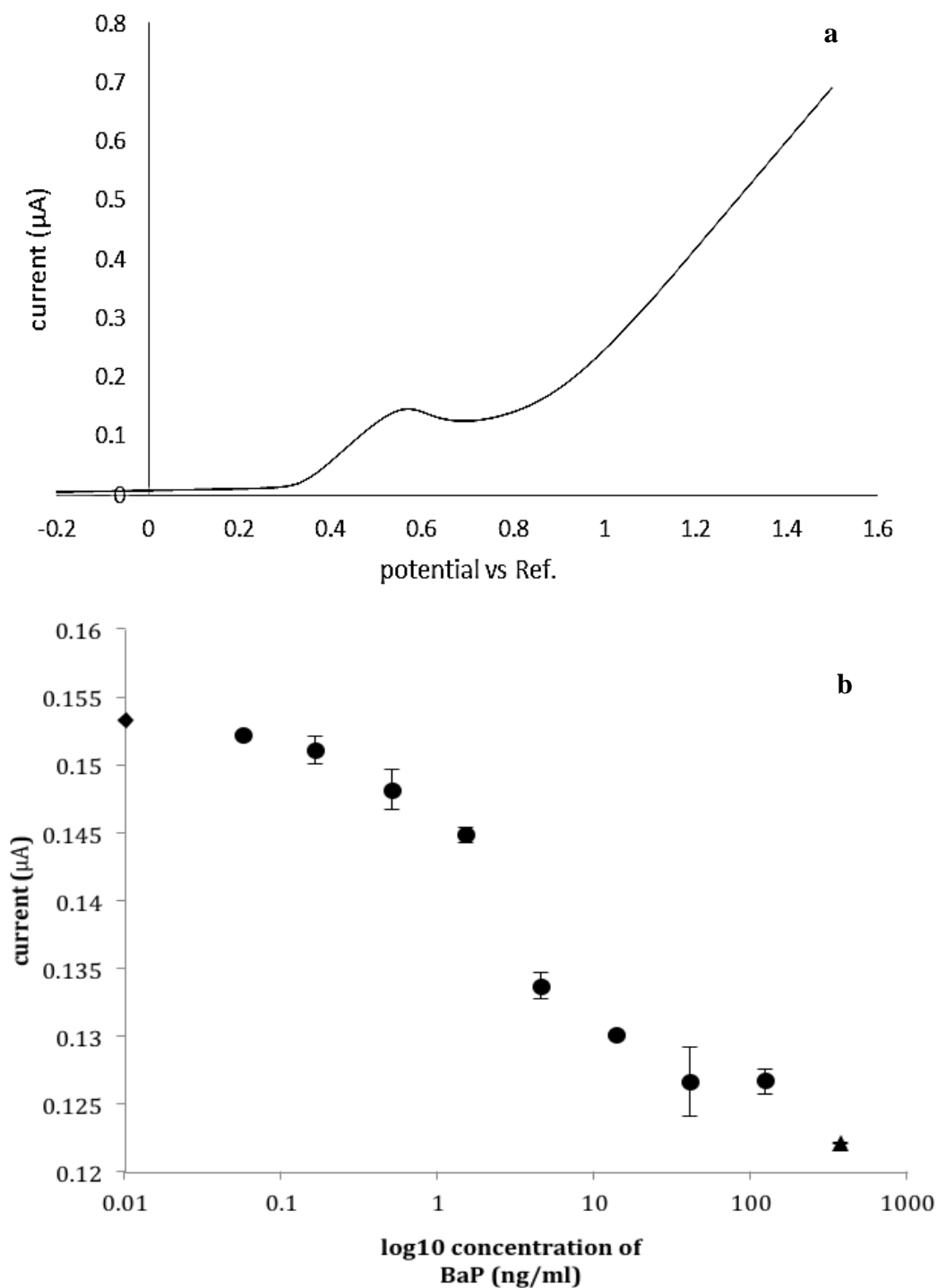


Figure 3.5.: (a) Linear sweep voltammogram obtained from the application of the displacement assay at concentration BaP of 0.166 ng/ml (b) Calibration curve obtained with the current peaks at a potential of 0.60 V found for each concentration Benzo[a]pyrene (BaP) (range of concentrations from 0.01 ng/ml to 10  $\mu\text{g/ml}$ )

As can be seen, the performance of the system shows a limit of detection of 0.07ng/ml. In addition, the response shows a linear range between 1 to 10 ng/ml. It was possible to prepare the assay onto the surface of the electrodes in about 2 hours, and a single measurement with linear sweep voltammetry was done in 16s.

#### **3.2.1.4 Conclusion**

The work presented the development of an immunochemical method of detection for BaP. An SPE electrode was used as the surface where all the immunoreactions occurred. Optimization of the immunoassay was done by isolating the different reagents and studying the response of the system before saturation. The use of linear sweep voltammetry in combination with the immunoassay-SPE offered a low limit detection (0.07 ng/ml) for the screening of Benzo [a] pyrene (BaP). Linear sweep voltammetry detection with SPEs allows a simple system that could be used as a small portable method for *in situ* water quality monitoring. Although the LOD reached were very low, further study will investigate the increase in sensitivity of the system in order to reach the value set by the European Drinking Water Directive, (0.01 ng/ml, as the limit for Benzo [a] pyrene (BaP) in drinking water). Future work will integrate the already developed lab-on-a-chip platform, which will reduce the number of steps and the incubation time, due to the increase of surface-to-volume ratio. The use of such a platform will also make it possible to automat the steps that the immunoassay requires. Therefore, the integration into a portable lab-on-a-chip solution could represent a future platform for monitoring water quality and avoid costly and non-efficient analysis of water samples in dedicated laboratories.

### **3.3 Objective of magneto-electrochemical immunoassay**

#### **3.3.1 Part 2: Nanoparticles (NPs)**

To overcome the difficulties of commercial techniques, this work presents the integration of electrochemical techniques in combination with a tailored immunoassay method that aims to

detect Benzo[a]pyrene (BaP) in water. Nanoparticles were used as a solid surface for the immobilization of antibodies, which were the main biomolecules of our immunoassay. The size of an antibody molecule is about 10 nm and nanoparticles of iron oxides are typically in the size range of 18-22 nm. Covalent binding has been developed. This method occurs through chemical processes, whereby the specific antibody with one of its functional groups (carboxyl) are linked to amine groups on the surface of the nanoparticles. This covalent immobilization method provides a strong bond between the antibodies and the nanoparticle, offering then a very reliable protocol for BaP detection. The limits of detection obtained (0.1ng/ml) are comparable to those of available state-of-the-art tools and close to the values requested by European Drinking Water Directive (0.01ng/ml). It also presents a linear range of (13.7 to 123 ng/ml) that is practical in the detection of PAHs in water. The use of a magnetic platform offers the opportunity to integrate it into a portable solution that could be used for in situ monitoring of PAH in water. Having an in situ monitoring device is important for real-time and early detection of the potential presence of PAHs in water. This is a potential solution for domestic testing that would allow consumers to control the quality of their drinkable water.

### **3.3.1.1 Introduction**

The work shows here presents the development of an electrochemical method to detect Benzo[a]pyrene (BaP), which aims to obtain a limit of detection at the values recommended by the European Drinking Water Directive (98/83/EC) (0.01ng/ml for BaP in drinking water [25]) The integration of an electrochemical method with an immunoassay principle can reach limits of detection [LOD] as low as required for the analysis of water samples in field and in real time. The development of this system is based upon the use of ferromagnetic particles (iron) that are integrated in the aforementioned methods. Ferromagnetic materials (iron-based materials that can form permanent magnets) have attracted research interest as a suitable material that can be used as a substrate [29-32]. The rapid growths of nanotechnology, and its

multiple uses, have generated great expectations. The use of nanoparticle [NP] on this work offered advantages due to their unique size and physicochemical properties. This nanomaterial behaviour makes nanoparticles present unique optical, catalytic, magnetic, electrical, and chemical properties [33]. Also due to their unique characteristics, e.g., biocompatible, reliable orientation effects, good adsorption capacity, structural properties, and structural compatibility, new functional nanomaterial contains the ability to immobilize biomolecules, such as DNAs, antibodies, and enzymes [34]. These new functional nanomaterials have also been used to label biomolecules, promoting electron transfer, catalysing reactions, and enhancing the amplification of electrochemical signals [35-41]. As with many other scientific fields, electrochemistry has taken advantage of nanotechnology to produce sensors with an extra enhanced sensitivity, thanks specifically to the enhanced surface area to volume ratio that these particles offer. In our particular case, we were interested in the study of nanoparticles as carriers for the antibodies that were a key part of our immunoassay.

Ferromagnetic materials were therefore used here as a solid phase where biomolecules attach, with the potential to increase the number of biomolecules being immobilised on them [41-43]. This is due to the high surface to volume ratio that nanoparticles have. Ferromagnetic materials are also of interest as an elegant and easy solution for integration of the immunoassay in a lab-on-a-chip platform. The coupling of an immunoassay with an automatic microfluidic system would be ideal for screening BaP, in addition to providing a portable option. It would also reduce the time required to do the measurements. Due to the high surface area, heat transfer would be highly efficient, thus, reducing incubation times. In addition, magnetic and fluidic manipulation of nanoparticles reduces drastically the amount of washing steps. The results presented here were obtained by adapting the protocol of an indirect displacement assay on the ferromagnetic particles surface.

We will show that such adaptation of the immunoassay protocol on nanoparticles reduces the detection time. The ability of this system to reduce the experimental time of a standard immunoassay, and the potential for integration into a portable lab-on-a-chip solution could represent a future magnetic platform for the home-testing of water quality, thereby avoiding costly and inefficient analysis of water samples in dedicated laboratories.

### **3.3.1.2 Experimental**

#### **3.3.1.2.1 Materials**

The following materials were purchased from Sigma (Dublin): O-(2-Aminoethyl) polyethylene glycol [DAPEG], 1-ethyl-3-(3-dimethylaminopropyl) carbodiimide (EDC), phosphate buffered saline (PBS), sodium hydroxide, sodium hydrogen carbonate, sodium chloride, detergent Tween-20, Tris salt, BaP, alkaline phosphatase (AP) labelled goat anti-mouse antibodies (whole molecule), magnetic iron oxide nanoparticles [ $\text{Fe}_3\text{O}_4$ ], Ammonium hydroxide solution, Potassium chloride (KCl) and Diethanolamine (DEA). Hydrochloric acid 37% was purchased from KMG ULTRA CHEMICALS LTD (England). Monoclonal mouse antibody 4D5 specific to BaP was purchased from Santa Cruz (Heidelberg, Germany). For the electrochemical detection, the substrate para-aminophenyl phosphate (pAPP) salt was purchased from Gold Biotechnology Inc., USA. All reagents were of analytical grade and any water used in the solutions was nanopure water (18.2 m $\Omega$ -cm). Disposable electrochemical screen-printed electrodes (Kanichi 3 mm Graphite, KRS-1001) were provided by Kanichi Research Services Ltd (UK).

#### **3.3.1.2.2 Instrumentations**

A CHI 1100 potentiostat (CH instruments, Inc. U.S.A) was used for the electrochemical measurements. For incubation, a Biometra OV3 Incubator (Gottingen, Germany) was set at 37 °C.

A Plasma Cleaner (45 watts) (Harrick Plasma, Ithaca, New York) was used for removing organic molecules from the surface of SPEs. A Nitrogen spray gun was used to dry the SPEs in between measurements. For shaking at room temperature, a Heidolph ROTAMAX (Heidolph, Germany) was used at 120 rpm.

### **3.3.1.2.3 Procedures**

- **Preparation of PEG-ferromagnetic particles.**

In order to enhance traditional immunoassays, it was included iron oxide [Fe<sub>3</sub>O<sub>4</sub>] (magnetic particles) were included as a solid surface. In order to do that, the research focused on developing an appropriate linkage of the ferromagnetic particles with the antibodies used in the immunoassay. To target BaP, a connection between BaP-specific antibodies and the ferromagnetic beads was required. We prepared magnetic particles by covering them with an O-(2-Aminoethyl) PEG, and then covalently connected them to the antibodies by using protein immobilization techniques. O-(2-Aminoethyl) polyethylene glycol polyethylene glycol [PEG] (0.10 g) was dissolved in 4 ml of nanopure water under N<sub>2</sub> purging with fast stirring. 2 ml of aqueous solution of magnetic iron oxide nanoparticles was then added (dropwise) to the O-(2-Aminoethyl) PEG solution. This solution was then made alkaline by the addition of 0.1 M ammonium hydroxide (4 ml) and left to react for 20 min at room temperature under the fume hood. Afterwards, the solution was centrifuged for a minute at 12000 rpm and then collected by magnetic force. The resulting brown-coloured material was washed off with nanopure water, rendering Amino-terminated PEG-magnetic beads.

- **Capture assay: Optimisation of monoclonal mouse antibody 4D5 specific to BaP**

For the optimisation of the primary antibody concentration, which is used as a captor for the target BaP, a serial dilution of monoclonal mouse 4D5 antibody (0.2mg/ml) was carried out in 50 mM carbonate/bicarbonate buffer pH 9.5 (nine different concentrations were prepared). 3ml of antibody solutions were introduced into 1 mL of Amino-terminated PEG-

magnetite solutions. 0.2 mg of 1-ethyl-3-(3- dimethyl-aminopropyl) carbodi-imide (EDC) was then added. Linkers can create bonds between specific functional groups, since they are chemical species with very reactive groups at one or both ends. The type of crosslinker (EDC) used in this work was a heterobifunctional crosslinker that has different reactive groups at both sides of the spacer arm. All the contents in the vial were left for 1 hour while shaking the content vial above Heidolph ROTAMAX 120 machine at room temperature.

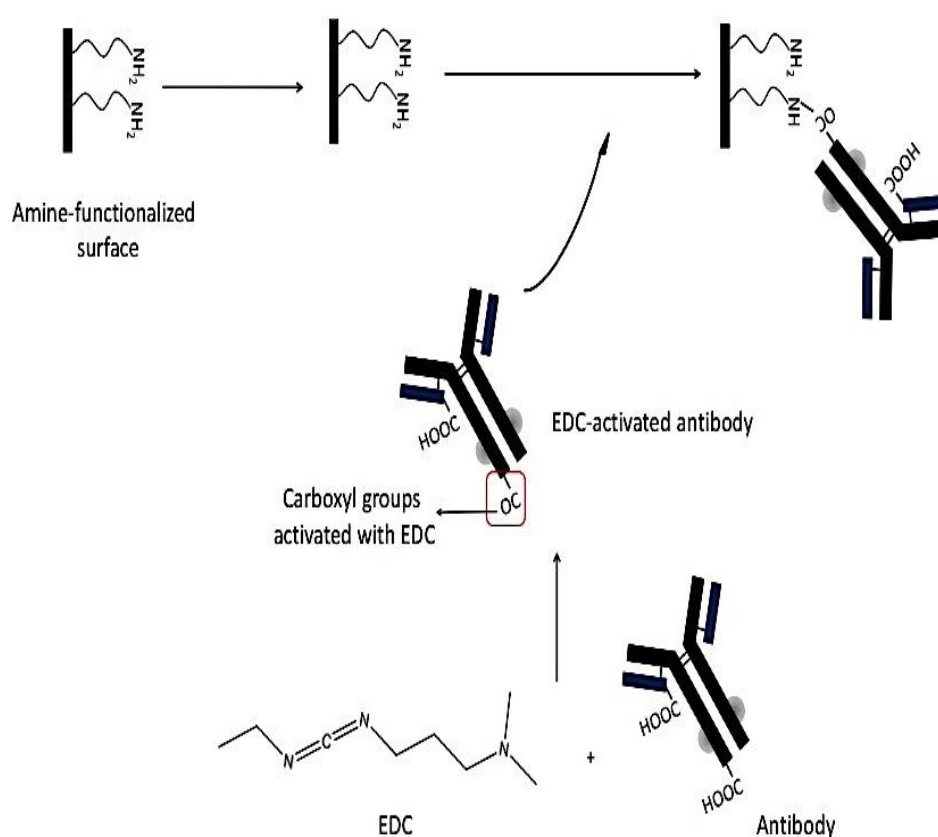


Figure 3.6: Schematic reaction of carboxyl-amine crosslinker. Carboxyl-amine crosslinker presents hetero-bifunctional chemistry (EDC). The carboxyl group of the antibody reacts with the amine on the surface.

After the last step of the capture assay, SPEs were connected individually to the electrochemical set up (potentiostat). Linear sweep voltammetry was used for the measurement of the reaction of the AP label and a solution of the substrate *p*APP in



Diethanolamine (DEA, 0.1M) in the presence of KCl (0.1M) pH 9.5. All measurements were done by depositing a drop of the final solution on the working area of the electrode. The SPEs were cleaned beforehand with isopropanol and then dried with a nitrogen gun. The SPEs were additionally treated in a plasma cleaner device for 30 minutes, in order to remove any organic compounds left on their surface. The SPEs were stored in dry and dark conditions for later electrochemical measurements.

- **Displacement assay on ferromagnetic particles surface**

The displacement assay is a test where the analyte displaces the antibody from the surface of the sensor. A serial dilution of BaP was prepared and was used to displace the primary antibodies that were bound to the surface. Optimised concentration values of the reagents were used for each particle's solution. All washing steps were done with washing buffer 7.4 pH. The prepared electrodes were connected to the potentiostat in order to measure their individual response in a linear sweep voltammetry setting (parameters: Initial voltage = 0.2 V, final voltage = -1.6 V, scan rate 0.05 V/s, sample interval = 0.005V).

### **3.3.1.3 Results and Discussion**

- **Development of immunoassay protocol for ferromagnetic particles.**

The main aim of this work was to develop an electrochemical immunoassay using ferromagnetic particles for detecting Benzo[a]pyrene (BaP) in water. In this study, optimization of different reagents was performed in order to obtain the optimal concentration for a maximum antibody-antigen binding. Indirect displacement assay was performed in order to ensure good limits of detection and sensitivity. This format is common when the target is small and possesses only one epitope.

• **Optimisation of monoclonal mouse 4D5 antibody specific to Benzo[a]pyrene (BaP).**

The objective of the experiment was to optimise the concentration of monoclonal mouse 4D5 antibody on the ferromagnetic particles surface. This was done by using a capture format assay (the antigen to be detected is sandwiched between two antibodies). The diagram for capture assay is shown in Figure 3.7. Amino-terminated PEG-magnetite was used as a substrate to link them into the primary antibodies (as detailed in 3.3.1.2). Linear sweep voltammetry detection was used. The graph in Figure 3.8 shows the response of the SPE electrode in the presence of a solution with the amino-PEG nanoparticles and different concentrations of the 4D5 antibody. In Figure 3.8 (a) the peak noted at 0.60 V in the linear sweep voltammogram and in (b) the calibration plot was constructed by plotting the current associated with peak at 0.60 V against the log of antibody concentration. The optimal concentration of monoclonal mouse 4D5 antibody is that which provides a maximum amplitude signal without reaching the system saturation level. In this case, as can be seen, the optimal concentration was 0.123  $\mu\text{g/ml}$ . This concentration was used in the final indirect displacement assay.

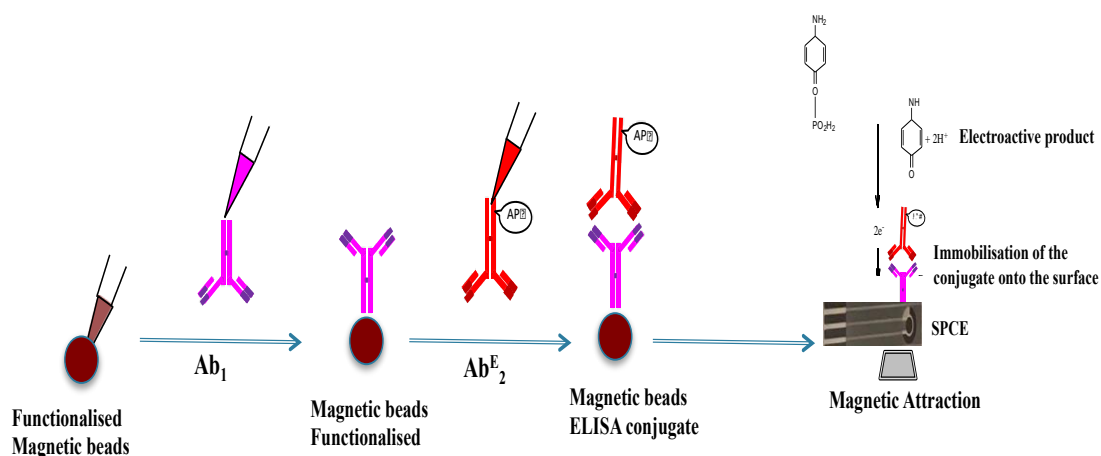


Figure 3.7: Schematic of typical EI steps using magnetic beads  $[\text{Fe}_3\text{O}_4]$  as solid surface material for immobilisation of immunoreagents. The immunocomplex is composed of a capture antibody ( $\text{Ab}_1$ ) and a secondary antibody ( $\text{Ab}_2$ ) labelled with redox enzyme (E). The magnetic bead-capture ELISA conjugate is attached to the screen-printed-electrode by magnetic attraction for electrochemical measurements.

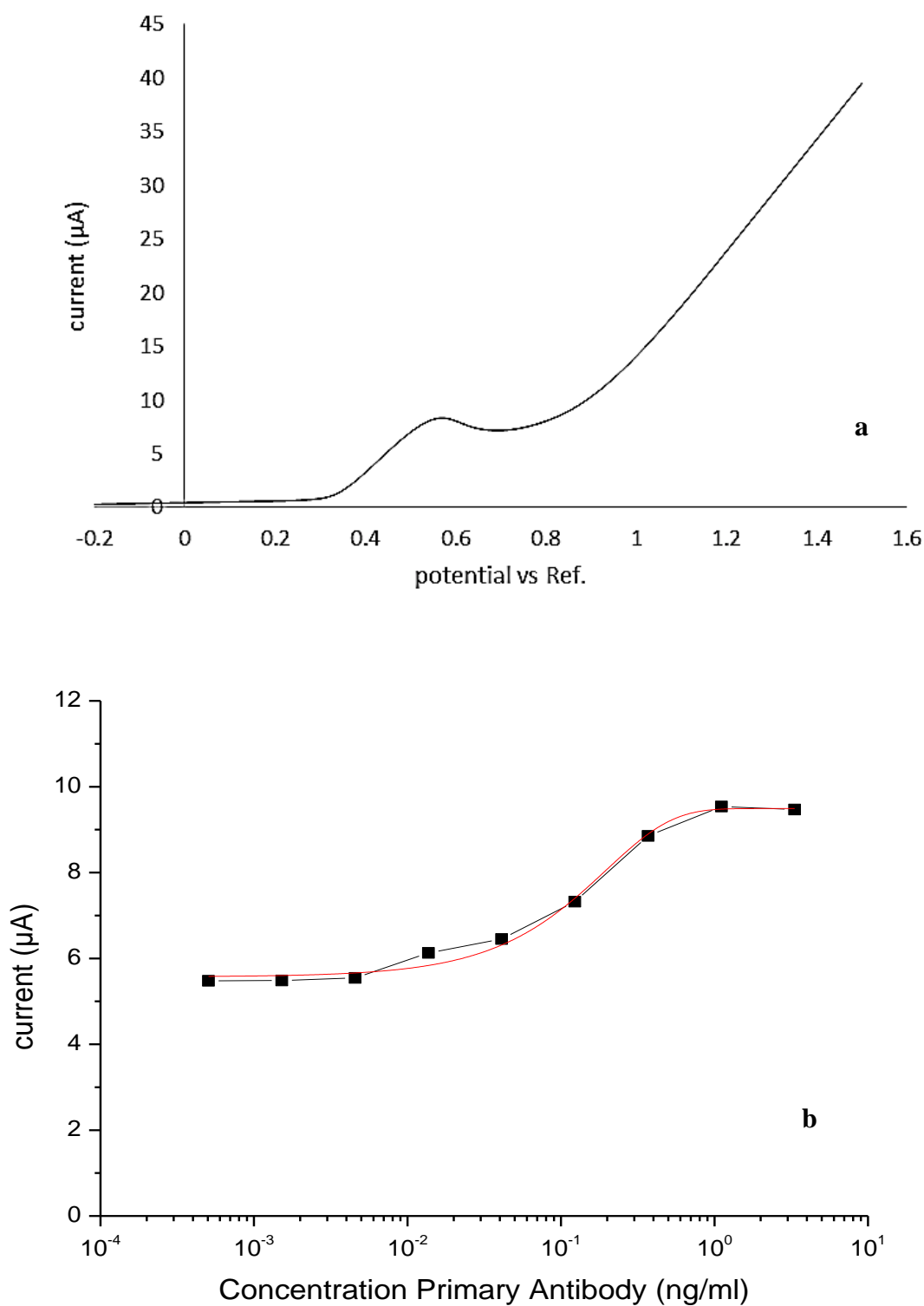


Figure 3.8: (a) Linear sweep voltammogram obtained from the application of the capture assay at concentration antibody of  $1.11 \mu\text{g/ml}$ . (b) Calibration plot for the monoclonal mouse 4D5 antibody using magneto-electrochemical immunoassay based on the current measured at the peak at 0.06 V in the linear sweep voltammogram.

- **Displacement assay on ferromagnetic particles**

This is the final experiment to detect BaP. In this study the ferromagnetic particles were coated with PEG polymer. The diagram for displacement assay is shown in Figure 3.9. Figure 3.10 shows the linear sweep voltammogram for BaP concentration of 13.7 ng/ml and the calibration curve of the assay. The performance of the system showed a limit of detection of 0.5 ng/ml. In addition, the response showed a linear range from 13.7 to 123 ng/ml. A single measurement with linear sweep voltammetry was done in 16s.

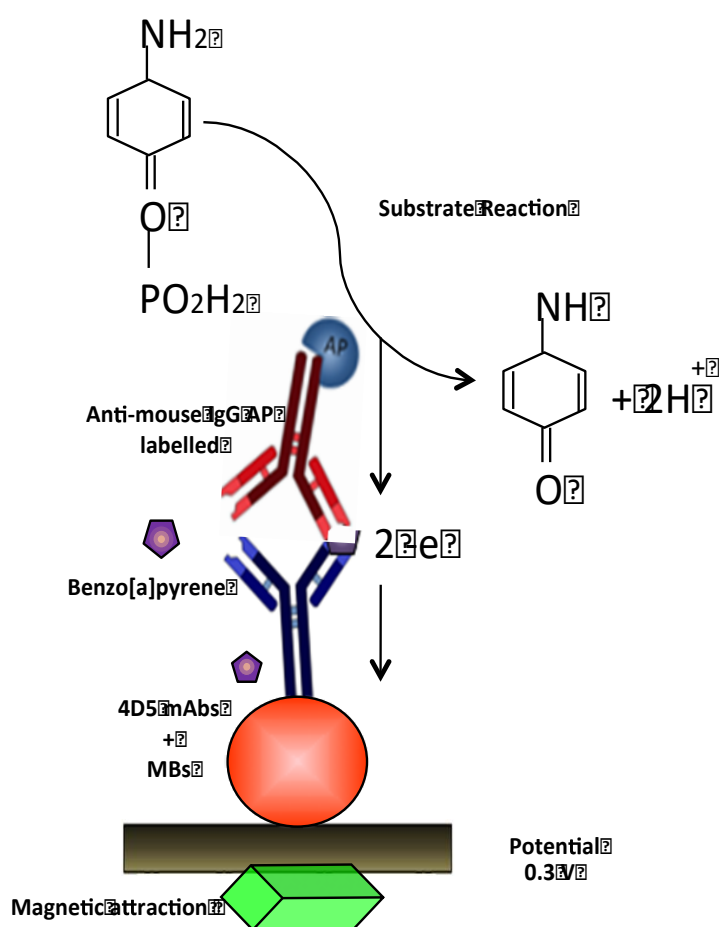


Figure 3.9: A schematic illustrates a typical ELISA format involved in the displacement assay.

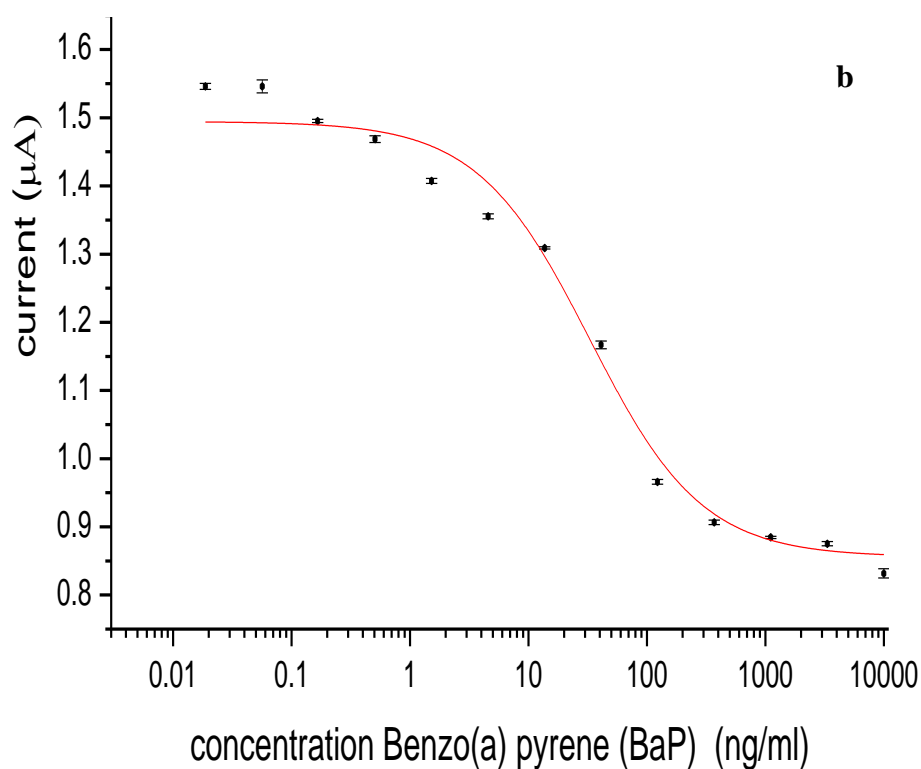
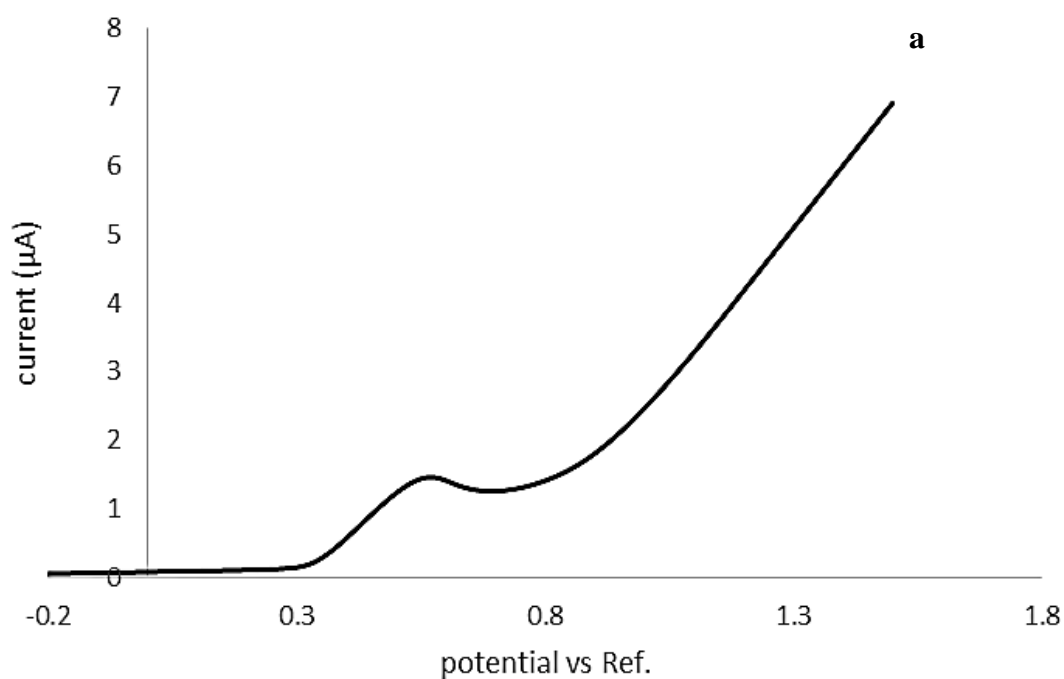


Figure. 3.10: (a) Linear sweep voltammogram obtained from the application of the displacement assay at concentration BaP of 13.7 ng/ml (b) Calibration curve obtained with the current peaks at 0.60 V found linear sweep voltammogram for each concentration Benzo[a]pyrene (BaP) (range of concentrations from 0.01 ng/ml to 10 μg/ml)

### 3.3.4 Conclusion

In this work we have presented the development of an immunochemical method of detection for (BaP).  $[\text{Fe}_3\text{O}_4]$  particles were used as solid surface where all the immunoreactions occurred. Optimisation of the immunoassay was done by isolating the different reagents and studying the response of the system before saturation. This is a detail that will be beneficial for the long term goal of a portable solution for the on-the-spot measurement of BaP in drinkable water, as it will be possible to carry out all the steps in the immunoassay in the lab, with the exception of the final addition of the sample; this then can be left to the operator who is in the field and providing the required information about real time situation of the measured drinking source, such as a river. The use of linear sweep voltammetry in combination with the immunoassay- ferromagnetic particles offered a low limit of detection (0.5ng/ml) for the screening of Benzo[a]pyrene (BaP).

The combination of linear sweep voltammetry detection with the particles provides a simple protocol that could be integrated in small portable systems. Although the limit of detection reached was not as low as we would have desired, further study will investigate the increase in sensitivity. One potential problem that may hinder the sensitivity was not having sufficient nanoparticles available to bind to our antibodies. This issue will be investigated by optimizing the concentration of magnetic nanoparticles. A second parameter that may be affecting our results is the orientation of the antibodies that are linked to the surface of the magnetic beads. It will be investigated by using alternative types of covalent immobilisation, such as direct chemistry (Periodate oxidation method) or introducing another kind of crosslinker (hemobiofunctional coupling).

Future work will integrate the already developed protocol based on magnetic nanoparticles into a lab-on-a-chip platform, which will help to reduce the number of steps and incubation time (this is due to the increase of surface-to-volume ratio). The use of such platforms will also make it possible to automat the steps that the immunoassay requires. Therefore, the integration into a portable lab-on-a-chip solution could represent a future platform for monitoring water quality and avoid costly and non-efficient analysis of water samples in dedicated laboratories.

### 3.3.5 References

1. Butler GJ, Neale R, Green AC, Pandeya N, Whiteman DC. Nonsteroidal anti-inflammatory drugs and the risk of actinic keratoses and squamous cell cancers of the skin. *Jour of the Amer Acad of Dermat.* 2005 Dec 1;53(6):966-72 .
2. Hayat A, Catanante G, Marty JL. Current trends in nanomaterial-based amperometric biosensors. *Sensors.* 2014 Dec;14(12):23439-61.
3. Fähnrich KA, Pravda M, Guilbault GG. Immunochemical detection of polycyclic aromatic hydrocarbons (PAHs). *Anal Letters.* 2002 May 8;35(8):1269-300.
4. Ramírez NB, Salgado AM, Valdman B. The evolution and developments of immunosensors for health and environmental monitoring: problems and perspectives. *Brazil Jour of Chem Eng.* 2009 Apr;26(2):227-49.
5. Zhang YH, Su Q, Xu JH, Zhang Y, Chen ST. Detecting of Benzo [a] pyrene Using a Label-free Amperometric Immunosensor. *Int. J. Electrochem. Sci.* 2014 Jul 1;9:3736-45.
6. Sassolas A, Prieto-Simón B, Marty JL. Biosensors for pesticide detection: new trends. *Ameri Jour of Anal Chem.* 2012 Mar 28;3(03):210.
7. Bansal V, Kumar P, Kwon EE, Kim KH. Review of the quantification techniques for polycyclic aromatic hydrocarbons (PAHs) in food products. *Crit Rev in Food Sc and*

Nutrition. 2017 Oct 13;57(15):3297-312.

8. Sassolas A, Prieto-Simón B, Marty JL. Biosensors for pesticide detection: new trends. *Amer Jour of Anal Chem.* 2012 Mar 28;3(03):210.

9. Ahmad A, Moore E. Electrochemical immunosensor modified with self-assembled monolayer of 11-mercaptoundecanoic acid on gold electrodes for detection of benzo [a] pyrene in water. *Analyst.* 2012;137(24):5839-44.

10. Zheng X, Tian D, Duan S, Wei M, Liu S, Zhou C, Li Q, Wu G. Polypyrrole composite film for highly sensitive and selective electrochemical determination sensors. *Electrochimica Acta.* 2014 Jun 1;130:187-93.

11. Rodriguez BA, Trindade EK, Cabral DG, Soares EC, Menezes CE, Ferreira DC, Mendes RK, Dutra RF. Nanomaterials for advancing the health immunosensor. In *Biosensors-Micro and Nanoscale Applications* 2015 Sep 24 (pp. 347-374). IntechOpen.

12. Hennion MC, Barcelo D. Strengths and limitations of immunoassays for effective and efficient use for pesticide analysis in water samples: A review. *Analytica Chimica Acta.* 1998 Apr 24;362(1):3-4.

13. Barathi P, Senthil Kumar A. Electrochemical conversion of unreactive pyrene to highly redox-active 1, 2-quinone derivatives on a carbon nanotube-modified gold electrode surface and its selective hydrogen peroxide sensing. *Langmuir.* 2013 Aug 13;29(34):10617-23.

14. Sharma S, Byrne H, O'Kennedy RJ. Antibodies and antibody-derived analytical biosensors. *Essays in Biochem.* 2016 Jun 30;60(1):9-18.

15. Yu X, Xu D, Xu DW, Lv R, Liu ZH. An impedance biosensor array for label-free detection of multiple antigen-antibody reactions. *Front Biosci.* 2006 Jan 1;11:983-90.

16. Baskeyfield DE, Davis F, Magan N, Tothill IE. A membrane-based immunosensor for the analysis of the herbicide isoproturon. *Analytica chimica acta.* 2011 Aug 12;699(2):223-31.



17. Wilson MS. Electrochemical immunosensors for the simultaneous detection of two tumor markers. *Anal Chem.* 2005 Mar 1;77(5):1496-502.
18. Kašná A, Skládal P. A four-channel electrochemical immunosensor for detection of herbicides based on phenoxyalkanoic acids. *Internl Jour of Environ & Anal Chem.* 2003 Feb 1;83(2):101-9.
19. Wolska L, Rawa-Adkonis M, Namieśnik J. Determining PAHs and PCBs in aqueous samples: finding and evaluating sources of error. *Anal and Bioanal Chem.* 2005 Jul 1;382(6):1389-97.
20. Law RJ, Klungsoyr J. The analysis of polycyclic aromatic hydrocarbons in marine samples. *Internl Jour of Enviro and Pollut.* 2000 Jan 1;13(1-6):262-83.
21. Lang V. Polychlorinated biphenyls in the environment. *Jour of Chromat A.* 1992 Mar 20;595(1-2):1-43.
22. Fuoco R, Ceccarini A. Polychlorobiphenyls in Antarctic matrices. In *Environl Contam in Antar* 2001 Jan 1 (pp. 237-273). Elsevier Science.
23. Kim KH, Jahan SA, Kabir E, Brown RJ. A review of airborne polycyclic aromatic hydrocarbons (PAHs) and their human health effects. *Environment international.* 2013 Oct 1;60:71-80.
24. Arey J. Atmospheric reactions of PAHs including formation of nitroarenes. In *PAHs and related compounds* 1998 (pp. 347-385). Springer, Berlin, Heidelberg.
25. Drinking water directive. Available online: [https://ec.europa.eu/environment/water/water-drink/legislation\\_en.html](https://ec.europa.eu/environment/water/water-drink/legislation_en.html) (Accessed on 27th November, 2019)
26. Brooks SL, Turner AP. Biosensors for measurement and control. *Measurement and Control.* 1987 May;20(4):37-43.
27. Ngo TT, editor. *Electrochemical sensors in immunological analysis.* Springer Science

& Business Media; 2013 Nov 11.

28. Atkins P, De Paula J, Friedman R. *Quanta, matter, and change: a molecular approach to physical chemistry*. Oxford University Press; 2009.
29. Olsson MB, Persson BR, Salford LG, Schröder U. Ferromagnetic particles as contrast agent in T2 NMR imaging. *Magnetic Resonance Imaging*. 1986 Jan 1;4(5):437-40.
30. Shinkai M, Honda H, Kobayashi T. Preparation of fine magnetic particles and application for enzyme immobilization. *Biocatalysis*. 1991 Jan 1;5(1):61-9.
31. Ito A, Teranishi R, Kamei K, Yamaguchi M, Ono A, Masumoto S, Sonoda Y, Horie M, Kawabe Y, Kamihira M. Magnetically triggered transgene expression in mammalian cells by localized cellular heating of magnetic nanoparticles. *Jour of Bios and Bioeng*. 2019 Apr 5.
32. Shinkai M, Wang J, Kamihira M, Iwata M, Honda H, Kobayashi T. Rapid enzyme-linked immunosorbent assay with functional magnetite particles. *Jour of Fermen and Bioeng*. 1992 Jan 1;73(2):166-8.
33. Langer R, Weissleder R. Scientific discovery and the future of medicine. *JAMA*. 2015;313:135-6.
34. Abdorahim M, Rabiee M, Alhosseini SN, Tahriri M, Yazdanpanah S, Alavi SH, Tayebi L. Nanomaterials-based electrochemical immunosensors for cardiac troponin recognition: An illustrated review. *TrAC*. 2016 Sep 1;82:337-47.
35. Ju H. Sensitive biosensing strategy based on functional nanomaterials. *Science China Chemistry*. 2011 Aug 1;54(8):1202.
36. Kamin RA, Wilson GS. Rotating ring-disk enzyme electrode for biocatalysis kinetic studies and characterization of the immobilized enzyme layer. *Anal Chem*. 1980 Jul 1;52(8):1198-205.
37. Ding L, Cheng W, Wang X, Ding S, Ju H. Carbohydrate monolayer strategy for electrochemical assay of cell surface carbohydrate. *Jour of the Amer Chem Society*. 2008 May

20;130(23):7224-5.

38. Pan M, Gu Y, Yun Y, Li M, Jin X, Wang S. Nanomaterials for electrochemical immunosensing. *Sensors*. 2017 May;17(5):1041.

39. Lim SA, Ahmed MU. Electrochemical immunosensors and their recent nanomaterial-based signal amplification strategies: A review. *RSC Adv*. 2016;6(30):24995-5014.

40. Hu W, Li CM. Nanomaterial-based advanced immunoassays. *Wiley Interdisciplinary Reviews: Nanomed and Nanobiotech*. 2011 Mar;3(2):119-33.

41. Zhu C, Yang G, Li H, Du D, Lin Y. Electrochemical sensors and biosensors based on nanomaterials and nanostructures. *Anal Chem*. 2014 Dec 19;87(1):230-49.

42. Wang F, Hu S. Electrochemical sensors based on metal and semiconductor nanoparticles. *Microchimica Acta*. 2009 Apr 1;165(1-2):1-22.

43. Wong SS, Jameson DM. Chemistry of protein and nucleic acid cross-linking and conjugation. *CRC Press*; 2011 Oct 10.

# **Chapter 4**

## **Development and Characterisation of a lab on a chip electrochemical immunosensor array**



#### 4.1. Aim and Novelty

The main objective of this study was to develop an electrochemical immunoassay using microfluidic-integrated system (lab on a chip) for screening of PAHs in environmental monitoring of water. Development of an electrochemical cell-on chip configured in a three-electrode system and its characterisation for electrochemical application has been described. In this study, the chips were tested using PalmSens and contact angle instrument. The influence of different scan rates was studied in order to investigate the electrochemical process. The important aspect of the immunosensor is the method of immobilisation of antibodies to ensure the correct formation on the surface. Self Assembled Monolayer (SAM) was developed in order to achieve a specific attachment of antibody to study the SAM behaviour, Characterisation of monolayers on gold electrode has been carried out using CV, and contact angle measurements. CV was performed to determine the mechanism of electrochemical reactions on the SAM layer. The goal of these electrochemical tests was to characterise the developed chip as a platform to be used in microfluidic-integrated system (lab on a chip). The alkaline phosphate (AP) enzyme used specifically converts the substrate (*para* –aminophenyl phosphate) (pAPP) into a measurable signal. The pAPP is dephosphorylated to form *p*- aminophenol (*p*AP) by reaction with enzyme, which was the oxidised at 0.300 mV to form the imino-quinone, thus 2 electrons were generated (figure 4.1). The pAPP was chosen because of the product of *p*AP can be oxidised at much less positive potential than the nitrophenol, an enzymatic product from nitrophenyl phosphate which would usually be used as an AP substrate for spectrophotometric detection.

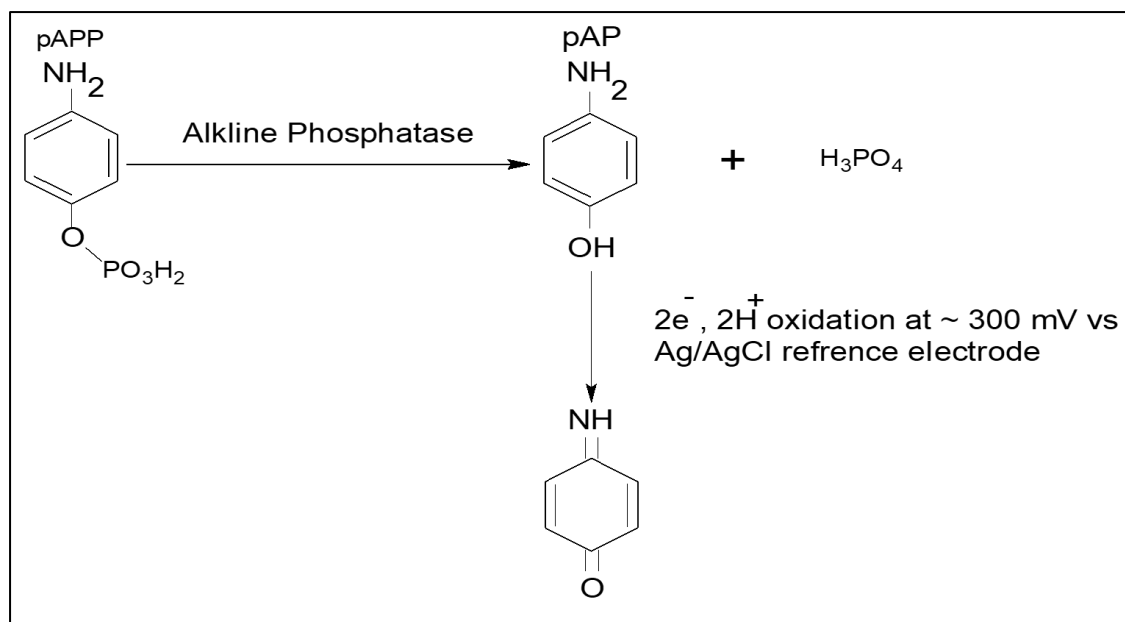


Figure 4.1: Amperometric detection using an AP used as enzyme label. The substrate used was pAPP. At the potential applied (300 mV) pAPP undergoes 2 electrons oxidation to generate p-aminophenol (pAP) as a final product.

## 4.2 Introduction

Electronic technology allows for the miniaturization of a variety of devices. In order to achieve this goal, the microfluidic technology has to be integrated and must be able to analyse complex samples having various antigens. The label free techniques will become more significant in the near future. Inexpensive screen-printed electrodes will become more prevalent, which will permit the thorough screening of a large number of samples. The diagnosis of human health, quality control of food and water supplies will be easily monitored by a combination of electrochemical immunoassay methods, namely lateral flow assays, ELISA and enzymatic glucose biosensors. Academic research indicates the presence of a variety of smart materials into the immunoassay system. [1-3]. The market for electrochemical immunoassays in the medical market in the U.S. has seen an annual increase of 6 % [4] Companies, such as Abbott Diagnostics, Beckman Coulter, bioMerieux, Roche Diagnostics and Siemens Healthcare are now

involved in manufacturing devices for oncology and endocrinology. It has been estimated that these devices will achieve a 75 % share by 2020, as a result of coupling the devices with cell phones and wireless technologies.

### **4.3 Materials and Methods**

#### **4.3.1 Reagents**

11-mercaptoundecanoic acid (11-MUA), EDC, NHS, Potassium ferricyanide/ferrocyanide, acetone, 1-isopropyl alcohol, and ethanol were purchased from Sigma Aldrich (Dublin, Ireland). Bovine serum albumin (BSA), 1-ethyl-3-(3-dimethylaminopropyl) carbodiimide (EDAC), Hydrochloric acid 37% were purchased from KMG ULTRA CHEMICALS LTD (England). Monoclonal mouse antibody 4D5 was bought from Santa Cruz (Heidelberg, Germany). Sodium hydrogen carbonate, sodium chloride, detergent Tween-20, Tris salt, BaP, alkaline phosphatase (AP), and labelled goat anti-mouse antibodies (whole molecules), all were bought from Sigma (Dublin, Ireland). For the electrochemical tests the substrate was para-aminophenyl phosphate (pAPP) salt, which was bought from Gold Biotechnology Inc., (USA). Potassium chloride (KCl) and Diethanolamine (DEA) were bought from Sigma (Dublin, Ireland). All reagents were of analytical grade or better, and any water used in the solutions was nanopure water.

#### **4.3.2 Instrumentations**

A PalmSens potentiostat (Palm Instrument BV, the Netherlands) was used for the electrochemical measurements. For incubation, a Biometra OV3 Incubator (Gottingen, Germany) was set at 37 °C. A Plasma Cleaner (45watts). (Harrick Plasma, Ithaca, New York) was used for removing organic molecules from the surface of the chip.



A Nitrogen spray gun was used to dry the chip between measurements. A nanopure water system was bought from ELGA.

#### 4.3.3 The fabrication of the biochip

The immunosensor consisted of an electrochemical cell- on- chip It was a three-electrode system (gold as working and counter electrode and Ag/AgCl reference electrodes). The chip was configured in a multi-electrode array screening for real time environmental measurements. An electrochemical immunosensor array was for the simultaneous detection of PAHs. Design and fabrication of this electrode as shown in Figure 4.2 was performed in the Tyndall National Institute. Each individual electrochemical cell has working electrode ( $1.822\text{ mm}^2$ ), counter electrode ( $3.280\text{ mm}^2$ ) and reference electrode ( $2.18\text{ mm}^2$ ). The overall chip size is ( $6.733\text{ mm} \times 24.7\text{ mm}$ ).

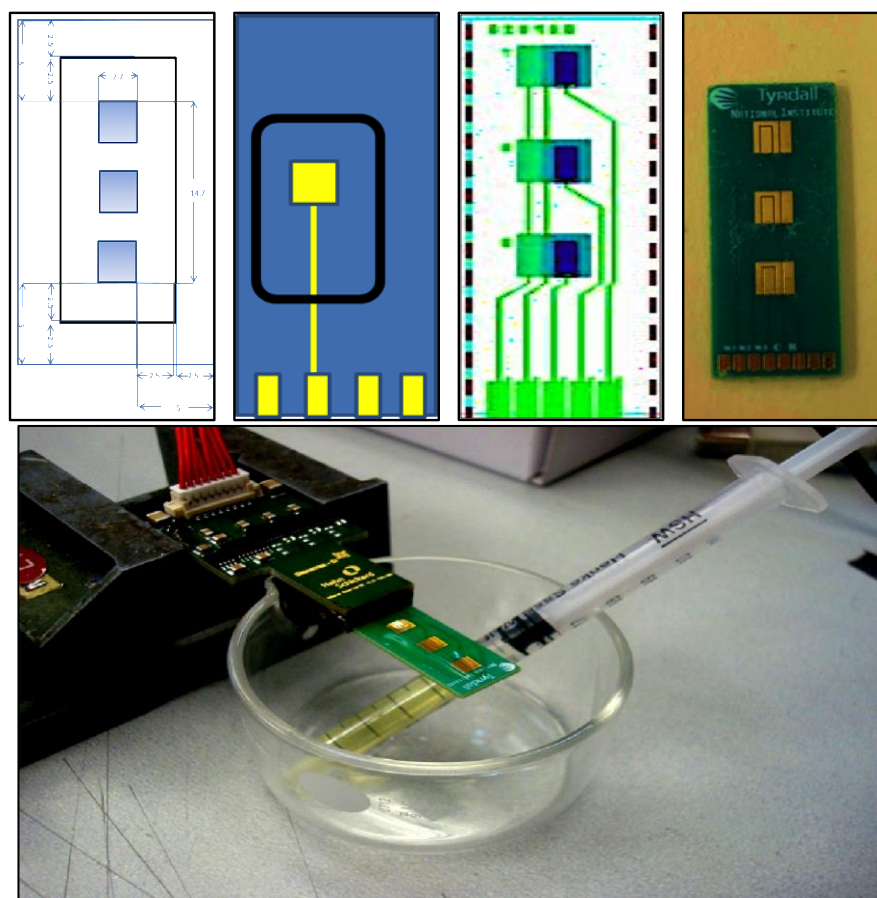


Figure 4.2: Fabricated chip in a three-electrode system.

#### 4.3.4 Characterisation and preparation of the gold chip

Electrochemical characterisation measurements were carried out with a PalmSens portable potentiostat. In order to connect the chip to the PalmSens, the interface for three-electrode system, which acts as a connector, was designed (see Figure 4.3). The PalmSens was connected to a laptop computer for conducting tests in the laboratory.

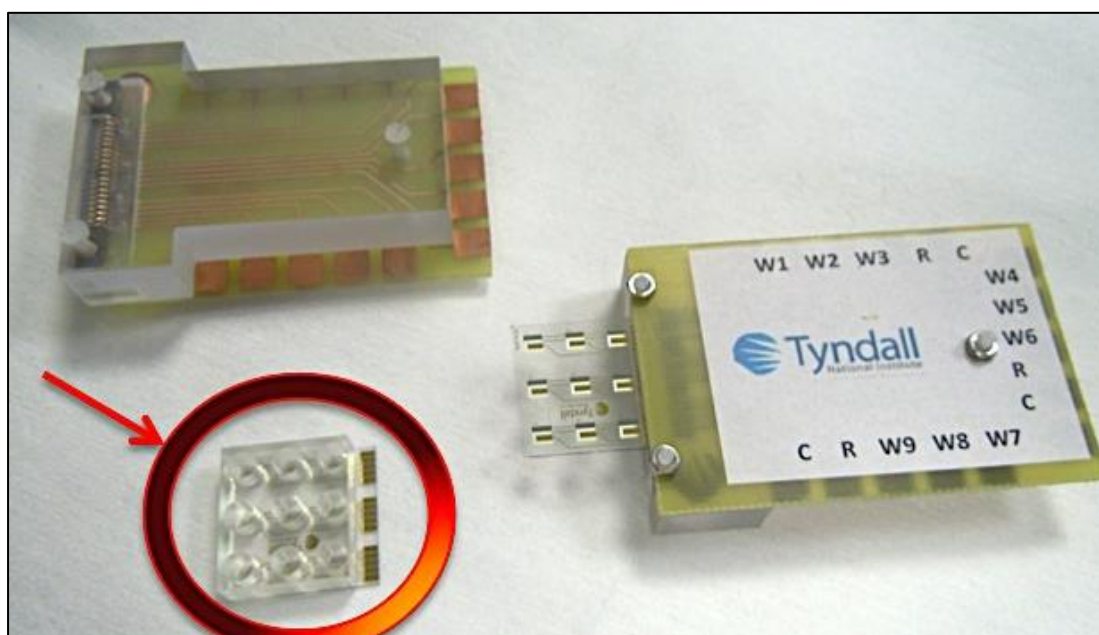


Figure 4.3: Electrochemical sensing array, with interface for connection to PalmSens detector and reservoir device for sample addition.

The gold chips were tested using cyclic voltammetry (CV). CV detects the redox behaviour of species within a potential range. CV measurements were performed in the presence of 5 mM ferri/ferrocyanide in 0.1M KCL at a scan rate of 50 mV/s between the applied potential ranges of -0.2 to 0.8 V.

##### 4.3.4.1 Studies on the influence of scan rate

In order to study the effect of the scan rate, the chip was characterised between -0.2 to 0.8 V in the aqueous electrolyte of ferri/ferrocyanide with the presence of

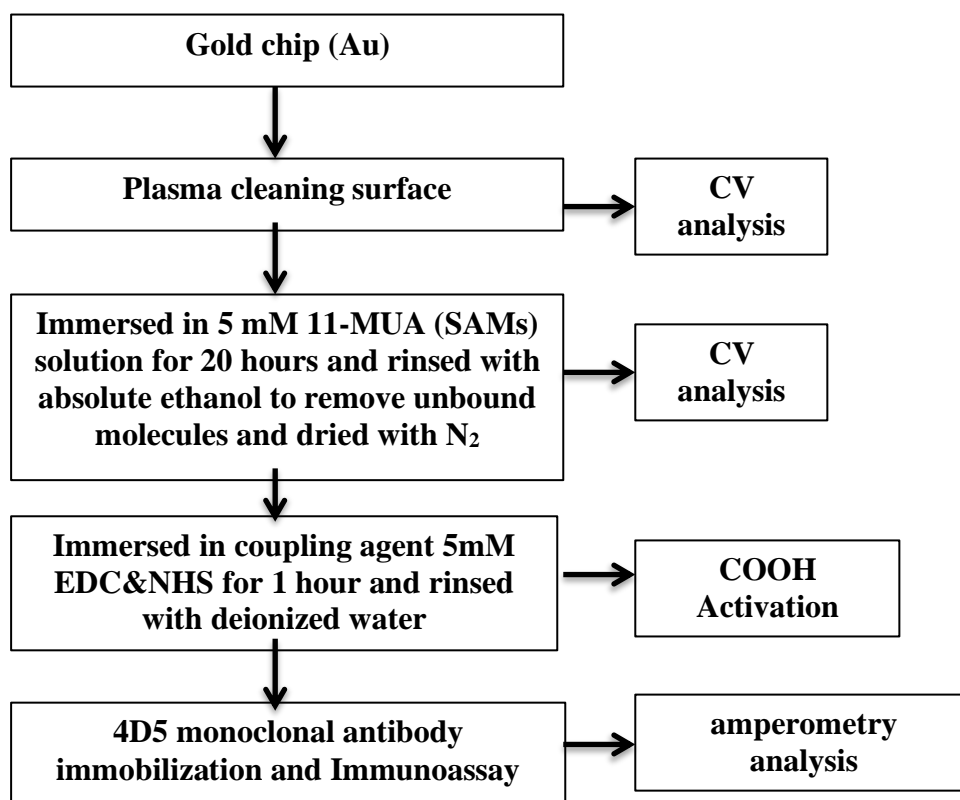
0.1M KCL. The CV measurements were performed in various scan rates from 5 to 200 mV/s at room temperature (25 °C).

#### 4.3.4.2 Gold chip cleaning protocols

In order to ensure that the gold chip surfaces were clean for electrochemical tests, the three-electrode systems were optimized with two cleaning protocols. The two cleaning protocols were ultrasonicating and plasma treatment. After this, the chips were cycled three times in the aqueous electrolyte of ferri/ferrocyanide with the presence of 0.1M KCL at a scan rate of 50 mV/s. The potential was selected between a range of -0.2 and 0.8 V.

- Ultrasonicating: The gold chips were cleaned firstly in acetone and then in 1-isopropyl alcohol and lastly in deionised water. Each clean took 5 minutes.
- The gold chips were cleaned in Plasma Cleaner for 20 minutes (45 watts).

#### 4.3.4.3. Gold chip modification procedure (Self Assembled Monolayers (SAM))



#### **4.3.4.4 Contact angle measurements**

Drop contact angle tests were performed in order to measure the surface hydrophobicity of the SAM surface. To form the droplet, the deionised water was pumped out of a syringe system at medium rate, namely 1  $\mu\text{l}$  / s. 1  $\mu\text{l}$  drop of water was placed on the surface. Tests were repeated for 3 drops on each chip (n=3).

#### **4.3.4.5 Amperometric detection**

Amperometric measurement with PalmSens allows for a simple device, which could be used as a portable solution for *in situ* measurement. The measurement was set to 60 seconds *pAPP* ds and the potential was applied at 0.3 V versus Ag/AgCl. The current was measured and was allowed to reach the stable baseline. The final concentration of the *pAPP* in the buffer was 3mM. The *pAPP* solution was freshly made up and stored in a dark area, as it was sensitive to light.

### **4.4 Lab on a chip design**

For the design of the fluidic interface, a fluidic cartridge was fabricated by the injection moulding. Injection moulding is a method of making plastic parts by melting the plastic substance and injecting this into an injection mould tool. This can be seen in Figure 4.4. Its main functions were to hold the fluids under analysis and to cover the whole surface of the gold chip. The fluid was driven via a set of valves and a portable pump, which were controlled by the electronic module .Figure 4.5 showing the fluidic channels across the chip and the portable pump and the valve control tab. Figure 4.6 shows an image of a euro coin to help clarify dimensions of the setup.

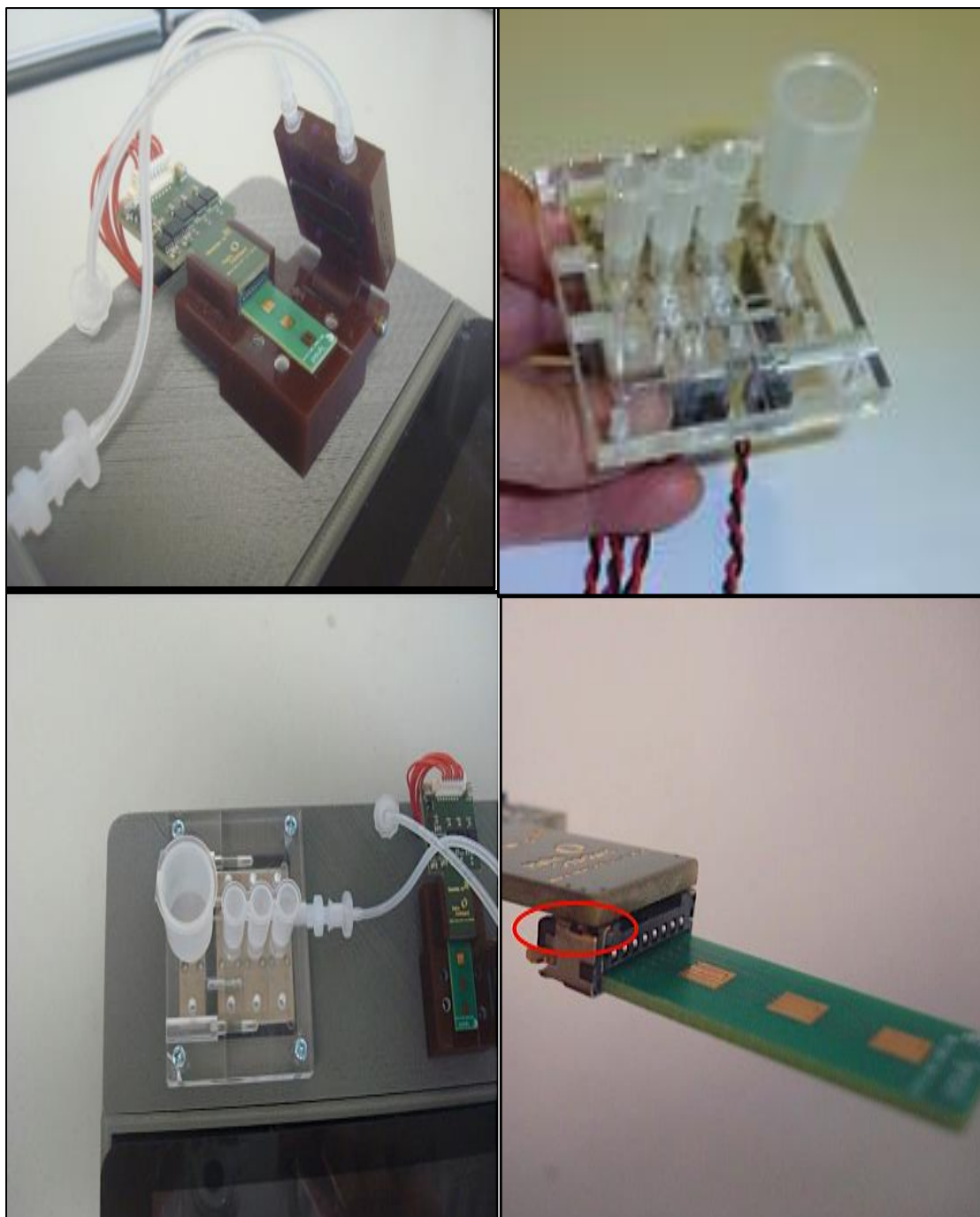


Figure 4.4: (left) Microfluidic cartridge with immunosensor and (right) fluidic manifold with valves to control fluid



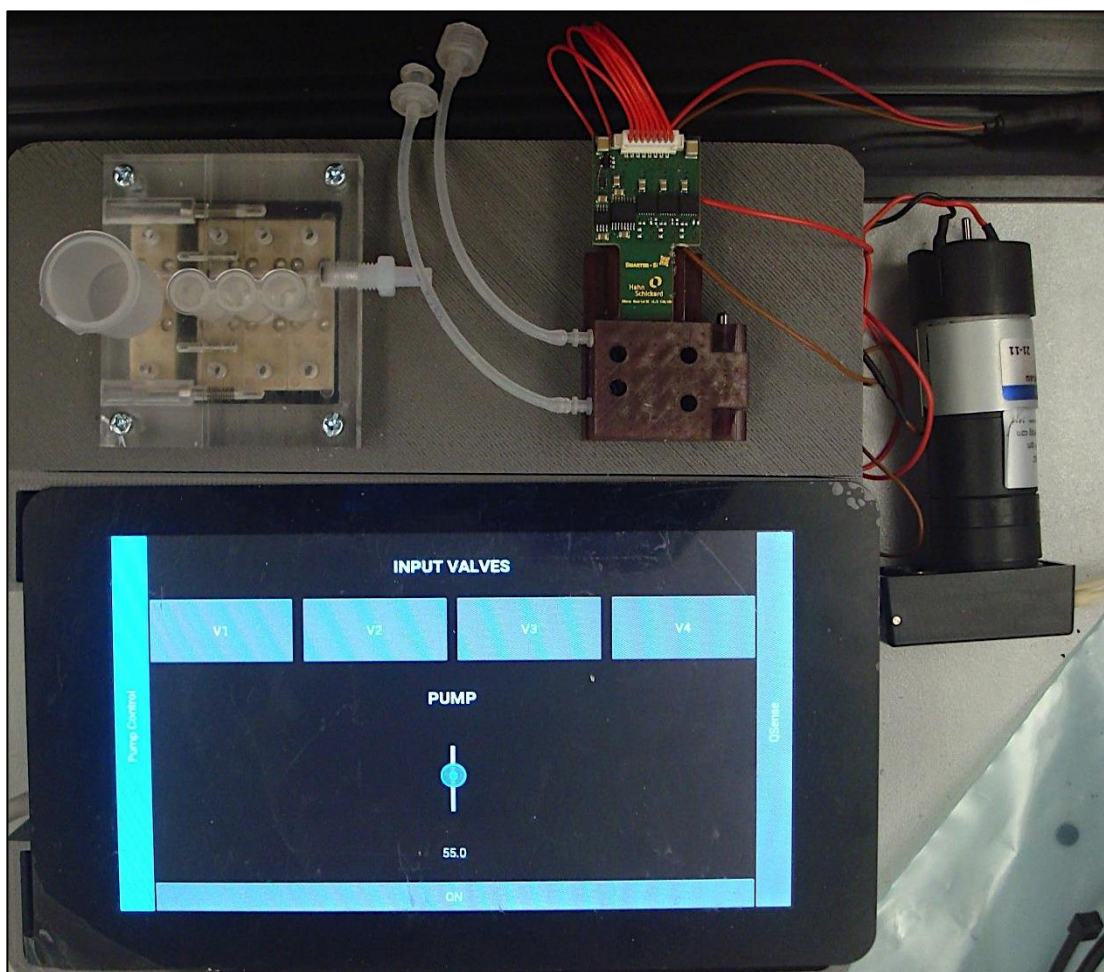


Figure 4.5: The fluid channels across the chip , fluidic cell with electrode chip electronics, portable pump and valve control Tab.

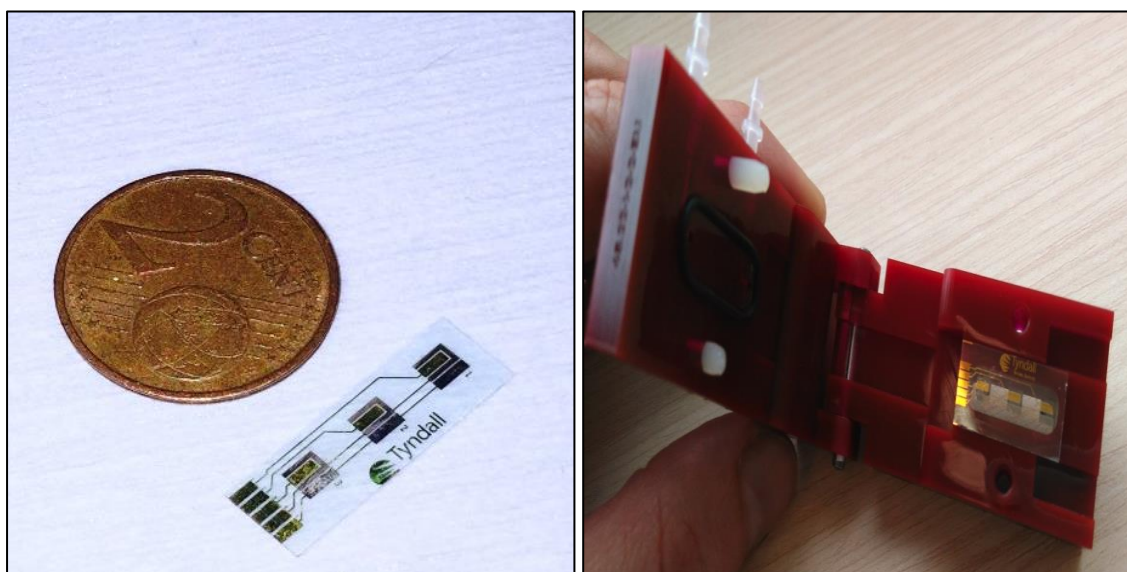


Figure 4.6: Images of a euro coin to help clarify dimensions of the setup and the microfluidic cell with the chip.

The electronic module unit was responsible for fluidic control (Figure 4.7). Amperometric electrochemical detection was embedded in a microfluidic device, which could be used to detect the presence of an electrochemically active species in the sample under study.



Figure 4.7: Control module, containing interfaces for microfluidics, immunosensor and user display.



## 4.5 Smarter-SI Q-Sense (Measurement GUI)

In the Q-Sense cell when the potential was applied to the system, electrostatic force was generated that could be made to cause liquid flows to move, merge, mix, spilt, and dispense from valves. The operation of the integrated system was achieved using Q-Sense GUI. The device was designed with a specific application. Figures [4.8- 4.12] show the images for the GUI of Q-Sense.

### 4.5.1. Raspian Desktop

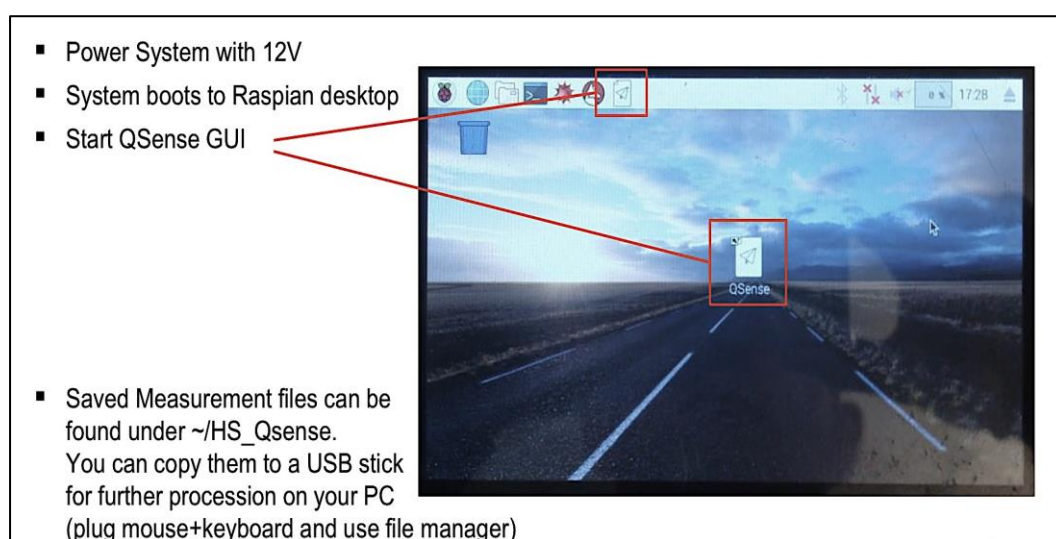


Figure 4.8: Q-sense system desktop

### 4.5.2. GUI – Tabs

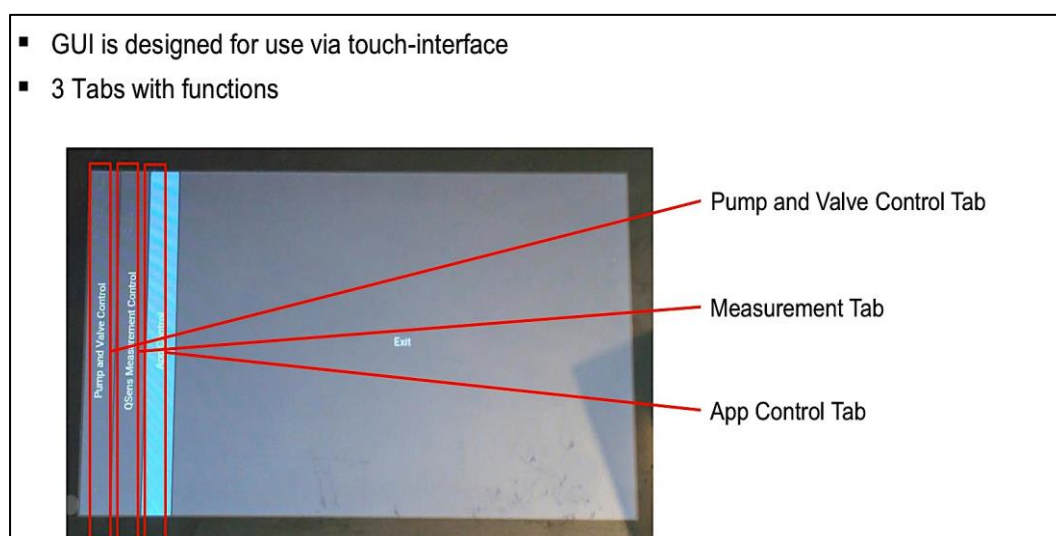


Figure 4.9: Q-sense system Tabs



### 4.5.3. GUI – Pump and Valve Control Tab

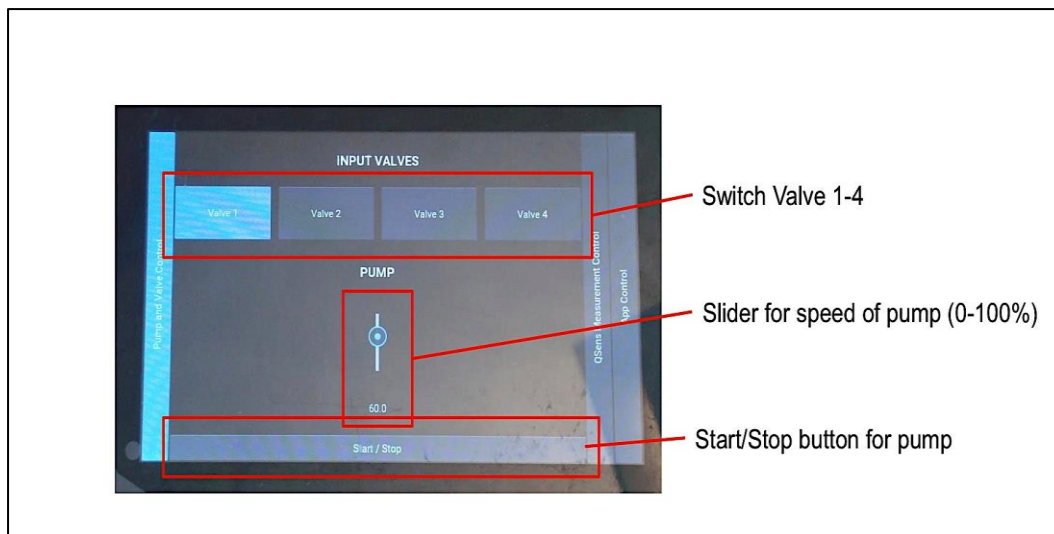


Figure 4.10: Q-sense system pump and valve control Tab

### 4.5.4. GUI – Measurement Control Tab

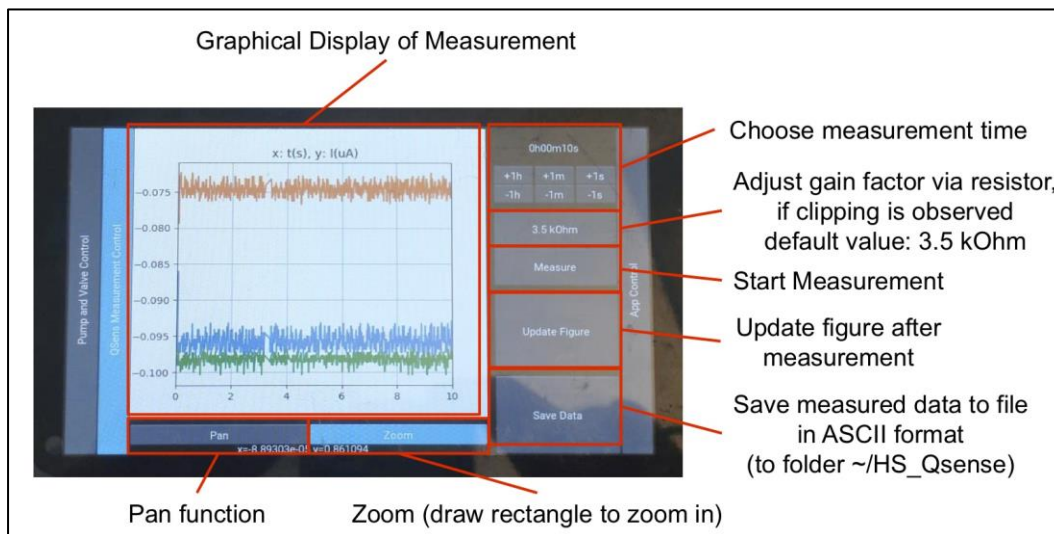


Figure 4.11: Q-sense system measurement control Tab

#### 4.5.5. GUI – App Control Tab

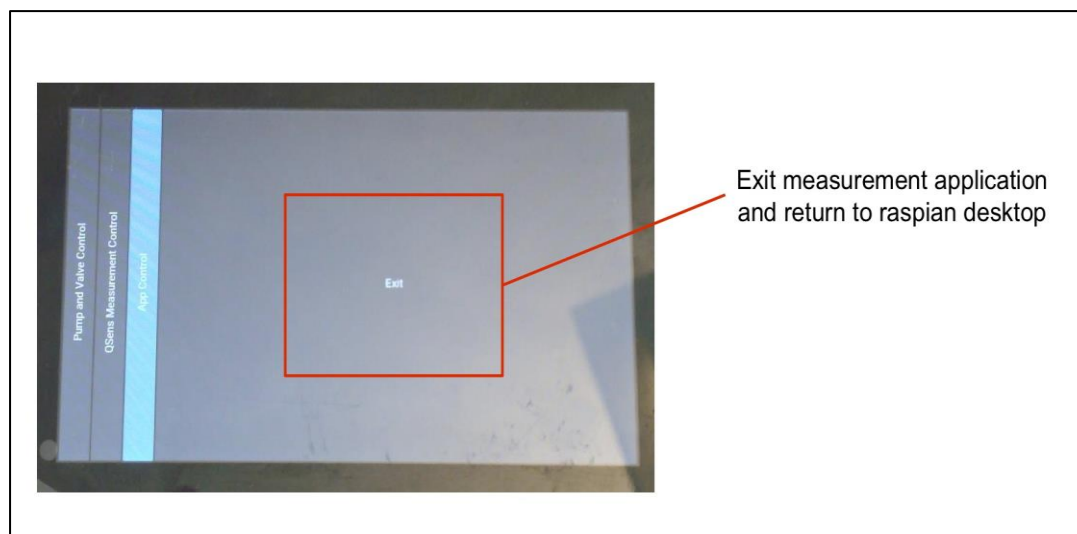


Figure 4.12: Q-sense system App control Tab

Simulations were also carried out to guarantee flow in the system. The software was called COMSOL (Figure 4.13). The simulation was liquid flow as it came in from the inlet and left at the outlet. It basically tells us the distribution of liquid in the chamber. Blue colour for higher quantity and lighter colour for less. These simulations provided an insight into how the liquid flow spreads in the area of the microfluidic capsule. Visualisation of the flow ensures the avoidance of dead areas that would not be covered by liquid. As can be seen in Figure 4.10, the liquid is expected to spread evenly in the space given by the microfluidic capsule. Velocity profile in microfluidic channels helps to understand how the fluid behaves while it is transported through the system and the nature of the fluid and direction of the fluid particles. Velocity profile shows the difference in intensity of resistance of fluid particles across the flow, due to cohesive and adhesive forces. The blue-to-red rainbow represents the flow-velocity magnitude distribution (laminar flow).

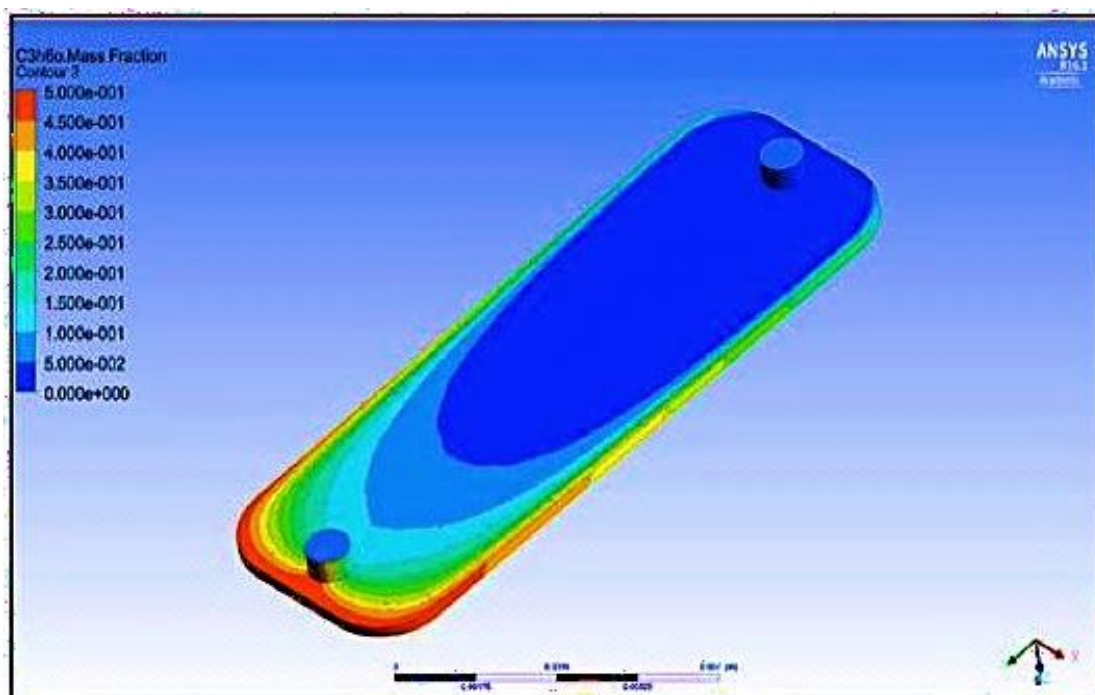


Figure 4.13: Simulations of liquid flow from inlet to outlet at microfluidic capsule (pressure driven flow).

## 4.6 Results and discussions

### 4.6.1 Characterisation of the gold chip

#### 4.6.1.1 Influence of scan rate

The effect of the scan rate was investigated using the CVs over the range of 5 to 200 mV/s for the ferrocyanide redox probe. As shown in Figure 4.12, large peak separation was observed by increasing the scan rate. The effect of increasing the scan rate resulted in the higher current. The current was found to be directly proportional to the square root of the scan rate indicating diffusion limited process, which is governed by the Randles–Sevcik equation

$$i_p = (2.69 \times 10^{-5}) n^{3/2} A D^{1/2} C v^{1/2} \quad \text{Equation (1)}$$

where  $i_p$  is the peak current,  $A$  is the area of the working electrode,  $C$  is the concentration of the electroactive species at the electrode,  $D$  is the diffusion coefficient

of the electroactive species,  $v$  is the scan rate, and  $n$  is the number of electrons in the redox reaction. A good linear correlation was obtained between the anodic peak height and the square root of the applied scan rates, as shown in Figure 4.14.

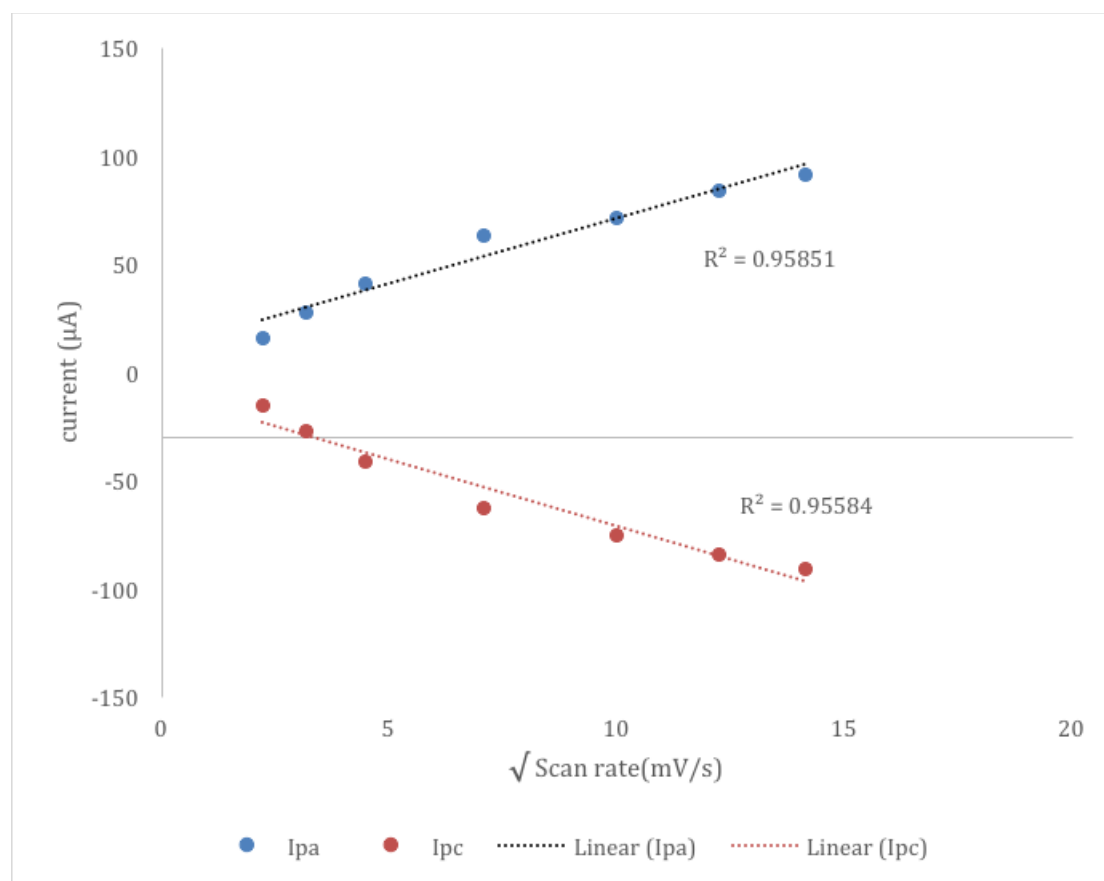


Figure 4.14: Influence of the square root of scan rates of 5 mM ferri/ferrocyanide at a bare chip. Supporting electrolyte was 0.1 M KCL

The table below indicates CV data for the oxidation of 5 mM ferri/ferrocyanide in 0.1 M KCL with different scan rates. CV tests were carried out at room temperature (25°C). A shift in anodic peak potential with increasing scan rate indicates a quasi-reversible or “irreversible” reaction.

Table 4.1: Influence of scan rate on the peak potential for 5 Mm ferrocyanide. The scan rate were 5 mV/s, 10 mV/s, 20 mV/s, 50 mV/s, 100 mV/s, 150 mV/s and 200 mV/s.

Scan rate (mV/s)	$E_{\text{mid}}$ vs Ref. (mV) <sup>a</sup>	$\Delta E_p$ (mV) <sup>b</sup>	$E_{\text{pa}}$ (mV/s) <sup>c</sup>
<b>5</b>	122	228	230
<b>10</b>	132	256	260
<b>20</b>	161	318	320
<b>50</b>	210	340	350
<b>100</b>	239	282	380
<b>150</b>	285	290	430
<b>200</b>	296	288	440

<sup>a</sup> Measured from the value  $\frac{1}{2} (E_{\text{pc}} + E_{\text{pa}})$  versus versus Ag/AgCl reference electrode

<sup>b</sup>  $\Delta E_p = (E_{\text{pc}} - E_{\text{pa}})$

<sup>c</sup>  $E_p$  anodic data here as a function of scan rate

#### 4.6.1.2 Influence of chip cleaning protocols

Cleaning and substrate preparation were important steps in order to study the surface phenomenon as they can improve the surface state for better electrochemical activates to take place. In this research, we employed two different established protocols to clean the chip for electrode regeneration. Chip cleanliness can be measured by looking at the potential differences between peak-to-peak separation of anodic and cathodic peaks. Figure 4.15 illustrates the CVs after treating the chips using all the considered cleaning protocols, as already described in section 4.3.4.2. Considering the theoretical value of  $\Delta E_p$  is 59 mV for single electron transfer of ferri/ferrocyanide redox couple, the closest experimental value of  $\Delta E_p$  (58 mV) was achieved when the CV was performed using

the chip treated with the plasma asher (45 watts). Plasma cleaning involves the removal of contamination from the surface through the use of energetic plasma created from oxygen gas species. Compared to other cleaning protocols, plasma-cleaning method shows well-defined peak. For this reason, we constantly used this method as our cleaning protocol for further electrochemical investigation.

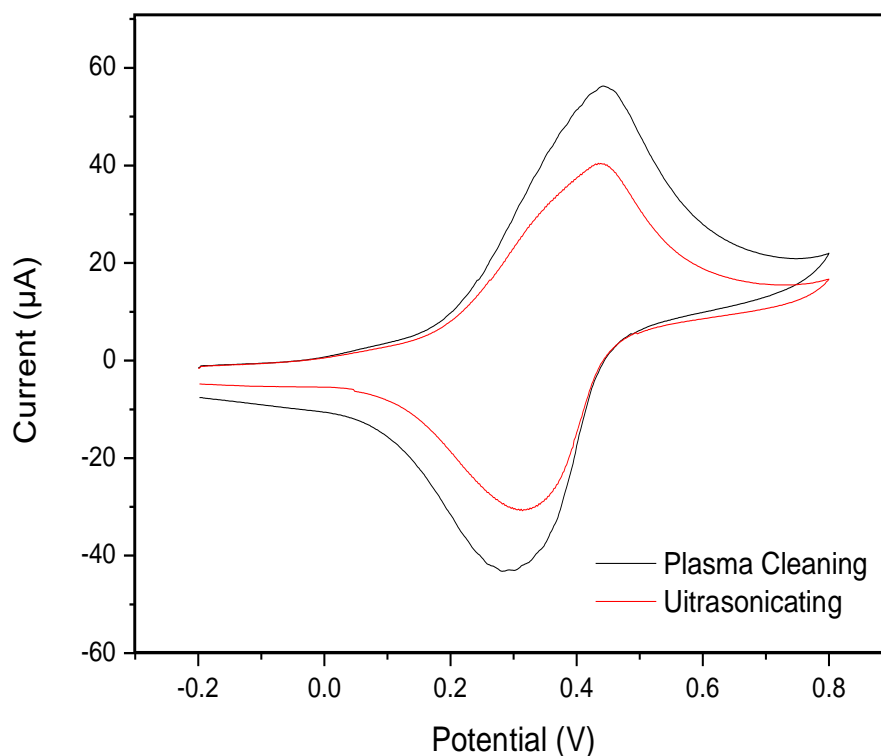


Figure 4.15: Studies on different chip cleaning protocols. CV was scanned in 5 mM ferri/ferrocyanide redox couple with a 50 mV/s scan rate.

#### 4.6.1.3 Gold chip arrays modification procedure (Self Assembled Monolayers (SAM))

A self-assembly of 11-MUA was used to modify the gold chip in order to control the orientation of the biomolecules (Abs) binding to the surface. The approach performed involved the modification of the gold chip using carboxylic acid terminated SAMs. The chemisorption of thiol and disulfides on gold chips has

become one of the most common applications of SAMs. CV measurements in Figure 4.16 show a decrease of ferri/ferrocyanide anodic and cathodic peak current after the immobilisation of 11-MUA SAM on the chip surface. This situation is caused by the reduced mass transport of highly ordered monolayers which blocked the probe molecules, thus preventing them to penetrate through the well-packed layer. Low current was observed for the 11-MUA SAM immobilised gold electrode, evidencing surface saturation and suggesting that a monolayer of fixed molecules was achieved. The addition of EDC/NHS to the carboxylic acid terminated SAMs increased the coverage of the antibodies. The primary monoclonal antibody was performed 30 minutes at 37 °C after the activation of EDC/NHS. As shown in CV, after the introduction of protein, the reaction became more and more irreversible.

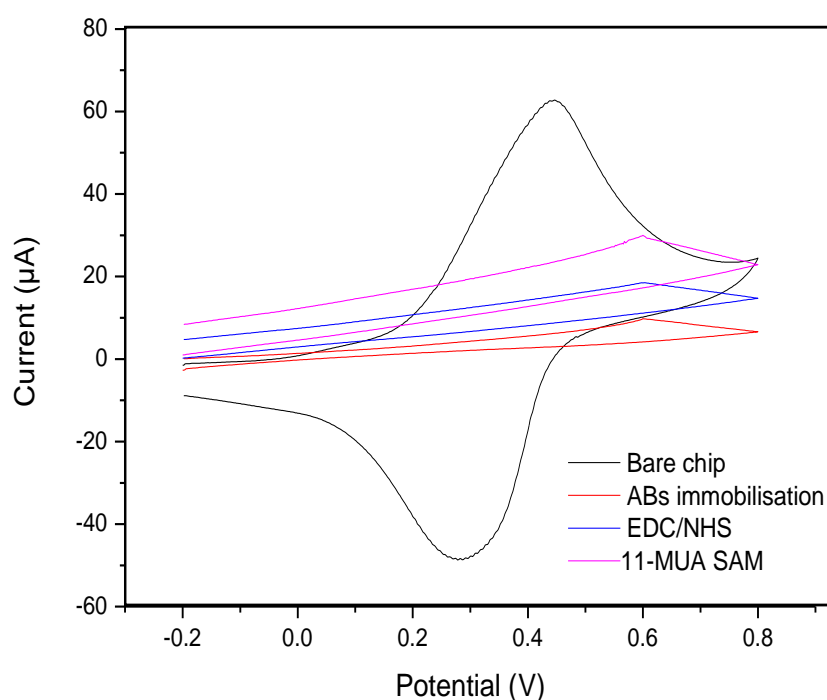


Figure 4.16: CVs of (i) bare Au: (ii) 20 hours 11-MUA SAM (iii) activation with EDC/NHS and (iv) immobilisation of primary monoclonal antibody. Electrolyte used was 5 mM ferri/ferrocyanide redox couple in 0.1M KCL with a 0.05 V /s scan rate.

#### 4.6.1.4. Contact angle measurements

The structural information and surface chemistry test of the modified gold surface was determined by using drop contact angle. Upon comparing the modified gold chip with a bare gold chip, it was found that the modification of the gold surface influenced the water contact angle. The bare gold chip had a contact angle of 55.07 degree. The modified gold chip had a contact angle of 35.58 degree. The contact angle of the modified gold chip had a lower value due to the SAM formation. The low contact angle revealed a hydrophilic surface of the carboxylic acid monolayer that consisted of the tail groups of the thiols. The tail groups of the thiols had a less hydrophobic surface. Figure 4.17 indicates the measurements of contact angle before and after the SAMs formations.

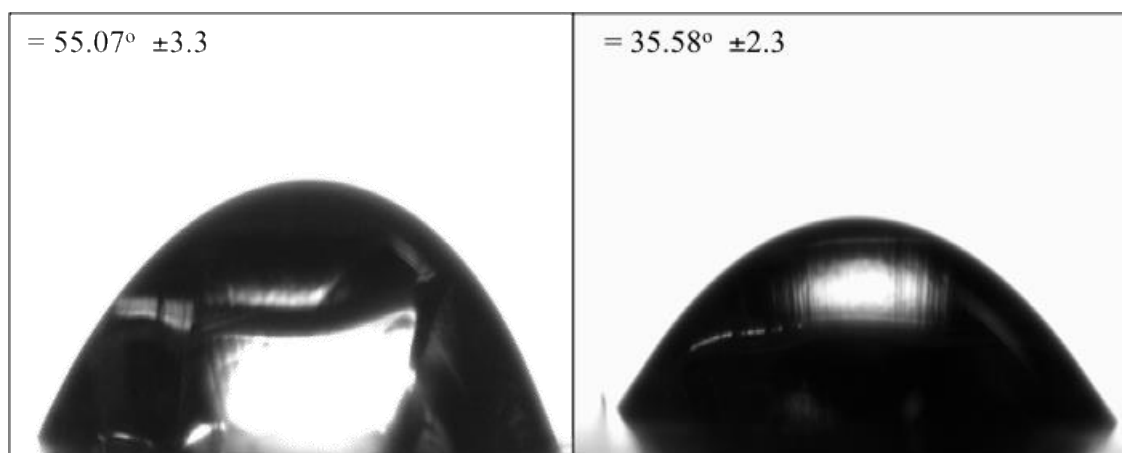


Figure 4.17: The contact angle tests before and after modification of the gold chip with 11-MUA SAM

#### 4.6.1.5 Amperometric detection

Amperometric measurements were performed using the PalmSens potentiostat. A sensing chip with small working electrode improves the signal to noise ratio and the lowers the limit of detection in low concentration. Before the measurements, the chip



coated with layers of biocomponents assay was stored in DEA buffer pH 9.5 at 4 °C to prevent the loss of antibody activity. The detection was conducted on the coated chip using the AP enzyme and the *p*APP substrate. Before carrying out the amperometric detection, the chip was rinsed with nanopure water and dried with nitrogen gun. A volume of 10 ml substrate solution was prepared. The chip was immersed into it and the chip active area was covered by the solution. The solution was stirred using a small magnetic bar. The measurement was 60 seconds and the potential was applied at 300 mV. The current was monitored and was allowed to remain the stable baseline (see the Figure 4.18). At 10 seconds, a 200  $\mu$ l of *p*APP (final concentration of 3mM) was injected into the buffer of the gold chip. The increase of current was recorded as the signal for data evaluation. Upon *p*APP injection, the increase of current was recorded as the signal for data evaluation.

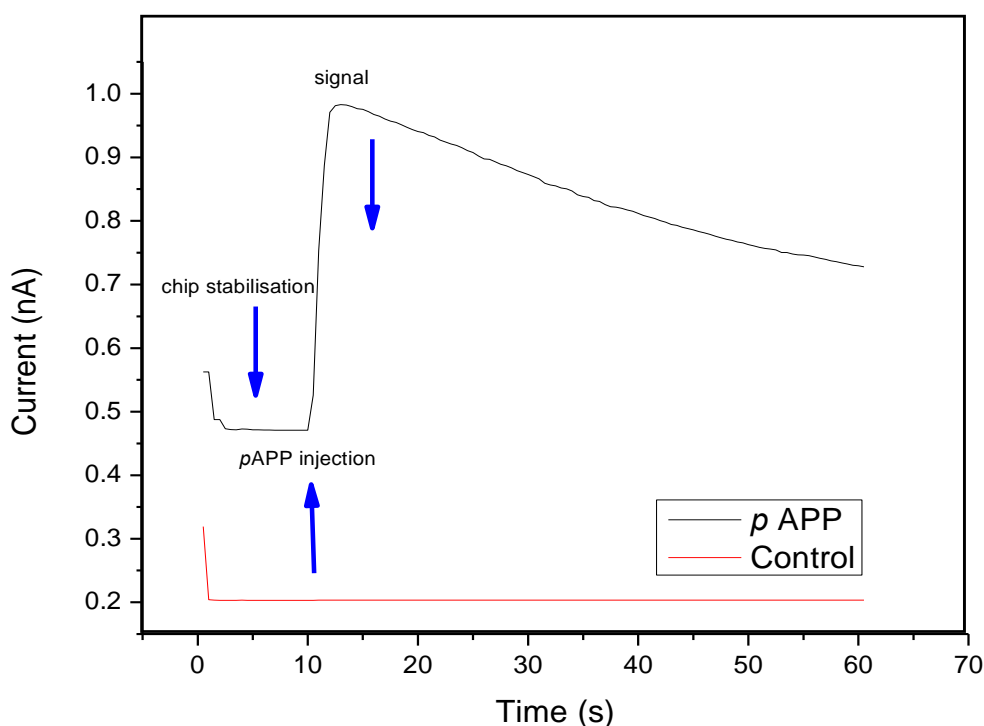


Figure 4.18: Typical signal for amperometric detection. The chip modified AP consisting bilayer (immunoassay format) was measured in DEA solution pH 9.5 at a potential of 300 mV. The substrate *p*APP was injected at 10 seconds

## 4.7 Development of an integrated sensing system (Lab On a Chip)

### 4.7.1. Proof of concept

In order to determine if the developed microfluidic system was compatible with electrochemical measurements, analysis tests were performed. This was to ensure that the system could hold and deliver the sample, and that the electrochemical chip connection worked correctly. The resulting graph, seen in Figure 4.19 shows the unmodified chip results when the chip was not coated with layers of biocomponents assay or any applied method.

The characterisation was investigated by performing the electrochemical detection. The resulting graph shows also that the connections of the system worked efficiently, with no problem in the electrochemical chip or leaking of sample.

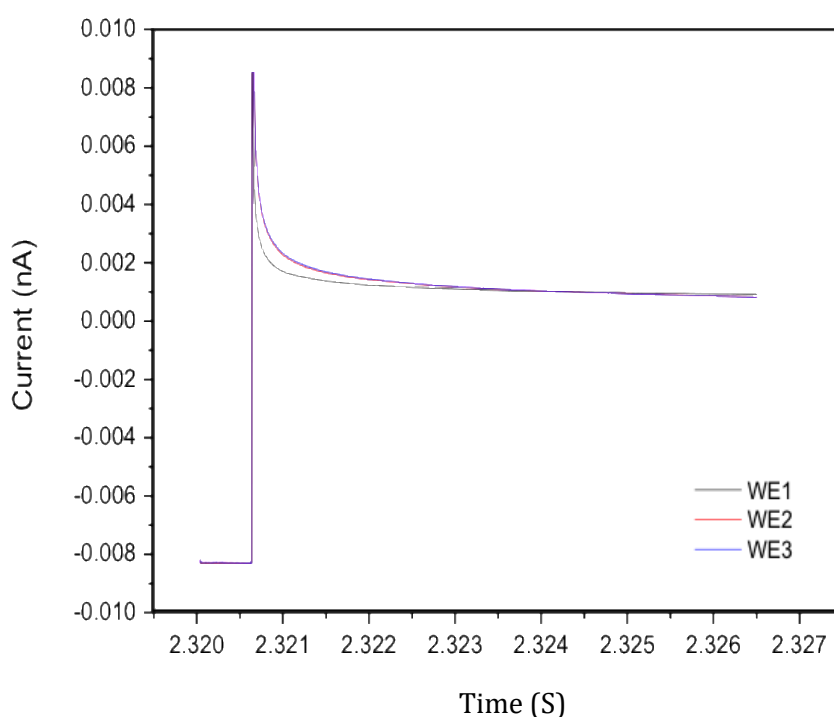


Figure 4.19: Electrochemical detection at bare chip. Electrolyte used was 5 mM ferri/ferrocyanide in 0.1M KCL.

The graph seen in Figure 4.20 shows the coated chip results. The detection was carried out on the coated chip using the AP enzyme and the *pAPP* substrate. Amperometric detection allowed simple device and integration of the sensor in a portable system for real-time and inexpensive measurement in the field [6]. SAMs formation was developed on a chip surface in order to achieve a specific immobilization of capture antibody. The capture antibody used was monoclonal mouse antibody 4D5. The enzyme AP was used in combination with *pAPP* substrate for detection. Capture ELISA format was used to ensure the correct formation on the chip surface. The amperometric result shows that the immunoassay complex was efficiently detected.

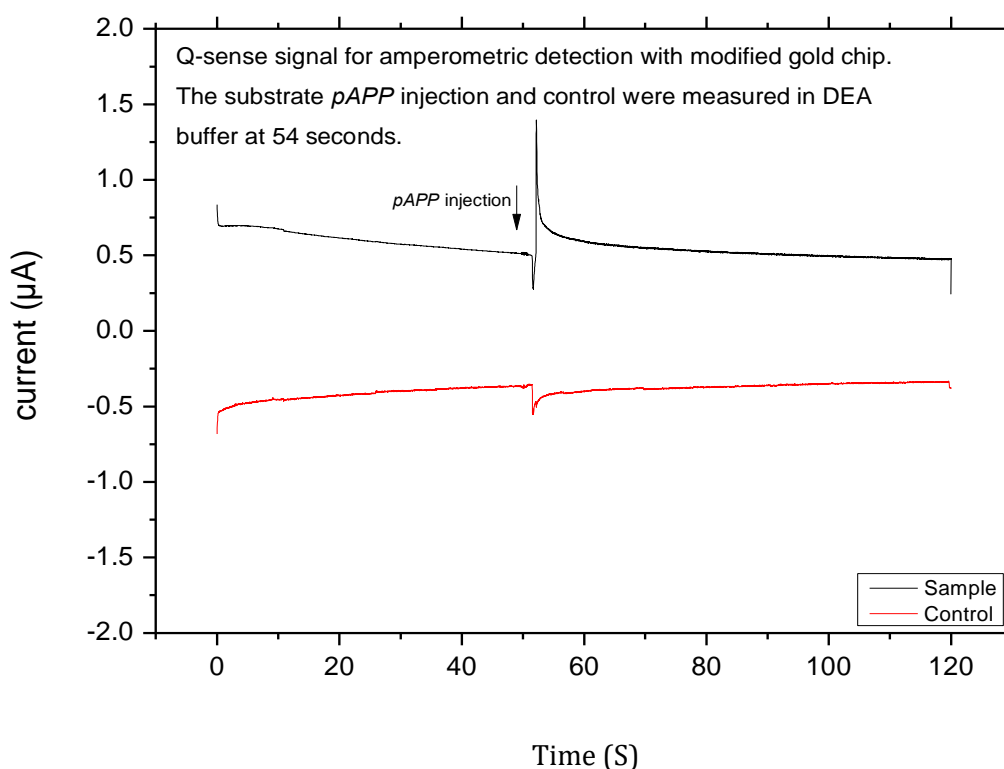


Figure 4.20: The amperometric tests with typical signal of Q-sense. The gold chip array modified AP consisting bilayer (immunoassay format) was measured in DEA solution.

Before carrying out the amperometric test, the chip was left over night in the DEA solution in order to maintain the activity of the antibodies. The finding showed a read-out obtained from the Q-sense system. The results indicated that there was a clear peak for the immunoassay components. At 54 seconds, *p*APP solution (final concentration of 3 mM) was delivered to the cartridge chip via the substrate valve, which was controlled by the electronic module. The increase of current was recorded as a signal for data evaluation. The sample with immunoassay yielded much higher positive current from amperometric measurements due to the AP concentration in the solution. It also appears on this plot that the current for immunoassay sample was decreasing exponentially whereas the control was almost linear. The overall aim of this section of research was to integrate the microfluidic design with a heterogeneous immunoassay and electrochemical methods to detect PAHs in water sample. The design of the system also allows for electrochemical chips to be inserted and removed easily. This shows the potential for inserting many other chips into the system, for the electrochemical analysis of a variety of parameters. The preliminary result for the above measurement is a proof of concept that the system works, both from an engineering and analytical chemistry perspective. Due to delays with the manufacture of the Q-sense system as proof of concept established. Future work will focus on the implementation of the device. The data representative of electro-analytical response of the Q-sense system for these immunoreactions, obtained us a useful starting point for development of the fully integrated system. Future work will also optimise different immunoassay parameters in order to achieve better assay performance. The next step then is to conduct on-site testing of the system in water. This can be carried out at any stage in the near future as the system is ready for use. From this, the device will be optimised for best fit into the production process.

#### **4.7.2 Troubleshooting and future work**

- Make the system and the chip more compact and integrated.
- Improve the battery performance and the software reliability.
- Integrate wireless connection in order to share data.
- Consider designing a tool/accessories box for the on-site tasks

It is necessary to redesign and refabricate the Pyrex 7740 glass substrate (Figure 4.21). The refabricated glass chip will be used for PAHs screening using an immunoassay format. PAHs are very nonpolar and lipophilic, and therefore can easily stick to plastics. This forces researchers to use glass for sampling and storage. For example, in collecting PAH samples for laboratory analysis, researchers noted that plastic materials should not be used for storage and sampling due to “the possible adsorption of the PAHs onto the plastic container material” [7]. The refabricated glass chip must be a three-electrode system consists of gold as working, platinum as counter electrode and an Ag/AgCl reference electrode. When applied them to electro-analysis, these materials are stable over the course of many measurements, and can be used several weeks after preparation with no loss of signal. Therefore, the new glass substrate should be thicker in order to avoid the breakage of glass when entering to the Q-sense system. In addition, the pads for chip electrodes must be long enough to easily facilitate connection to adaptors or electronics.

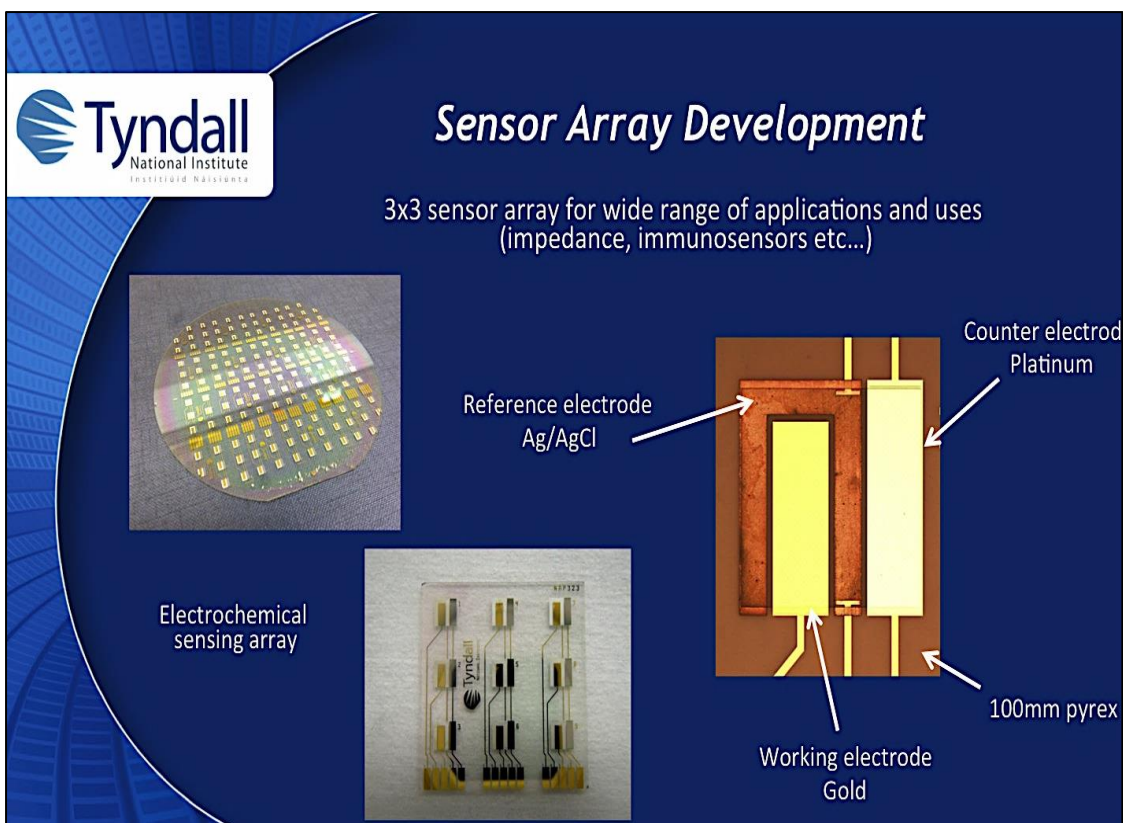


Figure 4.21: The Pyrex glass substrate, Example of Q-Sens immunosensor in H2020 project SMARTER-Si. This immunosensor is being used for water quality monitoring.

## 4.8 Conclusion

This chapter explained the development of a chip containing a three-electrode system and its characterisation in an electrochemical application. PalmSens portable potentiostat and contact angle device were used for the characterisations of the chips. Electrochemical behaviour of the chip was investigated using a redox probe in the presence of 0.10 M KCL. This redox probe is one of the most studied complexes in electrochemistry. The redox pair (ferri/ferrocyanide) was used to characterise electrochemical systems. CV was carried out in order to study the mechanism of the electrochemical reactions. Investigation of the influence of the scan rate was performed in order to study the electrochemical processes, in which the optimised scan rate was observed at 50 mV/s. The important factor in an immunoassay was to immobilise the desired antibody on

specific targeted sites with no non-specific binding. SAM formation was used in order to decrease random orientation of the antibodies binding to the surface. Modifications of SAM on the gold chip surface with (11-MUA) were performed. Activation of carboxylic acid-group with EDC in combination with NHS was used to the monolayer before the immobilisation of antibody. Characterisation of the SAM formation on gold surface was carried out using CV and contact angle tests. The SAM-modified chip surface was less accessible to redox pair. The chip surface became more insulated after the addition of modification layers. Contact angle test was performed to study the hydrophilic surface.

The end groups of thiol in SAM formation influenced the drop contact angle of coated SAM gold chip. Amperometric detection using the Q-sense system was developed. The system was based on detecting the specific antigen using an enzymatic reaction by measuring the chemical response to specific antibody. Amperometric detection with the microfluidic cell allows a simple tool that could be used as portable system for field measurements. The use of immunoassay method is viable for screening of PAHs. This technique allows for detecting multiple samples and analysis can be completed reasonably quickly. While the integrated system has proved successful in a lab-based setting, as the end aim of the research is to use this system in water environment, it will be brought into the water environment to carry out tests with their existing process. In this way, any issues that may arise from environmental setting can be rectified in an efficient manner.

The summary of evolution of Q-sense design and fabrication chip was outlined in the list above. In this way, any issues that may arise from environmental setting can be rectified in an efficient manner. The summary of evolution of Q-sense design and fabrication chip was outlined in the list above.

#### **4.9 References**

1. Burchiel SW, Luster MI. Signaling by environmental polycyclic aromatic hydrocarbons in human lymphocytes. *Clinic Immuno*. 2001 Jan 1;98(1):2-10.
2. Molaei S, Saleh A, Ghoulipour V, Seidi S. Centrifuge-less Emulsification Microextraction Using Effervescent CO<sub>2</sub> Tablet for On-site Extraction of PAHs in Water Samples Prior to GC–MS Detection. *Chromatographia*. 2016 May 1;79(9-10):629-40.
3. Wang W, Ma R, Wu Q, Wang C, Wang Z. Magnetic microsphere-confined graphene for the extraction of polycyclic aromatic hydrocarbons from environmental water samples coupled with high performance liquid chromatography–fluorescence analysis. *Jour of Chromat A*. 2013 Jun 7;1293:20-7.
4. Gilgenast E, Boczkaj G, Przyjazny A, Kamiński M. Sample preparation procedure for the determination of polycyclic aromatic hydrocarbons in petroleum vacuum residue and bitumen. *Anal and Bioanal Chem*. 2011 Aug 1;401(3):1059-69.
5. World Health Organization. Health criteria and other supporting information. Guidelines for drinking-water quality. 1996;2:796-803.
6. Southworth GR. The role of volatilization in removing polycyclic aromatic hydrocarbons from aquatic environments. *Bulletin of Environ Contamin and Toxico*. 1979 Jan 1;21(1):507-14.



7. Determination of Parent and Alkylated Polycyclic Aromatic Hydrocarbons (PAHs) in Biota and Sediment. Available online: <https://pdfs.semanticscholar.org/c83a/9554342d38c4eeab6004b44b9b285278714d.pdf> (accessed on 3 December 2019).

# **Chapter 5**

**Comparison with Gas**

**Chromatography Mass**

**Spectrometry (GC-MS)**



## **5.1 Comparative Study**

A comparative study using analytical chromatographic-based approach was performed in order to ensure that the already developed immunoassay sensor system met the requirements of the analytical methods for laboratory tests. The comparison was carried out to confirm that the procedure applied for a PAH test was suitable for its intended use. It was also conducted in order to compare the reliability and sensitivity of the developed immunoassay results. It was an important study of good analytical practice. The presence of PAHs has been detected by using Gas Chromatography-Mass Spectrometry (GC-MS). In particular, the work focused on the quantification of Benzo[a]pyrene (BaP). This study was performed in the Analytical Laboratory in the School of Chemistry at University College Cork (UCC).

## **5.2 Introduction**

### **5.2.1 Conventional PAHs Analysis Methods**

PAHs occur in different forms and concentrations in environmental areas, such as water, air, and soil. Consequently, this leads to the need for the application of different methods of analysis depending on each particular case [1]. Currently, the common traditional analytical methods used to detect PAHs include high-performance liquid chromatography (HPLC) with fluorescence detection, Gas Chromatography-Mass Spectrometry (GC-MS), and high-performance liquid chromatography with ultraviolet detection (HPLC–UV) [2]. There are several advantages that are associated with the use of these standard analysis techniques, such as accuracy, reliability and sensitivity.

However, there are limitations associated with these methods. Some of these disadvantages include the fact that their processes involve high-risk loss of analytes during sample separation. In addition, these methods require the use of an extensive amount of hazardous organic solvents [3]. This is a problem because it increases costs and contaminates the environment. Loss of analytes presents a major source of poor quality analytical data for PAH due to separation, pre-treatment, and sampling of analytes, which introduce errors that are not associated with the last quantification step. In addition, the application of these methods makes the procedure of sample analysis, preparation, and quantification quite time-consuming and tedious [4]

### 5.2.2 Environmental monitoring study (Drinking Water)

According to the World Health Organization (WHO), the PAHs with the highest concentrations in drinking water are anthracene, pyrene, phenanthrene, fluoranthene. These are measured in surface water for regulatory purposes because of their low solubility and high affinity for particular matter. Fluoranthene compound, in particular, is measured to a significant extent. Some PAHs compounds are toxic and considered as mutagenic, carcinogenic and teratogenic substance, e.g., Benzo[a]pyrene (BaP). BaP is the compound that has been studied and it has been identified as a hazardous environmental pollutant. The table outlines the physicochemical properties of BaP [5].

Table 5.1: physicochemical properties of BaP.

<b>Benzo[a]pyrene</b>  <b>MW</b>  <b>252.31 g/mol</b>	<b>Molecular Formula</b>	<b>No. Aromatic ring</b>	<b>Melting Point (°C)</b>	<b>Boiling Point (°C)</b>	<b>Vapour Pressure (kPa)</b>	<b>Water solubility (ug/L)</b>
	<b>C<sub>20</sub>H<sub>12</sub></b>	<b>5</b>	<b>178.1</b>	<b>496</b>	<b>7.3x10<sup>-10</sup></b>	<b>3.8</b>

In aqueous areas under aerobic conditions, PAH slowly biodegrades. In addition biodegradation occurs in accordance with increased number of aromatic rings. In one research study [6] the volatility of BaP in water was found to be low and the calculated half-lives for the selected analytes varied widely (from 500 to 1550 hours). The key process for PAH degradation in water is indirect photolysis under the influence of hydroxyl radicals. In another study a reaction of PAH and hydroxyl radicals showed the photodegradation half-lives was in the range of 3-11 hours [7-9].

### 5.2.3 Study with coal tar

In the past a common coating item used for distribution water pipes was coal tar. It was used for effective protection against corrosion. Coal tar is a mixture of 1000 compounds and 30 compounds of the mixture are PAHs [10]. According to the (WHO) it is clear from some reports in the recent literature that this practice was discontinued [5]. However, many countries still have a huge number of distribution pipes lined with coal tar. Coal tar coating is the main contamination source of drinking water with PAHs. Environmental levels of PAHs have been recorded in water after following repair work and the passage of water through distribution pipes [11]. The relative amount of PAHs in water relies on the solubility and the chemical profile of them. The effect of complex PAHs is different from that of individual PAHs. The interaction of PAHs in coal tar and in other materials may bring about higher or lower rates of tumor than can be obtained from their content of carcinogenic PAHs [12, 13]. A study based on the oral carcinogenicity experiment revealed that the guideline value for carcinogenic BaP in drinking water association with coal tar coating was estimated 0.7 ug/ L [14]. In order to support the validity of the previous study, another experiment was carried out, which yielded near similar results. [13, 15]. The presence of BaP in drinking water at notable amounts is a sign of the presence of deterioration of coal tar linings. In light of Irish research which shows that PAHs originate from many sources including coal-tar coating of drinking water pipes, soot, vehicle emissions and as combustion products of hydrocarbon fuels [16]. The recommendation of the (WHO) is that the use of coal tar linings and storage tanks to be discontinued and replaced by new ones. The WHO has also recommended that the levels of PAHs in individuals be monitored, along with its levels in their levels in drinking water.

### 5.3 Objective

The aim of this chapter is to compare the developed immunoassay system discussed in the previous chapters for the detecting of Benzo[a]pyrene (BaP) in drinking water. The European Union (EU) has produced a list of a series of (PAHs) found in the environmental that require monitoring. The determination and quantification of low concentration of PAHs have been extensively performed with chromatographic methods over the past decades. Here, a method based on Gas Chromatography-Mass Spectrometry (GC-MS) has been used. GC-MS is able to enter the volatile compound and into, the column rapidly and in as small a volume as possible. Standard and real sample tap water analyses were carried out targeting PAHs compounds that obtained a good sensitivity at UCC, Cork City. Analysis of a tap water sample with optical detections was also carried out.

#### 5.3.1 Experimental:

**5.3.1.1 Standards and reagents:** A PAH calibration mix containing 15 monitored compounds was obtained from Sigma (Dublin, Ireland). The working PAH mix was diluted separately in acetonitrile solvent with a final concentration of 7 µg/ml using glassware and pipets. The determination of the quantitative analysis was carried out a 5 point calibration curve. The concentrations of the standards were 3, 4, 5, 6 and 7 µg /ml (ppm). All samples were run in triplicate (n=3). Reagecon (PAH) Internal Standard (6 Compound Mix) in Dichloromethane was commercially obtained from Reagecon Diagnostics Ltd. (Shannon, Ireland). International standards solution was used in order to obtain the required response of the instrument for analytes and to identify the recovery of the particular analyte. Fiberglass filter paper coded Octadecyl C18



extraction disks 2215 with 47 mm in size was purchased from Supelco (Dublin). All reagents and solvents used were of analytical grade or better.

### 5.3.1.2 GC-MS conditions and instrumentation:

The study was performed on Agilent 6890/5973 gas chromatography-mass Spectrometry (GC-MS). Analysis of samples was performed on an Agilent 6890N GC equipped with a 5973 inert Mass Selective Detector. A capillary column HP-5MS [(5%-phenyl)-methylpolysiloxane] Agilent J & W GC column, 30 m, 0.25 mm i.d., coating thickness 0.25  $\mu\text{m}$  was used to separate analytes. Each sample was placed on an auto-sampler (Agilent) and injected in a volume of 5  $\mu\text{l}$  into the GC/MS with the splitless mode of injection. The GC/MS method consisted of a front inlet temperature of 280  $^{\circ}\text{C}$ , MS transfer line temperature of 280  $^{\circ}\text{C}$ , and the ion source temperature was 250  $^{\circ}\text{C}$ , and ionization voltage 70eV. The solvent delay was 4 min. The flow rate of helium through the column was kept at 1.0  $\text{mL}\cdot\text{min}^{-1}$ . The oven temperature was ramped as described in the Table 5.2.

Table 5.2: Agilent 6890/5973 gas chromatography-mass Spectrometry conditions

GC run conditions		MS conditions	
Analytical column	A 30.0 m, 0.25 mm i.d. HP-5MS capillary column with 5% phenyl-methylsiloxane (film thickness 0.25 $\mu\text{m}$ )	Solvent Delay	4 min
Injection volume	5.0 $\mu\text{l}$ Syringe size 10.0 $\mu\text{l}$	Acquisition mode	EI, SIM
Injection mode	Splitless mode of injection used to maximize sensitivity	Tune	Etune.u
Injection temperature	250 $^{\circ}\text{C}$	Gain factor	1
The carrier gas	Helium, constant flow mode, 1.0 $\text{mL}/\text{min}$ , Pressure 14.8 psi	Source Temperature	250 $^{\circ}\text{C}$

Oven Program	60 °C for 1 min raised to 120 °C at the rate of 25 °C/min, then to 160 °C at the rate of 10 °C/min and to 280 °C at the rate of 5 °C/min, held at final temperature for 15 min	Quadrupole Temperature	150 °C
--------------	--	------------------------	--------



Figure 5.1: Agilent 6890/5973 gas chromatography-mass Spectrometry (GC-MS) instrument.

Water should be eliminated from compounds before injection into the GC-MS because they could impact on GC column lifetime, inlets and detectors. Filtration is the most common method for removing water from the sample.

### 5.3.1.3 Water extraction

The water sample was filtered using fiberglass filtration in order to remove any solids that might prevent the extraction procedure. For this procedure fiberglass filter paper coded Octadecyl C18 extraction disks 2215 with 47mm in size was applied.

#### 5.3.1.4 Disks preparation

The disk had to be conditioned before using it in the extraction process. A solid phase extraction disk (SPED) was conditioned by inserting it into the 47 mm apparatus for filtering as shown in Figure 5.2. According to US Method 525.2 for GC-MS ethyl acetate (5ml) was used to soak the disk for 1 min. This is followed by vacuum drying of the disk. Ethyl acetate is a slight polar aprotic solvent that is immiscible with water and able to dissolve the organic compounds. This was followed by soaking the disk in methanol (5 ml) for 1 min. The disk was removed from the methanol in such a way that a layer of methanol was retained on the surface. The disk was rinsed with deionized water (5ml) in such a way that a layer of water remained on the disk.



Figure 5.2 The setup for disk conditioning

#### 5.3.1.5 Extraction of sample

Methanol (2.5 ml) and 50-ug ml<sup>-1</sup> (50 µl) of internal standard were added to the water sample before extraction of the sample. The mixture was added to the extraction reservoir and filtered under vacuum. The flow rate of the filtration was maintained at 5mL per min. The filtration top was removed from the filtration flask after the water sample (500 mL) was filtered.

The waste present in the reservoir flask was removed and cleaned. The resultant (eluent) was collected in a clean sample tube by fitting it to the filtration top (Figure 5.3).

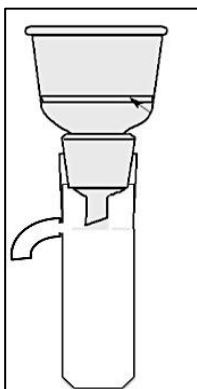


Figure 5.3: Elution apparatus

#### 5.3.1.6 Elution of the sample

Different solvents were used to elute the compounds attached to the disk. The sample bottle was rinsed and filled with acetonitrile (5ml). The disk was soaked in acetonitrile for 1 min followed by soaking of the disc in ethyl acetate for 1 min. Both the eluents- acetonitrile and ethyl acetate were allowed to pass through sodium sulphate (3 gm) in order to remove any water present in the sample. Sodium sulphate is an inert drying agent that is able to remove suspended water in solvent or absorb about 20-25 % of water after mixing with ethyl acetate. The sample test tube and the sodium sulphate were rinsed twice with ethyl acetate (5 ml). The eluents were collected in a concentrator tube that was heated to 28°C in a heating block so that the volume reduced to 0.5 ml under nitrogen atmosphere. The eluents were transferred to sample vials and stored at 4 °C. They were later analyzed using GC-MS.

### 5.3.2 Sample analysis with GC-MS

Identification of 15 priority PAHs in the samples was confirmed by the retention time [RT] and abundance. The ion mass program used for quantification is detailed in Table 5.3. A priority PAH (BaP) was utilized for the quantification using the response factors related to the respective internal standards based on 5-point calibration curve for PAH shown in Figure 5.4. The separation was accomplished in under 54 minutes on a 30 m, 0.25 mm i.d. HP-5MS capillary column. In PAH measurements using GC-MS, the selectivity of the column type was important to yield a good resolution for all PAHs compounds and also to improve peak shapes. In order to improve peak shapes and in order to have full understanding from the mass spectra, a short column type, tiny film thickness, and high operating temperature were required. The chromatogram of the individual compounds in the 15 PAHs compound mix is shown in Figure 5.5. All PAH compounds could be clearly separated, where the first peak of Naphthalene eluted at 6.67 min and the last peak of Benzo[ghi]perylene was at 40.49 min. The separation could be performed between PAH from the sample and its corresponding IS. For example, the retention time of BaP compound from the sample was (35.31min) and its deuterated internal standards (39.90 min) that could be separated using the method. The peaks had been confirmed using their measured mass to charge ratio value given in their data (mass spectra).

Table 5.3: GC-MS conditions under time scheduled selected ion monitoring

<b>Time Window (min)</b>	<b>Target Compounds</b>	<b>Target Acronyms</b>	<b>No. of rings</b>	<b>Molecular Mass</b>	<b>Retention Time (min)</b>
4.22-8.06	Naphthalene	Nap	2	128	6.67
7.92-11.78	Acenaphthylene	Acey	3	152	9.23
8.06-12.35	Acenaphthene	Acet	3	164	9.49
11.77-14.05	Fluoren	Flo	3	166	12.53
12.15-17.70	Phenanthre	Phe	3	178	14.07
12.35-17.89	Anthracene	Anth	3	178	14.76
17.70-22.84	Fluoranthene	Flan	4	202	18.20
17.88-23.78	Pyrene	Pyr	4	202	19.79
22.84-29.34	Benz [ <i>a</i> ] anthracene	B[a]a	4	228	25.23
23.78-29.53	Chrysene	Chry	4	228	27.57
29.42-34.07	Benzo[ <i>b</i> ]fluoranthene	B[b]f	5	252	32.50
34.06-35.25	Benzo[ <i>k</i> ]fluoranthene	B[k]f	5	252	34.48
35.26-35.43	Benzo[ <i>a</i> ]pyrene	B[a]p	5	252	35.31
39.49-39.51	Dibenz[ <i>a,h</i> ]anthracene	Ind	5	278	39.49
40.39-40.46	Benzo[ <i>ghi</i> ]perylene	Pery	6	276	40.46

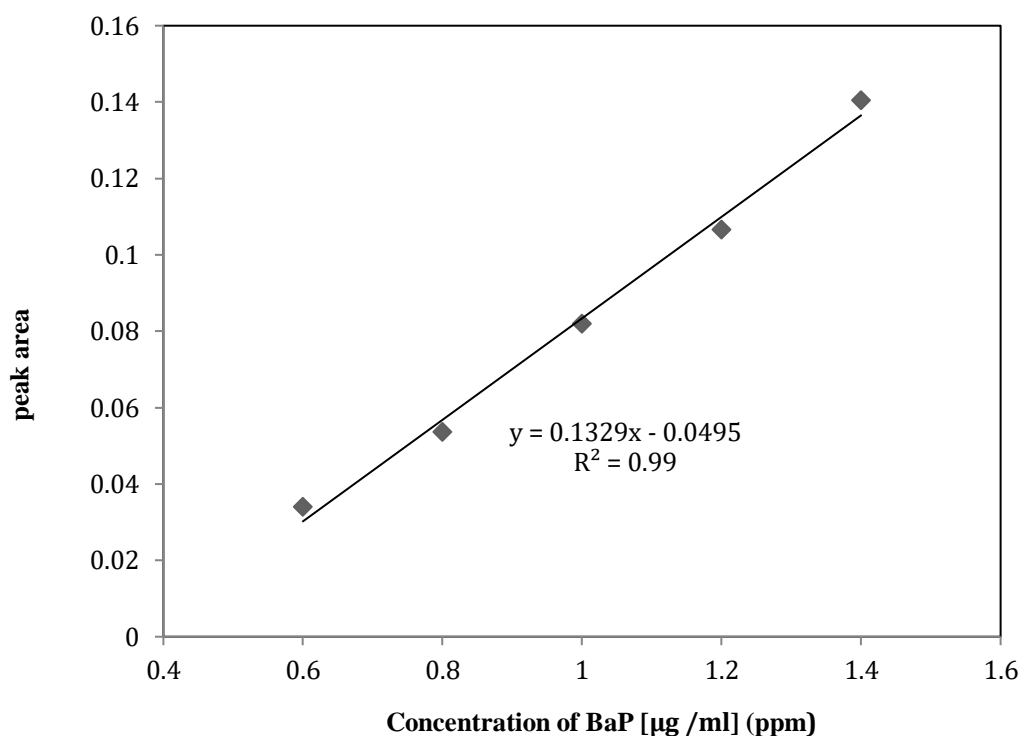


Figure 5.4: Standard curves obtained GC-MS for BaP .A 30.0 m, 0.25 mm i.d. HP-5MS capillary column, Injection volume 5.0 ul, Injection temperature 250 °C.

Figure 5.5 shows the mass spectrum or the total ion chromatogram for each compound on column. Mass spectrum pattern for each PAH allows for a highly specific and sensitive method for quantitation of a PAH in the matrix. Because the 15 PAHs have different chemical properties and retention times, 6 internal standards (Naphthalene D8, 1,4-Dichlorobenzene D4, Acenaphthylene D10, Phenanthrene-D10, Chrysene D12, Perylene D12) were used to monitor the PAHs.

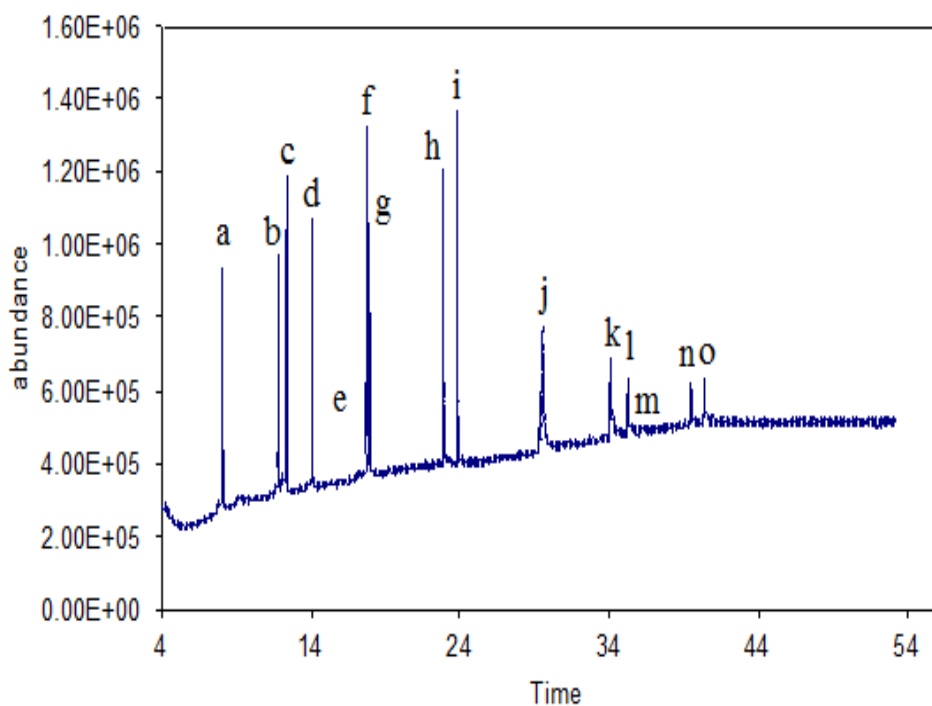


Figure 5.5: Chromatogram of the individual compounds in the 15 PAHs mix. Peak ID : (a) Nap, (b) Ace, (c) Flo, (d) Phe, (e) Anth, (f) Flan, (g) Pyr, (h) B[a]a, (i) Chry, (j) B[b]f, (k) B[e]a, (l) B[k]f, (m) B[a]p, (n) Pery and (o) Ind.

The total-ion chromatogram graph below shows the 6 internal standards cover the 15 PAH and distributed along the chromatogram (Figure 5.6). Usually, every PAH compound has a deuterated PAH with a more or less similar RT, ionization efficiency, detector response, and interactivity as the analyte of interest (Table 5.4). The internal standard must be inert and does not show any reaction to PAH sample or solvent diluted it for GC procedure.



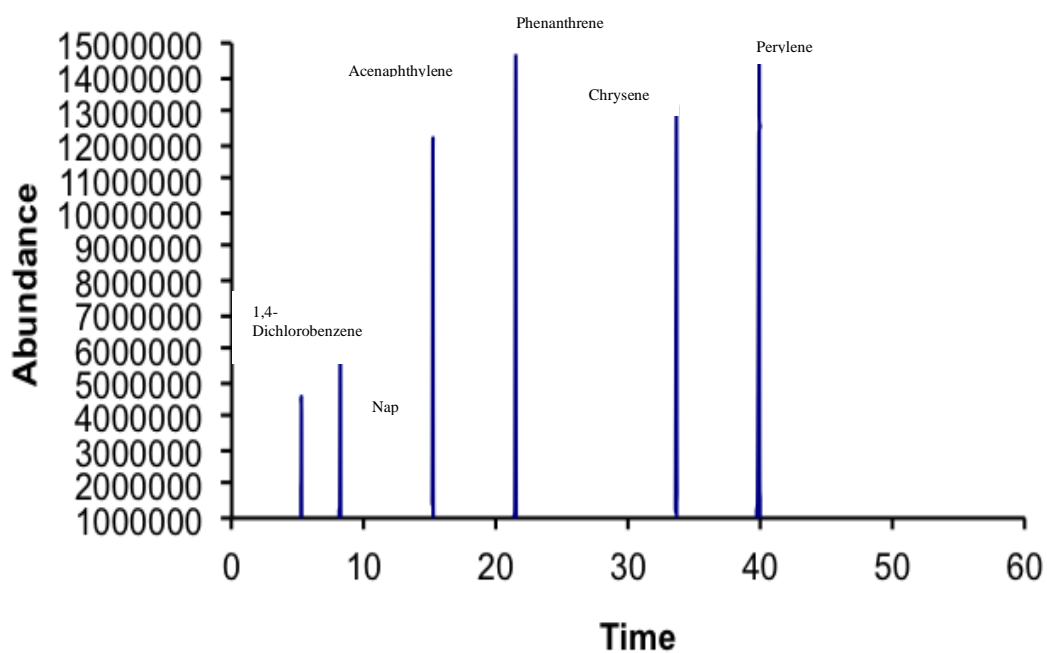


Figure 5.6: The total ion chromatogram of the 6 internal standards. Peak ID: Naphthalene D8,1,4-Dichlorobenzene D4, Acenaphthylene D10, Phenanthrene-D10, Chrysene D12, Perylene D12.

Table 5.4: Internal Standard with number of rings, molecular mass, and retention time

Internal Standard Compounds	No. of rings	Molecular Mass $\text{g}\cdot\text{mol}^{-1}$	Retention Time [RT] (min)
<b>1,4-Dichlorobenzene D4</b>	<b>1</b>	<b>147.00</b>	<b>5.278</b>
<b>Naphthalene D8</b>	<b>2</b>	<b>128</b>	<b>8.210</b>
<b>Acenaphthylene D10</b>	<b>3</b>	<b>152</b>	<b>15.205</b>
<b>Phenanthrene-D10</b>	<b>3</b>	<b>178</b>	<b>21.452</b>
<b>Chrysene D12</b>	<b>4</b>	<b>228</b>	<b>33.588</b>
<b>Perylene D12</b>	<b>5</b>	<b>25.316</b>	<b>39.805</b>

### 5.3.2.1 Response Factor (RF) and Relative Response Factors (RRFs) experiment:

Calibration curves were constructed from 3 to 7 ug/ml (ppm) (Table 5.5). GC-MS could obtain the required high response to BaP with liner calibration curves when the peak area was plotted against the concentrations (Figure 5.7). Using the same conditions as obtained in the experimental section, the separation could be completed between a BaP compound from sample and its corresponding IS. IS comparison is a good quantification method where each PAH can be quantified against the most appropriate IS. SI technique is a suitable way for calculating the ratio between the responses produced (peak area) and the concentrations of compound that generate the signal. In chromatography this ratio is defined as the Response Factor [RF].

$$\text{RF} = \text{peak area (response) (A)} / \text{concentration(C)}$$

$$R_{x/is} = \frac{A_x / A_{is}}{c_x / c_{is}} \quad (\text{Equation 1})$$

Where: A = integrated abundance of the quantitation ion of the analyte x A = integrated abundance of the quantitation ion internal is standard C = quantity of analyte injected in concentration units x C= quantity of internal standard injected in concentration units is.

$$\text{RRF}_A = \text{Response factor } x / \text{Response factor } is \quad (\text{Equation 2})$$

The response from the PAH (BaP) peak was compared to the internal standard. This procedure corrected for minor variations in the injection volume. Samples were fixed mass of internal standard and, different masses of standard analyte (PAH). The calibration curve must showed linear response. Slope = response factor.

Table 5.5: Calibration Curve with Internal Standard.

GC calibration curve of PAH ( BaP) with internal standards						
Standards	PAH $\mu\text{g/ml (cx)}$	Int Std. $\mu\text{g/ml ( cis)}$	$c_x/c_{is}$	$A_x$	$A_{is}$	$A_x/A_{is}$
1	3	5	0.60	53204875	1813679	0.034088
2	4	5	0.80	53204875	2854252	0.053646
3	5	5	1.00	53204875	4361052	0.081967
4	6	5	1.20	53204875	5673043	0.106626
5	7	5	1.40	53204875	7474412	0.140483

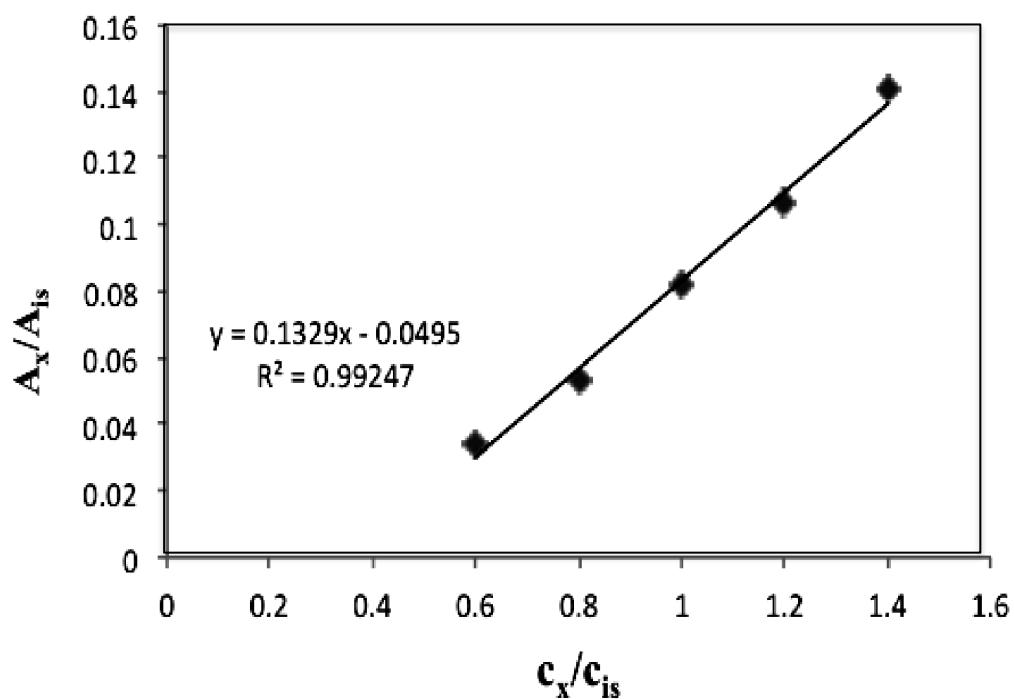


Figure 5.7: GC calibration curve of PAH with internal standard (Naphthalene D8, 1,4-Dichlorobenzene D4, Acenaphthylene D10, Phenanthrene-D10, Chrysene D12, Perylene D12).

### 5.3.2.2 Relative standard deviation (RSD)

In order to achieve the optimal conditions of PAH (n=6) it was necessary to calculate the average and standard deviation of the PAH solutions and real sample (tap water) and the relative standard deviation of the retention times and the peak areas as indicated in Table 5.6. The % RSD was used to express the precision and repeatability of the assay. It found that the RSD of the retention times and the peak areas for both samples were less than 0.5 % for retention times and less than 1% for peak area, which was an acceptable result and express the precision.

#### For the average results:

$$\text{The Average} = \text{Mean} = \frac{\text{Sum of Observations}}{\text{Number of Observations}} \quad (\text{Equation 3})$$

#### For the standard deviation:

$$s = \sqrt{\frac{\sum (x - \bar{x})^2}{n - 1}} \quad (\text{Equation 4})$$

#### For the relative standard deviation:

$$100 * s / \bar{x} \quad (\text{Equation 5})$$

Table 5.6: The average and standard deviation of the PAH solutions and real sample (tap water) and the relative standard deviation of the retention times and the peak areas

Target Compounds	Avg $\pm$ SD of peak areas [PAHs in standard solution]	Avg $\pm$ SD of retention times PAH in real sample (extracted tap water)
<b>1,4-Dichlorobenzene D4</b>	23264219 $\pm$ 1879	5.26 $\pm$ 0.0213
<b>Naphthalene D8</b>	12327713 $\pm$ 2615	8.192 $\pm$ 0.0043
<b>Acenaphthylene D10</b>	24353818 $\pm$ 1560	15.183 $\pm$ 0.0024
<b>Phenanthrene-D10</b>	37601895 $\pm$ 3175	21.435 $\pm$ 0.0025
<b>Chrysene D12</b>	50414877 $\pm$ 7286	33.577 $\pm$ 0.0011
<b>Perylene D12</b>	46499372 $\pm$ 6338	39.776 $\pm$ 0.0081
<b>RSD (%)</b>	<b>0.800</b>	<b>0.405</b>
	<b>0.212</b>	<b>0.053</b>
	<b>0.640</b>	<b>0.016</b>
	<b>0.844</b>	<b>0.011</b>
	<b>0.144</b>	<b>0.003</b>
	<b>0.136</b>	<b>0.020</b>

### 5.3.2.3 Spiked and recovery experiments:

Sample spiking can provide method validation accuracy. The separation and quantification of BaP (PAH) in the spiked samples were carried out using the same GC-MS conditions as the standard solutions. The spiked sample was run in triplicate (n=3). Table 5.7 shows the presence of the spiked internal standard in the water samples. A chromatogram of sample is shown in Figure 5.8.

Recovery of the spiked sample shows if the expected result can be measured accurately. If the recovered result differs significantly from the result expected, this can be a sign that some factor in the sample matrix can be causing a falsely depressed result. 90-120% recovery is generally considered valid.

$$\% \text{ Recovery} = (\text{amount of spike substance (recovered)}) / (\text{amount of substance originally taken (standard)}) \times 100 \% \quad (\text{Equation 6})$$

Table 5.7: The recovery percentages of spiked (IS) found in tap water sample.

<b>Sample</b>	<b>1,4Dichloro benzene D4 %</b>	<b>Naphthalene D8 %</b>	<b>Acenaphthylene D10 %</b>	<b>Phenanthrene D10 %</b>	<b>Chrysene D12%</b>	<b>Perylene D12 %</b>
<b>Tap water</b>	<b>93.4</b>	<b>104</b>	<b>108</b>	<b>91.3</b>	<b>91.1</b>	<b>89.2</b>

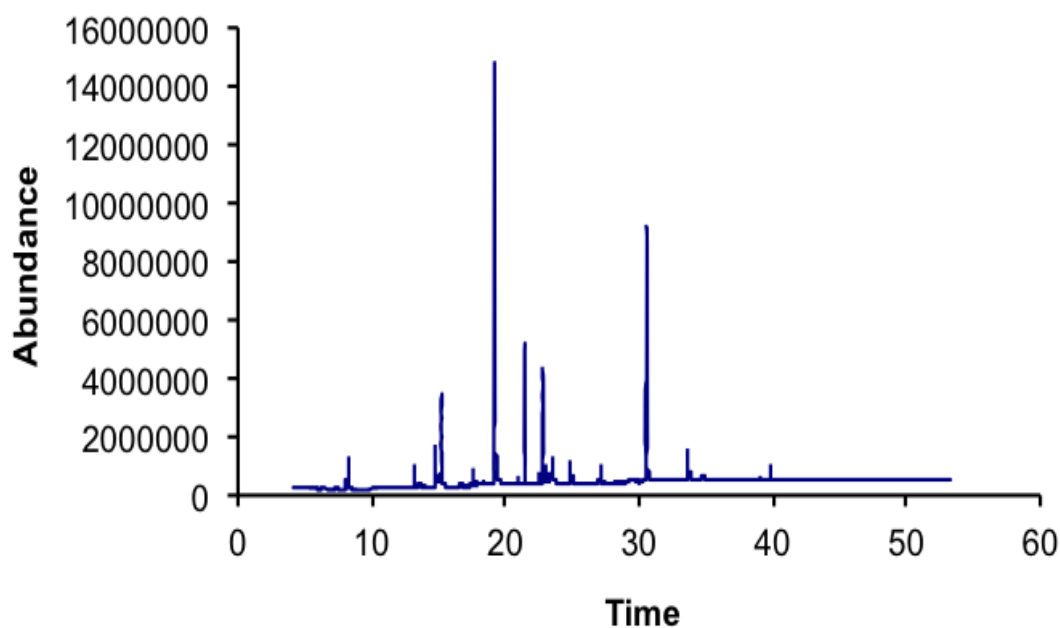


Figure 5.8: the total ion chromatogram of real sample (tap water). All the spiked ISs were found in the sample.

There were no PAHs observed in the samples and the low recoveries were related to the number of PAHs rings. As stated in [17] the recovery method of PAHs family decreases according to the number of their aromatic rings. Sometimes the poor results may be due to the presences of interfering substances arising from handling before the extraction process. As reported by [18] the presence of suspended particular matter during transportation can decrease the recovery percentage for PAHs. Table 5.6 and figure 5.8 illustrate the spiked (IS) results in tap water. Based on the high recovery percentages of the 6 isotopes spiked in real sample before the extraction. It can be confirmed that the pre-treatment extraction was effective. As previously mentioned the GC-MS technique could detect at very low concentrations of PAHs. The electrochemical bio-immunosensors (SPEs and magnetic platform) illustrated a good performance and exhibited increased sensitivity compared to colorimetric immunoassay. Table 5.9 shows the comparison of the optical and electrochemical and GC-MS.

Table 5.8 Comparison of optical and electrochemical immunosensors performance with GC-MS.

<b>Detection</b>	<b>Support</b>	<b>Material for immunoreaction</b>	<b>LOD</b>	<b>Linear Rang (ng/ml)</b>
<b>Optical</b>	<b>96 well plate</b>	<b>Hydrophobic polystyrene</b>	<b>0.0137 µg/ml</b>	<b>0.37 to 0.0137 µg/ml</b>
<b>Electrochemical</b>	<b>SPEs</b>	<b>Direct on bare surface</b>	<b>0.07 ng/ml</b>	<b>1 to 10 ng/ml</b>

<b>Electrochemical</b>	<b>NPs</b>	<b>On SPEs under magnetic force</b>	<b>0.1 ng/ml</b>	<b>13.7 to 123</b>
<b>GC-MS</b>	<b>-</b>	<b>-</b>	<b>3.0 µg/ml</b>	<b>-</b>

### 5.3.3 Conclusions

An analytical method for the detection of BaP (PAH) in tap water sample was developed using GC-MS. Findings revealed a low concentration of BaP. The alternative commonly used method for the quantitative analysis of PAH could be carried out using HPLC-florescence detection (FD). GC-MS is a powerful method for determining volatile compounds in a variety of sample. The internal standards were spiked in the tap water sample before the extraction procedure. The mass spectrum of the internal standard was compared to the real sample. The method was applied to the tap water. The tap water was spiked with (6 compound mix internal standard) and good recovery was obtained in the range of 89 to 108 % (n=3). It can be concluded that this method was reliable and effective.

### 5.3.4 References

1. Burchiel SW, Luster MI. Signaling by environmental polycyclic aromatic hydrocarbons in human lymphocytes. Clinic Immuno. 2001 Jan 1;98(1):2-10.
2. Molaei S, Saleh A, Ghoulipour V, Seidi S. Centrifuge-less Emulsification Microextraction Using Effervescent CO<sub>2</sub> Tablet for On-site Extraction of PAHs in



- Water Samples Prior to GC–MS Detection. *Chromatographia*. 2016 May 1;79(9-10):629-40.
3. Wang W, Ma R, Wu Q, Wang C, Wang Z. Magnetic microsphere-confined graphene for the extraction of polycyclic aromatic hydrocarbons from environmental water samples coupled with high performance liquid chromatography–fluorescence analysis. *Jour of Chromat A*. 2013 Jun 7;1293:20-7.
  4. Gilgenast E, Boczkaj G, Przyjazny A, Kamiński M. Sample preparation procedure for the determination of polycyclic aromatic hydrocarbons in petroleum vacuum residue and bitumen. *Anal and Bioanal Chem*. 2011 Aug 1;401(3):1059-69.
  5. World Health Organization. Health criteria and other supporting information. Guidelines for drinking-water quality. 1996;2:796-803.
  6. Southworth GR. The role of volatilization in removing polycyclic aromatic hydrocarbons from aquatic environments. *Bulletin of Environ Contamin and Toxico*. 1979 Jan 1;21(1):507-14.
  7. Atkinson R. A structure-activity relationship for the estimation of rate constants for the gas-phase reactions of OH radicals with organic compounds. *Internl Jour of Chem Kinet*. 1987 Sep;19(9):799-828.
  8. Lyman WJ, Blau GE. Estimation of physical properties. In *Environmental exposure from chemicals 1985* (pp. 13-47). CRS Press Inc.
  9. Mill T, Mabey WR, Lan BY, Baraze A. Photolysis of polycyclic aromatic hydrocarbons in water. *Chemos*. 1981 Jan 1;10(11-12):1281-90.
  10. Wallcave L, Garcia H, Feldman R, Lijinsky W, Shubik P. Skin tumorigenesis in mice by petroleum asphalts and coal-tar pitches of known polynuclear aromatic hydrocarbon content. *Toxi and Applied Pharma*. 1971 Jan 1;18(1):41-52.

11. Vu DT, Huynh CK. Organic micropollutants in water. Preliminary results on haloforms and polycyclic aromatic hydrocarbons. *Sozial-und Praventivmedizin*. 1981 Oct;26(5):315.
12. Culp SJ, Beland FA. Comparison of DNA adduct formation in mice fed coal tar or benzo [a] pyrene. *Carcinogenesis*. 1994 Feb 1;15(2):247-52.
13. Culp SJ, Gaylor DW, Sheldon WG, Goldstein LS, Beland FA. DNA adduct measurements in relation to small intestine and forestomach tumor incidence during the chronic feeding of coal tar or benzo [a] pyrene to mice.
14. Neal J, Rigdon RH. Gastric tumors in mice fed benzo (a) pyrene: a quantitative study. *Texas Reports on Bio and Med*. 1967;25(4):553.
15. Wynder EL, Hoffmann D. The carcinogenicity of benzofluoranthenes. *Cancer*. 1959 Nov;12(6):1194-9.
16. World Health Organization. Selected non-heterocyclic polycyclic aromatic hydrocarbons. 1998

**Chapter 6**

**General Conclusions and**

**Suggestions for Future**

**Perspective**



## **6.1 Conclusion:**

Pollution of PAHs in water environments has resulted in the advancement of new methods to obtain higher quality solutions to monitor this issue more effectively. Mixtures of PAHs exist in different matrices normally, which make them difficult to detect. Large-scale investigation has been carried out in the areas of PAH extraction, separation and detection. For the last few years, scientists have developed various methods of detection, depending on the properties of the compounds to be measured, for instance the amount of target, physicochemical characterization, etc. They are mostly focused on chromatographic procedures in combination with various detectors, such as, mass spectrometry and UV spectrophotometry. However, these procedures depend on expensive laboratory based-devices with additional cost needed to conduct the analysis. Chromatographic procedures are not suited to in-field evaluations and on-line water monitoring. Immunoassay procedures are another proposed alternative for PAHs detection in water monitoring. Immunoassay procedure is designed to determine specific chemicals by screening the compounds response to specific antibodies. This procedure has been broadly used in the field of clinical science. Recent developments have seen its uses extended to areas, for instance detection of chemicals in the environment. Electrochemical enzyme immunoassay format offers the advantages of specificity and sensitivity compared with other enzyme immunoassay detection methods. Moreover, electrochemical enzyme immunoassay introduced miniaturized system that allows for easy and low cost and volume required. There are a number of solid supports (transducers) that have been used in electrochemical format detection including amperometric and voltammetric. These electrochemical transducers are used in the measurement of pollution in water.

In this project, a portable electrochemical system based on an integrated lab on a chip platform consisting of (a) Microfluidic cartridge with immunosensor (b) Fluidic manifold with valves to control fluid (c) Control module, containing interfaces for microfluidics, immunosensor and user display has been described. The immunosensor was fabricated in a three-electrode system (working, counter and reference electrodes) at Tyndall national institute. This sensor was configured in a multi-electrode array screening for real time environmental measurements. This microfluidic platform allows quick time and portable measurement and requires only small volumes of sample. Modification of the immunosensor array surface could enhance the binding of the target to its specific antibody, thus increasing the sensitivity of the sensor towards environmental pollutants. Preliminary result on sample was conducted using this platform. However, no further studies were carried out to optimise the parameters and to develop the sensitivity as the timeframe of the research study, it was difficult to acquire quantitative data for standard and real samples. Optimisation experiments on different format components were performed in order to achieve the ideal conditions for a maximum immunoassay binding. Even though the tests for optimisation of solvents used to dilute PAHs were not performed for the assay using electrochemical, it has been considered that DMSO is the optimal solvent for the best organic solvents. This consideration was made based on the tests conducted for the optimisation of organic solvent using optical detection. This consideration was also supported by [1], where it has been reported that the use of DMSO to dilute PAHs for their electrochemical screen-printed-electrode resulted in a good assay performance. The displacement assay format used in this project could be of interest for individual targeted compounds (BaP). A key aspect in an immunosensor development is to immobilize the antibody to the solid surface.

In order to enhance the sensitivity of the developed immunosensor, the working electrode was modified with the 11-MUA SAM. Activation of water-soluble carbodiimide was performed using EDC and NHS before the antibody immobilisation. The performance of 11-MUA SAM in ethanolic solution has been demonstrated as a result to improve the binding of the antibody towards the surface for the detection of BAP in the water samples. Characterisation of the 11-MUA formations on the immunosensor surface was carried out using cyclic voltammetry (CV) and contact angle measurements. The results confirmed that with the presence of 11-MUA formations on the immunosensor surface, the immobilisation of antibodies to the chip was improved and thus the sensitivity of the sensor increased. In this project, another electrochemical method for PAHs detection was that based on the screen-printed-electrode and nanoparticles as the solid surfaces were also developed. Screen- printed-electrode and nanoparticles were able to detect PAH analytes and also provide quantitative analysis. The electrochemical methods with an immunoassay principle showed a limit of detection (0.07 ng/ml) and a linear range (1 to 10 ng/ml). Displacement assay was carried using optical immunoassay for determination of benzo[a]pyrene in water. However, there was no benzo[a]pyrene was detected. Spiking of 5 and 50 ng ml of benzo[a] pyrene showed high percentages of in each sample, indicating that our system was actually working. As this system was unable to detect the benzo[a]pyrene without spiking was probably because of the very low amount of benzo[a]pyrene presence in the samples, or might be no presence of benzo[a]pyrene in the water at the time the samples were collected. These results were supported by the results using GC-MS, in which there was no benzo[a] pyrene detected.

To validate the developed immunosensors, Gas Chromatography-Mass Spectrometry was carried out for determination of PAHs in tap water. GC-MS is one of the promising traditional techniques for detection of PAHs in different sample matrices. Analysis of tap water samples showed high percentages of recovery in tap water sample and there was no presence of PAHs. GC-MS analysis indicated that the system was actually working. In general, the up-and-coming performance of the developed electrochemical system could satisfy the need of excellent biosensors. However, these developed systems will not replace standard methods for the detection of PAHs, but will rather complement them.

## **6.2 Suggestions for Future perspective**

The challenges throughout the tests were maintained. Our immunosensors array could be re-used, by cleaning the chips with the protocols that was optimised in Chapter 4. It was great to improve the regeneration of the chip, thus it could be used for multiple times. To date, gold materials have been used in the most studies as sensing material because of their favorable properties, including electronic property and easy surface modifications. However, researches on indium tin oxide could be considered for quantitative immunoassay applications as this thin film material provides a good electrical conductivity, electrochemical potential window, and high optical transparency [2]. According to Aziz et al., this thin film material was used in immunosensor, in which it has been successful in developing a platform based on indium tin oxide to detect mouse IgG with a LOD of 1.0 pg/ml [3]. Finally, the serious challenge associated with any environmental assay is the treatment of interferences. Interferences affect the read-out values and lifetime of the system. The simple and low cost solution could be by using revolver like filtration system. 3D printing technology



could be easily implemented to increase lifetime of the system. Environmental monitoring still faces various challenges, table 6.1 representing the feasibility of printing technologies that can be used to overcome them.

**Table 6.1:** The challenges environmental monitoring and the possible solutions

<b>Features</b>	<b>Challenges Environmental monitoring</b>	<b>Possible solutions</b>
<b>Materials (lifetime)</b>	<b>Metals (oxidant condition)</b>	<b>Conductive polymer</b>
<b>Stability</b>	<b>Reactants involved (low stability)</b>	<b>Avoid using biomolecules due to their bioactivity and capability decrease drastically in environment conditions</b>
<b>Energy supply</b>	<b>Battery</b>	<b>Photovoltaic cell</b>
<b>Production cost</b>	<b>Traditional fabrication used to produce deployable devices is costly</b>	<b>Printing technologies used to produce deployable devices for analytical purposes is low cost</b>

It is obvious that unaddressed technologies gaps could be filled in the near future with 3D printing technology and ink printing. Printing technologies will not only solve the challenges environmental monitoring but also will be the standard technology to

produce full deployable devices at low cost. LOC system will excel as promising miniaturized platform for in situ and real time monitoring of pollutants.

### **6.3 References**

1. K.A. Fährnich, M. Pravda, and G.G. Guilbault. Biosensors and Bioelectronics. 2003. 18: p. 73-82.
2. D. Yu and K. Kim. Bull. Korean Chem. Soc. 2009. 30(4): p. 955-958.
3. M.A. Aziz, K. Jo, M.A. Qaium, C.-H. Huh, I.S. Hong, and H. Yang. Electroanalysis. 2009. 21(19): p. 2160-2164.

## **1 List of Publications**

### **1. Shifa Felemban, Patricia Vazquez and Eric Moore**

Future Trends for In Situ Monitoring of Polycyclic Aromatic Hydrocarbons in Water

Sources: The Role of Immunosensing Techniques.

### **3. Shifa Felemban, Patricia Vazquez and Eric Moore. Article:**

Magnetic Iron Oxide Nanoparticles-based electrochemical immunosensor of

Polycyclic Aromatic Hydrocarbons .In preparation

### **4. Shifa Felemban, Patricia Vazquez and Eric Moore. Article: Determination of**

Polycyclic Aromatic Hydrocarbons from water samples using a microfluidic

immunosensor system. In preparation

## **2 Dissemination Activities**

- (Poster) at MTAS 2016 (Dublin) + Workshops
- ISC 2016 at UCC (Attendee)
- Demonstration for Master degree (S1/S2) 2016
- Passing 3 modules 2016
- Poster at AIT 2017 (Athlon) + Workshops
- Oral talk at SPIE 2017 (Barcelona)
- Demonstrating for Master's degree S1/S2 2017
- 4 outreach at Tyndall 2017
- Passing 1 module 2017
- Smart systems integration, Cork City, Ireland [2017] (Attendee)
- Attending a LSI day at Tyndall [2017] (Oral)
- Attending 2<sup>nd</sup> /3<sup>rd</sup> Year Post graduation day at UCC (Poster)
- CIT conference 2018 (Oral) + Workshops

- SSI Dresden 2018 (Oral)
- ISE conference (Bologna) 2018 (Oral)
- 2nd /3rd Year Post graduation day at UCC (Oral)
- 2 outreaches at Tyndall 2018
- Passing 1 module 2018
- Demonstrating for Master's degree S1/S2 2018
- ISE conference (Dublin) 2019 (Poster)
- Demonstrating for Master's degree S1/S2 2019